Control and management strategies for a microgrid

Ngoc An Luu

THÈSE

Pour obtenir le grade de

DOCTEUR DE L'UNIVERSITÉ DE GRENOBLE

Spécialité : **Génie Electrique**

Arrêté ministériel : 7 août 2006

Présentée par

Ngoc An LUU

Thèse dirigée par **Quoc Tuan TRAN** et
par **Seddik BACHA**

préparée au sein du **CEA-INES et du Laboratoire de Génie Electrique de Grenoble**
École Doctorale Electronique, Electrotechnique, Automatique & Traitement du Signal

Control and management strategies for a microgrid

Thèse soutenue publiquement le **« 18/12/2014 »**,
devant le jury composé de :

M. Brayima DAKYO
Professeur, Université du Havre, Président
M. Kim Hung LE
Professeur, Université de Da Nang, Rapporteur
M. Demba DIALLO
Professeur, Université Paris Sud, Rapporteur
M. Quoc Tuan TRAN
Responsable scientifique, HDR, CEA/INES, Directeur de thèse
M. Seddik BACHA
Professeur, Université Joseph Fourier, Co-Directeur de thèse
M. Lambert PIERRAT
LJK-LAB, Stat-M3S, Université de Grenoble, invité

Acknowledgments

First and foremost, I would like to express my deepest gratitude to my supervisor, Dr. Tran Quoc Tuan, for his guidance, advice and support during three years of my study in CEA/INES and in G2Elab of the University of Grenoble. He taught me how to do a research. All of my works in this dissertation cannot be accomplished without his support.

I would like to thank my supervisor, Prof. Seddik Bacha for his help and the opportunities he gave me to improve myself during the time in G2Elab.

I would like to thank my friends, especially all members in G2Elab for their discussion and friendship.

Special thanks to my parents, my brother and my sister in law for their love and support.

Most of all, I would like to express my appreciation to my wife DUNG for her love and encouragement. Thanks for her understanding, staying by my side and taking care our baby.

Luu Ngoc An

Grenoble, France

December, 2014

Abstract

Today and in the future, the increase of fuel price, deregulation and environment constraints give more opportunities for the usage of the renewable energy sources (RES) in power systems. A microgrid concept is needed in order to integrate the renewable sources in the electrical grid. It comprises low voltage (LV) system with distributed energy resources (DERs) together with storage devices and flexible loads. The integration of RES into a microgrid can cause challenges and impacts on microgrid operation. Thus, in this thesis, an optimal sizing and security, reliability and economic efficiency operation strategies of a microgrid including photovoltaic productions (PV), battery energy storage systems (BESS) and/or diesels is proposed. Firstly, the iterative optimization technique is used to find the optimal sizing of a microgrid. Secondly, the voltage and frequency control strategies for an island microgrid by using droop control methods are studied. Furthermore, we propose intelligent voltage and frequency control strategies by using fuzzy logic. By this way, the frequency is expressed not only as the function of active power but also the state of charge of BESS and the operation states of microgrid. And finally, a method to optimize the energy management in operation of a microgrid is proposed in this thesis. Dynamic programming is used to find the minimum the cost of fuel considering the emissions by scheduling of distributed energy resources (DERs) in an island microgrid as well as to minimize the cash flows and the exchanged power with the main grid in a grid-connected mode. The simulation results obtained show the accuracy and efficiency of the proposed solutions

Abrégé

Aujourd'hui et à l'avenir, l'augmentation des prix du carburant, la déréglementation et les contraintes de l'environnement donnent plus de possibilités pour l'utilisation des sources d'énergie renouvelables (SER) dans les réseaux électriques. Un concept de microgrid est nécessaire afin d'intégrer les sources d'énergie renouvelables dans le réseau électrique. Ce microgrid comprend un réseau de basse tension (BT) avec les ressources d'énergie distribuées (DER) ainsi que les moyens de stockage et des charges flexibles. L'intégration des énergies renouvelables dans un microgrid peut causer des enjeux et des impacts sur le fonctionnement du microgrid. C'est pourquoi dans cette thèse, un dimensionnement optimal et les stratégies de fonctionnement en sécurité, fiabilité et efficacité d'un microgrid comportant des productions photovoltaïques (PV), des systèmes de stockage d'énergie de la batterie (BESS) et / ou les diesels sont proposés. Tout d'abord, la technique d'optimisation itérative est utilisée pour trouver le dimensionnement optimal d'un microgrid. Deuxièmement, les stratégies de contrôle de tension et de fréquence pour un microgrid en mode îloté en utilisant les statismes sont étudiées. De plus, nous proposons les stratégies intelligentes de contrôle de tension et de la fréquence à l'aide de la logique floue. De cette manière, la fréquence est exprimée non seulement en fonction de la puissance active, mais aussi de l'état de charge de BESS et des régimes de fonctionnement de microgrid. Et enfin, une méthode pour optimiser la gestion de l'énergie dans l'exploitation d'un microgrid est proposée dans cette thèse. La programmation dynamique est utilisée pour trouver le minimum du coût du carburant compte tenu des émissions par la planification des ressources énergétiques distribuées (de DER) dans un microgrid en mode îloté ainsi que pour minimiser le coût d'énergie et les puissances d'échange avec le réseau en mode connecté. Les résultats de simulation obtenus montrent la précision et l'efficacité des solutions proposées.

Table of Contents

List of Figures

List of Abbreviations

PV	– Photovoltaic
LV	– Low voltage
DER	– Distributed Energy Resources
AI	– Artificial intelligent
GA	– Genetic algorithm
PSO	– Particle swarm optimization
LP	– Linear programming
MILP	– Mix-integer linear programming
DP	– Dynamic programming
MOEAs	– Multi-objective evolutionary algorithms
QP	– Quadratic programming
ADP	– Advance dynamic programming
MADS	– Mesh adaptive direct search
MG	– Microgrid
MC	– Microsource controller
LC	– Load controller
MGCC	– Microgrid system central controller
DMS	– Distribution management system
PCC	– Point of common coupling
BESS	– Battery energy storage system
SOC	– State of charge
SOH	– State of health
FR	– Renewable energy fraction
EER	– Excess energy ratio

SS – Static switch

CB – Circuit breaker

DC – Direct current

ACS – Annual cost of system

ACC – Annual capital cost

AOM – Annual operation maintenance cost

ARC – Annual replacement cost

AFC – Annual fuel cost

AEC – Annual emission cost

ABC – Annual buying cost

ASC – Annual selling cost

CS – Cost of system

FC – Fuel cost

EC – Emission cost

BrC – Battery replacement cost

CF – Cash flow

CP – Cash pay

CR – Received cash

CHAPTER I :

Introduction

SUMMARY

I.1. **Context**

I.1.1. Development of photovoltaic

Today and in the future, the power system is characterized by sharing of renewable energy sources. The part of variable renewable sources for electricity generation in four regions is shown in Figure I.1 [1]. This figure shows a continuous huge increase of renewable sources participation.

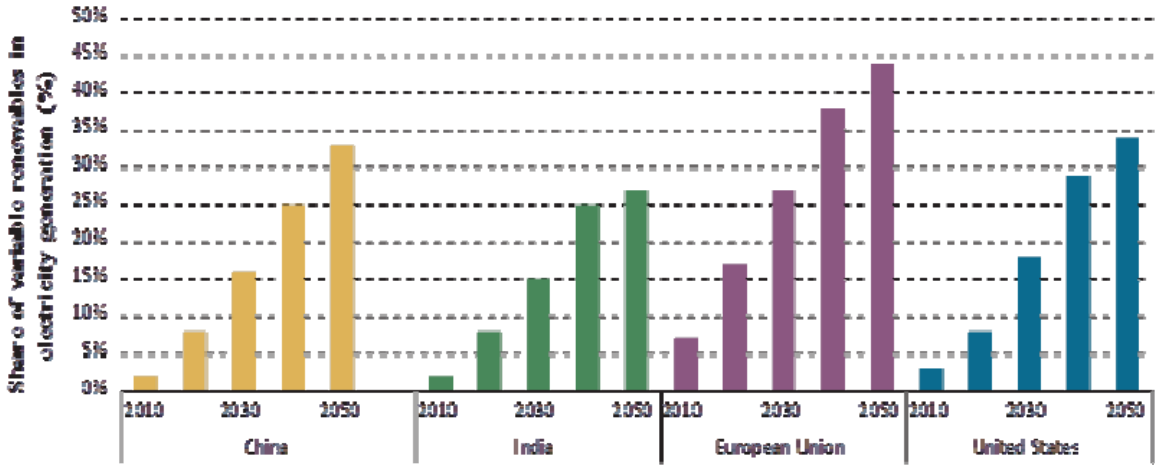

Figure I.1: The sharing of variable renewable sources of electricity generation in 4 regions

(Source: http://www.iea.org; Technology Roadmap: Energy Storage)

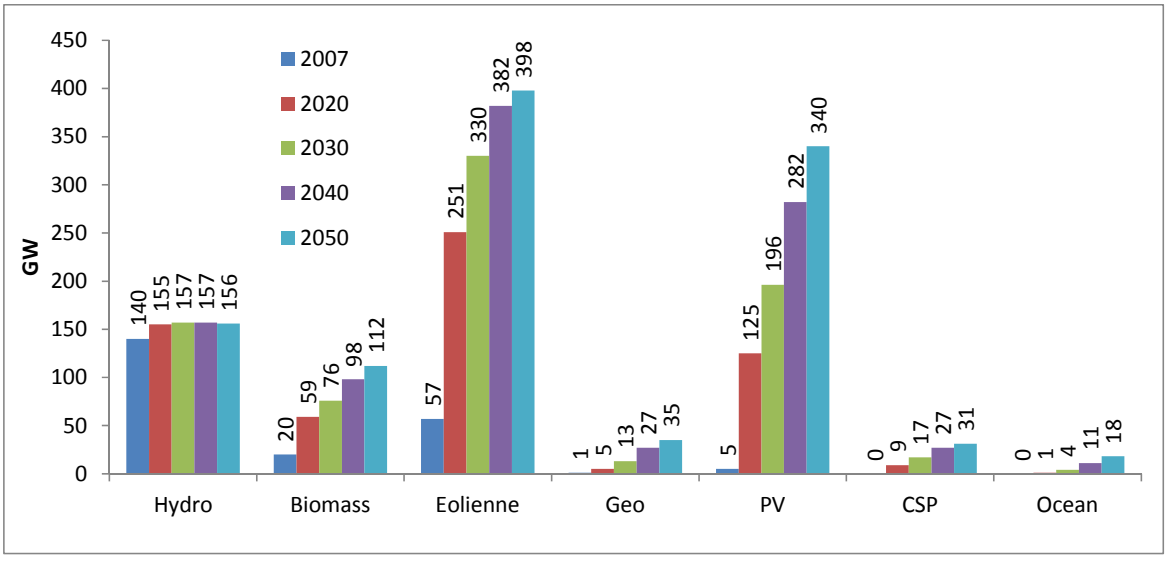

Figure I.2: The contribution of renewable sources in the total electricity generation

(Source: http://www.greenpeace.org; Energy (R)evolution-

Towards a fully renewable energy supply in the EU 27)

The installed power of renewable resources in Europe nationals are predicted to 2050, are shown in Figure I.2. As can be seen from this Figure, the photovoltaic and wind energy productions are given as the fastest growth.

Figure I.3 shows the installed power of renewable sources in Germany. It can be seen from this Figure, the solar installed is given up to 37.5GW in July 2014; Furthermore, this value is given in France about 4.3GW (Figure I.4).

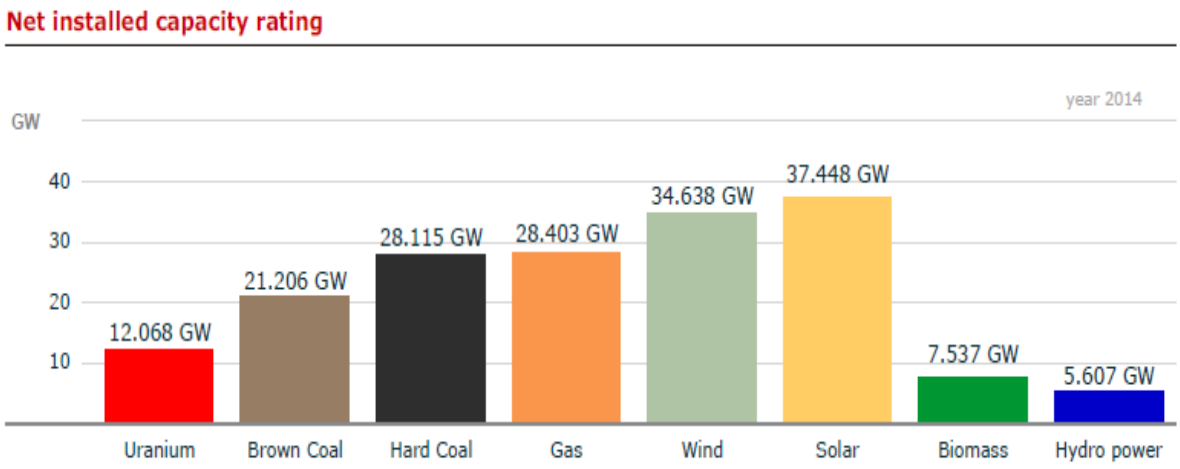

Figure I.3: the installed power of renewable sources in Germany

(Source : http://www.ise.fraunhofer.de/en; B.Burger, Fraunhofer ISE, data : Bundesnetzagentur)

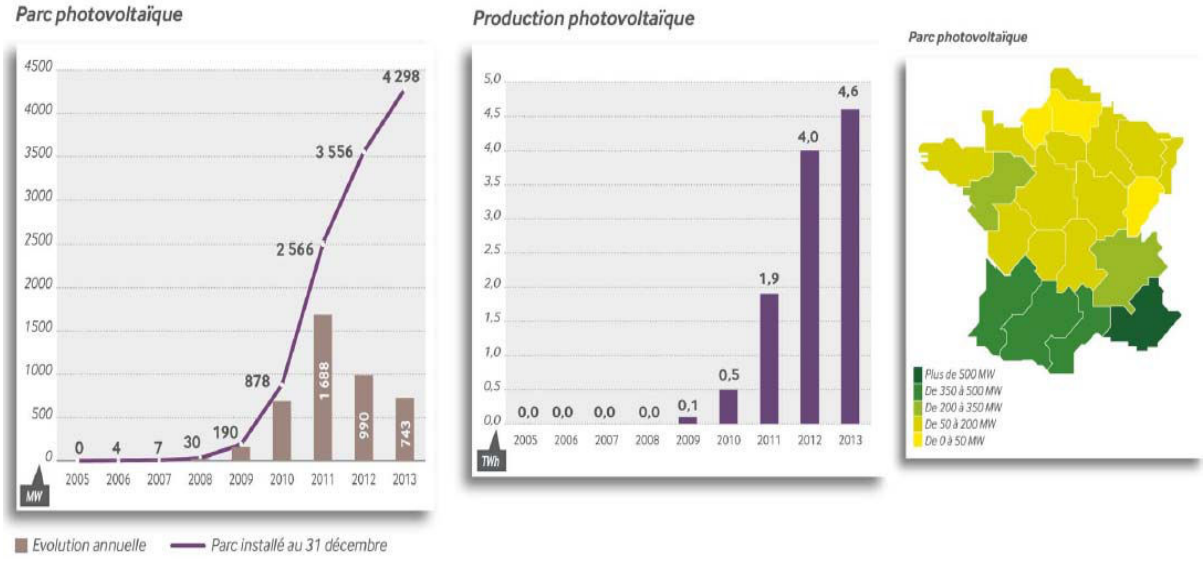

Figure I.4: Evolution of installed photovoltaic in France

(Source : Bilan électrique français 2013, RTE, 23 Janvier 2014)

The installed PV price in United States is shown in Figure I.5. From this Figure, one can see that the installed price dramatically declined from 2008 to 2013.

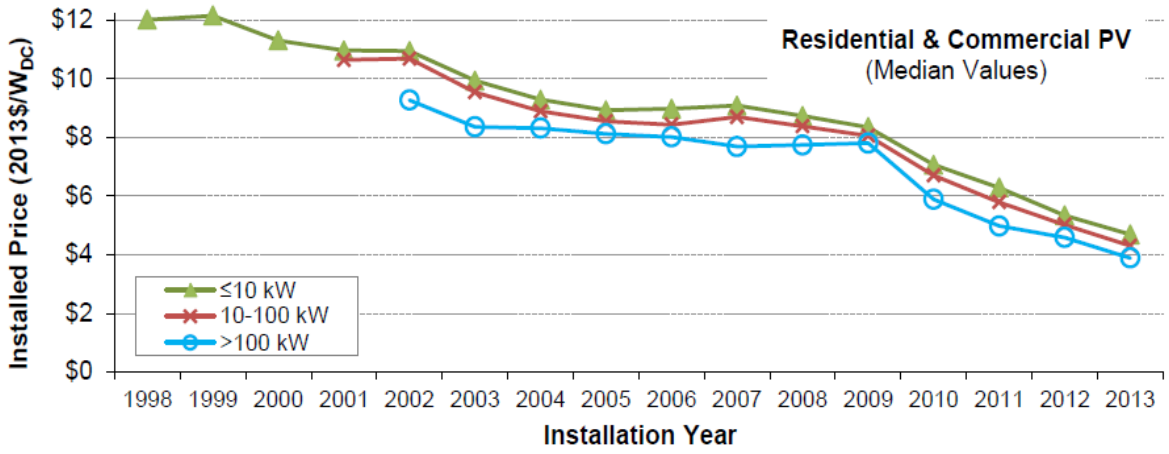

Figure I.5: The installed PV price in United States

(Source: http://www.emp.lbl.gov; Tracking the Sun VII: An Historical Summary of the Installed Price of Photovoltaics in the United States from 1998 to 2013)

Figure I.6 illustrates the installed PV price in Germany. This price will decrease continually from 2013 to 2030

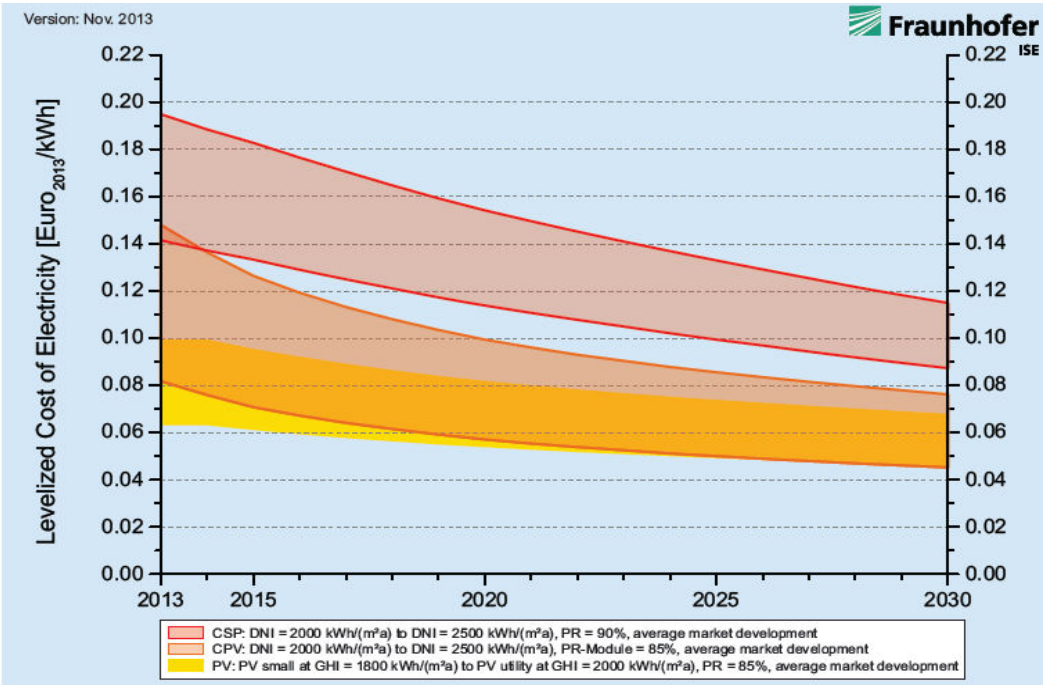

Figure I.6: The installed PV price in Germany

(Source : http://www.ise.fraunhofer.de/en/)

I.1.2. Development of Electrochemical Energy Storages

The electricity storage capacity for daily electricity storage by four regions in 2011 and 2050 is described in Figure I.7. From this Figure, there are significant growth rates of electricity storage capacity in all regions.

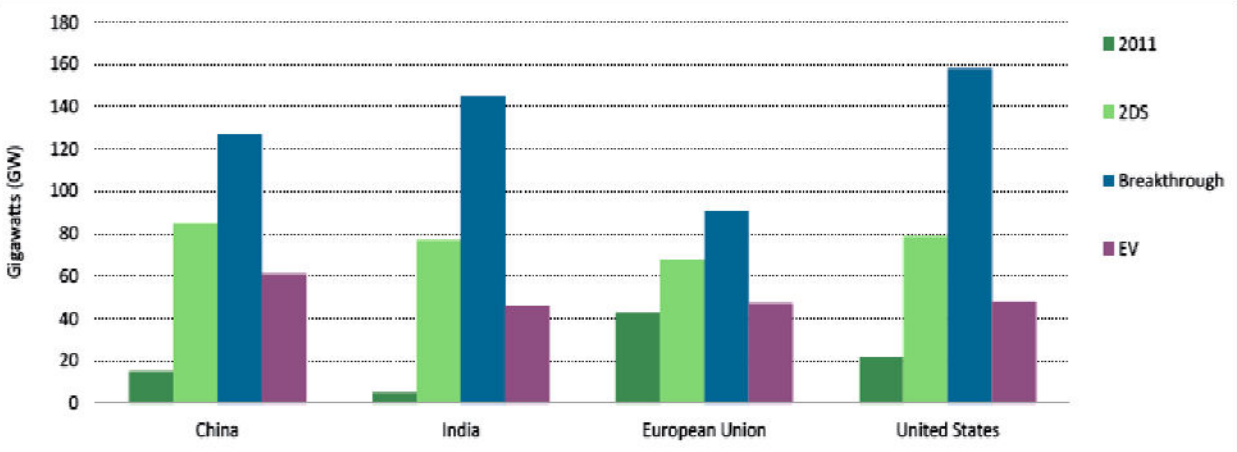

Figure I.7: Electricity storage capacity for daily electricity storage by region in 2011 and 2050

(Source: http://www.iea.org; Technology Roadmap: Energy Storage)

The battery prices evolution from 2009 to 2013 is demonstrated in Figure I.8. As it can be seen from this Figure, the price dropped from about 2000$ in 2009 to around 700$ in 2013.

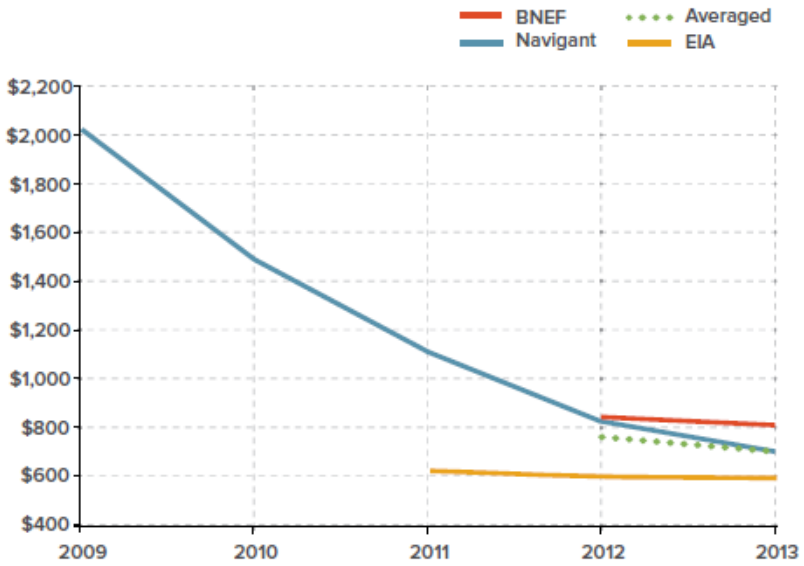

Figure I.8: The Battery price from 2009 to 2013

(Source: www.rmi.org; RMI - The Economics Of Grid Defection - When And Where Distributed Solar Generation Plus Storage Competes With Traditional Utility Service)

Figure I.9 shows the future trend of the battery price; the price is predicted to decrease continually to 2030, and after it stabilizes to 2050.

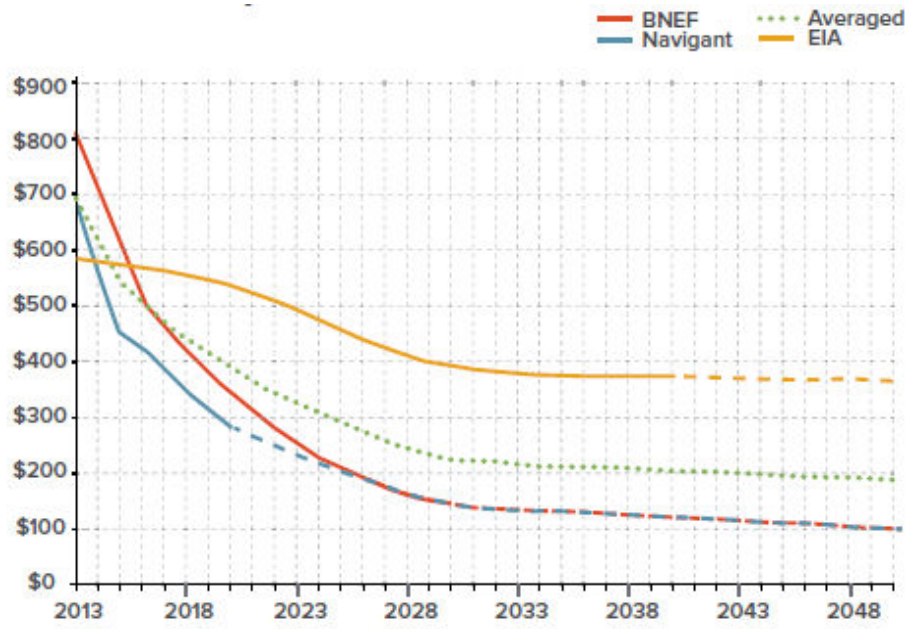

Figure I.9: The Battery price provision from 2013 to 2050

(Source: www.rmi.org; RMI - The Economics Of Grid Defection - When And Where Distributed Solar Generation Plus Storage Competes With Traditional Utility Service)

It's well known that the grid must be balanced at each instant; therefore, the generated electricity must meet the varying demand. When there is an imbalance between supply and demand, it will damage the stability and even quality (voltage and frequency) of the power supply. On the other hand, the sources are usually located far from the load. Generators and consumers are connected through transmission lines and transformers. This may cause congestion. If a failure on a line occurs, the supply of electricity will be interrupted and the loads can be shed. Thus, energy storage is needed and the roles of this are presented in the following [2]:

- High generation cost during the peak demand periods

As can be seen from Figure I.10, the price for electricity at peak demand periods is given as higher than at off-peak periods. During peak periods when electricity consumption exceeds average, the output of power plants has to be increased, which means that increasing the fuel sources with oil and gas... This leads to an increase in price. Then, during the off peak periods, demand load is less than production; some generators have to be interrupted. In order to overcome these drawbacks, energy source storage is needed. The

storages will be charged during low-cost power and discharge into the power grid during peak periods. The surplus energy from renewable sources (PV, wind) can be stored in storage and used to reduce generation costs. On the other hand, consumers who charge batteries during off-peak hours can use it during the expensive price (peak load periods) and may even sell electricity to utilities or to other consumers during peak hours.

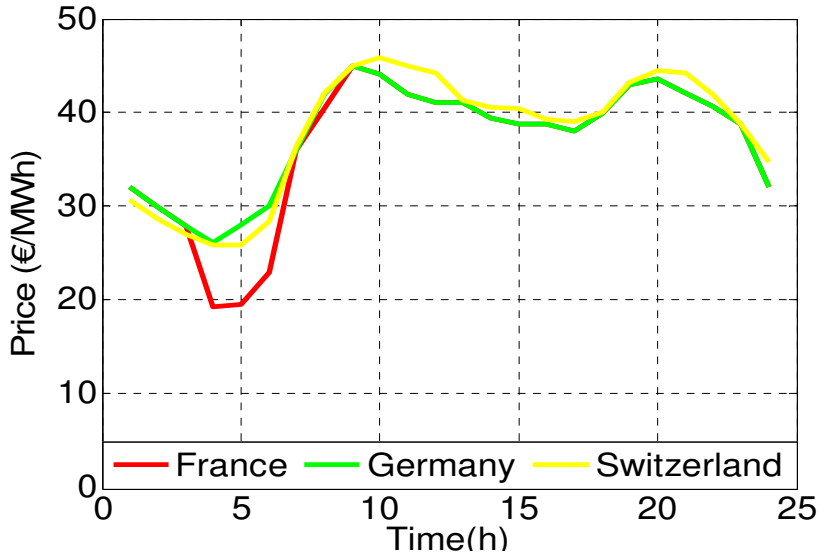

Figure I.10: The comparison of daily electricity prices between three countries (27/8/2014)

(Source: www.epexspot.com)

- Increasing penetration of renewable energy

The benefit of energy storage is to increase the penetration of renewable energy on the grid. In fact, storage can "smooth" the delivery of power generated from wind and solar technologies, in effect, increasing the power of renewable sources [3] - [6]. Additionally, when energy storage is used with distributed generation, it can improve the reliability of those assets by providing power-conditioning value [2].

- Reducing line-congestion

Storage can reduce line-congestion and line-loss by moving electricity from the peak load periods to off-peak times. Therefore, it reduces the peak loading (and overloading) of transmission and distribution lines. Thus, storage can contribute to extending the life of existing infrastructure.

- Energy storage for vehicles

The storage is needed not only for the deployment of batteries in vehicles, but also for potential second-life applications for electric vehicle (EV) batteries. It means that the integration of energy between vehicles and the grid will gain more interest and get

developed.

Regarding the issues above, the PV grid integration is an important subject to be considered. The storage is one of the levers which can increase the PV penetration rate. . Other additional functions can be taken from the storage like ancillary services and other power quality aspects. Thus, a microgrid concept, including PV and batteries, will be a new solution for a 'smart grid'.

I.1.3. Microgrid

There are microgrid projects which were successfully completed, providing several innovation technical solutions. For example, the EU Microgrid Research Project (1998-2002), The EU More Microgrid Research Project (2002-2006), EU demonstration sites (Greece: The Kythnos island microgrid, Netherlands: Continuon's MV/LV facility), CERTS microgrid introduction, CERTs microgrid test bed, GE global research microgrid, NEDO microgrid projects…

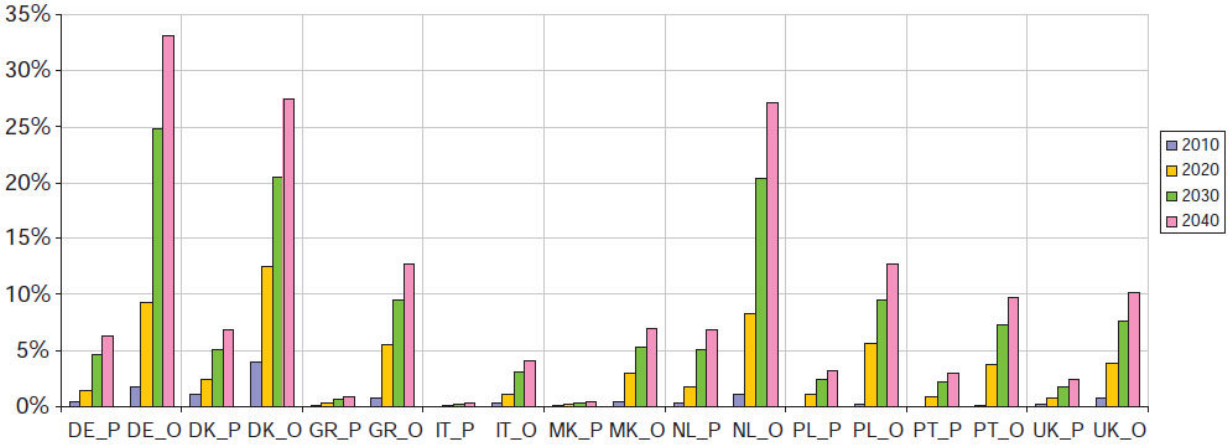

Figure I.11: Microgrid dissemination ratio in EU national grids scenarios [1]

(O = optimistic assumptions, P = pessimistic assumptions). (DE=Germany, DK=Denmark, GR=Greece, IT=Italy, MK=FYROM, NL=The Netherlands, PL=Poland, PT=Portugal, UK=United Kingdom)

To illustrate the development of the European national microgrid, four scenarios are presented for 2010, 2020, 2030 and 2040. The share of typical microgrids within national power systems (microgrid dissemination ratio) per country and region are assumed to be as shown in Figure I.11, for 2010, 2020, 2030 and 2040, with pessimistic (P) and optimistic (O) assumptions [1]. It can be seen from this Figure, the growth rate of microgrid is given and predicted to increase continually of the European national microgrid

Microgrid is an important and necessary part of the development of smart grid. The microgrid is characterized as the "building block of smart grid" [1]. It comprises low voltage (LV) system with distributed energy resources (DERs) together with storage devices and flexible loads. The DERs such as micro-turbines such as, fuel cells, wind generator, photovoltaic (PV) and storage devices such as flywheels, energy capacitor and batteries are used in a microgrid. The microgrid can benefit both the grid and the customer [1].

From the customer's view: microgrids answer to both thermal and electricity needs and enhance local reliability, reduce emission, improve power quality by supporting the voltage and frequency and potentially lower costs of energy supply.

From the utility's view: a microgrid can be seen as a controlled entity within the power system as a single dispatchable unit (load or generator) or ancillary services provider.

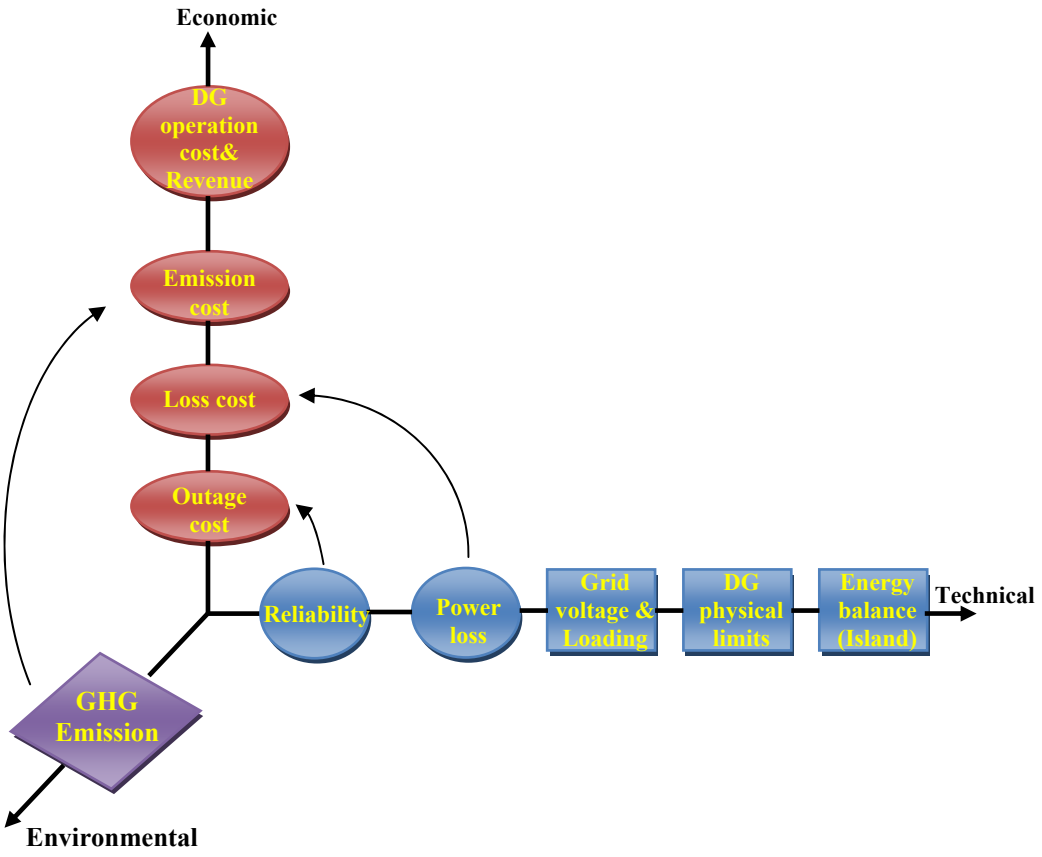

Figure I.12: Microgrid operation strategy [1]

Normally, a microgrid has two modes of operation: the island mode and the grid-connected mode. In the island mode, the production is required to meet the loads demand.

On the other hand, when the microgrid is connected to grid, it can either receive or inject power into the main grid. Furthermore, the gird connected microgrid can provide power supporting to its local loads demand. When a disturbance occurs, the microgrid is disconnected from the distribution network as soon as possible in order to avoid any further damage. In that case, the microgrid will operate in an island mode. Furthermore, the operation mode is related to the elasticity supply, local loads demand and the electricity market. Thus, the objectives of the optimal operation scheduling in microgrids concern with the economical, technical and the environmental aspects.

A microgrid can provide a large variety of economic, technical, environmental, and social benefits to both internal and external stake-holders depending on its operation strategy [1].

Microgrid control can be divided into the coordinated control (supervisory control or energy management) and local control. First, the coordinated control optimizes to allocate the power output among DER, the cost of energy production and emission. The forecast values of loads demand, the generation and the market electricity price in each hour on the next day are collected and calculated to find the optimal output power of DER, the consumption level of utility grid and the cost and the emission. Second, the intelligent local controllers for DER can enhance the efficiency of microgrid operation. In fact, these controllers participate to control the frequency and voltage in different operation modes of microgrid such as: islanded mode and grid connected mode.

I.2. **Literatures review**

Optimal sizing, control and energy management strategies are known as important research issues. First, several methods for optimal sizing have been proposed in the literature. Some of the authors use the artificial intelligent (AI) methods such as genetic algorithm (GA), Particle Swarm optimization (PSO), whereas others utilize the iterative method to find the optimal configuration of a microgrid which satisfies the optimal operation strategy. Second, the optimal for microgrid energy management is also presented in some researches. The Rule-based method, optimal global methods (Linear programming (LP), Mix-Integer-Linear-Programming (MILP) and dynamic programming (DP)) as well as the artificial intelligent (AI) methods are used to find the optimal energy management for a microgrid. Last, the local controllers for DER can enhance the efficiency of

microgrid operation by using the conventional methods (single master (centralize control), master/slave and droop control). Furthermore, the variations of conventional droop control are also addressed in some publications.

I.2.1. Optimal sizing of a microgrid

Optimal sizing of an island microgrid

The optimization sizing of island microgrid has been presented in the literature. It has two main aspects, which are the architecture sizing and the energy fluxes. Dealing with these problems, various simulation and optimization software tools on PV hybrid systems have been reviewed in the literature [7]-[12]. On the other hand, two main methods of optimization that are iterative and artificial intelligent (AI) based methods have been proposed in [13]

Genetic Algorithm (GA) has been proposed for optimal sizing of a PV-diesel-battery system in [14]. The main objective is to define the optimum number of PV panels, battery banks and DG capacity. In [15], the GA is used to optimize a hybrid PV/diesel generator system which is divided into two parts. The first part aims to find the optimal configuration of the system. Then, the latter part optimizes the operation strategy by using each calculated configuration in the first part. The optimal configuration is the one that leads to the minimum cost of the system. A multi-objective optimization for a stand-alone PV-Wind –diesel system with battery storage by using Multi-Objective Evolutionary Algorithms (MOEAs) is described in [16]. The levelized cost of energy (LCOE) and the equivalent CO_2 life cycle emission (LCE) are known as the objectives. In [17], a multi-objective evolutionary algorithms (MOEAs) and a GA have been used to minimize the total cost, pollutant emissions (CO_2) and unmet loads.

An iterative optimization technique for a stand-alone hybrid photovoltaic/wind system (HPWS) with battery storage was proposed in [18]. The aim is to find the optimum size of system in order to respond to the demanded load and to analyze the impact of different parameters on the system size. In [19]-[20], another iterative optimization technique is used to optimize the capacity sizes of different components of hybrid solar-wind power generation systems employing a battery bank. The sizing optimization of this hybrid system can be achieved technically and economically according to the system reliability requirements. An optimal sizing model based on iterative technique in order to

optimize the capacity sizes of different components of hybrid photovoltaic/wind power generator system using a battery bank was proposed in [21].

Optimal sizing a grid-connected microgrid

The optimization of the grid-connected microgrid has been presented in the recent literature. For instance, in [22], a method is proposed to determine the size of battery storage for grid connected PV system. The objective is to minimize the cost considering the net power purchase from grid and the battery capacity loss (state of health). A methodology for the optimization sizing and the economic analysis dedicated to PV grid-connected systems is presented in [23]. In which, the number, type of the PV units and converters are given as the decision variable. In [24], an optimum sizing of PV-energy storage methodology for small autonomous islands is studied. The main parameters of this paper are the PV-rated power and the storage capacity. The artificial intelligent (AI) techniques are used to optimize such architecture based on PV Grid-connected systems. In [25], the author uses GA to determine the optimal allocation and sizing of PV grid connected systems. On the other hand, the Particle Swarm optimization (PSO) is used for optimal sizing of a grid connected hybrid system in [26]. A comparison between the two methods which are PSO and genetic algorithm (GA) is carried out in advance to evaluate the efficiency of the proposed method.

I.2.2. Energy management of microgrid

When a microgrid has more than two DERs, the energy management system (EMS) is needed to impose the power allocation among DER, the cost of energy production and emission.

The EMS in a microgrid is shown in the Figure I.13. As can be seen from this Figure, the forecast values of load demand, the distributed energy resources and the market electricity price in each hour on the next day are denoted as inputs. Furthermore, the operation objectives are considered to optimize the energy management, are given as follows:

- Economic option
- Technical option
- Environmental option
- Combined objective option.

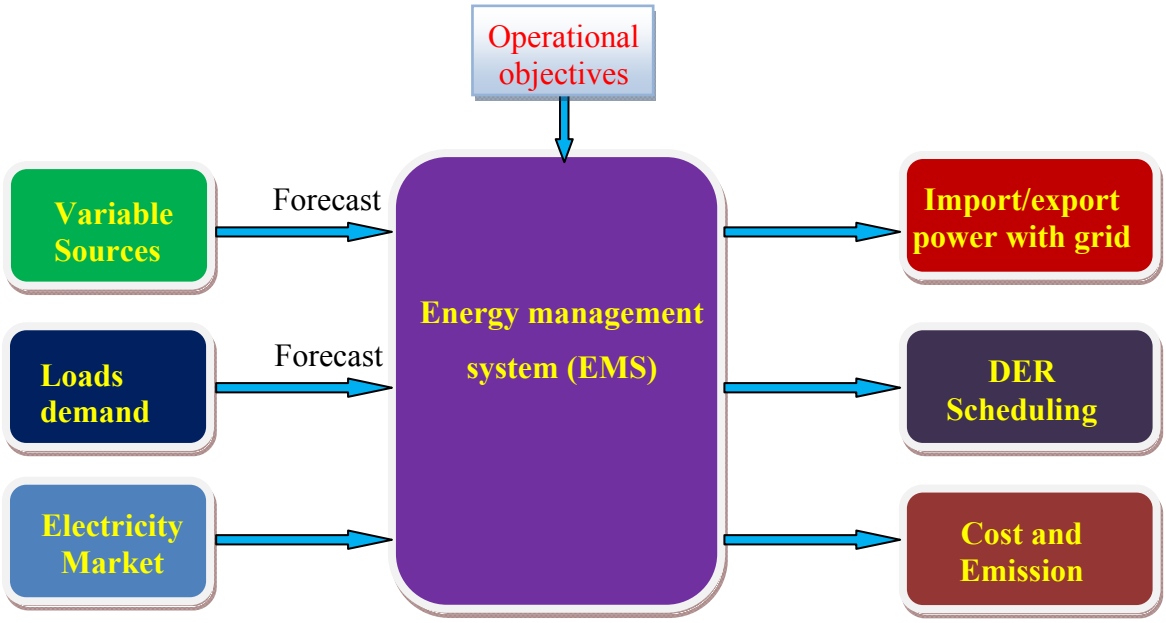

Figure I.13: The energy management system (EMS)

Some algorithms for the optimization of microgrid energy management are proposed [27-40]. The optimal energy management of an island microgrid is presented in [27], [28] by using a rule-based management. The operation of the system depends on the developed rules; thus, the constraints are always satisfied, but the optimization is not global results. In [29], [30], fuzzy logic is used to estimate the rule to improve the rule-based technique. The linear programming (LP) and mix integer linear programming (MILP) are used to find the optimal energy management in [31], [32]. This method gives good results; however, the main limitation is known as the need of a specific mathematical solver [31]. In [33], [34], the optimal energy management for a grid connected with PV/battery and a vehicular electric power system is addressed by using the quadratic programming (QP). The good results achieved, however, the limit of this method is to need the objective function to be convex. In [35], the optimal energy management of a microgrid is solved by using Game Theory and multi-objective optimization. The operating cost and the emission level are given as two objectives functions. The Mesh Adaptive Direct Search (MADS) algorithm is used to optimize the microgrid operating cost function in [35]. A matrix real-coded genetic algorithm (MRC-GA) optimization module is used to search the optimal generation schedule in [36]. The particle swarm optimization (PSO) technique was proposed in [37], [38]. The dynamic programming (DP) and advance dynamic programming (ADP) are used

to optimize the energy management in [39] and [40]. The achieved results are proved the efficiency of these methods.

I.2.3. Microgrid control

Microgrid control was addressed in some literatures.

- The European R&D project [1], [41], [42]

The microgrid control is presented in Figure I.14 [1], [41], [42].

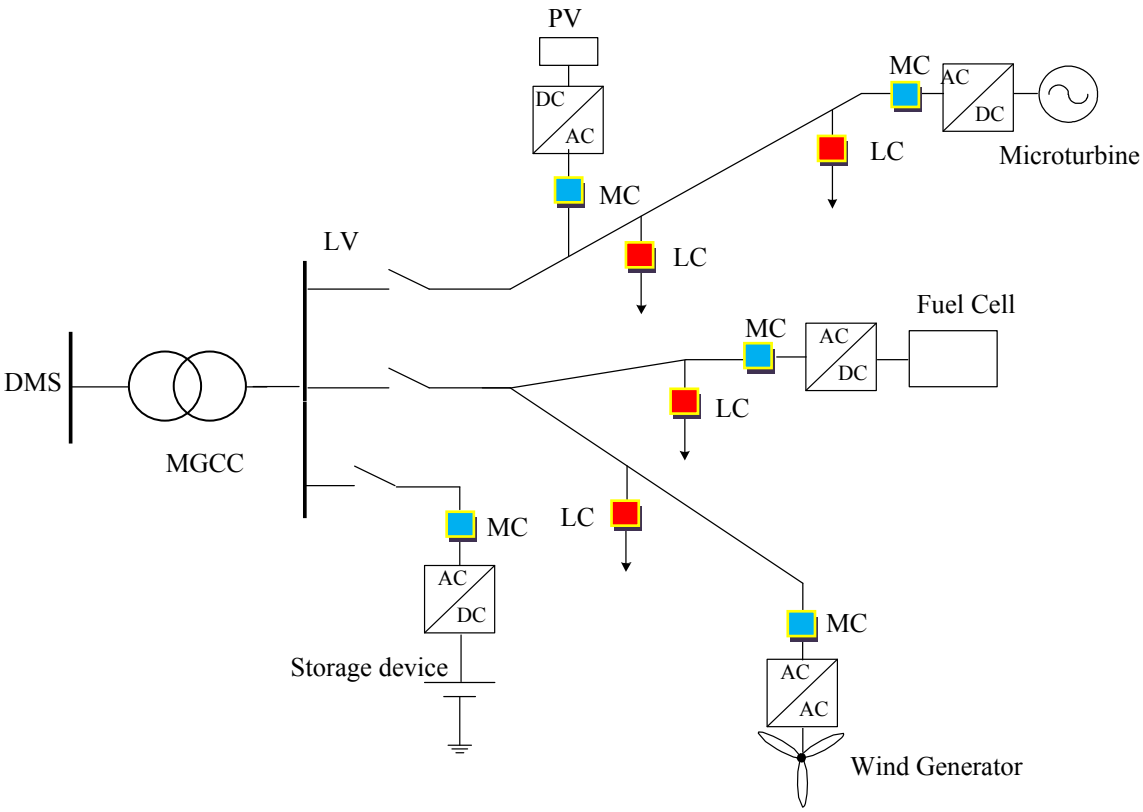

Figure I.14: The microgrid control architecture

The microgrid control includes:

• Micro Source Controllers (MC) and Load Controllers (LC)

• Microgrid System Central Controller (MGCC)

• Distribution Management System (DMS).

+ The Micro Source Controller (MC):

Power electronics interfaces are the privileged mean for energy fluxes control. The local information is measured for controlling and monitoring DERs

+ Microgrid System Central Controller (MGCC)

The Microgrid Central Controller proposes the interface of a microgrid with the other actor such as distribution system operation (DSO) and optimizes the microgrid operation

+ Distribution Management System (DMS).

Distribution Management Systems (DMS) is used for distribution areas management and control, comprising several feeders including several Microgrids

- Hierarchical control of microgrid

The hierarchical microgrid control with its various levels [43] -[52] is presented in Figure I.15 [43]

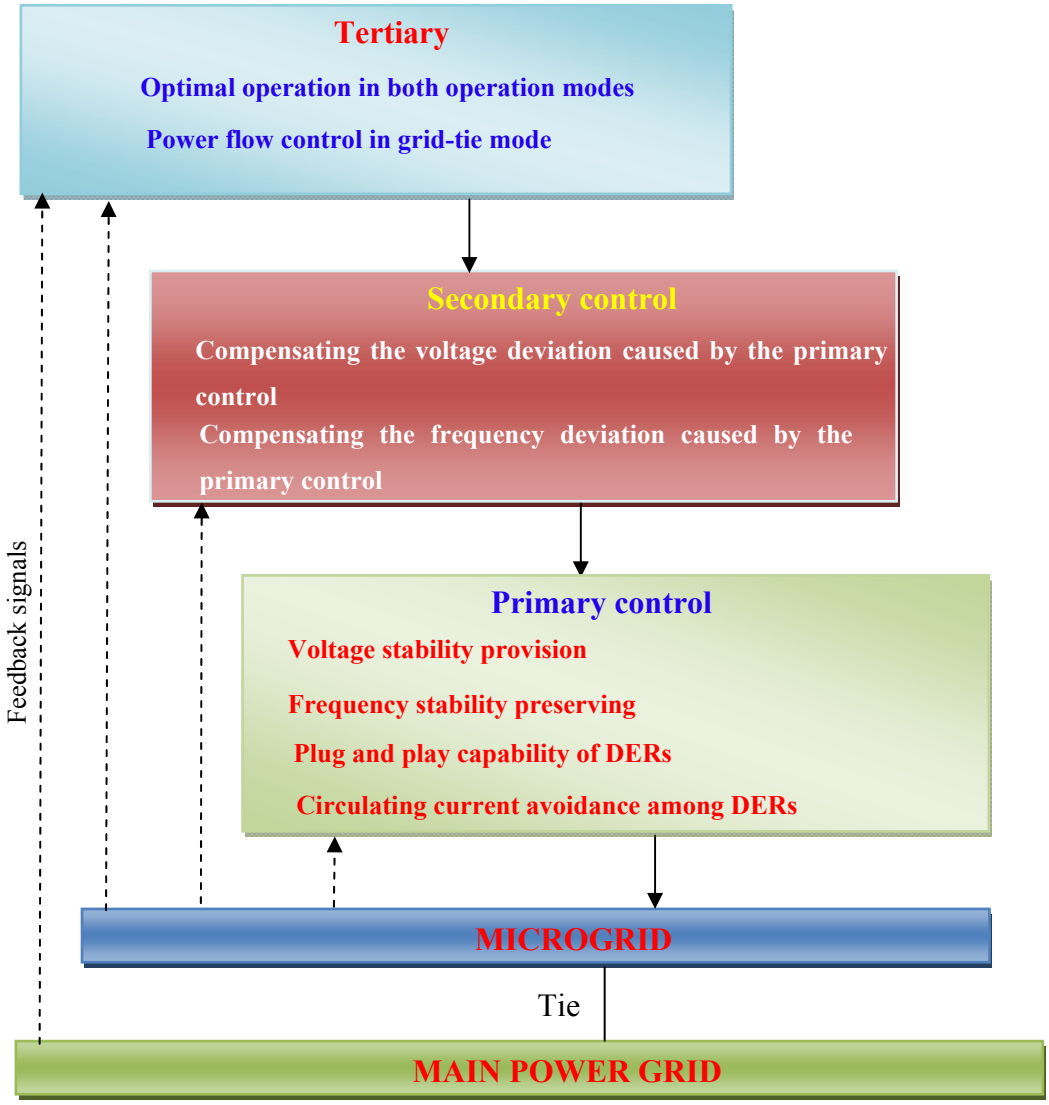

Figure I.15: the requirement at each control hierarchy level [43]

From the two above microgrid control architectures, the primary control is known as the Micro Source Controllers (MC) in The European R&D. In addition, the second and third level is performed by Microgrid System Central Controller (MGCC). The MC will be presented in this part; then, the Distribution Management Systems (DMS) will be mentioned in the future work section of this thesis.

*** Micro sources controller (MC)**

- Centralized control

The centralized control, also known as concentrated control is shown in Figure I.16 [53]. The basic principle of this method is an average current sharing scheme. From the total load current, the current reference of each module is expressed by dividing the total load current by the number of modules [54]. After that, the current error is obtained and delivered to a current control loop. Then, the outputs of the current regulators are sent to the PWM to produce the control signals for each inverter.

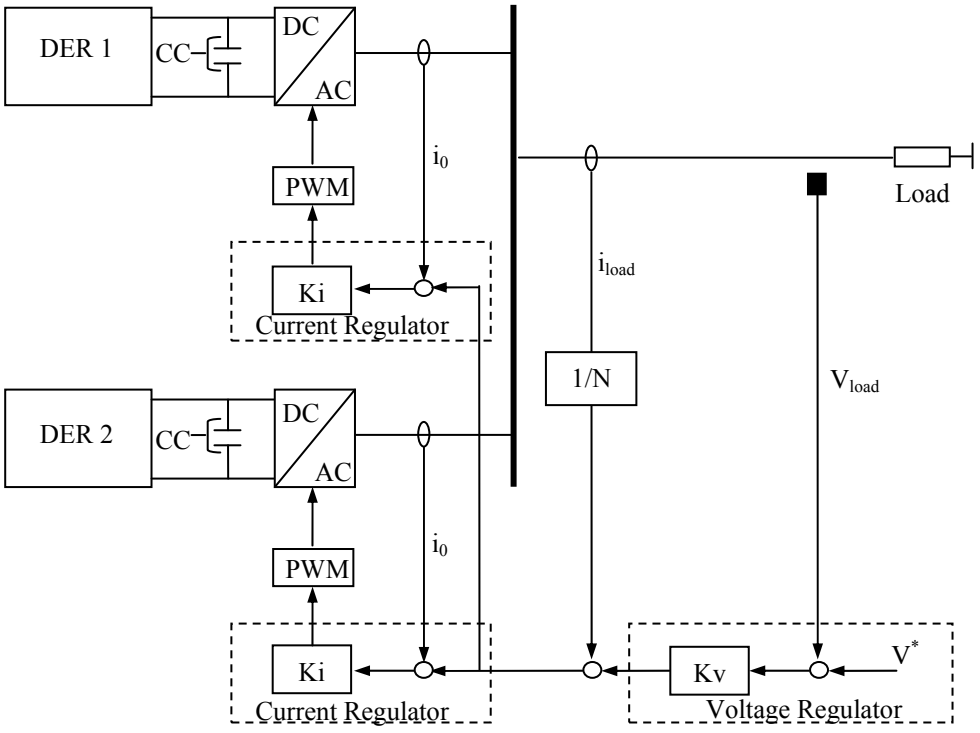

Figure I.16: The centralized control [53]

- Master/slave control

In this control scheme, only one inverter behaves like a master to regulate the voltage

and frequency and the other units keep the constant power. The master unit is V/f controlled and the remaining units are the P/Q controlled. The master/slave is shown in Figure.I.17 [53].

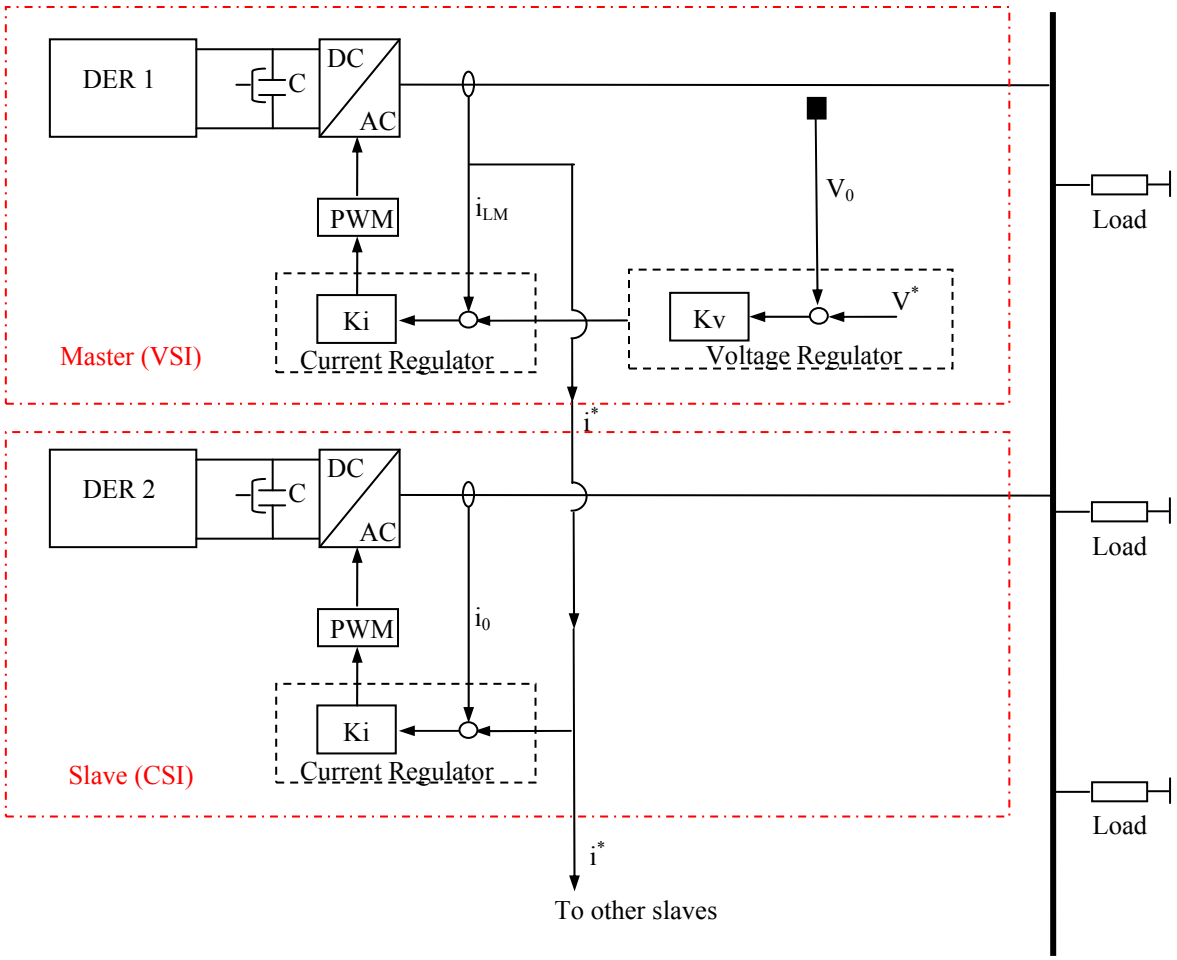

Figure I.17: The master/slave control [53]

- Droop control

Droop methods are based on the behavior of synchronous generators in the power system. In this control technique, the active and reactive power sharing by the inverters are estimated by adjusting the output frequency and voltage amplitude. It is able to avoid critical communication links. The droop control is presented in the Figure I.18 [53], in which m, n are the droop coefficients.

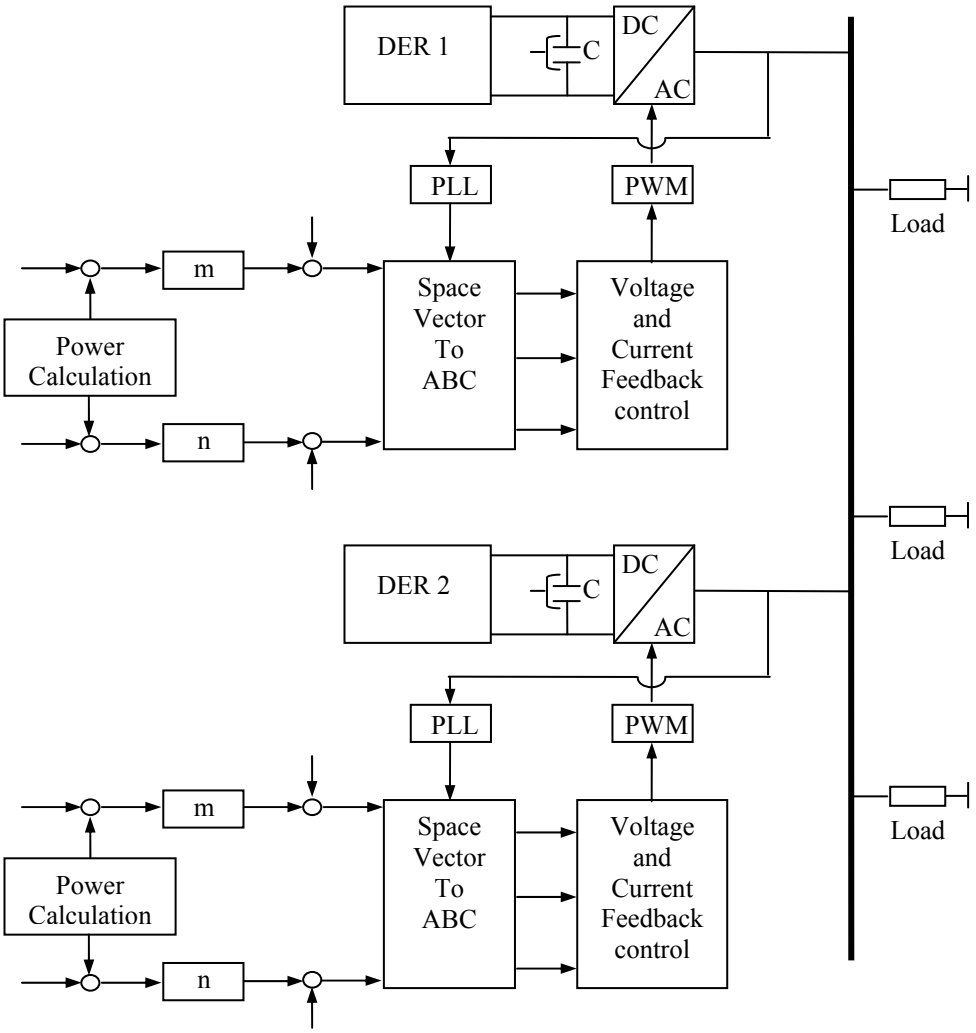

Figure I.18: The droop control [53]

The main advantages and drawbacks [55]–[57] of the conventional droop method are presented as follows [58].

Advantages of the conventional droop control	**Disadvantages of the conventional droop control**
- Avoid of communications - Great flexibility - High reliability - Free laying - Different power ratings	- Trade-off between voltage regulation and load sharing - Poor harmonic sharing - Coupling inductances - Influence of system impedance - Slow dynamic response - Integration of renewable energies

In order to overcome the main disadvantages of the conventional droop method, the variations of this method were addressed in some literature. Each drawback can be solved with some variation methods as follows [58]:

- *Trade-off between voltage regulation and load sharing:*

  Restoration controls [57], [59]
  Dynamic slopes [60], [61]
  High gain angle droop control instead of frequency droop control [62]

- *Harmonic load sharing*

  Additional loop for the bandwidth [63]
  Virtual impedance [64], [65], [66]
  Cooperative harmonic filtering strategy [67]

- *Coupling inductances*

  Virtual impedance [64]
  Virtual impedance variations [65], [66]

- *Line impedance*

  Additional loop with grid impedance estimation [68]
  Voltage droop coefficients by output active and reactive powers [69]

- *Dynamic response*

  Angle droop [70]
  Adaptive decentralized droop [71]
  Droop based on coupling filter parameters [72]
  Controllable droop slopes [73]

- *Integration of renewable energy resources*

  Non-lineal droop control [74]
  Hybrid MPPT with droop control [75]

I.3. **Objective of the thesis**

The aim of this thesis is to present optimal configuration and control strategies to ensure secure, reliable and efficient operation of a microgrid including photovoltaic productions (PV), battery energy storage system (BESS) and/or diesels. In this thesis, the optimal sizing, control and energy management of microgrid are proposed in both modes: island and grid connected modes. The objectives of this thesis are described as follows:

- Optimal sizing of a microgrid is designed to find the minimum cost considering the optimization of the operating conditions with highest reliability and lowest emission

- Optimizing the power sharing among DERs, the cost of fuel and emission for island microgrid

- Optimizing the cost of production, the exchanged power between the microgrid with the main grid and the power allocation among DERs

- Controlling the microgrid voltage and frequency in the island mode and transition from grid connected mode to island mode.

I.4. **Thesis contributions**

The main contributions of this thesis can be listed as follows:

- The thesis proposes a method to optimize the sizing of a microgrid. The iterative optimization technique has been used to follow the renewable energy fractions (FR), the excess energy ratio (EER) and the annual cost of system (ACS) considering the CO_2 emission

- The thesis proposes a method to optimize the energy management in operation of a microgrid with its configuration achieved from the above part. Dynamic programming (DP) method is used to find the minimum fuel cost considering the emissions in an island microgrid as well as to minimize the cash flows and the exchanged power with the main grid in a grid-connected mode. The balance of power between supply and load demand in each time interval and the limitations of each DER and microgrid operations are given as the constraints.

- The thesis proposes voltage and frequency control strategies for an island microgrid by using droop control methods

- The thesis further proposes intelligent voltage and frequency control strategies by using fuzzy logic to adaptively adjust the droop control. By this way, the frequency is expressed not only as the function of active power (in the above strategy) but also the state of charge of BESS and initial operation conditions.

I.5. **Thesis organization**

This thesis comprises seven chapters. Contents of each chapter are briefly described as follows:

- Chapter I: introduces the context, the literature review, the thesis objective, the thesis contribution and the thesis outline.

- Chapter II: presents the microgrid concept with the definition of microgrid, the microgrid operation, the microgrid control and the microgrid protection.

- Chapter III: brings out the modeling of the microgrid components: Photovoltaic productions (PV), battery energy storage systems, diesels and loads.

- Chapter IV: proposes the optimal sizing for two types of the microgrid: island microgrid and grid-connected microgrid.

- Chapter V: presents the optimal energy management for the island and the grid connected microgrid

- Chapter VI: introduces the microgrid control. The voltage and frequency control strategy by using classical droop control for an island microgrid is presented in the first part. In the second part, an intelligent control strategy (fuzzy logic control) is proposed for the island mode and transition from the grid connected to the island mode.

- Chapter VII: contains the conclusion and future works.

CHAPTER II :

Microgrid concept

SUMMARY

II.1. **Definition of microgrid**

Currently, there are a lot of microgrid definitions presented in various reports by researching organizations in all over world. Some descriptions of microgrid are shown as follows:

The U. S. Department of Energy (DOE) has provided the following definition of Microgrids in [76]:

"A Microgrid, a local energy network, offers integration of distributed energy resources (DER) with local elastic loads, which can operate in parallel with the grid or in an intentional island mode to provide a customized level of high reliability and resilience to grid disturbances. This advanced, integrated distribution system addresses the need for application in locations with electric supply and/or delivery constraints, in remote sites, and for protection of critical loads and economically sensitive development. (Myles, et al. 2011)"

The Congressional Research Service (CRS) presents a Microgrid definition in [77]. It has a slight difference with the above description:

"A Microgrid is any small or local electric power system that is independent of the bulk electric power network. For example, it can be a combined heat and power system based on a natural gas combustion engine (which cogenerates electricity and hot water or steam from water used to cool the natural gas turbine), or diesel generators, renewable energy, or fuel cells. A Microgrid can be used to serve the electricity needs of data centers, colleges, hospitals, factories, military bases, or entire communities (i.e., "village power"). (Campbell 2012)"

The definition from the EU research projects [78], [79] is provided as follows:

"Microgrids comprise LV distribution systems with distributed energy resources (DER) (microturbines, fuel cells, PV, etc.) together with storage devices (flywheels, energy capacitors and batteries) and flexible loads. Such systems can be operated in a non-

autonomous way, if interconnected to the grid, or in an autonomous way, if disconnected from the main grid. The operation of microsources in the network can provide distinct benefits to the overall system performance, if managed and coordinated efficiently"

From these definitions, the features of a microgrid include:

- Microgrid is an integration of microsources, storage units and controllable loads located in a local distribution grid.

- A microgrid can operate in grid-connected or disconnected modes

- The energy management and coordination control between available microsources are demonstrated in a microgrid,

II.2. **Microgrid structure and components**

A microgrid includes distributed energy resource (DER) (photovoltaics, small wind turbines, fuel cells, internal combustion engines, microturbines, etc.), distributed energy storage devices (flywheels, superconductor inductors, batteries, etc.), and loads. DERs can be divided into two main groups: (i) DER directed-coupled conventional rotating machines (e.g., an induction generator driven by a fixed-speed wind turbine), and (ii) DER grid-coupled with the inverter (e.g. Photovoltaic, fuel cells, etc.). Distributed energy storage devices can be charged with the power excess and discharge to cover the power deficit. Thus, they help to enhance the reliability of microgrid as well as making it efficient and economical. Furthermore, energy storage is known as fast response devices. Therefore, they also prevent transient instability and participate to control the voltage and the frequency of the microgrid by providing the balance reserve ranging from short time.

The diagram of a microgrid which includes many systems: PV, a variable-speed wind generator, fuel cell, microturbine and a battery energy storage system is shown in Figure II.1. Each distributed energy resource is interfaced with its corresponding bus through a power-electronic converter. The microgrid is connected to the upstream network at the Point of common coupling (PCC). The power is furnished from a Low-voltage (LV) transmission grid, through a substation transformer. The microgrid operates with two modes: the grid-connected mode and the islanded mode. In the grid-connected mode, the PCC is closed and the microgrid is connected with the main grid. It leads that the microgrid can exchange energy with the main grid. When the upstream network occurs the

disturbance or the microgrid gets the optimal operation state, the switch at PCC can be opened to disconnect the microgrid. Thus, the microgrid can continue to operate in the so-called islanded mode.

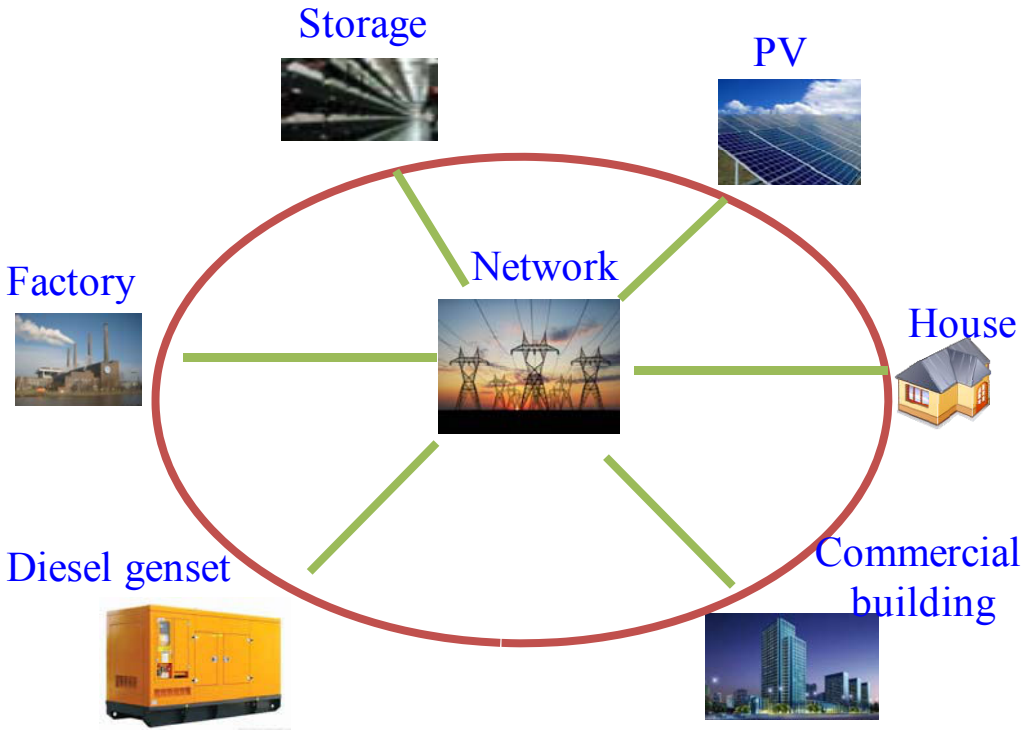

Figure II.1: A studied Microgrid structure

II.3. **Microgrid operation**

Two operation modes of microgrid can be defined as follows [80]:

• Grid-connected Mode: the microgrid (MG) is connected to the upstream network. The MG can receive totally or partially the energy by the main grid (depending on the power sharing). On the other hand, the power excess can be sent to the main grid (when the total production exceeds consumption).

• Island Mode: when the upstream network has a failure, or there are some planned actions (for example, in order to perform maintenance actions), the MG can smoothly move to islanded operation. Thus, the MG operate autonomously, is called island mode, in a similar way to the electric power systems of the physical islands.

Furthermore, the operation of the microgrid may depend on conflicting interests among different stakeholders involved in electricity supply, such as system/network operators, DG owners, DER operators, energy suppliers, and so on, as well as customers or regulatory bodies. Optimal operation of microgrid is based on economic, technical, or environmental aspects [1], [79].

The microgrid operation strategies are presented in Figure II.2 [79]

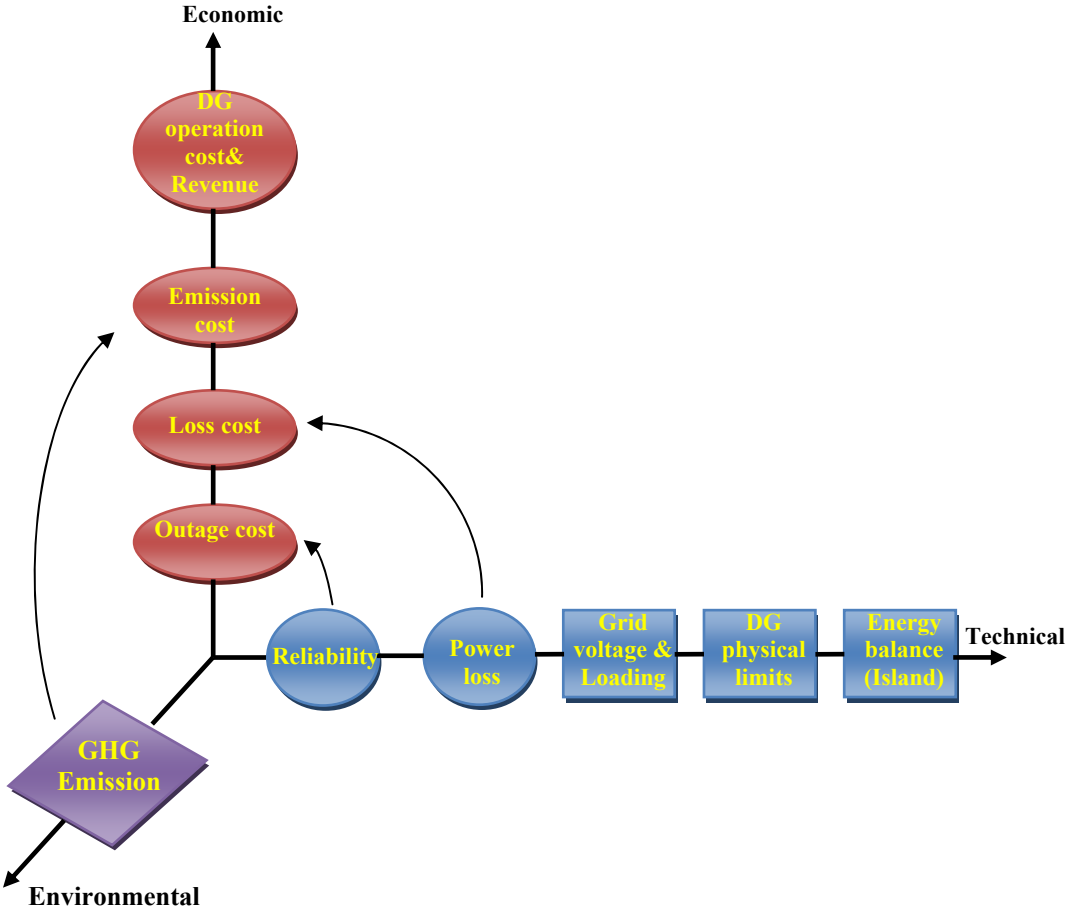

Figure II.2: The microgrid operation strategies

There are four operational options as follows:

- Economic option
- Technical option
- Environmental option
- Combined objective option.

*** The economic option**

In the economic option, the objective function is to minimize total costs of DER operation and Revenue. This option assumes lost cost and emission obligations. The constraints are expressed as the physical constraints of DER and energy balance. The economic mode of microgrid operation is shown in Figure II.3 [79]

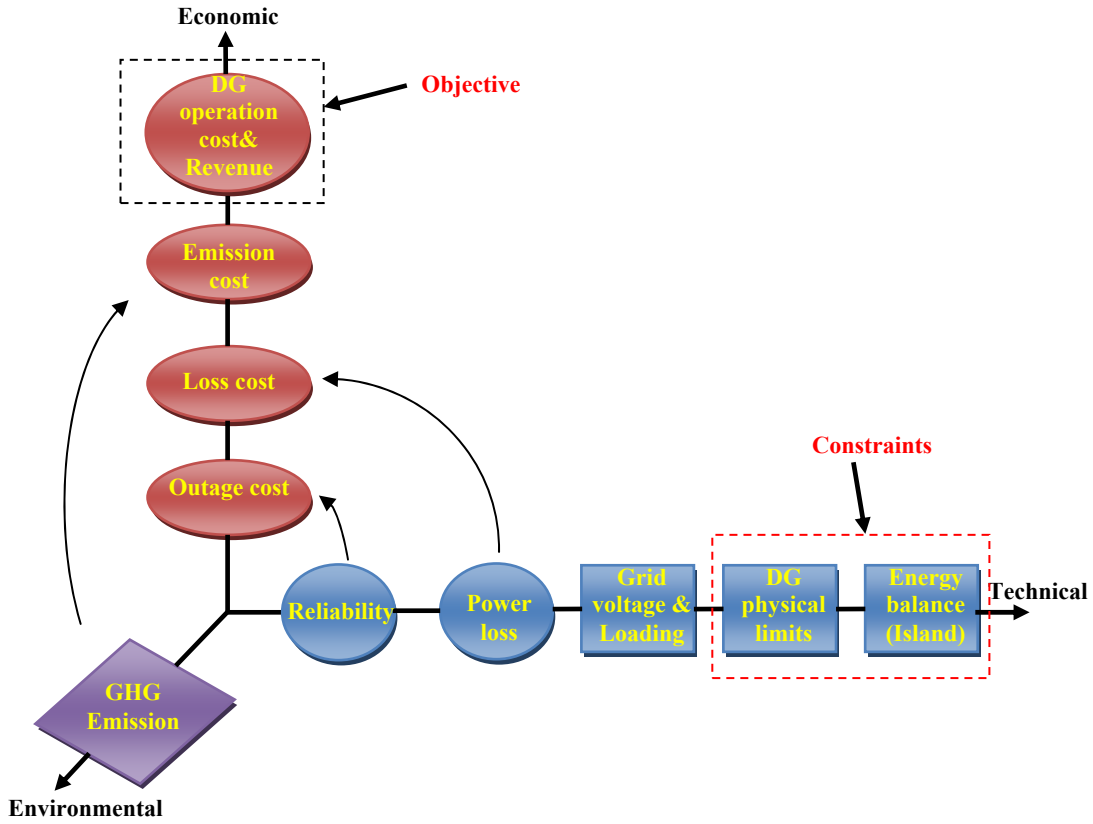

Figure II.3: The economic mode of microgrid operation

*** The technical option**

The technical mode of microgrid operation is presented in Figure II.4. The power loss is demonstrated as the objective function. The voltage variation and device loading, DER physical limits and energy balance are the constraints.

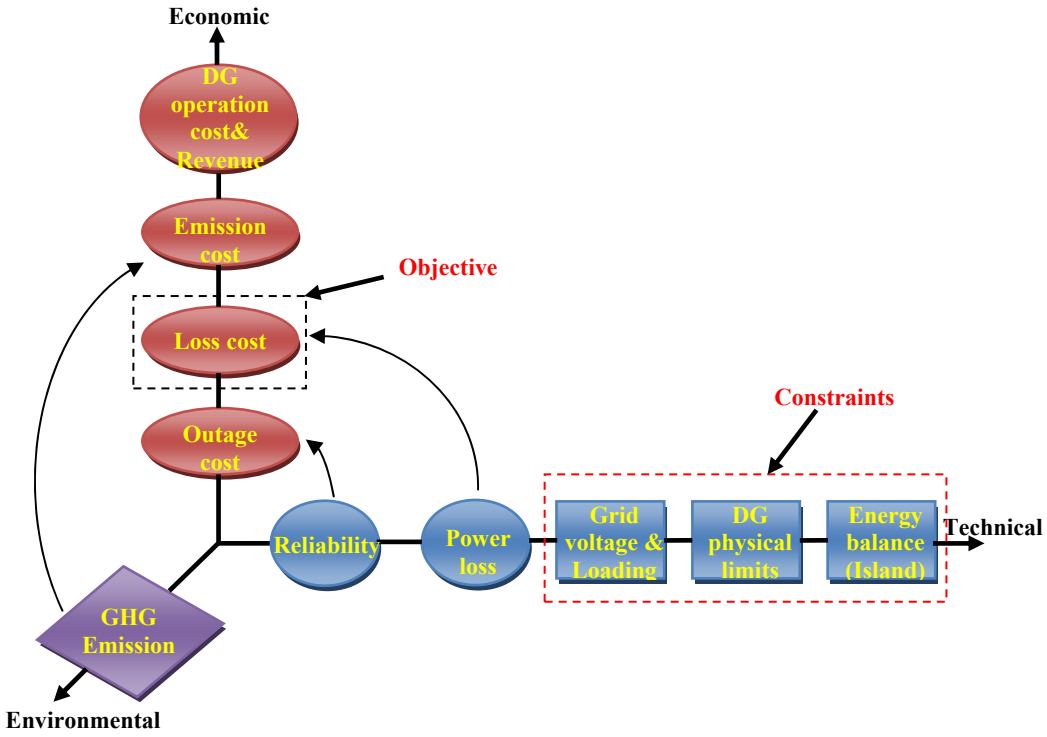

Figure II.4: The technical mode of microgrid operation

*The environmental option

The environmental mode of MG operation is shown in Figure II.5.

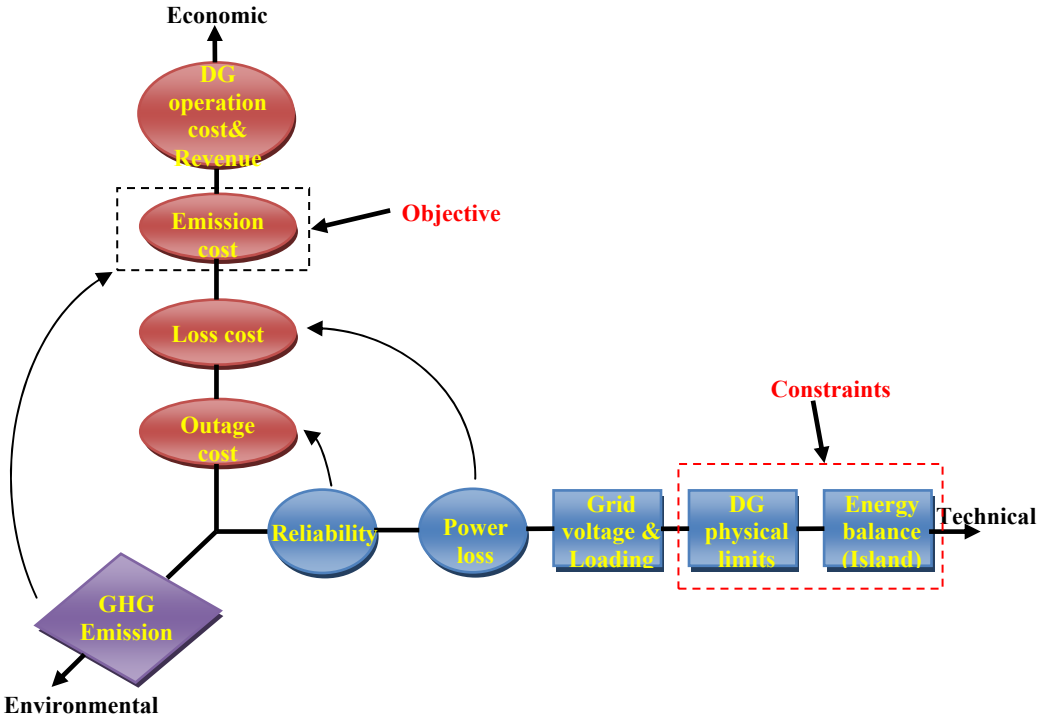

Figure II.5: The environmental mode of microgrid operation

The DER units with lower specific emission levels will be the target of choice which does not consider the financial or technical aspects. The emission cost is given as the objective of this option.

***The combined option**

The combined option solves a multi-objective problem to satisfy all of the economic, technical and environmental aspects. The objective function includes the economic and the economic equivalents of the technical and environmental, considering constraints from the voltage variation and loading, DER physical limits and the balance energy. The combine mode of microgrid operation is shown in Figure II.6.

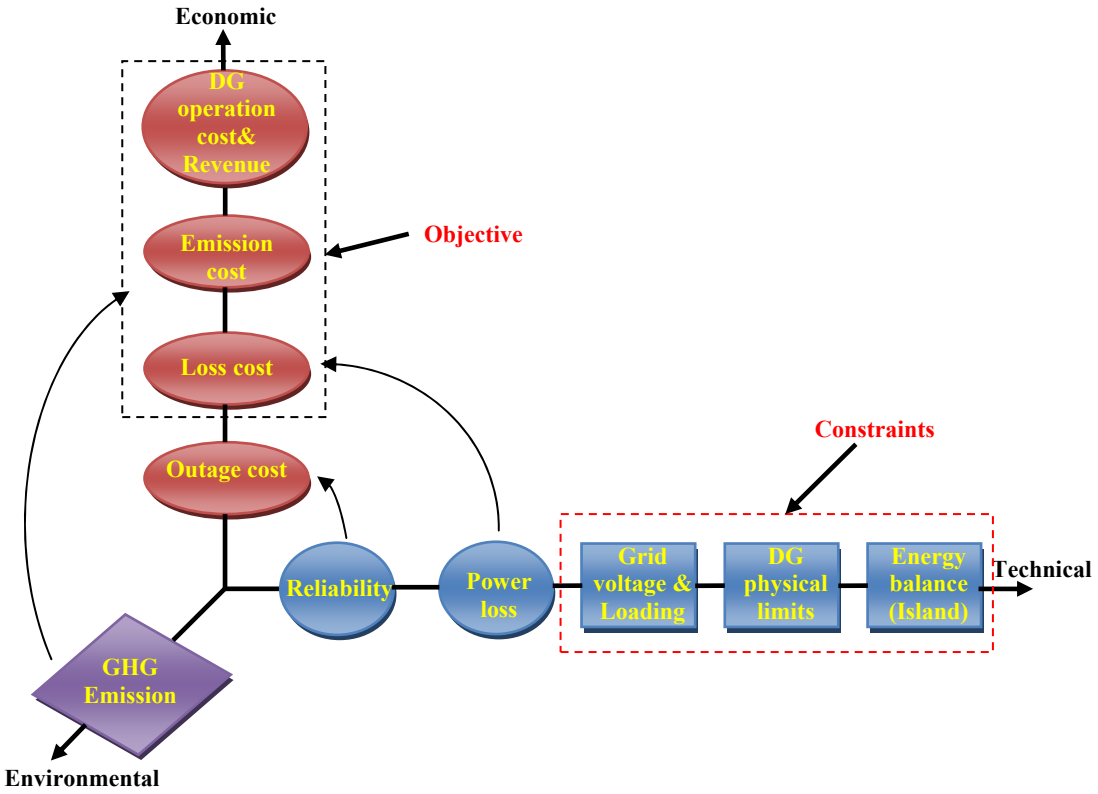

Figure II.6: The combined objective mode of microgrid operation

II.4. **Microgrid control**

The basic principle of the microgrid control is presented in this part. The details of microgrid control will be illustrated in chapters V, VI.

The typical microgrid control structure is described in Figure II.7.

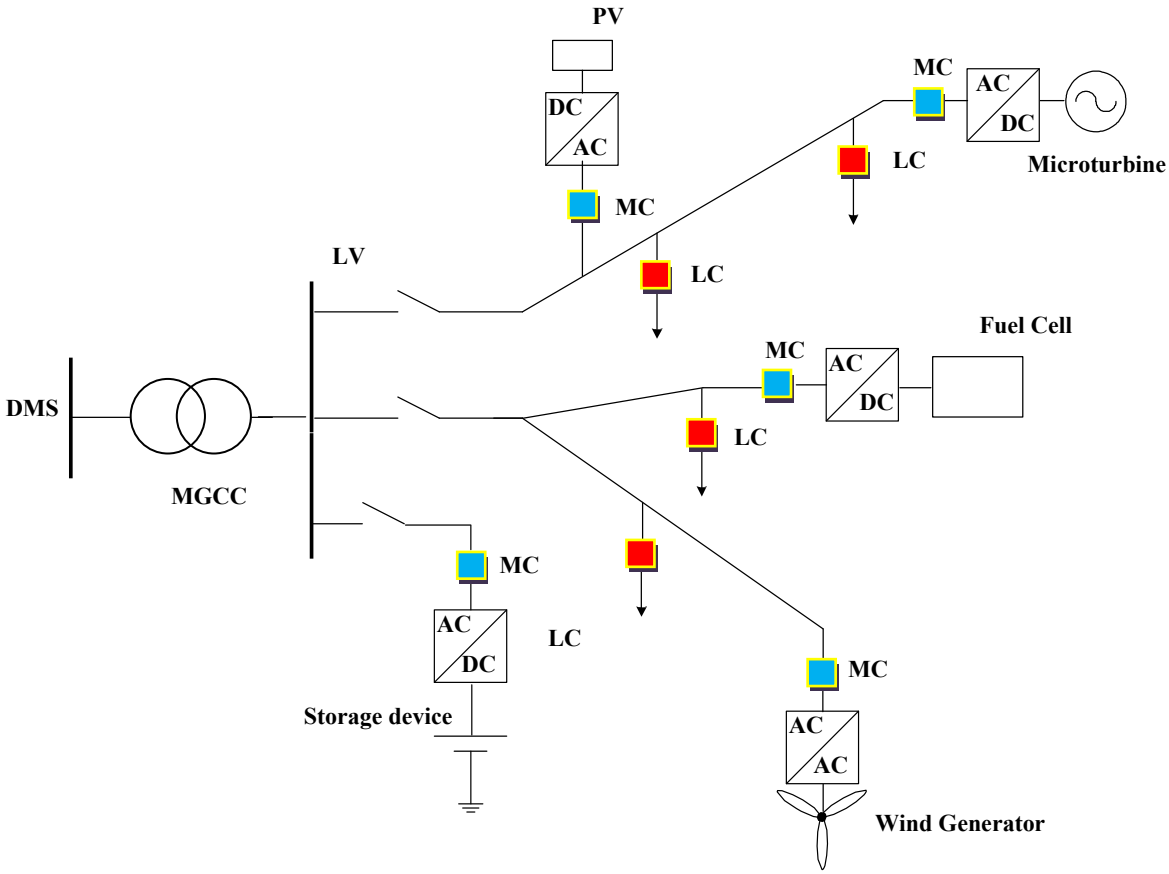

Figure II.7: The typical microgrid control structure

A microgrid control includes:

- Micro Source Controllers (MC) and Load Controllers (LC)
- MicroGrid System Central Controller (MGCC)
- Distribution Management System (DMS).

*** The control functionalities in a microgrid are presented as follows [1]:**

- Distribution management system (DMS)

  - Decision for island/interconnected mode
  - Market participate
  - Upstream coordination

- Central controller functions (MGCC):

  - Secondary voltage/ frequency control
  - Secondary active/ reactive power control

- Load consumption/shedding
- Black start

- Microsource controller (MC)

- Primary voltage/ frequency control
- Primary active/ reactive power control
- Battery management

The controlling of a microgrid will be focused on this thesis. Thus, the DMS will be not presented on this thesis.

- Microsource controller (MC)

MC plays controlling and monitoring distributed energy resources, storage devices and loads, including electrical vehicles. The power electronic interface of the micro source is used for the microgrid source controller. The local information is measured for controlling the voltage and the frequency of the microgrid. The basic configuration of the microsource is shown in Figure II.8 [79]. It includes:

- The Microsource (PV, fuel cell, microturbine, etc).
- A DC-link (capacitor C), which connects the MS to the DC-AC inverter (grid-side inverter);
- A low-pass LC filter, which cancels out high order harmonics;
- A coupling inductance.

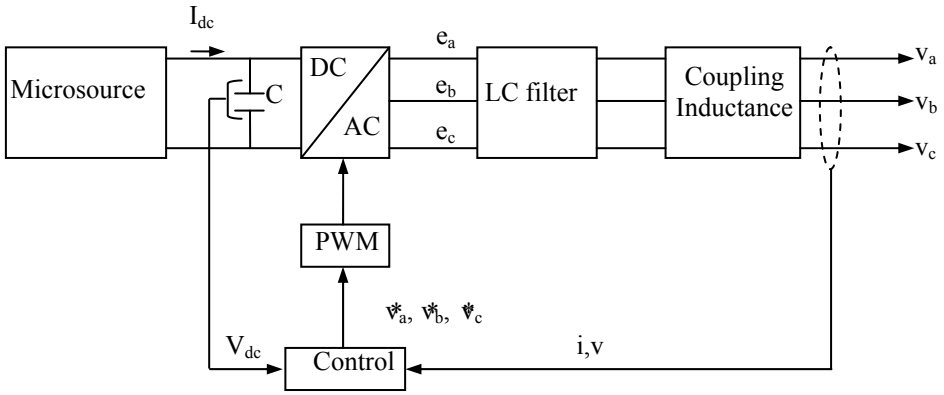

Figure II.8: The basic configuration of the microsource

In Figure II.9, the complete control of the microsource is presented [81]. The inputs are either measurements (like the voltages and currents) or set-points (for nominal voltage,

power and the nominal grid frequency). The outputs are the gate pulses. The inverter voltage and current are measured. Then two blocks are used to calculate instantaneous active and reactive power injected by the inverter. After that the signals is transferred through low-pass filter to prevent the higher order harmonic. Following, the active-frequency droop and the reactive-voltage blocks are used to determine the frequency and voltage. The voltage is calculated from the stationary frame components of the filtered instantaneous voltages. The desired and measured voltage values are compared in the voltage control block. The output is given as the desired voltage magnitude to be implemented by the gate pulse generator block.

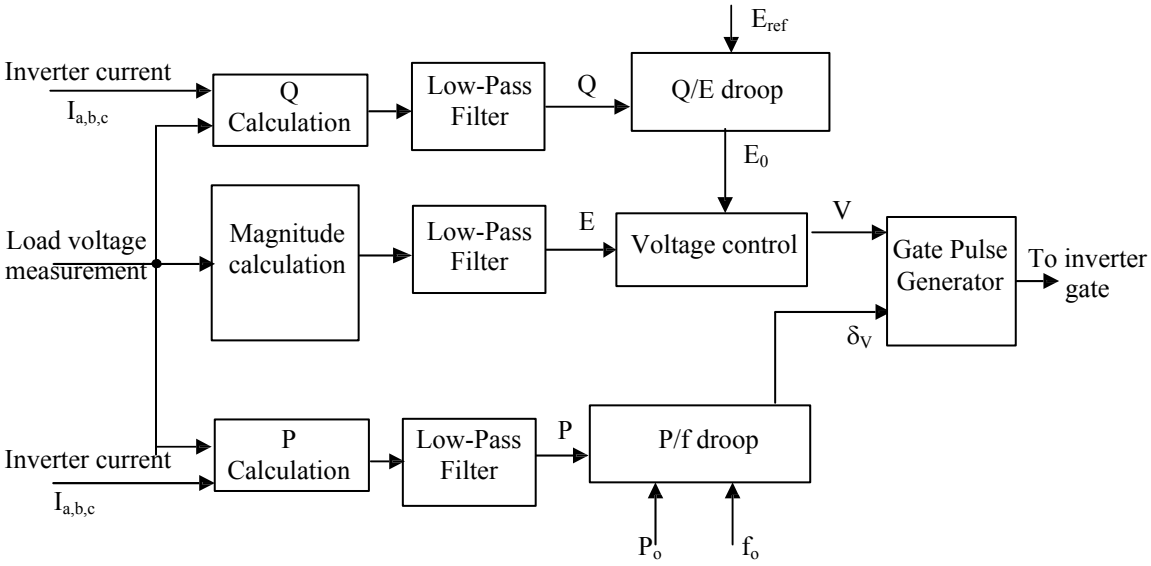

Figure II.9: The complete control of the microsource

- The microgrid central controller (MGCC):

The microgrid central controller (MGCC) plays an important role in microgrid control. In fact, it provides the main interface between microgrid and other actors. In addition, the MGCC will response depending on the different roles for entire microgrid or local MCs from difficult to simple. For example, it can provide set-points for the MCs or simply monitor or supervise their operation [1]. A microgrid can be operated in a centralized or decentralized way.

a) Centralized control

In the centralized control, the MGCC responsibilities are the maximization of using microgrid value and the optimization of its operation. From the taken information such as:

price of electricity, gas costs as well as ancillary service and grid security, the MGCC calculate the power exchange with grid and optimizing local production or consumption capabilities. The principle of centralized control is shown in Figure II.10 [1].

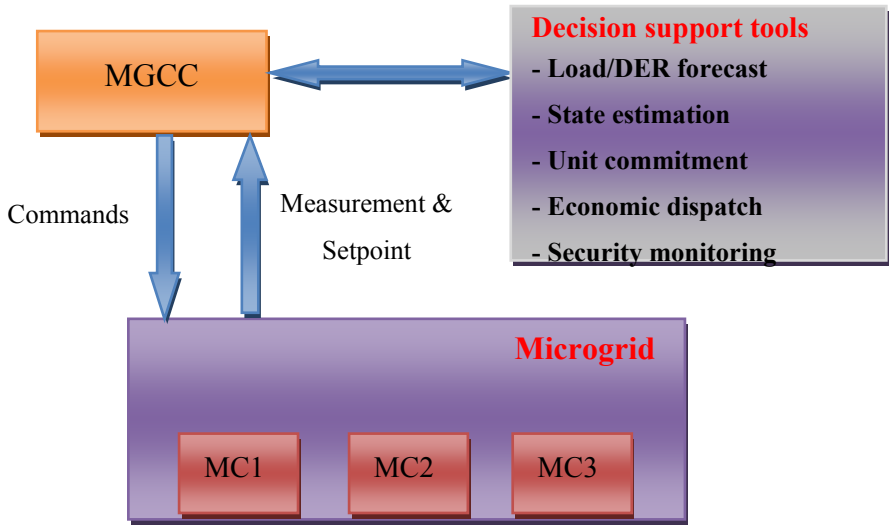

Figure II.10: the principle of centralized control [1]

The optimization problem is formulated differently according to the market policies assumed. Two possible operation policies are presented. In the policy I, a microgrid is disconnected from the main grid and operates in a stand-alone mode or an island microgrid. On the other hand, in the Policy II, a microgrid is connected to the main grid and is exchanged power with the main grid in [1].

- Market Policy 1

According to the market prices and the production costs, the MGCC tries to meet the active power demand by using its local production as much as possible without exporting power to the main grid.

In this case, in [1], MGCC is provided with:

+ The market prices active and reactive power

+ The active and reactive power demand

+ The micro-generators bids

+ The demand bids (if the demand side is considered)

$$\text{cost} = \sum_{i=1}^{N} \text{active\_ bid } (x_i) + AX + \sum_{j=1}^{L} \text{active\_ bid } (y_i) \qquad \text{(II.1)}$$

where

x_i: the active power production of the i-th DER source.

X: the active power bought from the grid.

N: the number of the DER sources that offer bids for active power production.

A: the price on the open market for active power.

If demand side bid is considered, then y_j refers to the bid of the j^{th} load of the L loads bidding.

The constraints for this optimization problem are:

+ Technical limits of the DER sources, such as the minimum and maximum limits of operation;

+ Active power balance of the microgrid

$$\sum_{i=1}^{N} x_i + X + \sum_{j=1}^{L} y_i = P_{demand} \quad \text{(II.2)}$$

where

P_{demand}: the active power of load demand

- Market Policy 2

The Microgrid participates in the market by buying and selling active and reactive power from/to the grid. It is assumed that the microgrid serves its own needs, but it also participates in the market. The MGCC expect to maximize the value of the microgrid and maximizing the gain from the power exchange with the grid

In this case, in [1], the MGCC is provided with:

+ The market price for buying and selling to the grid (A).

+ The active and reactive power demand

+ The bids of each microsource

+ The maximum capacity allowed to be exchanged with the grid.

The MGCC provides:

+ Set points of the microsources.

+ Active power X and reactive power Y bought from the grid

+ Active and reactive power sold to the grid.

The objective function:

Maximize (Income - Expense)

The MGCC sell energy to answer the consumers of the microgrid and the excess production is sold to the upstream network with the market price. If the load demand exceeds the local production, the energy is bought from the grid and sells to the end-users. Conversely, the X (in equation II.3) is given as zero. The 'income' term is estimated as follow:

$$\text{Income} = A\sum_{i=1}^{N} x_i + A.X \tag{II.3}$$

The term "Expenses" includes: the costs for the active power bought from the grid, the DER sources and the relevant costs (if demand side bid is considered). The 'Expenses' is estimated as follow:

$$\text{Expenses}=\sum_{i=1}^{N} \text{active\_ bid } (x_i) + AX + \sum_{j=1}^{L} \text{active\_ bid } (y_i) \tag{II.4}$$

Thus, the objective function is expressed as follows:

$$\text{Maximize}\left(A\sum_{i=1}^{N} x_i - \sum_{i=1}^{N} \text{active\_ bid } (x_i) - \sum_{j=1}^{L} \text{active\_ bid } (y_i) \right) \tag{II.5}$$

The constraints for this optimization problem are:

+ Technical limits of the DER sources,

+ At least the active power of the microgrid

$$\sum_{i=1}^{N} x_i + X + \sum_{j=1}^{L} y_i \geq P_{demand} \tag{II.6}$$

b) Decentralized control

In the decentralized control, the MCs responsibility is to optimize the microsource, to meet the demand and provide the maximum possible export power to the grid following

the current market prices. In this control, each MC isn't able to achieve the maximum revenue of the corresponding unit; however, the overall performance of the microgrid can be improved. The principle of decentralized control is shown in Figure II.11 [1]

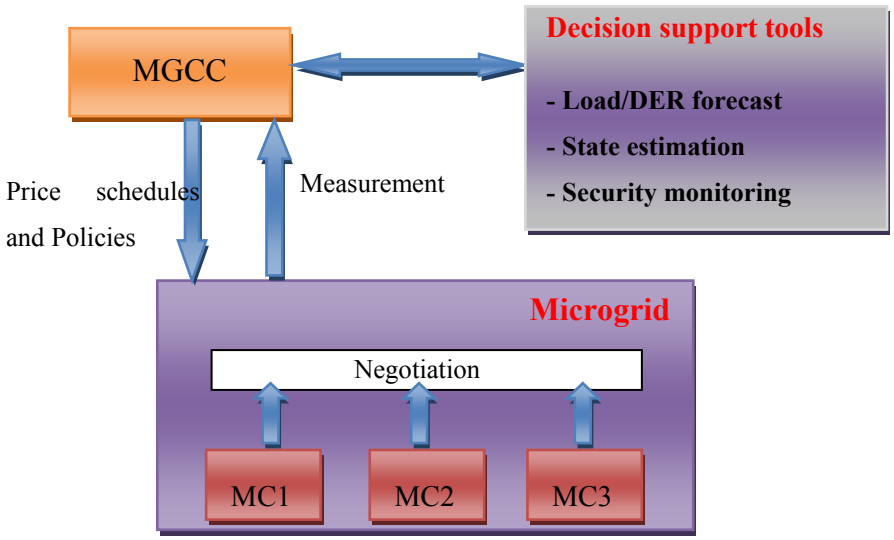

Figure II.11: The principle of decentralized control

The choice between the centralized and decentralized approach for microgrid control, depends on the personnel and equipment. It can be seen that the centralized control is more suitable when the DER and load owners have common goals [1].

II.5. **Microgrid protection**

The microgrid protection must respond when the disturbance occurs in the utility grid system as well as in the microgrid. If the disturbance appears in the utility grid, the protection has to be tripped to disconnect the microgrid with the main grid as rapidly as possible by a fast semiconductor switch called static switch (SS). If the fault is within the microgrid, the protection system isolates the smallest possible section of the distribution feeder to eliminate the fault [1].

In the distribution system, the conventional protection is based on short-circuit current sensing. Directly coupled rotating- machine-based micro sources will increase short-circuit currents. In contrast, the inverter fault currents are limited by the ratings of the silicon devices to around 2p.u. rated current. Fault currents in islanded inverter based microgrids may not have adequate magnitudes to use traditional over-current protection techniques. This possibility requires an expanded protection strategy [82].

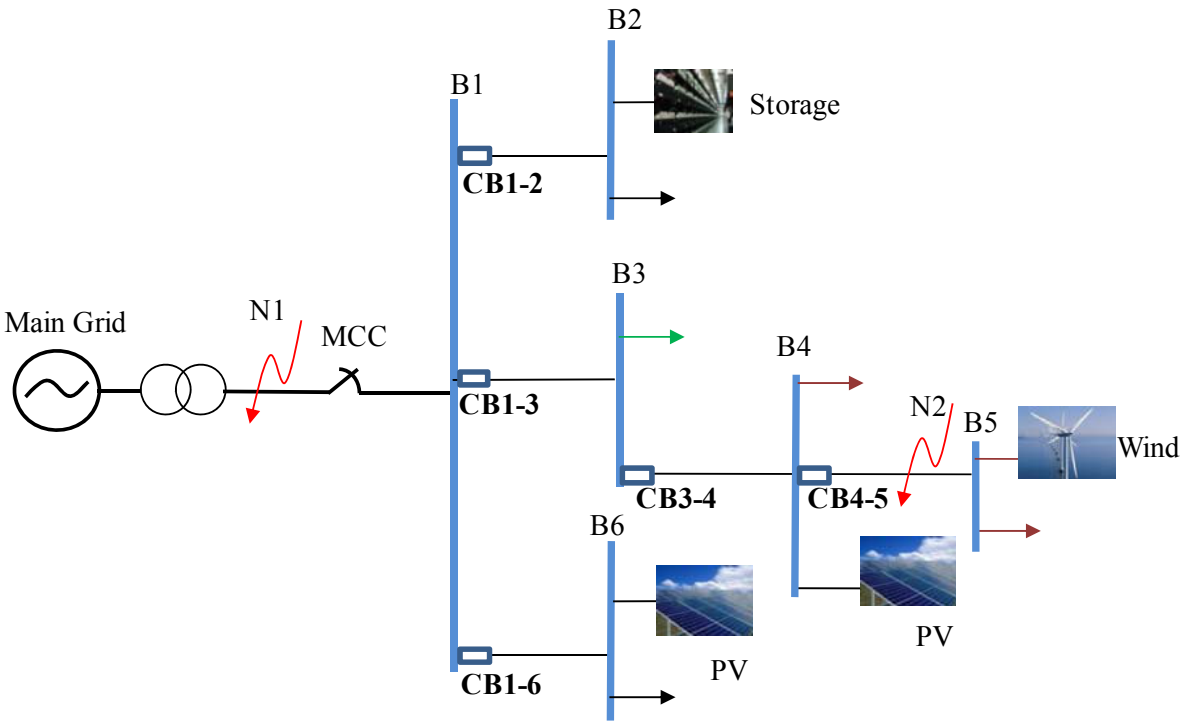

Figure II.12: External and internal fault scenarios in a microgrid

Locating faults quickly and accurately is very important for economy, safety and reliability of power system. In [83]-[84], a fault location algorithm is presented. Figure II.12 describes the external and internal fault scenarios in a simple microgrid. For example, a fault occurs at the N1. This point lies in the utility grid; the static switch at MCC opens to isolate the microgrid with the main grid. After that, the microgrid will operate in the island mode. If the disturbance appears at N2, the circuit breaker CB4-5 would open but the CB 3-4 would not. The source at the bus B5 has to shut down whereas remaining sources still operate.

Currently, the automatic adaptive protection is presented as a new solution, has been addressed in [1]. This change of protection settings depends on the microgrid configuration based on pre-calculated or on real-time calculated settings.

CHAPTER III :

Modeling of the microgrid components

SUMMARY

III.1. Introduction

In this chapter, model of components within a microgrid is illustrated. In each device, one will concentrate on researching the controlling model which is shown in chapter VI. Furthermore, the mathematical model of these components is also designed to apply for optimal sizing of microgrid which is described in chapter IV. In this thesis, the presented microgrid includes the photovoltaic (PV) system, diesel, storage system and load. Thus, the modeling of these components is shown on this chapter.

III.2. Photovoltaic system Modeling

III.2.1. Photovoltaic module

Photovoltaic cells produce DC electricity from the sunlight. Cells are connected together and placed in the supportive material covered by the glass layer known as module. The PV module is connected to the grid or the isolated grid through inverters. Currently, there are three main groups of PV modules and inverters as shown in Figure III.1:

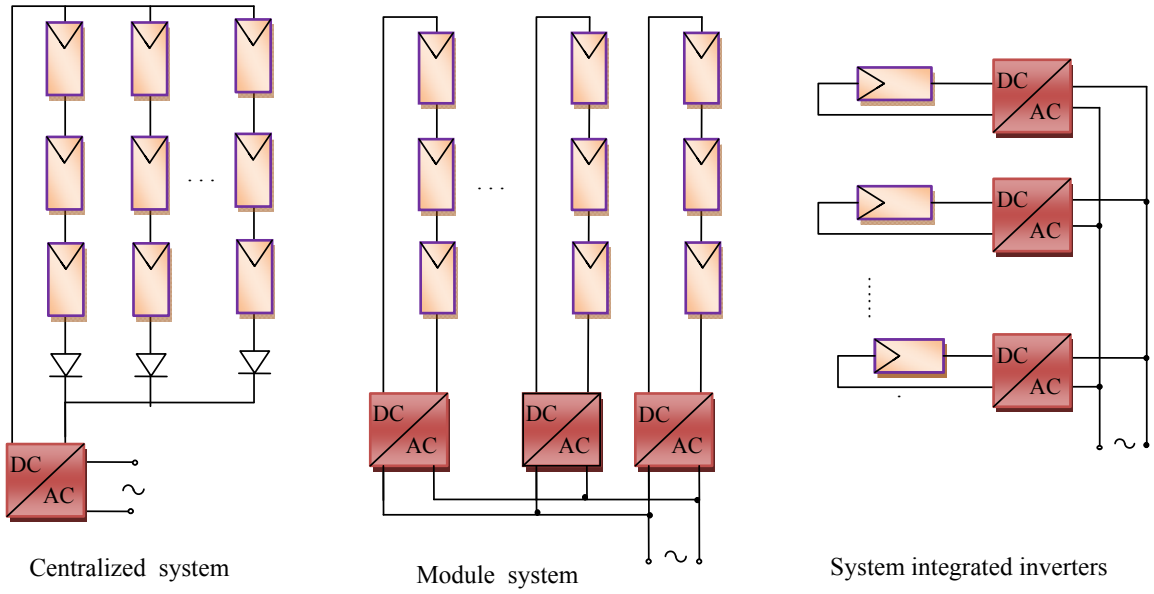

Figure III.1: PV module and inverter

- Centralized system uses a single inverter to transfer the total power. It is useful for small installations

- For modular system, several inverters are connected to a series of PV modules.

- System integrated inverters is useful for PV modules with high power installations.

III.2.2. PV system sizing

The PV sizing is presented in this subsection. This will be used in chapter IV to determine the optimal sizing of microgrid. The PV sizing variables are given as the PV panel number and the amount of string in a PV array.

The required number of PV panels in series is estimated by the number of panels needed to match the bus operation voltage. Thus, the PV panel number in series is calculated as follows:

$$n_{pv\ series} = \frac{U_{bus}}{U_{panel}} \quad \text{(III.1)}$$

where

U_{bus}: the bus operation voltage

$U_{panel:}$ the PV panel voltage

$n_{pv,series}$: the number of PV panel in series

Each PV string includes $n_{pv,series}$ connected in series. In order to match the current requirement of the system, this PV string is needed to be installed in parallel with other strings. The parallel string number is the sizing variable that needs to be optimized.

Because the parallel PV string number $x_{pv,parellel}$ relates with the amount of the available output current from the overall PV array. Thus, when one changes the value of $x_{pv\ parallel}$, the value of the output current is also changed. Therefore, in the optimal sizing system, the parallel PV string number is handled as a variable value to be found through the optimization algorithm. The current output of PV array at time t is calculated as follows [85]:

$$I_{PV,array}(t) = I_{pv,panel}(t, x_{size,type,PV}).x_{pv,parallel}.f_{mm} \quad \text{(III.2)}$$

where

$x_{size,type,PV}$: PV panel size of a certain PV panel type

$I_{pv,panel}(t, x_{size,type,PV})$: the PV panel output current at time t depending on panel type

f_{mm}: mismatch factor

The PV panels number can range from 0 to the highest amount of the PV panels needed when a PV stand alone system can cover the load demand [85]. Thus, $x_{pv,parellel}$ is bounded as follows [85]:

$$0 \leq x_{pv,parallel} \leq \frac{E_{L\_day}}{\eta . W . n_{pv\ series} . Hours_{sunshine/day}} \quad \text{(III.3)}$$

where

η: efficiency loss of conversion,

W: the expected PV panel output power (W).

$Hours_{sunshine/day}$: the average number of estimated sunshine hours per day (h)

The output power of the PV array is calculated as follows:

$$P(t) = I_{pv,panel}(t, x_{size,type,PV}).U_{panel}.n_{pv,series}.x_{pv,parallel}.f_{mm} \quad \text{(III.4)}$$

III.2.3. PV system Modeling

A photovoltaic system is modeled by a current source with its power control. The PV simplifier system model is given as an injected current source with P/Q control. The purpose of this control is to impose the output active and reactive power following the set-point value P_{sp} and Q_{sp}, respectively. In reality, the P_{sp} is determined by the MPPT of PV module and Q_{sp} is zero. The operation of this model is shown in Figure III.2 [86], [87]

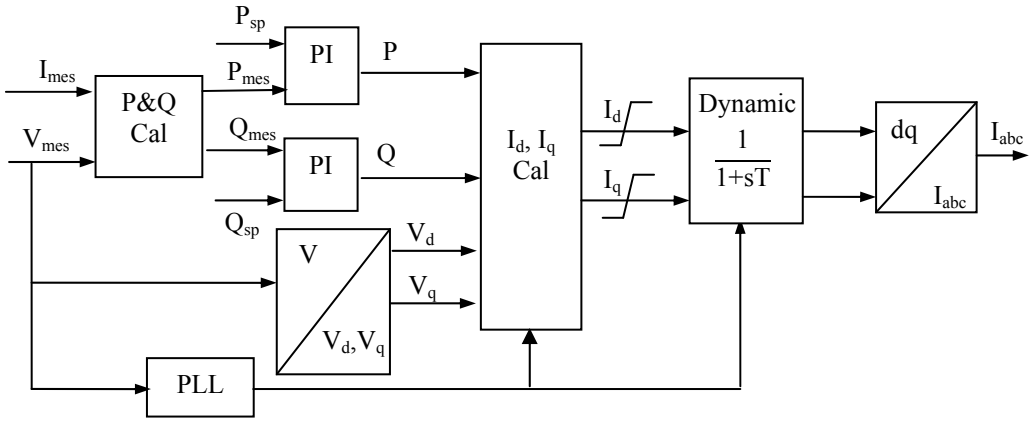

Figure III.2: Photovoltaic system with power electronic interface – P/Q control

- P and Q calculation

The values of active and reactive power use the information of instantaneous values of line to line voltages and line currents. The equations are shown as follow [81]:

$$P_{mes} = V_{bc}i_c - V_{ab}i_a \quad \text{(III.5)}$$

$$Q_{mes} = \frac{V_{bc}(2i_a + i_b) + V_{ca}(2i_b + i_a)}{\sqrt{3}} \quad \text{(III.6)}$$

In [39], the active and reactive power can be calculated following the rotating frame components of voltage and current as follows:

$$P_{mes} = \frac{3}{2}(V_d.I_d + V_q.I_q) \quad \text{(III.7)}$$

$$Q_{mes} = -\frac{3}{2}(V_q.I_d - V_d.I_q) \quad \text{(III.8)}$$

- Voltage magnitude

The voltage is converted from the polar to Cartesian, is presented as follows [81]

$$V_d = \frac{V_c - V_b}{\sqrt{3}} \quad \text{(III.9)}$$

$$V_q = \frac{2}{3}(V_a - \frac{1}{2}V_b - \frac{1}{2}V_c) \quad \text{(III.10)}$$

- The direct and quadratic current calculation

The direct and quadratic currents are calculated as follows:

$$I_d = \frac{2}{3}\frac{(P.V_d + Q.V_q)}{(V_d^2 + V_q^2)} \quad \text{(III.11)}$$

$$I_q = \frac{2}{3}\frac{(P.V_q - Q.V_d)}{(V_d^2 + V_q^2)} \quad \text{(III.12)}$$

- The Proportional Integral (PI) block

Two block Proportional Integral (PI) play a role to regulate the active and reactive power at their reference value. In order to calculate the coefficient k_i and k_p, we have loop

control of active power in Figure III.3

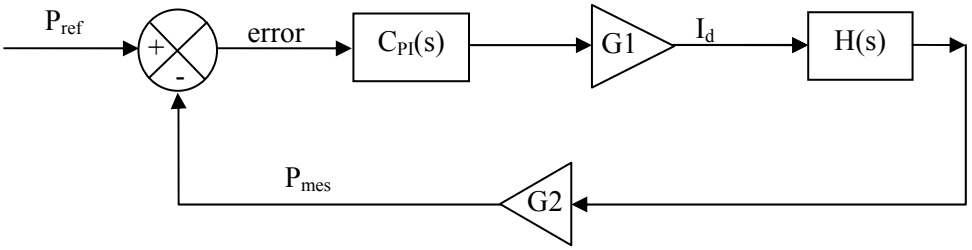

Figure III.3: Control loop for active control

The transfer function G_1 is expressed as follows:

$$G_1=\frac{2}{3.V_d} \tag{III.13}$$

The transfer function G_2 is expressed as follows:

$$G_2=\frac{3}{2}.V_d.I_d \tag{III.14}$$

Equation III.13 and III.14 are rewritten from the equations III.11, III.12, respectively with the $V_q=0$, V_d=constant.

The transfer function $C_{PI}(s)$ of classical PI is expressed as follows:

$$C_{PI}(s)=k_p+\frac{k_i}{s} \tag{III.15}$$

The transfer function H(s) of the dynamic block is given as follows:

$$H(s)=\frac{1}{1+\tau.s} \tag{III.16}$$

The transfer function of the loop control in Figure III.3 is given as two-order transfer function. It is presented as follows:

$$K(s)=\frac{N(s)}{1+\frac{2\xi}{\omega_n}.s+\frac{1}{\omega_n^2}.s^2}=\frac{C_{PI}(s).\,G_1.H(s)}{1+C_{PI}(s).\,G_1.G_2.H(s)}=\frac{G_1.(k_p.s+k_i)}{1+\frac{G_1.G_2.k_p+1}{k_i.G_1.G_2}s+\frac{\tau}{k_i.G_1.G_2}s^2} \tag{III.17}$$

Thus

$$\frac{2\xi}{\omega_n}=\frac{G_1.G_2.k_p+1}{k_i.G_1.G_2} \tag{III.18}$$

and

$$\frac{1}{\omega_n^2}=\frac{\tau}{k_i.G_1.G_2} \tag{III.19}$$

We have $\omega_n=\frac{1}{\tau}$ and $\xi < 1$, the coefficient k_i, k_p are estimated as follows:

$$k_i = \omega_n \quad \text{(III.20)}$$

$$k_p = 2.\xi\text{-}1 \quad \text{(III.21)}$$

Similar to the loop reactive power, the same results are obtained with both the correction coefficients.

III.3. **Electrochemical storage Modeling**

In this thesis, electrochemical storage is used. Therefore in this part the modeling of these storage units will be presented. Currently, six battery types are listed: lead acid, NiCd/NiMH, Li-ion, metal air, sodium sulphur and sodium nickel chloride [88]. This thesis has been performed with lead acid technology. Furthermore, the model is presented corresponding to this type of battery.

III.3.1. Battery Parameters

- *Voltage*

In [89], the batteries voltage is expressed as a function of the SOC; thus it has been considered as linear function. From experimental results carried out at the INES institute, the voltage of batteries in charge and discharge are calculated by (III.22) and (III.23), where "N_{Bat}" is the 12V batteries number connected in series. The experimental results and linear interpolation are presented in Figure III.4

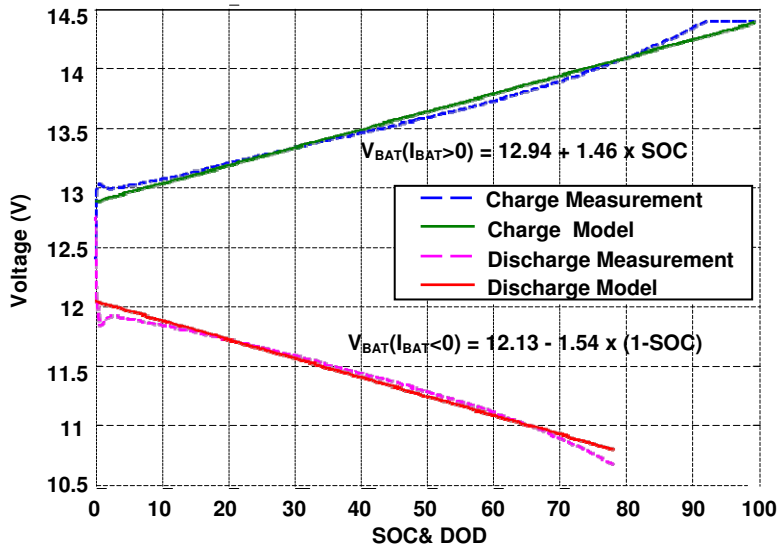

Figure III.4: Experimental measures and linear modeling of the charge and discharge voltage (12-V lead acid battery and I_{BAT} is constant at a rate of 5 h)

- If $I_{BAT} \geq 0$ (Charge or rest)

$$V_{BAT}(t) = (12.94 + 1.46.SOC(t)).\ N_{BAT} \quad \text{(III.22)}$$

- If $I_{BAT} < 0$ (discharge)

$$V_{BAT}(t) = (12.13 - 1.54.(1-SOC(t)))\ .N_{BAT} \quad \text{(III.23)}$$

- *State of charge (SOC)*

The state of charge SOC is calculated in [89], [90], [91]. It takes into account the variation of the quantity of charge in the process which is expressed as a function of the current rates and the ambient temperature [39]. The battery state of charge is estimated as follows

$$SOC = \frac{C(t)}{C_{ref}} \quad \text{(III.24)}$$

where

C_{ref}: the reference capacity.

C(t): the batteries capacity at each instant

The batteries capacity at each time C(t) is calculated as follows [39]:

$$C(t) = Q(t_o) + Q_c(t) + Q_d(t) \quad \text{(III.25)}$$

where

$Q(t_o)$: the initial quantity of charge

$Q_c(t)$: the quantity of charge exchange during the charge

$Q_d(t)$: the quantity of charge exchange during the discharge process

- *State of Health (SOH)*

The State of Health (SOH) of batteries is defined as follows [39]

$$SOH = \frac{C_{ref}(t)}{C_{ref,nom}} \quad \text{(III.26)}$$

where

$C_{ref,nom}$:the nominal capacity of reference available from the manufacturer data

At each step size, the new capacity reference is estimated as follows:

$$C_{ref}(t) = C_{ref}(t-\Delta t) - \Delta C_{ref}(t) \quad \text{(III.27)}$$

In which, the capacity losses is calculated:

$$\Delta C_{ref}(t) = C_{ref,nom}.\ Z\ .(\ SOC(t-\Delta t) - SOC(t)) \quad \text{(III.28)}$$

From the equations III.26, III.27 and III.28, the SOH can be expressed as follows:

$$SOH(t)= \frac{C_{ref}(t-\Delta t)}{C_{ref,nom}} - Z.(SOC(t-\Delta t)- SOC(t)) \quad \text{(III.29)}$$

where

Z: linear ageing coefficients

III.3.2. Battery Interface

The BESS are connected to the grid via power electronics interface which the power can be fed into or taken from the grid directly. In this thesis, the inverter of battery is controlled by a V/f controller. These set-points can be expressed as the voltage reference and frequency reference. The V/f controller of the battery inverter is shown in Figure III.5.

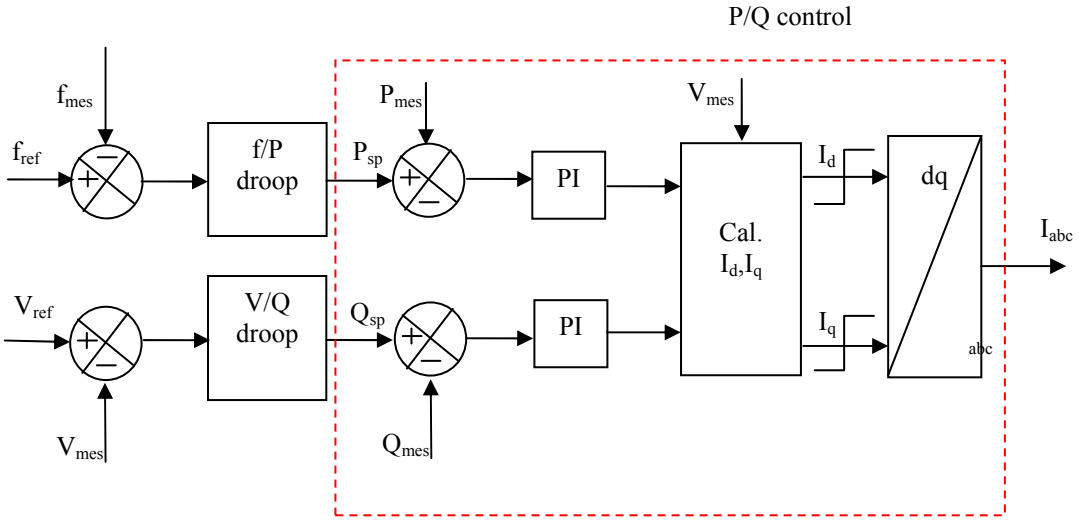

Figure III.5: Battery model with power electronic interface – V/f control

The inverter control block implements the droop characteristics which are determined by the droop constants. The P_{sp} and Q_{sp} are given as the output of the droop control blocks, response to voltage and frequency deviations. This leads to ensure that frequency and voltage remain closed to their set point values. The P_{sp}, Q_{sp} are given as input of P/Q controls presented in the above part.

A simple island microgrid modeling includes PV, BESS and load, is presented in this part. The matlab simulink model of this microgrid is shown in Figure III.6. The simulation is performed to show the performance of the PV, BESS control modeling

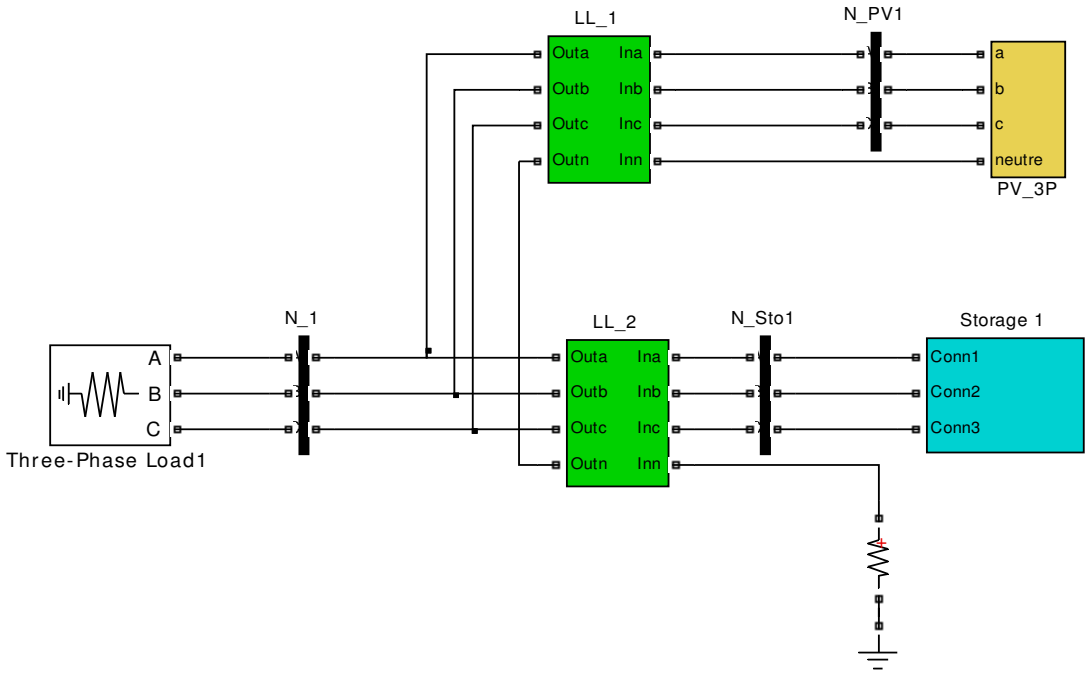

Figure III.6: Matlab simulink model of an example of microgrid

- The hybrid system includes:

  * Three-phase PV productions (bus N_PV1):

    P_PV_3P_1 (max) = 15kW

  * BESS (bus N_Sto1):

    Sto1: P_{max} = 20kW

  * Load:

    Three phase loads (bus N_1): P_{Load} = 15kW

- The simulations are performed with two scenarios:

  * Scenario1: Load variation

  * Scenario2: PV variation

Scenario1: Increasing the loads

In this case, assumed that the PV system (with the P_{PV} = 15kW) initially supplies to the load with P_{load} =15kW. At time t=4s the load increases from 15kW to P_{load} =18kW (increasing 20% of load power).

As can be seen from the Figure III.7, the BESS with the interface V/f control plays a role as a master unit. It discharges the power (3kW) to match the load demand after the consumption suddenly increases to 20%.

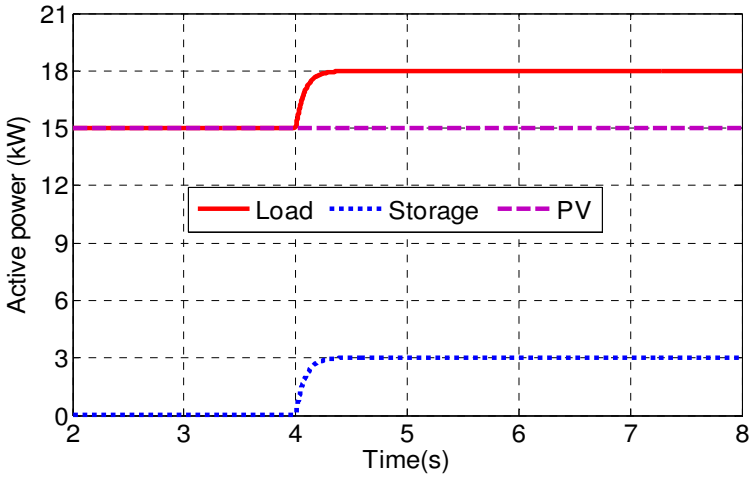

Figure III.7: The variation of active power

The system frequency is shown in Figure III.8. The system frequency drops immediately after the increase of load. Then, the system frequency obtains the new state (it will be explained clearly in chapter VI). After that, the frequency turns back to the nominal value (50Hz).

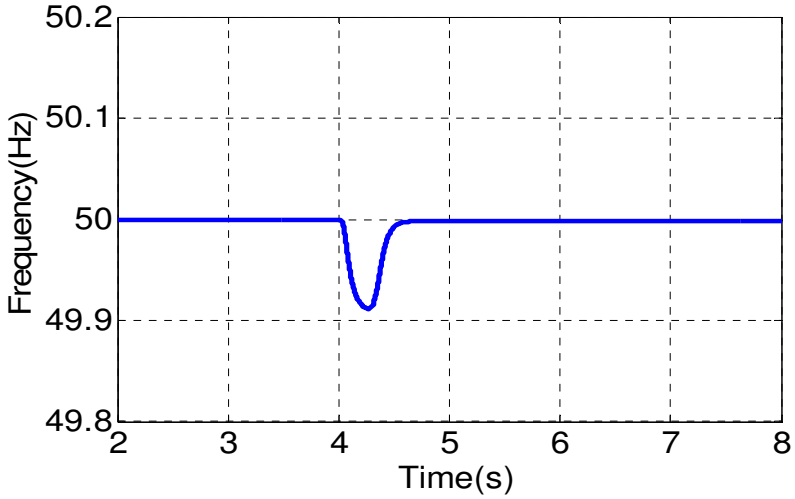

Figure III.8: The system frequency

Scenario2: PV system production variation

In this case, assume that the PV system power is reduced from 100% to 40% and then it increases from 40% to 90%.

* Initial scenario:

- Total load: P_{Load} =15kW
- PV productions: P_{PV} = 15 kW
- BESS: P_{sto_max} = 20kW

- The BESS with initial power equal to zero (or charge or discharge).

* Assumed that

- T = 3s: PV production is reduced from 100% to 40%
- T = 7s: PV production is increased to 90%.

The active power variation of system is shown in Figure III.9. After the PV production is reduced from 100% to 40%, the BESS discharges to maintain the balance between production and consumption. Then, at time t = 7s, PV production is increased to 90%, it leads to increase the frequency. In order to prevent this increase, the BESS have to reduce the discharged power.

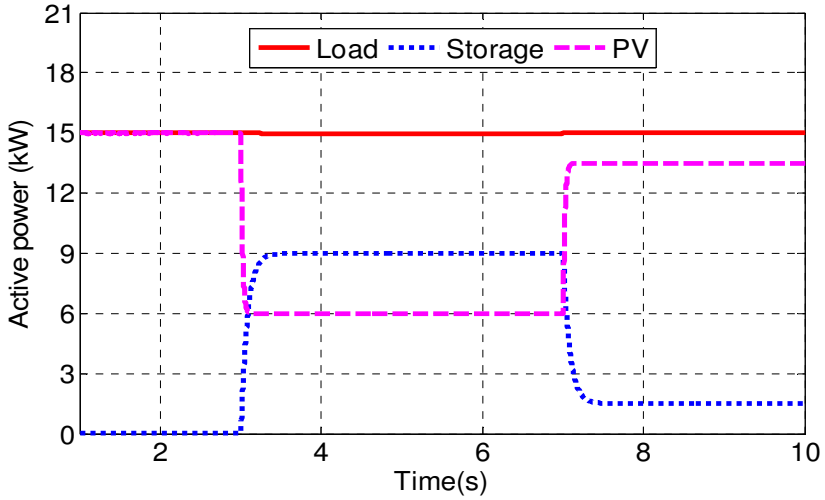

Figure III.9: The active power variation of system

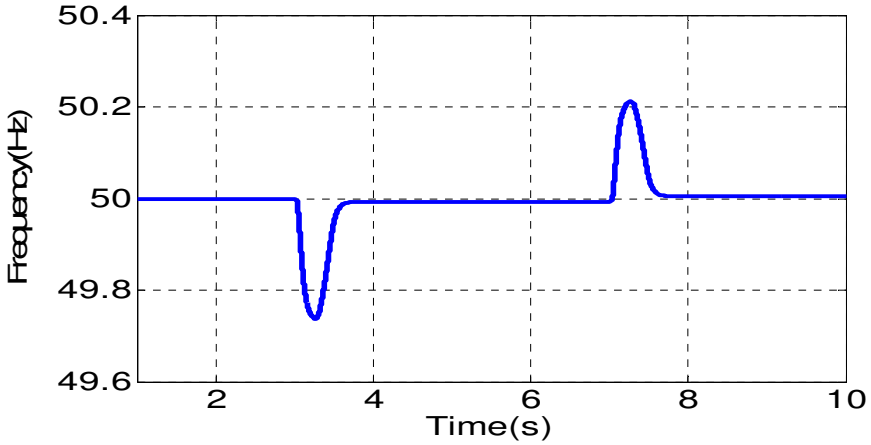

Figure III.10: The frequency of system

As can be seen from Figure III.10, the frequency drops after the PV power reducing. Then the BESS adjusts to bring the frequency back to nominal value (50Hz). After that, when the PV production increases from 40% to 90%, the frequency goes up to the new

value which is higher than nominal value. Finally, the BESS changes the output power to restore the frequency to 50Hz.

III.4. **Diesel Modeling**

A diesel generator (DER) includes of an internal combustion (IC) engine coupled to a synchronous generator. The schematic diagram of DG is shown in Figure III.12 [92].

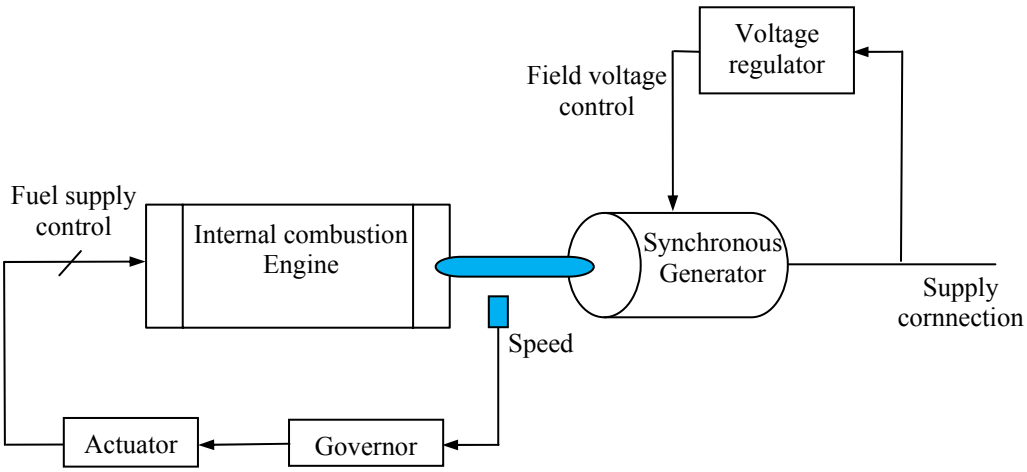

Figure III.11: The schematic diagram of the diesel genset

The IC engine is integrated with a governor to control the output speed of the engine shaft by adjusting the amount of fuel supplied to the engine. A PID controller is used for controlling the governor.

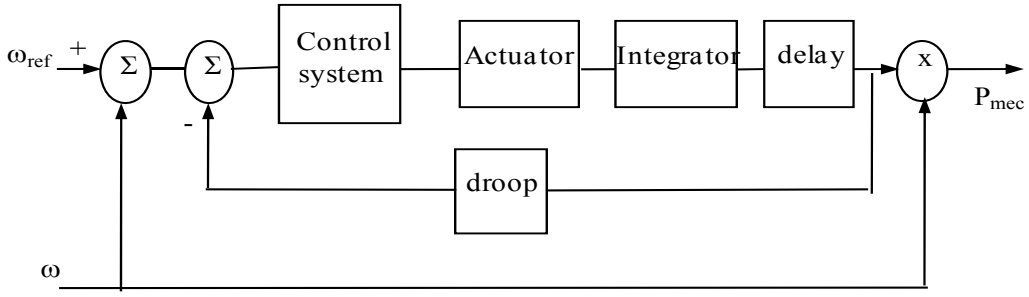

Figure III.12: Block diagram of speed governing system

The synchronous generator is incorporated with an exciter and a voltage regulator. The voltage regulator control maintains the required terminal voltage

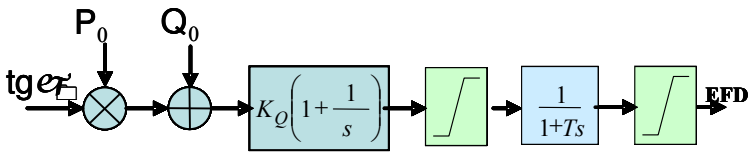

Figure III.13: VAR/PF regulation

Simulation studies of the system, which include a diesel and five loads, are performed to demonstrate the performance of the diesel model. The studied system is presented as follows:

* Diesel Generator: 60kW (rated power)

* Loads

- Total load: P= 40kW; Q=7kVAr
- 3 Single-phase loads (nodes 2, 4 and 6)
- 2-three phase loads (nodes 3, 5).

Figure III.12 presents the studied system model with Matlab/simulink. At t= 4s, a three phase load 7 (P_{L7} =10kW, Q_{L7} =1kVAr) is connected with the system.

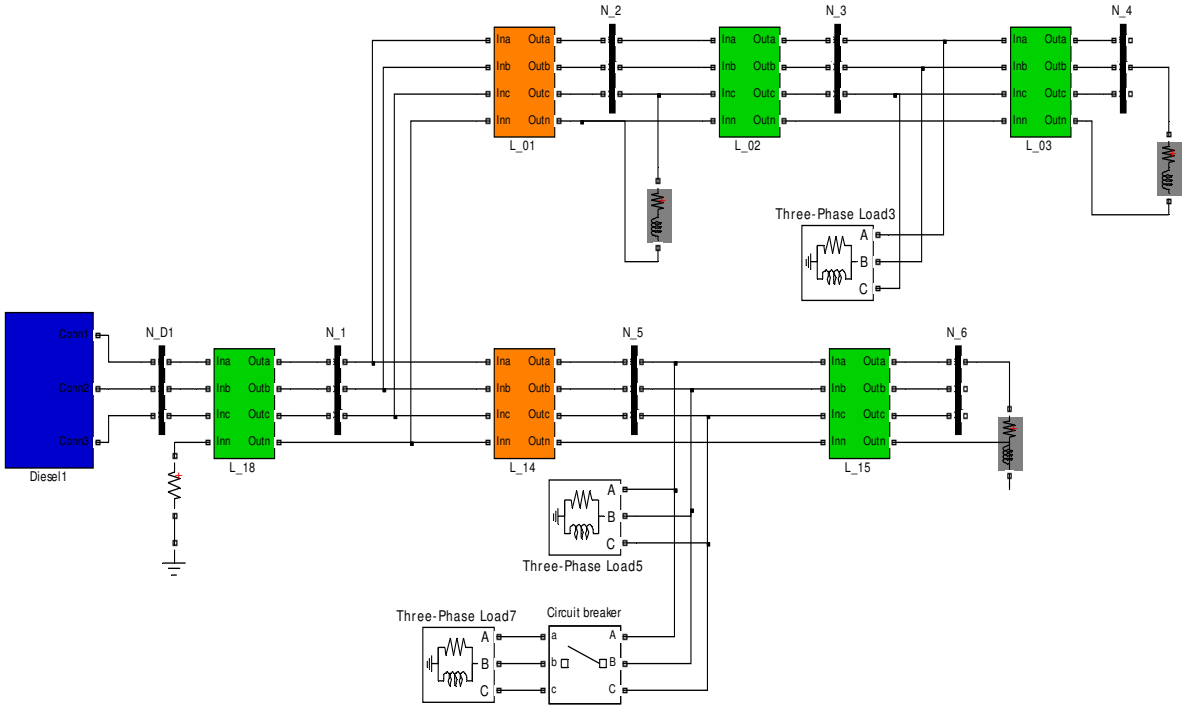

Figure III.14: The studied system model by matlab simulink

In Figure III.13, the active and reactive power variations of diesel are presented. One

can see that the diesel genset changes the power output according to the variation of load demand.

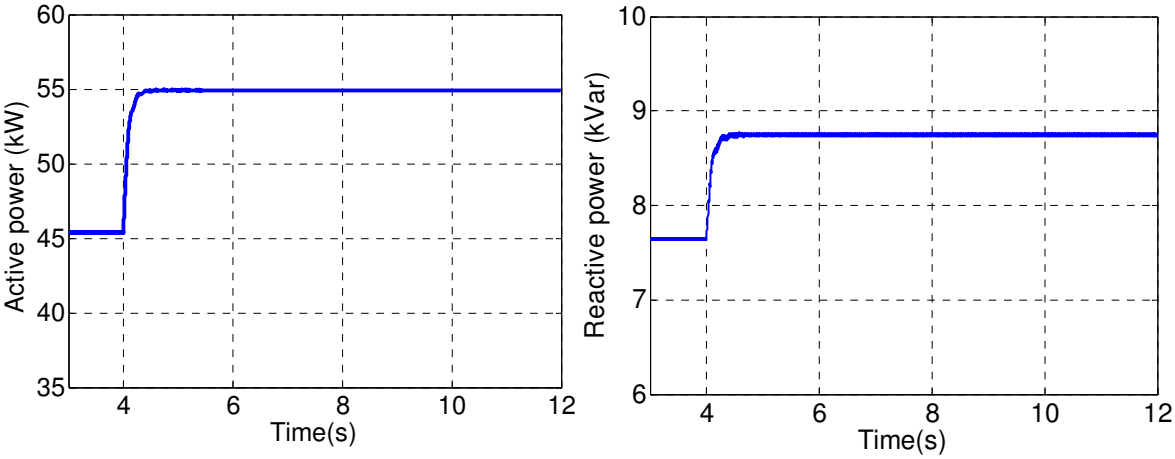

Figure III.15: the active and reactive power variation of diesel

The frequency behavior and voltage variation at bus 3 are shown in Figure III.14. The governor of diesel genset responds to bring the frequency to the nominal value. On the other hand, the voltage at bus 3 is still kept within a permitted limit.

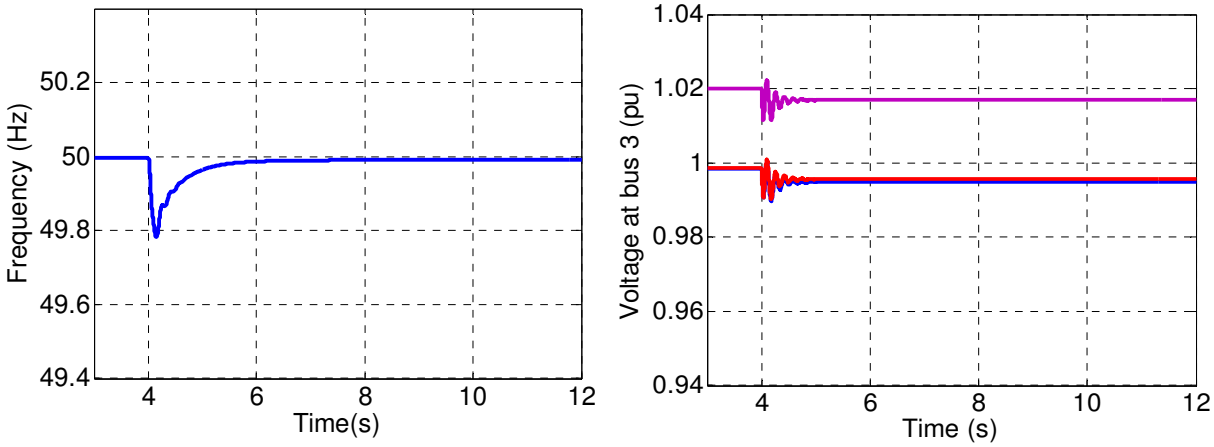

Figure III.16: The frequency behaviour and the voltage at bus 3

- Diesel genset sizing

The diesel should be run at high load levels to maximize fuel efficiency and designed such that it meets the load reliability [85]. Thus, the rated power of diesel generator (P_R) is limited between 0 and the maximum demand which a diesel has to cover. Therefore, the boundary of the diesel general sizing is given by:

$$0 \leq P_R \leq P_{L\_peak} \tag{III.30}$$

where

P_R: The rated power of diesel generator

$P_{L\_peak:}$ The peak loads power.

When the diesel operates to cover the load, it will consume an amount of fuel which is calculated as follows [93]:

$$F(t) = (0.246.\ P_D(t) + 0.08415.\ P_R) \quad \text{(III.31)}$$

where

F(t): the hourly fuel consumption (liter/hour)

$P_D(t)$: the diesel power at time t

From the equation III.31, we can see that the fuel consumption of diesel generator is expressed as a function of the rated power and the generated power. Thus, the diesel generator should not be operated under its minimum value which is given by the manufacturer.

Therefore, the generated power of genset has to be bounded in range as follows

$$P_{Die\_min} \leq P_D(t) \leq P_{Die\_max} \quad \text{(III.32)}$$

III.5. **Load Modeling**

The load modeling is complicated because of the large set of connected devices such as refrigerator, heater,… Thus, it is difficult to estimate the exact load modeling. Furthermore, the load changes depending on many factors such as time, weather conditions, and economy [94]. In [94], the load model can be divided in two types: static model and dynamic model. In static load model, the load is expressed as algebraic function of bus voltage magnitude and frequency at that instant. It can be presented as constant power constant current or constant impedance characteristic. On the other hand, studies of inter-area oscillations, voltage stability and long-term stability require load dynamic modeling such as the motors [94]. In this thesis, the load model is assumed as the active and reactive power constants. The daily load curve in two days which are summer day and winter day, is shown in Figure III.15

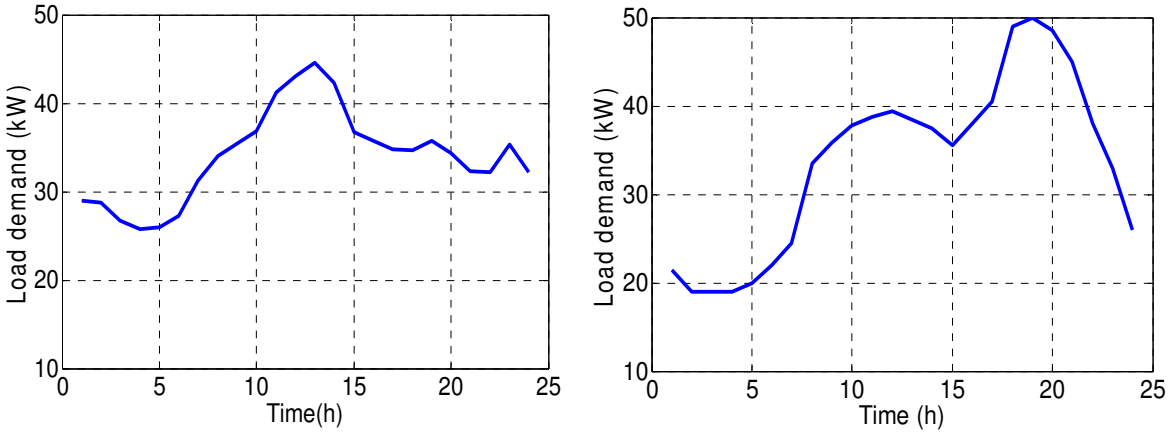

Figure III.17: Daily loads in a summer day and winter day

III.6. **Conclusion**

In order to optimize the sizing and the controlling, the microgrid components are modeled for different investigation purpose. Furthermore, each model has been tested and assessed through simulation results. These developed models will be used in the following chapters.

CHAPTER IV :

Optimal sizing of microgrid

SUMMARY

IV.1. **Introduction**

A microgrid is a small-scale power system with distributed energy resources (DER) such as renewable (photovoltaic system, wind turbines and biomass) and non-renewable (internal combustion engine, micro-turbine and fuel cells) resources with storage. Recently, the increase of fuel price and the development of renewable energy technologies give more opportunities for using the renewable sources in microgrid. However, PV and wind energy are intermittent sources due to the fact that they depend on the weather. Therefore, it is difficult to match production and demand. That makes the sizing process complex in many technical/economics aspects combined with social concerns. The optimization problem concerns not only the components sizing but also the operation strategies. Thus, an optimal sizing of a microgrid necessitates optimizing the whole set of components and energy fluxes control.

The optimal sizing of a microgrid takes into account not only the added value of direct profits but also other issues like power availability, reliability, environmental foot print, power quality, renewable integration and thus for both grid connected /disconnected modes.

In this chapter, optimal sizing of an isolated photovoltaic-diesel-BESS hybrid system (off-grid microgrid) and grid connected PV-BESS (on-grid microgrid) are presented. The iterative optimization technique is used to follow the renewable energy fractions (FR), the excess energy ratio (EER) and the annual cost of system (ACS) considering the CO2 emission. Firstly, based on an iterative simulation, the possible configurations of system are calculated in order to fulfill the desired load system. Then, these configurations are assessed based on FR, EER and the annual cost of the system with respect to low CO_2 value (PV-diesel-BESS hybrid) in order to find the optimum configuration.

IV.2. **Optimal sizing of a microgrid in island mode**

IV.2.1. System configuration

In this section, an island microgrid which includes PV, Diesel and BESS is shown in Figure.IV.1. The diesel generators are connected with AC bus system, which supply directly the load. While the PV and BESS are coupled with the inverter. The gensets can be used as the main source or as a backup (associated or not with BESS) in the case, for

instance, of insufficient PV production. Furthermore, the PV production has to be used with the highest efficiency. Therefore, it is necessary for an operation strategy to find the optimal economic solution for solving this problem. On the other hand, the capacity of BESS has to be large enough to be charged from the power excess and cover the power deficit

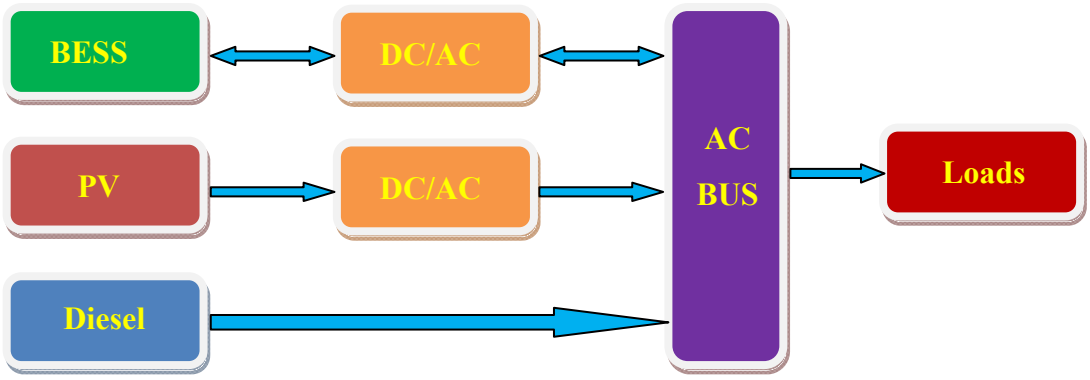

Figure IV.1: The PV-diesel-battery hybrid system

IV.2.2. System components

IV.2.2.a. Photovoltaic model

The optimal sizing of an island microgrid is concerned in this chapter. Therefore, a simple PV model is chosen. The PV output power is expressed as function of the area, solar radiation conditions and its efficiency [95].

$$P_{PV}(t)=\eta.Ap.N_{PV}.E(t) \qquad (IV.1)$$

where

η: the energy conversion efficiency (%)

A_p: the area of single PV panels

N_{PV}: the number of PV panels

E(t) : the solar radiation value.

In this chapter, PV panels are used as Photowatt PW2300-235 (235W). The solar radiation of summer and winter days are shown in Figure IV.2

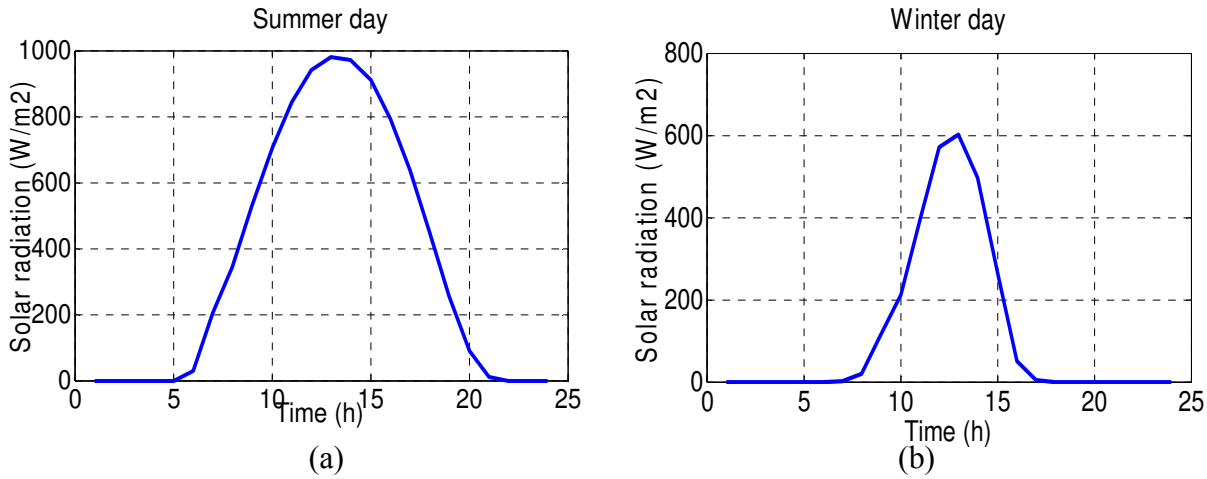

(a) (b)

Figure IV.2: Solar radiation in a summer day (a) and winter day (b)

IV.2.2.b. Diesel generators

The diesel gensets are used to cover the entire load in the case, for instance, of insufficient PV system and BESS production. Diesels are started to meet the load demand and may be shut off whenever the PV and BESS production are sufficient to supply the load. The diesel generators should not be operated when the generated power is below the minimum power recommended by the manufacturer. The operation of diesel genset is bounded as follows:

$$P_{Dmin} \leq P_D(t) \leq P_{Dmax} \qquad \text{(IV.2)}$$

In this chapter, the minimum/maximum power of diesel generators is given:

$$P_{Dmin} = 0.3\ P_R \text{ and } P_{Dmax} = P_R \text{ (diesel rated power).}$$

IV.2.2.c. BESS model

The BESS are charged /discharged depending on the operation strategy. Whenever the total power of PV and diesel exceeds the load demand, the BESS will be charged. On the other hand, if the available production is less than consumption, the BESS will discharge to cover the deficit.

The state of charge is given by the equation:

$$SOC(t) = \frac{C(t)}{C_{ref}} \qquad \text{(IV.3)}$$

where

C(t) and C_{ref}: the BESS capacity at time t and the reference capacity, respectively.

The state of charge SOC(t) is estimated by the previous value SOC(t-1) and the rejected /absorbed power during the time from t-Δt to t. The state of charge at hour t can be calculated by the following equation:

$$SOC(t)=SOC(t-1)+\frac{P_{PV}(t)+P_{grid}(t)-P_L(t)}{C_{ref}}.\Delta t \quad (IV.4)$$

In this chapter, Δt: is a unit time interval: Δt = 1 (1 hour)

C_{ref}: is BESS capacity (kWh)

In [15], the SOC related constraint is expressed as follows:

$$SOC^{min} \leq SOC(t) \leq SOC^{max} \quad (IV.5)$$

The constraint (IV.5) means that the battery should not be charged or discharged when SOC is out of the limits.

IV.2.2.d. Load model

The load data utilized in this chapter is based on hourly load data in one summer day and one winter day as shown in Figure.IV.3.

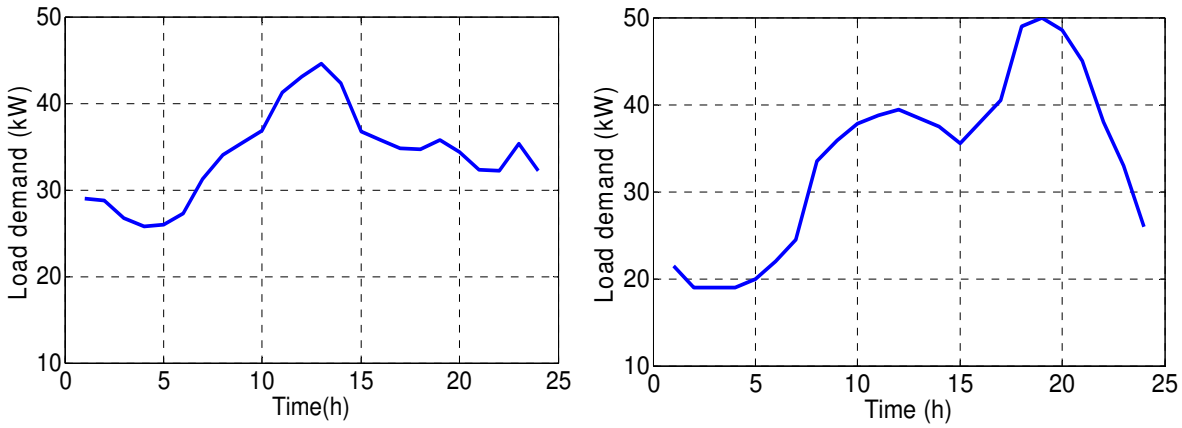

(a) (b)

Figure IV.3: Daily load curves in a summer day (a) and winter day (b)

IV.2.3. Methodology

IV.2.3.a. Objective function

The objective function is to minimize the annual cost of system (ACS) considering the CO_2 emission. It comprises the initial investment cost and payments cost throughout

the life time of installation. For this chapter, the lifetime of components is considered the same, apart for the BESS (since it has to be replaced during their lifetime).

In this section, the annual cost of system can be proposed with elements as follows:

- Installation cost of PV system, diesel battery bank and inverter.
- Replacing cost of devices during the lifetime of the system
- Maintenance cost of Photovoltaic, battery bank.
- Consumption fuel cost for diesel during the lifetime
- Operation and maintenance costs of diesel generator

IV.2.3.b. Economic model

The annual cost of system (ACS) includes the annual capital cost (ACC), annual operation maintenance (AOM), annual replacement cost (ARC), annual fuel cost of DG (AFC) and annual emission cost (AEC) as in [96]. ACS is estimated as follows:

$$ACS=ACC + AOM + ARC + AFC + AEC \quad (IV.6)$$

- The annual capital cost of PV system, diesel and inverter is calculated in the following equation as [6]:

$$ACC=C_{cap}.CRF(i,y) \quad (IV.7)$$

in which

$$CRF= \frac{i.(1+i)^y}{(1+i)^y-1} \quad (IV.8)$$

where

C_{cap}: the capital cost (US$)

CRF, : capital recovery factor

y: project lifetime

i: annual real interest rate.

The annual real interest rate can be calculated as follow [18]

$$i= \frac{i'-f}{1+f} \quad (IV.9)$$

where

i’ : loan interest (%)

f: annual inflation rate (%).

- The annual operation maintenance cost:

$$AOM=C_{cap}\ \frac{1-\lambda}{y} \tag{IV.10}$$

where

λ: reliability of components.

- The annual replacement cost:

$$ARC=C_{rep}.SFF(i,y_{rep}) \tag{IV.11}$$

where

C_{rep}: replacement cost of battery bank

SFF: sinking fund factor, it can be calculated as follow [18]:

$$SFF=\frac{i}{(1+i)^{y}-1} \tag{IV.12}$$

- The annual fuel cost of diesel:

$$AFC=C_f\sum_{t=1}^{8760}F(t) \tag{IV.13}$$

where

C_f: fuel cost per liter

F(t): hourly consumption of diesel generator.

F(t) is calculated in [96], [15]:

$$F(t)=(0.246.P_{DG}(t)+0.08415.P_R) \tag{IV.14}$$

where

P_R : rated power of diesel generators.

$P_{DG}(t)$: diesel power at time t

- The annual emission cost (CO_2 emission):

$$AEC=\sum_{t=1}^{8760}\frac{E_f.E_{cf}P_{DG}(t)}{1000} \tag{IV.15}$$

where

E_f: the emission function (kg/kWh)

E_{cf} : the emission cost factor ($/ton)

Table IV.1: The economic data

Project life time (year)	20
Interest rate i' (%)	3
Inflation rate (%)	1.6
PV panel lifetime (years)	20
Inverter lifetime (years)	20
Battery lifetime (years)	10
Reliability of PV panel (%)	0.98
Reliability of inverter (%)	0.98
Reliability of battery (%)	0.98
Reliability of diesel (%)	0.9
Cost of diesel generator (US$/kW)	500
Cost of PV panel (US$/W)	0.92
Cost of battery bank (US$/kWh)	200
Cost of inverter (US$/kW)	1000
Fuel cost (C_f) (US$/l)	0.7
Emission function (kg/kWh)	0.34
Emission cost factor (US$/ton)	55

IV.2.3.c. The operation of the PV-diesel-BESS hybrid system

The operation strategy of the PV-diesel-BESS hybrid is shown in Figure IV.4 and performed as follows:

* $P_{PV}(t)>P_L(t)$:

The BESS will be charged to the minimum value between the full state of BESS (with amount of power $\Delta P_{B\_ch} = (C_{Bmax} - C_B(t))/\Delta t$) and the power excess $(P_{pv}(t) - P_L(t))$

$$P_B(t) = \min (P_{pv}(t) - P_L(t), \Delta P_{B\_ch}) \quad \text{(IV.16)}$$

* $P_{PV}(t)<P_L(t)$:

The power is supplied by Diesel and battery banks

- If the power deficit value ($P_{dif}(t) = P_L(t)-P_{PV}(t)$) is less than the amount of minimum

diesel power (P_{Dmin}).

- If the remaining BESS power ($\Delta P_{B\_dis}(t) = (C_B(t)-C_{Bmin})/\Delta t$) is enough to cover $P_{dif}(t)$, the BESS will discharge and the Diesel is switched off.

$$P_B(t) = P_{dif}(t) \quad \text{(IV.17)}$$

- If $P_{dif}(t) > \Delta P_{B\_dis}(t)$, the diesel will operate at P_{Dmin} and the BESS will be charged with the value defined as

$$P_B(t) = P_{dif}(t)-P_{Dmin} \quad \text{(IV.18)}$$

- If $P_{dif}(t) > P_{Dmin}$, we have three cases such as:

- If $P_{dif}(t) \leq \Delta P_{B\_dis}(t)$, the BESS will discharge ($P_{dif}(t)$) and the Diesel is switched off.
- If $P_{dif}(t) > P_{Dmin}+\Delta P_{B\_dis}(t)$, the BESS will discharge ($\Delta P_{B\_dis}(t)$) and the diesel operates with the power value:

$$P_D(t) = P_{dif}(t)- \Delta P_B(t) \quad \text{(IV.19)}$$

- If $\Delta P_{B\_dis}(t) < P_{dif}(t) \leq P_{Dmin}+\Delta P_{B\_dis}(t)$, the diesel operates at P_{Dmin} and the BESS will discharge with value:

$$P_B(t) = P_{Dmin} - P_{dif}(t)$$

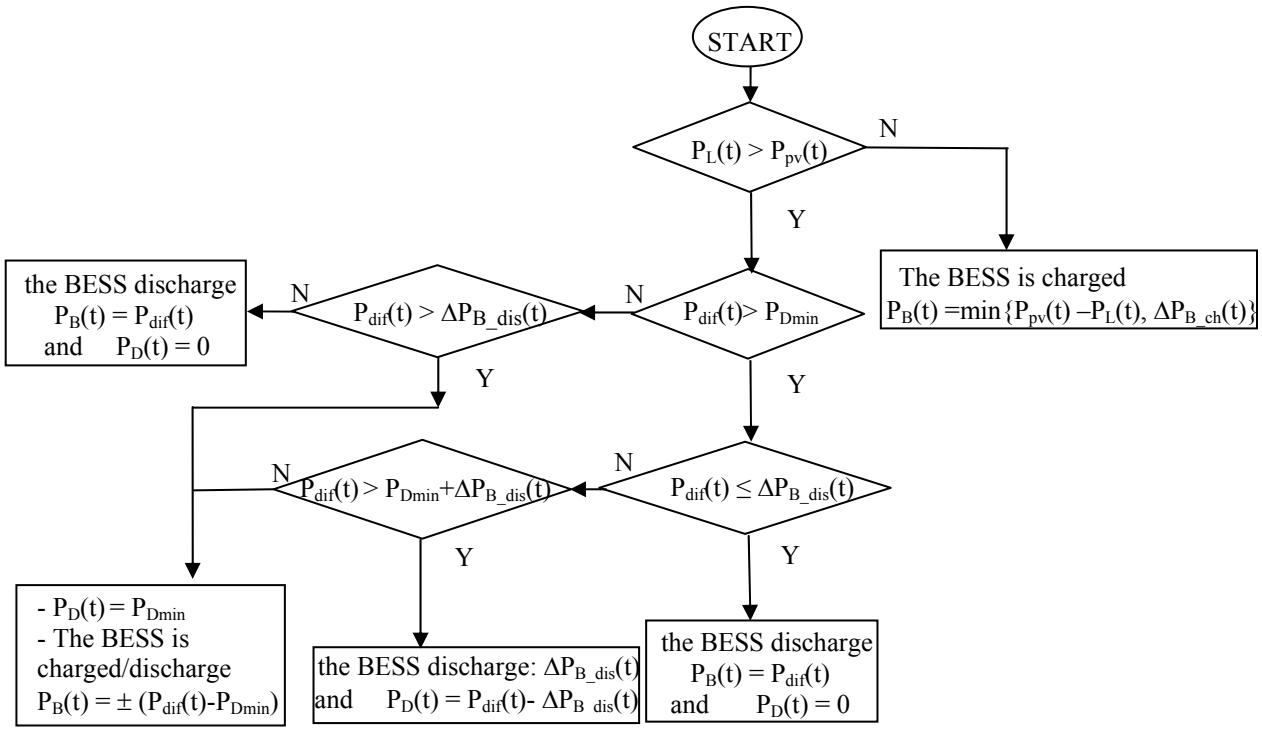

Figure IV.4: The operation strategy of PV – diesel – BESS hybrid system

IV.2.3.d. Constraints

** The configuration constraints*

- The PV sizing variables (Npv):

The number of PV panels can range from 0 to the highest amount of PV panels needed when a PV stand-alone system can cover the load demand. Thus, N_{pv} is bounded as follows [85]:

$$0 \leq N_{pv} \leq \frac{E_{L\_day}}{\eta.W.Hours_{sunshine/day}} \quad \text{(IV.20)}$$

where

η: Efficiency loss of conversion,

W: The expected PV panel output power.

$Hours_{sunshine/day}$: The average number of estimated sunshine hours per day.

- The BESS sizing variable (C_b):

The capacity of BESS (kWh) is calculated by equation in [13] as follows:

$$C_b = \frac{E_{L\_day}.D}{DOD.\eta_b} \quad \text{(IV.21)}$$

where

D: Number of autonomy days

DOD: Depth of discharge %

The capacity of BESS is limited to a value from 0 (no BESS) and its value for 5 days of autonomy day. This value means that during this time, the BESS has to cover the load demand without PV, diesel. The capacity of BESS is bounded as follow

$$0 \leq C_b \leq \frac{5.E_{L\_day}}{DOD.\eta_b} \quad \text{(IV.22)}$$

- The diesel sizing (P_R):

The size of diesel generator is bounded from 0 (no diesel generator) to the size for a diesel single source system to meet the peak demand power in W.

$$0 \leq P_R \leq P_{L\_peak} \quad \text{(IV.23)}$$

** The operation constraints*

The operation constraints are summarized in [16] as follows

$$P_L(t)=P_{PV}(t) + P_B(t) + P_D(t) \quad \text{(IV.24)}$$

$$SOC_{min} \leq SOC(t) \leq SOC_{max} \quad \text{(IV.25)}$$

$$P_{Bmin} \leq P_B(t) \leq P_{Bmax} \quad \text{(IV.26)}$$

Equation (IV.24) comes from the balance of energy law. The battery physical constraints are given by (IV.25-26). The state of charge and power of BESS are bounded by predefined limit.

** The other constraints*

In order to maximize the renewable energy utilities, the renewable energy fractions and excess power ratio have been considered during the optimal process

- Renewable energy fractions (FR)

The renewable energy fraction is defined as the ratio of renewable energy to the total energy production of the hybrid system. The equation for FR is shown as in [97]

$$FR= \frac{E_{RE}}{E_{RE}+P_{DG}} = \frac{E_{solar}}{E_{solar}+E_{DG}} \quad \text{(IV.27)}$$

where $0 \leq FR \leq 1$, the fraction Fr =0 means that the load demand is supplied by diesel gensets sources. On the other hand, Fr = 1 the system is fed only by renewable sources.

$$FR_{design} \leq FR \leq 1 \quad \text{(IV.28)}$$

- Excess energy ratio (EER)

The excess energy ratio is calculated by dividing the excess renewable energy by the total energy production.

$$EER= \frac{E_{excess}}{E_{RE}+E_{DG}} = \frac{E_{excess}}{E_{solar}+E_{DG}} \quad \text{(IV.29)}$$

The excess energy ratio has to be below the design value.

$$0 \leq EER \leq EER_{design} \quad \text{(IV.30)}$$

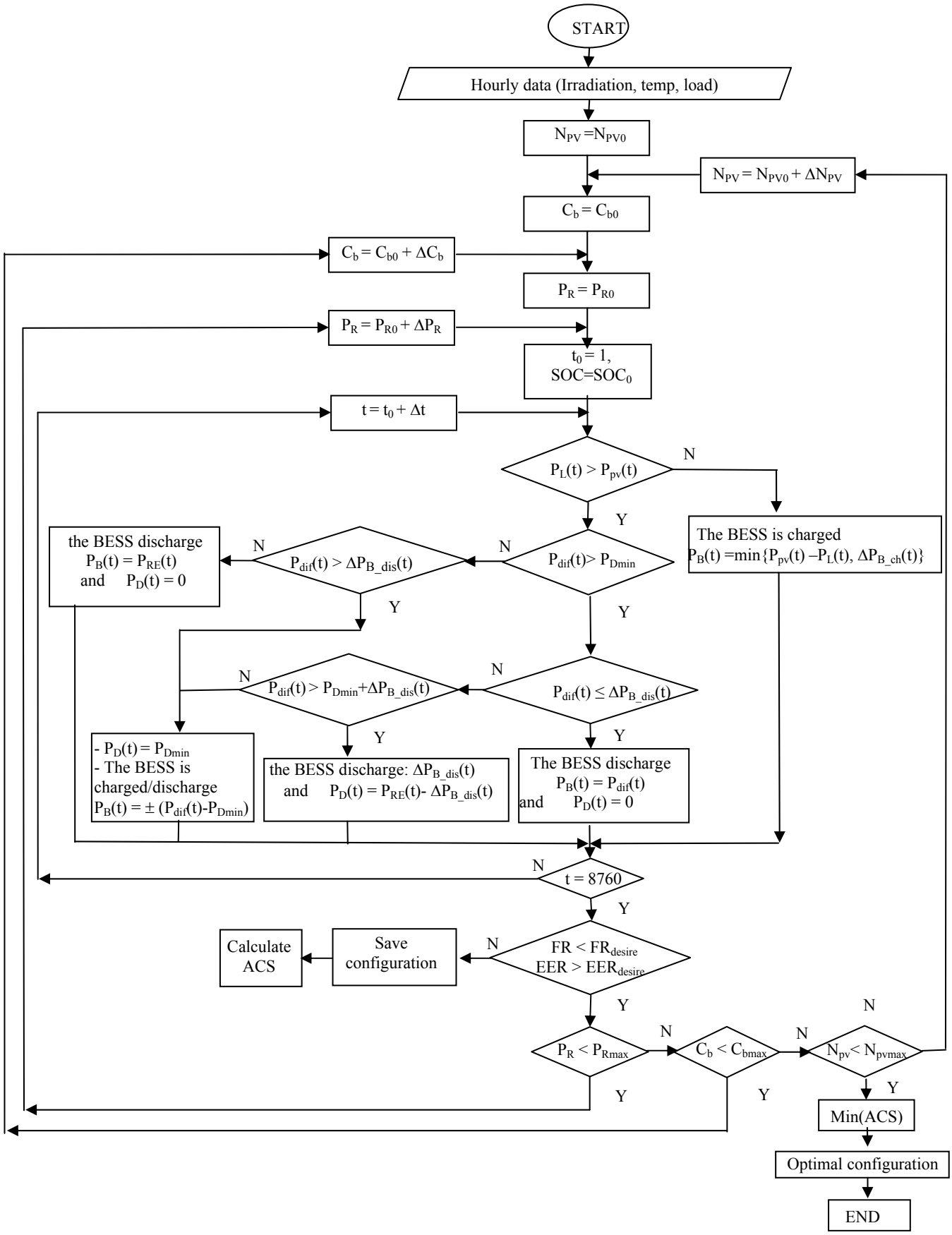

Figure IV.5: The optimal sizing algorithm

IV.2.4. Simulation results and discussion

Optimal sizing of isolated PV-diesel-BESS hybrid system is to be revealed in this subsection. The irradiation data, load profile and the other factors are shown in IV.2. The annual simulation is performed to determine the ACS and the CO2 emission. The simulation will be finished when the variables reach their maximum values. In this section, the renewable energy fraction (FR_{design}) is set at 0.5 and 0.25 in the summer and winter days, respectively. The excess energy ratio (EER_{design}) in all days is fixed at 0.01.

Table IV.2: Optimal sizing PV-diesel-BESS hybrid results

	Hybrid system	Baseline (Diesel only)
Maximum PV power (kW)	103.4 (440x235)	-
BESS capacity (kWh)	495	-
Diesel generator capacity (kW)	50	50
Diesel generator minimum power (%)	30	30
SOC_{min} (%)	20	-
SOC_{max} (%)	90	-
FR (%)	50	-
EER (%)	1	-
Annual load energy (kWh)	286853.5	286853.5
Annual CO_2 emission (Ton/year)	34.8	100.6
Annual cost of system ACS (US$)	53.296	71.060
Price (US$/kW)	0.19	0.24

In Table IV.2, the optimal sizing of hybrid system results is shown and is compared to diesel only system. From this result, one can see that the optimal sizing of hybrid system is achieved with the number of PV panels as 440 (peak power generated 104.3kW) and the capacity of BESS and diesel generators are estimated as 495kWh, 50kW. It can be seen from this Table, the annual cost of system ACS in the hybrid system (53.296US$) is smaller than that in the baseline case (71.060US$). It is due to the fact that the combination operation of the components in system can make the total annual cost decrease. In addition, the operation of proposed hybrid system generate CO_2 emission lower than the baseline

system. Thus, we can conclude that the hybrid system is more economical (price: 0.19US$/kWh compared to 0.24US$/kWh) as well as less emission than diesel only system.

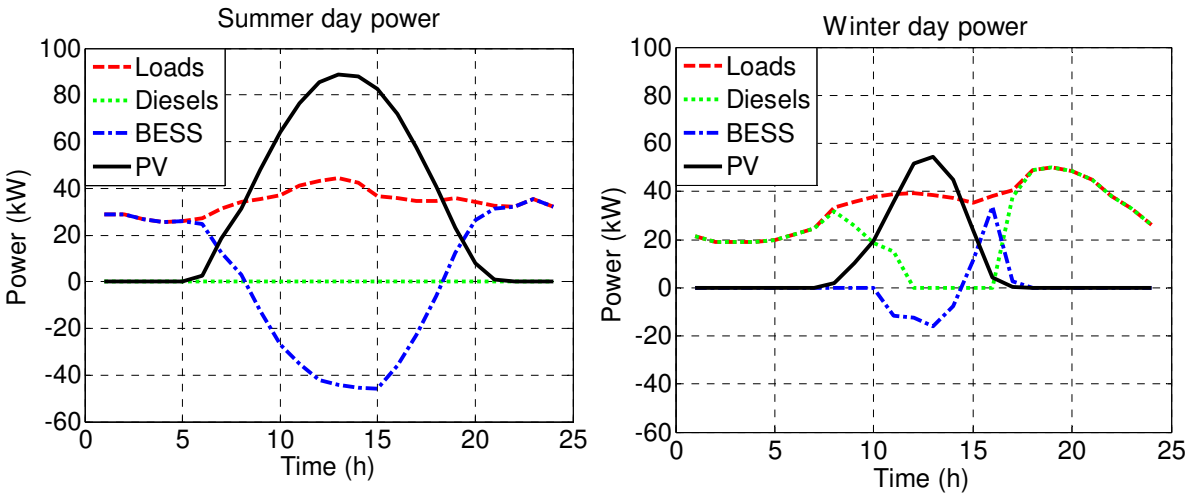

a) b)

Figure IV.6: Variation in load, PV, diesel and BESS power in a day under the optimal size

Figure.IV.6 describes the power flow balance in the proposed system. It can be seen that the load demand is supplied by the sources in the optimal configuration. For the entire day, no load shedding is found and the energy from PV is totally used (since EER=0). Thus, this system can reach the high reliability. As can be seen from Figure IV.6a, in summer day (clear day) the diesel is not used during whole day. Therefore, a large amount of the fuel consumption and CO_2 emissions are reduced. On the other hand, in winter day (cloudy day) due to small PV radiation the diesel gensets only stop during 4 hours from 12am-4pm (Figure IV.6b).

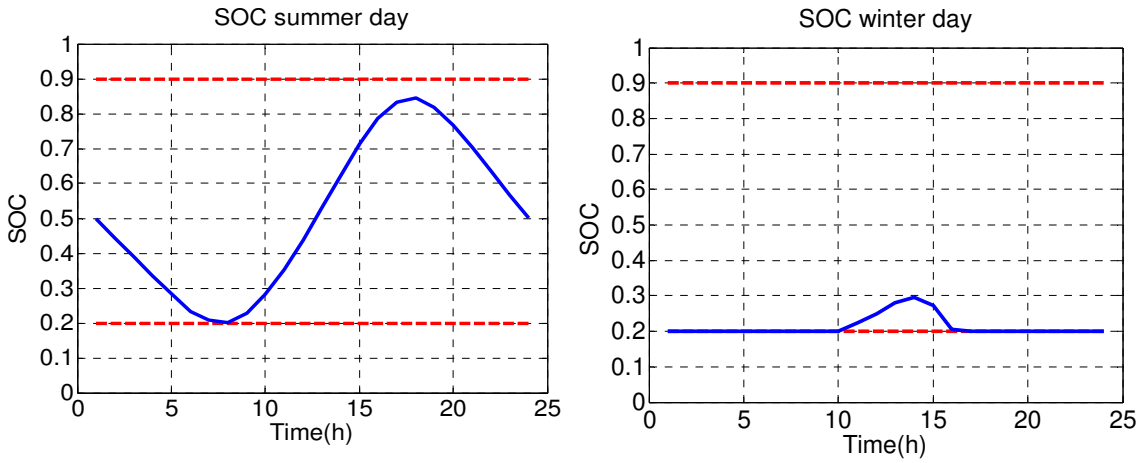

a) b)

Figure IV.7: Battery SOC in a day of the optimal configuration

In Figure IV.7, the battery SOC value is always bounded by the limit values during a day. Thus, the BESS are well controlled and in good operating condition. In the summer day (the clear day), the BESS will discharge at the beginning and the end of the day and is charged with the power excess from the PV system.

The annual electricity production of each unit is shown in Figure IV.8. The ratio between PV production and total production reaches 55%. The remaining power will be handled by BESS or diesel generators. The annual participation ratio from the BESS and diesel are determined as 16% and 29%, respectively.

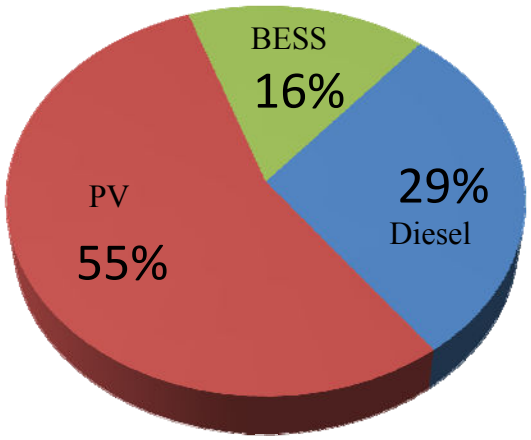

Figure IV.8: The annual electricity production from various units

In the simple way, if we increase the PV panels, the annual cost of system would decrease. However, because of the system operation constraints and the technology conditions, increasing the PV panels will not change the annual cost. It can be seen from Figure IV.7, on a sunny day, the load demand is fulfilled by the PV panels and BESS. Thus, if the number of PV panels increases, the excess energy ratio will overcome the EER design. Furthermore, the BESS capacity is also increasing; hence, it leads to a rise in capital cost and O&M. Therefore, increasing the number of PV panel is unable to obtain the high efficiency. The minimum storage level of BESS (C_{bmin}) (the limit value which the BESS can discharge) also affects the fuel cost. In fact, when C_{bmin} value is large, the diesel generators would have to be operated more times than that for the small C_{bmin} value. Thus, the CO_2 emission produced by diesel will also increase. Consequently, increasing the minimum storage value of BESS will lead to the increase of both the fuel cost and the CO_2 emission.

IV.3. Optimal sizing of a microgrid in grid connected mode

IV.3.1. System configuration

In this subsection, the grid connected PV- BESS system is described in the Figure IV.9. In this case, the diesel generator is not available; thus, the main grid will supply power whenever the load demand exceeds the PV and BESS power. On the other hand, when the PV power is superior to the load demand, the power excess can be sold back to the main grid or be charged to BESS. In this system, the charge/discharge processing of BESS and buying/ selling the power from the main grid can be reached after solving the optimal economics based on the system operation.

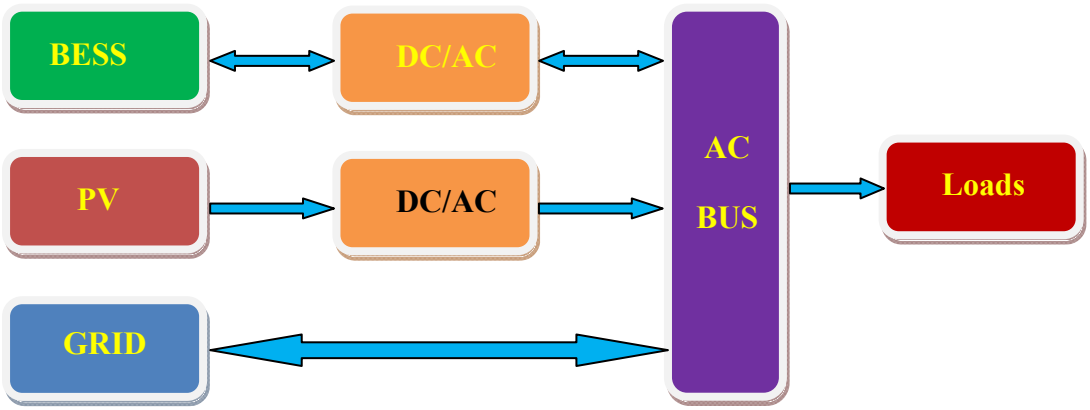

Figure IV.9: The grid connected PV-BESS system

IV.3.2. System components

IV.3.2.a. Photovoltaic model

The simple model of PV is chosen for this system. The output power from the PV panel is expressed by a function of the area, solar radiation conditions and its efficiency. In this section, the PV panels are used as Photowatt PW2300-235. The data radiation is given in Figure IV.2

IV.3.2.b. BESS model

The BESS will be charged when the production exceeds the consumption. On the other hand, the BESS discharges to cover the power deficit. The state of charge is

calculated by equation (IV.4). The battery bank is bounded as in equation (IV.6).

IV.3.2.c. Load model

The load data is shown in Figure IV.3 for a summer day load and winter day load

IV.3.2.d. Utility of power system

Electric power can be purchased from the grid whenever the PV system and BESS are not sufficient to meet the load demand. On the other hand, when the PV production exceeds the consumption, the power excess will be sold back to the grid (high tariff) or/and charged to the BESS (low tariff).

The power exchange with the main grid $P_{grid}(t)$ has to be bounded in this chapter as follows:

- $P_{grid}(t) > 0$: The power is purchased from the grid, and the constraint is defined as:

$$P_{grid}(t) \leq P_{grid}\,max \tag{IV.31}$$

- $P_{grid}(t) < 0$: The power is sold to the grid, and the P_{grid} has to be lower-bounded as:

$$P_{grid}(t) \geq P_{grid}\,min \tag{IV.32}$$

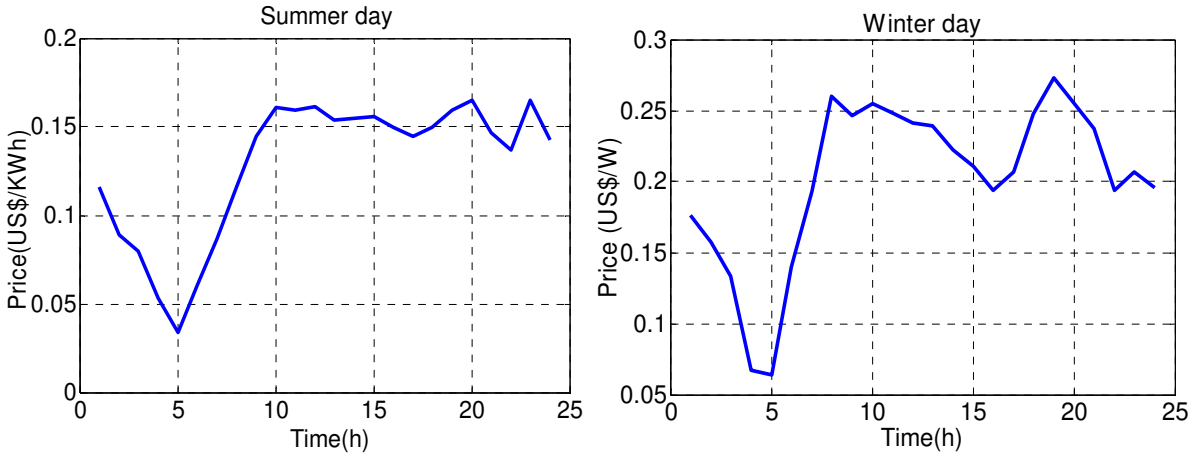

Figure IV.10: The daily electricity tariff of the main grid

IV.3.3. Methodology

IV.3.3.a. Objective function

In this subsection, the objective function is to minimize the annual cost of the system (ACS). It comprises of the initial investment cost, payments cost throughout the life time

of installation and the revenue obtained from selling power back to the main grid. The annual cost of the system in this part can be proposed with elements as follow:

- Purchase cost of PV, BESS and inverter.
- Replacement cost of devices during the lifetime of the system
- Maintenance cost of Photovoltaic, BESS.
- Purchase cost from the main grid
- Income from selling the electricity to the main grid

IV.3.3.b. Economic models

In this part, the annual cost of system (ACS) includes the annual capital cost (ACC), annual operation maintenance (AOM), annual replacement cost (ARC), annual buying cost (ABC) and the income from selling the electricity to the main grid (annual selling cost-ASC). ACS is estimated as follows:

$$ACS=ACC + AOM + ARC +ABC-ASC \quad (IV.33)$$

The values ACC, AOM, ARC are calculated following equation (8), (11) and (12) respectively. The ABC value can be estimated according to the day tariff. The income from selling the electricity to the main grid can be calculated as in [15]:

$$ASC_{feed\text{-}in}= \sum_{t=1}^{8760} rate_{feed\text{-}in}.\left|P_{grid}^{feed-in}\right| \quad (IV.34)$$

where

$rate_{feed\text{-}in}$: feed-in tariff rate

$P_{grid}^{feed\text{-}in}$: power excess sold back to main grid

IV.3.3.c. Operation of the grid connected PV-BESS system

The operation strategy of the grid connected PV - BESS system is shown as follows:

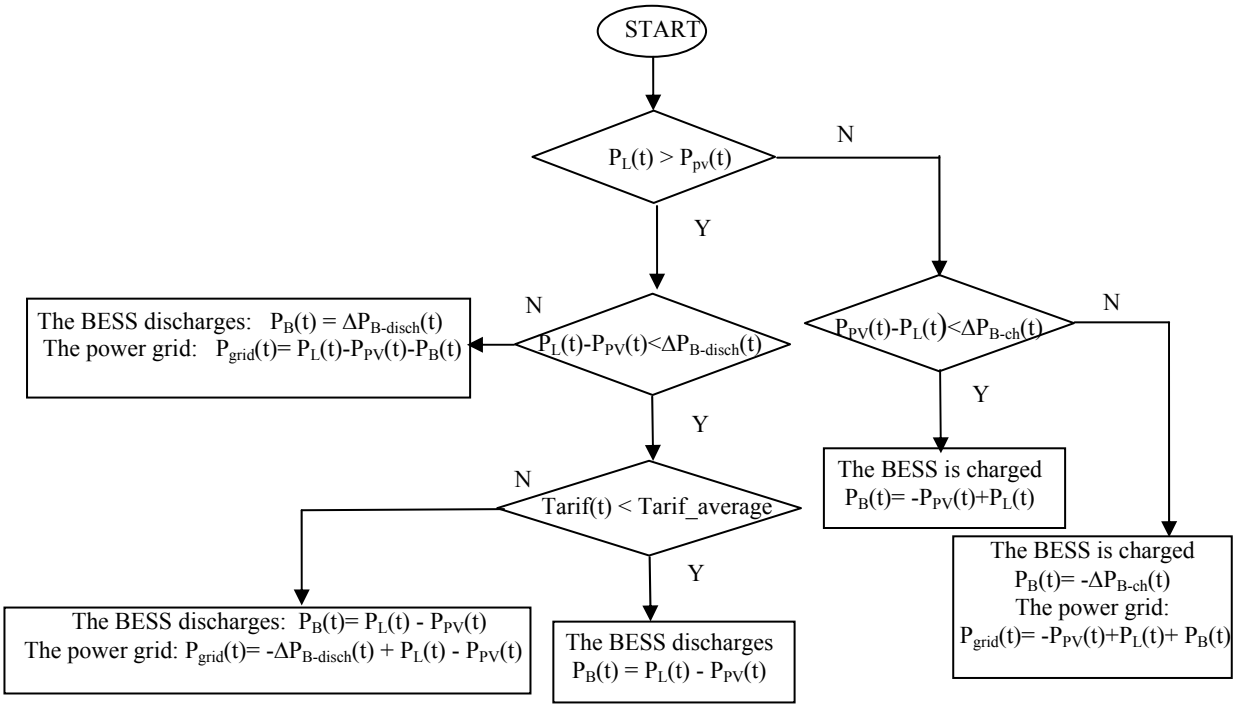

Figure IV.11: The operation strategy of grid connected PV-BESS system

* *$P_{PV}(t)>P_L(t)$:*

The power excess $P_{PV}(t)-P_L(t)$ will be charged to the BESS and be sold back to grid as

- If $P_{PV}(t)-P_L(t) > \Delta P_{B\text{-}ch}(t) =(C_{B\_max} – C_B(t))/ \Delta t$, the BESS will be full charged and the remaining power will be sold to grid ($P_{grid} < 0$)

$$P_{grid}(t)= -P_{PV}(t)+P_L(t)+ \Delta P_{B\text{-}ch}(t) \quad \text{(IV.35)}$$

- If $P_{PV}(t)-P_L(t) < \Delta P_{B\text{-}ch}(t)$, the BESS will be only charged ($P_B < 0$) with value

$$P_B(t) = -P_{PV}(t)+P_L(t) \quad \text{(IV.36)}$$

* *$P_{PV}(t)<P_L(t)$:*

The grid or/and BESS will cover the power deficit

- If the power deficit $P_L(t)-P_{PV}(t)$ is inferior the remaining BESS power ($\Delta P_{B\text{-}disch}(t) = (C_B(t)-C_{B\_min})/\Delta t$)

- If Tariff < average tariff for a day, the BESS discharges to cover the power deficit ($P_B > 0$)

$$P_B(t) = P_L(t)-P_{PV}(t) \quad \text{(IV.37)}$$

- If Tariff > average tariff for a day, the BESS supplies the power deficit and sell the remaining power to the grid until SOC = SOC_{min}.

$$P_{grid}(t)= -\Delta P_{B\text{-}disch}(t) + P_L(t)-P_{PV}(t) \quad \text{(IV.38)}$$

- If $P_L(t)-P_{PV}(t) > \Delta P_{B\text{-}disch}(t)$, the BESS will discharge with $\Delta P_{B\text{-}disch}(t)$ and the deficit will be supplied by grid

$$P_{grid}(t)= P_L(t)-P_{PV}(t)-P_B(t) \quad \text{(IV.39)}$$

IV.3.3.d. Constraints

** The configuration constraints*

The PV (N_{pv}) and BESS (C_b) sizing are bounded as in equation (IV.21), (IV23), respectively.

** The operation constraints*

The operation constraints of BESS and the balance energy constraint between generators and consumptions are shown in (IV.26) and (IV.27). The power exchange with main grid is limited as follows

$$P_{grid}^{min} \le P_{grid} \le P_{grid}^{max} \quad \text{(IV.40)}$$

** The other constraints*

In order to maximize the renewable energy utilities, the renewable energy fractions and excess power ratio have been concerned during the optimal process

- Renewable energy fractions (FR)

The equation for FR is shown as in [22]

$$FR= \frac{E_{RE}}{E_{RE}+P_{Grid}}=\frac{E_{solar}}{E_{solar}+E_{Grid}} \quad \text{(IV.41)}$$

where $0 \le FR \le 1$, the fraction Fr =0, it means that the load demand is supplied by grid. On the other hand, Fr = 1 the system only includes renewable sources.

$$FR_{design} \le FR \le 1 \quad \text{(IV.42)}$$

- Excess energy ratio (EER)

$$EER= \frac{E_{excess}}{E_{RE}+E_{Grid}}=\frac{E_{excess}}{E_{solar}+E_{Grid}} \quad \text{(IV.43)}$$

The renewable energy fraction has to be below the design value

$$0 \le EER \le EER_{design} \quad \text{(IV.44)}$$

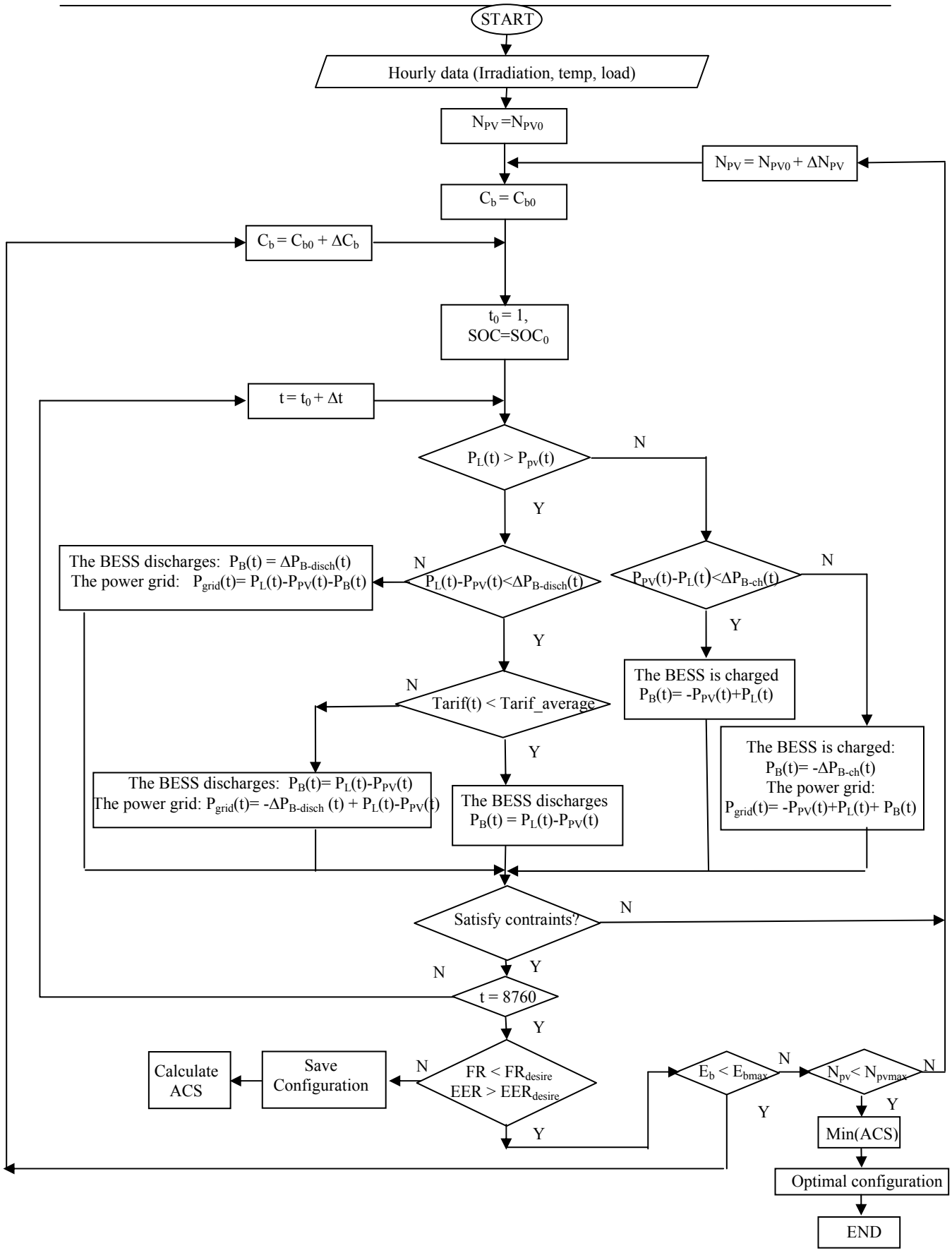

Figure IV.12. The topology of optimal sizing of grid connected system

IV.3.4. Simulation results and discussion

Optimal sizing of grid connected PV-BESS system has been performed in this subsection. The irradiation data, load profile and the other factors are shown in section IV.1.2. The topology of the proposed method is described in Figure IV.12. The annual simulation is performed to determine the ACS. The simulation will stop when the variables (N_{pv} and E_b) reach their maximum values. The renewable energy fraction (FR_{design}) is fixed as 0.5 in the summer and 0.25 in winter day. The excess energy ratio (EER_{design}) is set as 0.01 in all days.

Table IV.3: Optimal sizing grid connected PV-BESS system results

	Grid connected PV-BESS system	PV- diesel-BESS system
Maximum PV power (kW)	108.1 (460x235)	103.4 (440x235)
BESS capacity (kWh)	295	495
Diesel generator capacity (kW)	-	50
Diesel generator minimum power (%)	-	30
SOC_{min} (%)	20	20
SOC_{max} (%)	90	90
FR (%)	50	50
EER (%)	1	1
Annual load energy (kWh)	286853.5	286853.5
Annual cost of system ACS (US$)	45.861	53.296
Annual average price (US$/kW)	0.16	0.19

In Table IV.3, the optimal sizing of grid connected PV-BESS system result is shown and is compared with PV-Diesel-BESS hybrid system. The optimal configuration of the grid connected system includes the PV panel number and the BESS capacity is estimated at 460 (Maximum PV power: 108.1kW) and 295kWh, respectively, compared with 460 (103,4kW) and 495kWh in the hybrid system. This is due to the fact that the required

power can be regulated by the main grid. Thus, the BESS capacity will be smaller than its value in off grid system. Furthermore, after the surplus power is fully charged to the BESS, the remaining power can be sold back to the grid. To sum up, the annual cost of system (ACS) in on-grid and off-grid configurations are determined as 45.861US$ and 53.296US$, respectively. Thus, one can conclude that the grid connected system is more economic point of view (price: 0.16US$/kWh compared with 0.19US$/kWh) than island system.

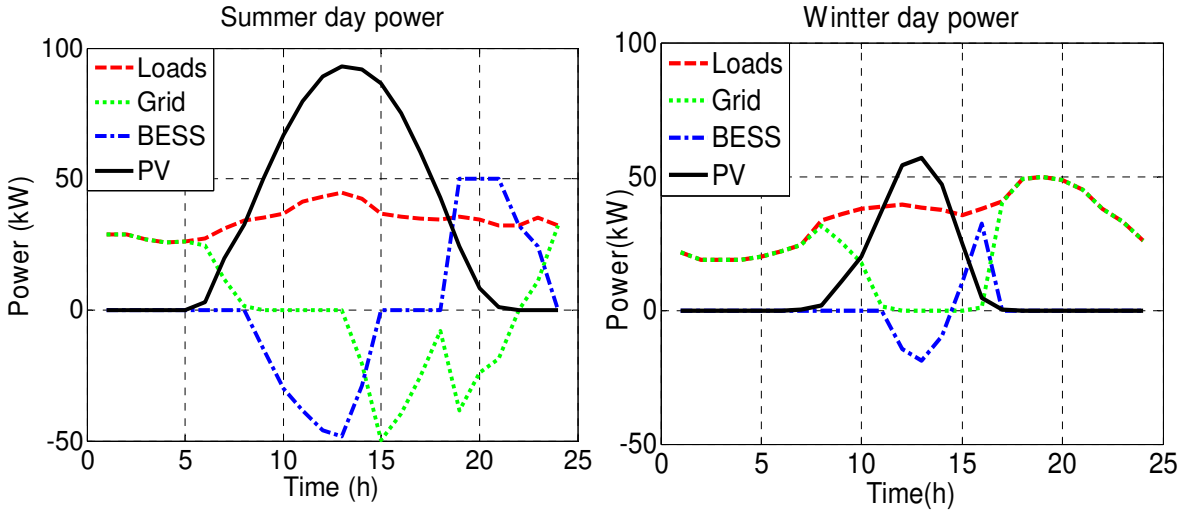

a) b)

Figure IV.13: Variation in load, PV, grid and BESS power in a day under the optimal size

The power variation of grid, BESS, PV system and loads is shown in Figure IV.13. It can be seen from this figure that the load demand is fulfilled by the sources in the optimal configuration. For the entire day, no load shedding is found and the energy from PV system is totally used (EER=0). As can be seen from Figure IV.13a, the consumption is supplied by the grid during the first hours of the day. After that, the power excess is fully charged for BESS due to the fact that the PV power exceeds load demand. Then, the remaining power will be sold back to the grid during the high demand periods. And finally, the load demand is covered by the BESS until 10pm and by grid and BESS at the end of the day. The bought/sold power is always bounded following the constraint (IV.44). In these summer days (clear days), because the power excess is fed back into the grid, the annual cost of the system also declines.

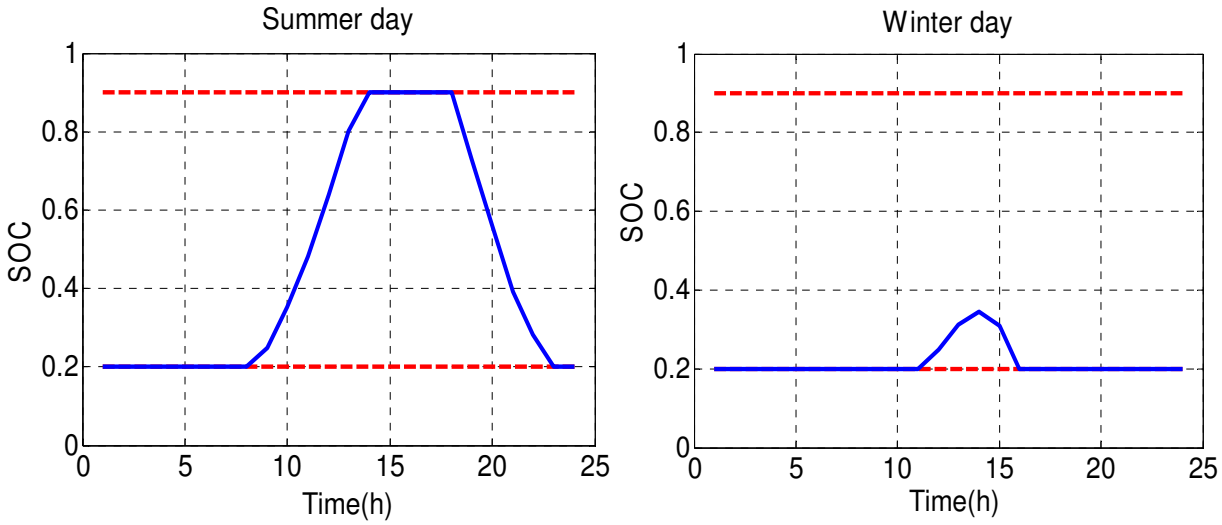

a) b)

Figure IV.14: Battery SOC in a day of the optimal configuration

As can be seen from Figure IV.14, the battery SOC values in summer day and winter day are always bounded by the limit values during a day. On the summer days, the BESS is fully charged. Then, the BESS discharges until SOC_{min}.

Table IV.4: Comparison between grid-connected PV-BESS system and grid only system

	Grid connected PV-BESS system	Grid only system
Annual load energy (kWh)	286853.5	286853.5
Annual cost of system ACS (US$)	45.861	51.783
Annual average price (US$/kW)	0.16	0.18

From Table IV.4, we can see that the annual cost system (ACS) value in grid connected PV-BESS system is less than this of grid only case (45.861US$ compared with 51.783US$). Therefore, the grid connected PV-BESS system built from the proposed optimal sizing method is the best solution.

IV.4. **Conclusion**

In this chapter, the optimal sizing of island microgrid (PV-diesel-BESS hybrid system) and grid-connected microgrid (grid-connected PV-BESS system) has been

presented. An iterative technique is used to find the optimal configuration of the number of PV panels, BESS capacity and diesel capacity (in the hybrid system). Then, the comparisons of the optimal configuration system with the diesel and grid only system have been carried out to assess the proposed method.

In the optimal sizing of the PV-diesel-BESS system, the total number of PV panels and the BESS capacity are estimated at 440 (the peak power generated power is produced as103.4kW) and 495kWh, respectively. The annual cost system ACS of hybrid system is determined by 53.296US$. From Table IV.2, one can conclude that the hybrid system is better from an economic as well as emission point of view than the diesel only system.

In the optimal sizing of the grid connected system, the total PV panel and the BESS capacity are carried out with 460 (the peak power generated power is produced 108.1kW), 495kWh, respectively. The annual cost system ACS of grid connected system is estimated as 45.861US$. From Table IV.3, one can see the economic efficiency of this system.

CHAPTER V :

Optimal energy management for microgrid

SUMMARY

V.1. **Introduction**

When a microgrid has more than two DERs, it is necessary to have an energy management system (EMS) which is expected to optimize the power sharing among DER, the cost of energy production and emission. The functions of proposed EMS are shown in Figure V.1. The energy management system receives the forecast values of load demand, the distributed energy resources and the market electricity price in each hour on the next day to impose the scheduling output power of DER, the import/export power with main grid, the cost and the emission. The microgrid configuration estimated in chapter IV, will be used in this chapter.

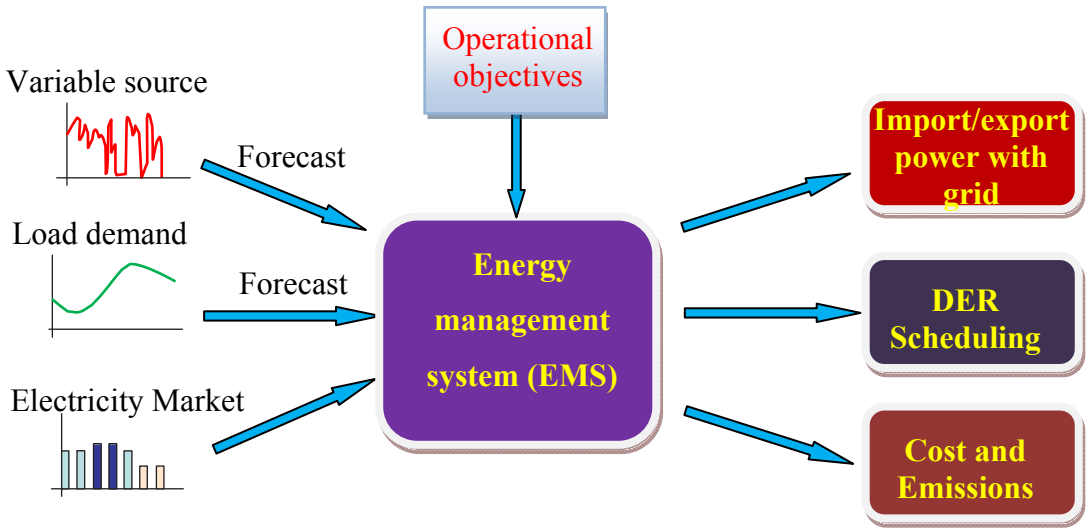

Figure V.1: The EMS in a microgrid

Based on the operation objectives, the optimal energy management will be achieved by EMS. In this chapter, the operational objectives are shown as follows:

- Minimizing the cost
- Minimizing the emissions
- Maximizing the renewable energy
- Minimizing the net power import from the main grid.

The optimal energy management for a microgrid performs under two operational modes that are island and grid connected modes by using DP method. In the island microgrid, the objective function is to minimize the fuel cost and to reduce emissions by scheduling of DERs. While for the grid connected mode, the aim is to minimize the cash

flow of the system as well as to satisfy the net power import from the main grid, which is viewed as one constraint of the optimization problem. Moreover, the maximum renewable energy is always reached by this DP method. The constraints are given by the balance power between the supply and the load demand and the limitations of each DER. The energy management obtained by DP method is compared to a Rule-based method. The simulation results are carried out to assess the efficiency of the proposed method (DP).

V.2. **Optimization methods**

In this chapter, the dynamic programming is used to determine the optimal energy management. The DP algorithm and its application are addressed in the following.

V.2.1. Dynamic Programming and Bellman Algorithm

Dynamic programming is known as an optimization technique which transforms a complex problem into simpler problem by breaking up a problem into a series sub-problems. The advantages of this approach are addressed such as: it is applied both in discrete time and continuous time settings as well as no specific mathematical solver. A Dynamic Programming algorithm called the Bellman algorithm is used to find the shortest path from all nodes of a graph. In order to understand this algorithm, one reminds a basic technology [98]: a graph is set elements called nodes or vertices, with edges between some of the nodes. One uses V to denote the set of vertices and E to denote the set of edges. A directed graph G = (V, E) is a graph where the edge has a direction. In other definition, the weighted graph is given as a graph where its edges have weight such as cost or length. We have a definition for the basic shortest path problem as follows:

"Given a weighted, directed graph G, a start node s and a destination node t, the s-t shortest path problem is to output the shortest path from s to t. The single-source shortest path problem is to find shortest paths from s to every node in G. The (algorithmically equivalent) single-sink shortest path problem is to find shortest paths from every node in G to t."

The Bellman Ford algorithm is shown as follow [98], [99], [100]:

Given a directed graph G = (V, E), a start node S and a destination node T

1. Initialization. If $u \in V$, we get dist(u):=∞. If u=S, we get dist(S) =0

2. if i = /N/-1, stop. If each (u,v) ∈E, we get

dist(v):= min{dist(u), dist(u)+lent(u,v)}

if dist(v) is changed, we put v=u. Update i, i:=i+1, return 2

A flowchart of Bellman method is shown in [39]. In Figure V.2, a edge $u(x_i, x_j)$ is given by node x_j, and previous node x_i. A path that leads to the summit "x_i" is an available path between the initial node "x_0" and node "x_i". The cost of a path is the sum of weights of an edge on the way. The cost of the path that leads to the node "x_i" is denoted by $C(x_i)$.

Based on the above algorithm, the cost of a path leading to node x_j is written as follows:

$$C(x_j) = P(u_{xi, xj}) + C(x_i)^* \quad \text{(V.1)}$$

where :

$C(x_i)^*$: cost of the shortest path that leads to node i

$P(u_{xi,xj})$: weight between node i and node j

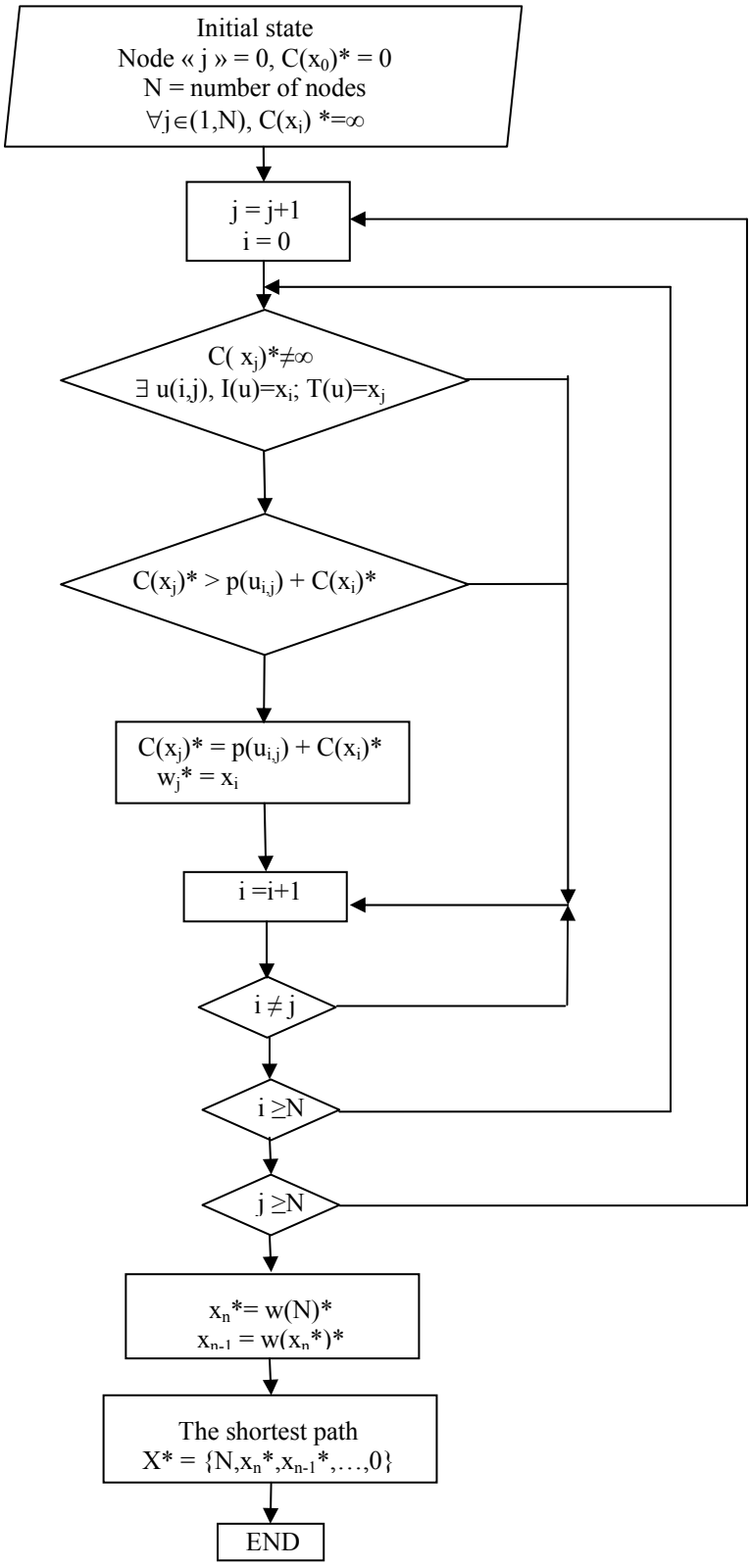

Figure V.2: The flowchart of the shortest path R.Bellman algorithm

In order to explain the shortest path of Bellman algorithm, an example is given in Figure VI.3. One finds the shortest path from the initial node (node 0) to the final node (node 5). The graph G (V, E) is shown in Figure V.3.

- {V}= {0,1,2,3,4,5}
- {E}={$e_{0,1}$, $e_{0,2}$, $e_{1,2}$, $e_{1,3}$, $e_{1,4}$, $e_{2,3}$, $e_{2,4}$, $e_{3,4}$, $e_{3,5}$, $e_{4,5}$}

The weights of the edges are

- {P}={1, 3, 5, 2, 3, 4, -2, 3, 4, 6}

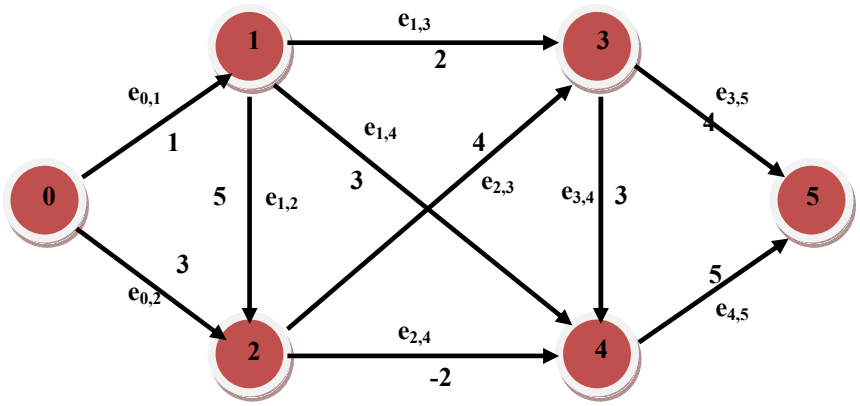

Figure V.3: A example of a directed graph G(V,E)

The Bellman algorithm for this graph is explained as follows:

- The initial node is node 0. We have $C(x_0)^*=0$.
- x_1, a node, is put together with the previous node x_0 to get an edge. Thus, the path is calculated as follow

$$C(x_1)^*=\min(P(e_{0,1}) + C(x_0)^*) = 1$$

- The shortest path is calculated from node 0 to node 2

$$C(x_2)^*=\min[P(e_{0,2}) + C(x_0)^*, P(e_{1,2}) + C(x_1)^*] = \min[3,6]=3.$$

→ the shortest path, leads to the node 2, is from node 0.

- The shortest path is calculated from node 0 to node 3

$$C(x_3)^*=\min[P(e_{1,3}) + C(x_1)^*, P(e_{2,3}) + C(x_2)^*] = \min[3,9]=3.$$

→ the shortest path, leads to the node 3, is from node 0 and via node 1.

- The shortest path is calculated from node 0 to node 4

$$C(x_4)^*=\min[P(e_{1,4}) + C(x_1)^*, P(e_{2,4}) + C(x_2)^*, P(e_{3,4}) + C(x_3)^*,] = \min[4,1,6]=1.$$

→ the shortest path, leads to the node 3, is from node 0 and via node 2.

- The shortest path is calculated from node 0 to node 5

$$C(x_5)^*=\min[P(e_{3,5}) + C(x_3)^*, P(e_{4,5}) + C(x_4)^*] = \min[7,6]=6.$$

Thus, the shortest path from the initial node (node 0) to final node (node 5) has to pass node 2 and 4.

V.2.2. Application of Bellman algorithm to finding the nominal state of charge (SOC) of batteries

As defined in V.2.1, the program now includes sub-problems like a system is divided into multi-stage decision process. The state of the system at each time is estimated by a set of state variables. It is discretized with a step size "δSOC". The initial state of charge (SOC_0) is given as initial node without the previous node. Similarly, one sets for the final state of charge (SOC_T). All edges are oriented in one direction from t time to t+Δt time. Thus, the change SOC process is seen as a directed graph with initial node (SOC_0) and the final node (SOC_T). Hence, from the definitions in the previous part, the Bellman algorithm for the searching SOC is described as in Figure V.4

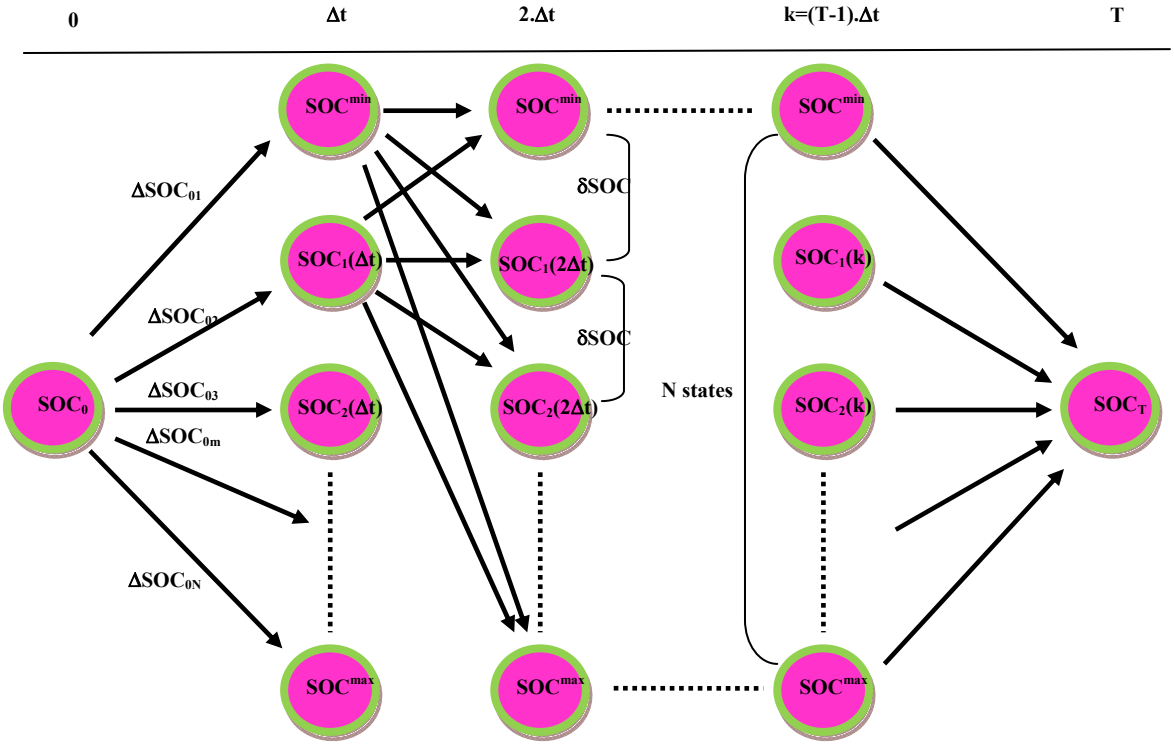

Figure V.4: Bellman algorithm application for battery's SOC space

A state of charge (SOC) variation between two states x_i and x_j during one step is written ΔSOC, calculated as follows [39]:

$$\Delta SOC\ (x_i,x_j,t) = SOC\ (x_j,t) - SOC\ (x_i,t-\Delta t) \qquad (V.2)$$

If $\Delta SOC < 0$: Battery discharge

If $\Delta SOC > 0$: Battery is charged

If $\Delta SOC = 0$: Battery rest

The number of states is estimated as follows:

$$N = \frac{SOC^{max} - SOC^{min}}{\delta SOC} \quad (V.3)$$

V.3. Optimization of energy management for a microgrid in isolated mode

The configuration of an island microgrid, which has been estimated in chapter IV, includes PV system, Diesels and BESS. The diesel systems are connected by AC systems bus, directly supply to the load demand. When the PV power is not sufficient to meet the load demand, the remaining power will be covered by diesel and BESS. On the other side, the power excess from the PV production will be charged to the BESS. Thus, the energy management is used to estimate the optimal power sharing between sources. In this section, the data of load is taken from the Chapter IV, while that of the PV radiation is given as equal to two out of three of the data in summer day in Chapter IV.

V.3.1. Objective function

The objective is to minimize the cost of system (CS) considering the CO_2 emission. The CS includes the cost of fuel (FC), the emission cost (EC) and the batteries replacement cost (BrC). In this chapter, the day-ahead cost of system can be determined as follows:

$$CS = \sum_{t=1}^{24} FC(t) + EC(t) + BrC(t) \quad (V.4)$$

- The fuel cost is calculated as follows:

$$FC(t) = C_f . F(t) \quad (V.5)$$

where

C_f: the fuel cost per liter

F(t): the hourly consumption of diesel generator.

F(t) is calculated as:

$$F(t) = (0.246.P_D(t) + 0.08415.P_R) \quad (V.6)$$

where

P_R : the rated power of diesel generators.

$P_D(t)$: the diesel power at time t

- The emission cost (EC) is estimated as follows (in Chapter IV)

$$EC(t)= \frac{E_f.E_{cf}P_D(t)}{1000} \quad (V.7)$$

where

E_f: The emission function (kg/kWh)

E_{cf} : The emission cost factor

- The replacing batteries cost (BrC)

In this chapter, the cost of replacing batteries (BrC) at each time step corresponds to the cost of the capacity lost during the time interval. It is calculated according to the variation of SOH (ΔSOH) at each time step. The variation of state of health (ΔSOH) is estimated in equation (V.8). On the other hand, the ΔSOH can be estimated by (V.9) which is a linear function of the variation of the state of charge (ΔSOC) and the ageing coefficient (Z). The ΔSOH is calculated only during the discharge process.

$$\Delta SOH(x_i,x_j, t)= SOHx_i(t-\Delta t)-SOHx_j(t) \quad (V.8)$$

$$\Delta SOH(x_i,x_j, t)= Z.(SOCx_i(t-\Delta t)-SOCx_j(t)) \quad (V.9)$$

The batteries' replacement cost BrC is estimated as follows [64]

$$BrC(t)= BiC\ \frac{\Delta SOH(t)}{1-SOH_{min}} \quad (V.10)$$

And it has to satisfy

$$\sum_{t \text{ such as } SOH=1}^{t \text{ such as } SOH=SOHmin} BrC(t)= BiC \quad (V.11)$$

where

BiC: the batteries' investment cost

SOH_{min}: The state of health minimum

In this chapter, $Z = 3.10^{-4}$[64].

V.3.2. Constraints

** Power balance constraint:*

$$P_L(t)=P_{PV}(t) + P_B(t) + P_D(t) \quad (V.12)$$

where

$P_L(t)$: the load power at t

$P_{PV}(t)$: the PV system power at t

$P_B(t)$: the BESS power at t

$P_D(t)$: the Diesel generators power at t

** BESS power output:*

$$P_{Bmin} \leq P_B(t) \leq P_{Bmax} \quad (V.13)$$

- If $P_B(t) < 0$: BESS is charged
- If $P_B(t) > 0$: BESS discharge
- If $P_B(t) = 0$: BESS rest

The BESS power $P_B(t)$ corresponds to a transition between two states during one time step. Thus, the constraint to the SOC variation constraint is described as follows [89]

$$\Delta SOC_{min} \leq \Delta SOC(t) \leq \Delta SOC_{max} \quad (V.14)$$

** Battery state of charge constraint:*

The battery state of charge is bounded in predefined limit as follows:

$$SOC_{min} \leq SOC(t) \leq SOC_{max} \quad (V.15)$$

** Battery ageing constraint:*

Battery state of health (SOH) is limited by the equation as follows

$$SOH(t) \geq SOH_{min} \quad (V.16)$$

** Diesel generators constraint:*

The power output of diesel generators is bounded as follows:

$$P_{die\_min} \leq P_D(t) \leq P_{die\_max} \quad (V.17)$$

V.3.3. A rule-based energy management strategy

In this subsection, a 'constraint' management strategy is proposed based on the predefined rules. The system operation is imposed depending on the power of PV and consumption. This management method is restricted due to the fact that the state of battery is not taken into account in the predefined rules.

The principle of the ruled based energy management is based on the following main rules:

- PV energy is primarily used to supply for the loads
- The BESS only discharge when the PV system and Diesels are not sufficient
- The BESS is charged as soon as possible with the power excess (when the production is more than the loads).

The proposed ruled based energy management has to assure the following constraints:

$$P_L(t)=P_{PV}(t) + P_B(t) + P_D(t)$$

$$SOC_{min} \leq SOC(t) \leq SOC_{max}$$

$$P_{Bmin} \leq P_b(t) \leq P_{Bmax}$$

$$P_{die\_min} \leq P_D(t) \leq P_{die\_max}$$

The method topology is shown in Figure V.5. The approach is performed as follows:

- The diesel power is expressed as the function of the PV system and the loads power.
- The corresponding BESS power is calculated by the equation V.12
- Verification of compliance with the BESS and Diesel constraints (the constraints V.12- V.15).

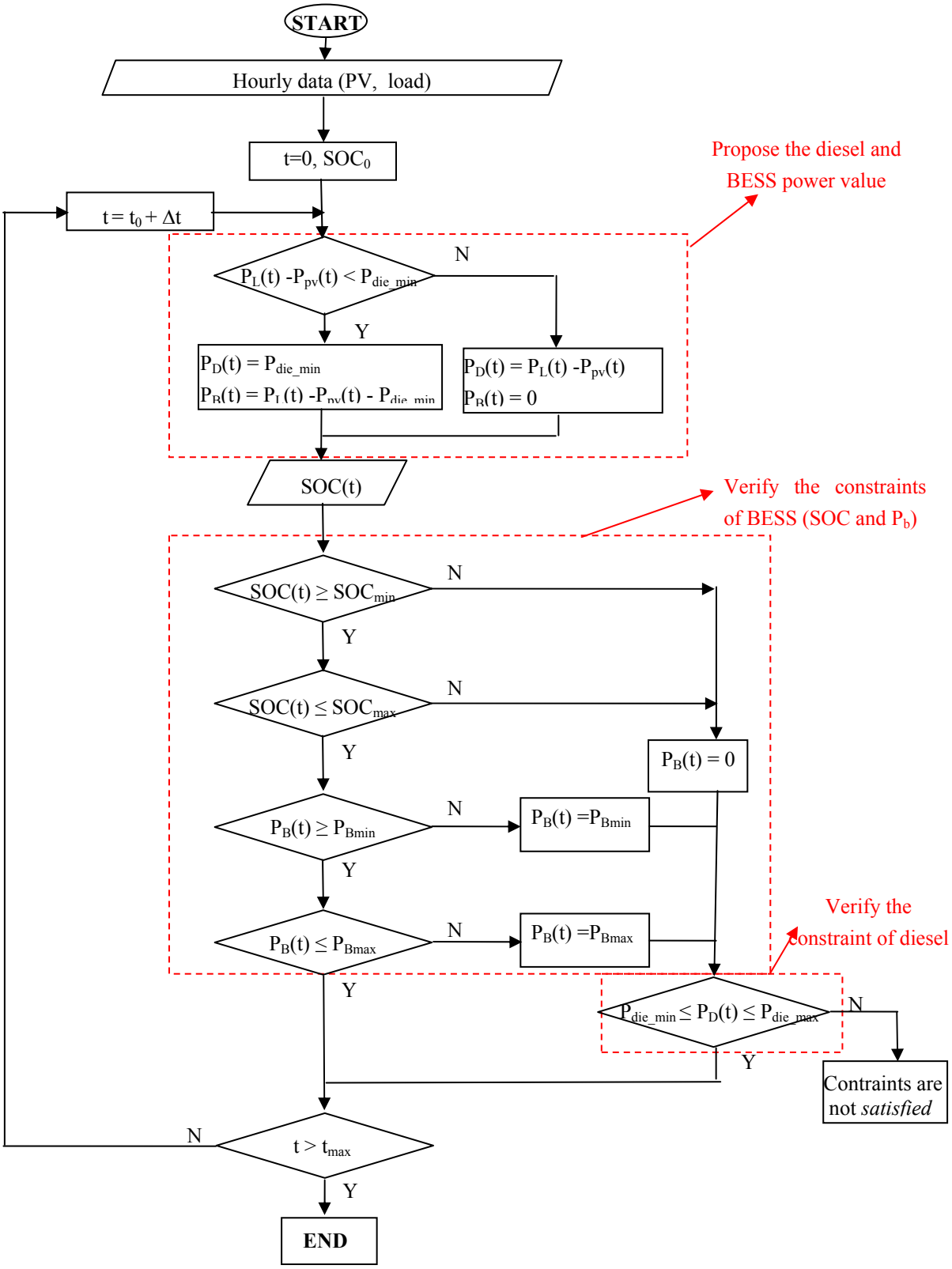

Figure V.5: Flowchart of rule-based management in an island microgrid

V.3.4. Bellman algorithm application in optimal energy management for an island microgrid

The Bellman algorithm is applied for this hybrid system to achieve the minimum day-ahead cost of system by the way to find the optimal sequence of SOC transition from the initial time to final time. The optimal problem is now discretized in time Δt. Thus, the cost of system (CS) can be described as follows:

$$CS= \sum_{t=1}^{24} C_f.FC(t)+\frac{E_f.E_{cf}P_D(t)}{1000}+BrC\,(t) \tag{V.18}$$

Substitute (V.5)-(V.10) to (V.18), we obtain the objective function as follows:

$$\min(CS)=\min \sum_{to}^{24} C_f(0.246.P_D(t) + 0.08415.P_R)+\frac{E_f.E_{cf}P_D(t)}{1000}+BiC\frac{Z.(SOCx_i(t-\Delta t)-SOCx_j(t))}{1-SOH_{min}}$$

The objective function is expressed as a function of diesel power and the SOC variation. Furthermore, the SOC variation (ΔSOC) is related to the battery power. Thus, for each ΔSOC the P_B is determined and the P_D is estimated according to the P_B and the forecast value of P_{PV}, P_L. The calculated process of P_D is shown in the Figure V.6 [39]. Therefore, the CS now is a function of the SOC variation. Hence, the optimal cost of system (CS) is obtained by applying the Bellman algorithm described in Figure (V.4) to find the optimal sequence (the shortest path) of state of charge from the initial time to the final time.

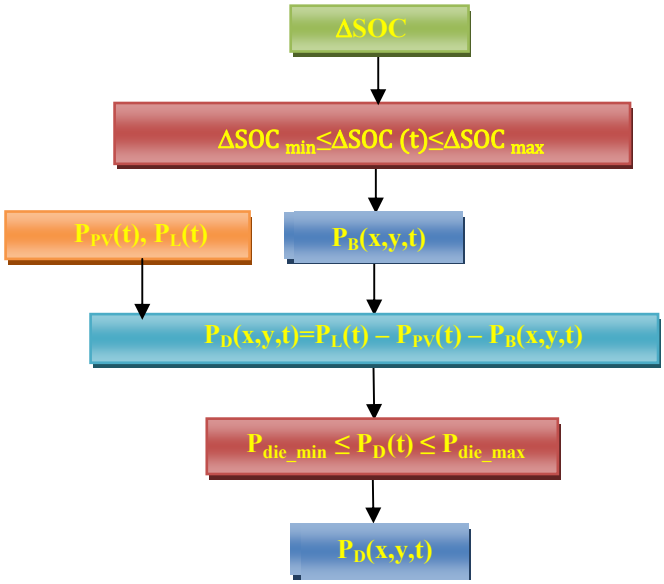

Figure V.6: Process of calculating P_B and P_D

The flowchart of the algorithm with the detail computation of the weight of the edges is shown in Figure V.7.

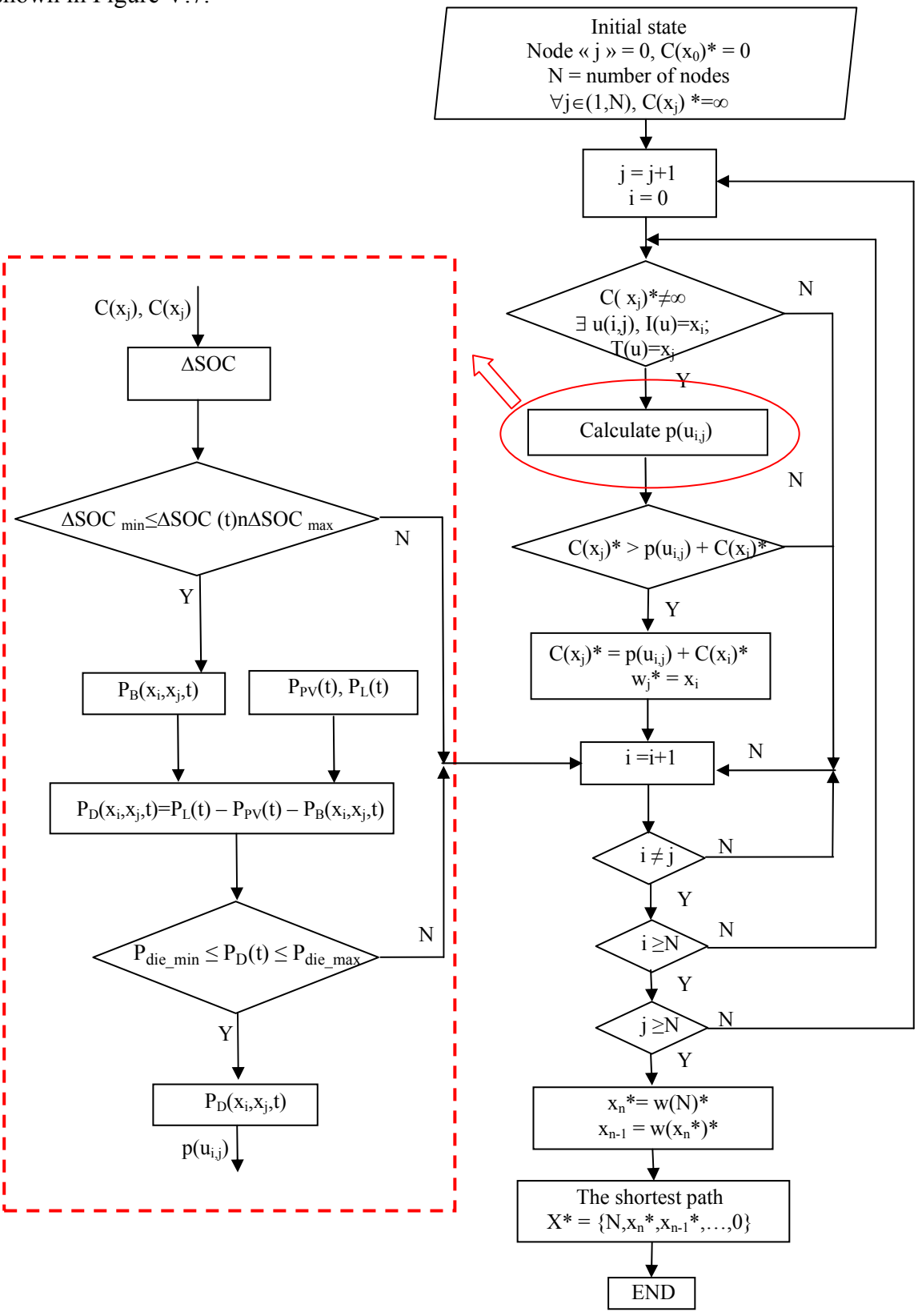

Figure V.7: The flowchart of proposed method

V.3.5. Simulation results and discussion

Optimal energy management of isolated PV-diesel- BESS hybrid system is to be revealed in this subsection. The flowchart of the proposed method is shown in Figure V.7. In this section, the results of the Chapter IV are used to carry out the efficiency of the proposed optimal method. The day-ahead forecast values of load and PV are taken for a summer day in Chapter IV, are shown in Figure V.8. The day-ahead simulation is performed to determine the minimum of CS, the CO2 emission as well as the optimal schedule of diesels and BESS. The simulation is finished when the state of charge SOC variable reaches its final state. In this part, three scenarios are performed as:

Scenario1: initial state of charge $SOC(t_0) = 0.5$

Scenario2: initial state of charge $SOC(t_0) = 0.2$

Scenario3: initial state of charge $SOC(t_0) = 0.9$

The optimal problem is briefly introduced as follows:

Objective :

$$CS= \sum_{t=1}^{24} C_f.FC(t)+\frac{E_f.E_{cf}P_{DG}(\Delta t)}{1000}+BrC\,(t)$$

with

$$P_L(t)=P_{PV}(t) + P_B(t) + P_D(t)$$

$$P_{Bmin} \leq P_B(t) \leq P_{Bmax}$$

$$SOC_{min} \leq SOC(t) \leq SOC_{max}$$

$$SOH(t) \geq SOH_{min}$$

$$P_{die\_min} \leq P_D(t) \leq P_{die\_max}$$

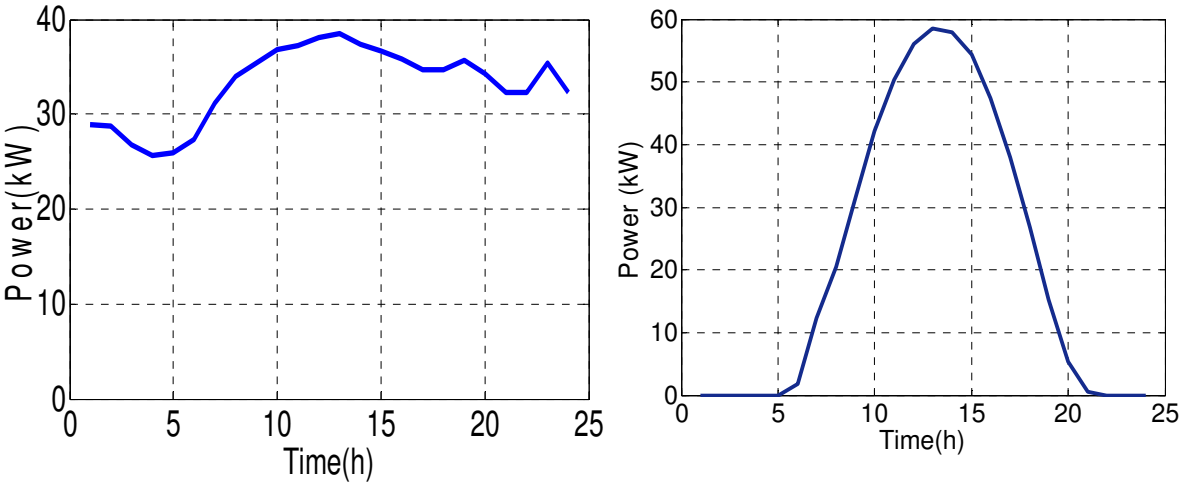

Figure V.8: The day-ahead forecast value of load and PV system

The Table V.1 provides the simulations parameter values. In addition, the economic data is taken from Table IV.1 in chapter IV.

Table V.1: The simulation parameter values

Name	Value	Unit
T	24	h
Δt	1	h
δSOC	0.001	
SOC_{min}	0.2	
SOC_{max}	0.9	
ΔSOC_{min}	-0.7	
ΔSOC_{max}	0.7	
SOH_{min}	0.7	
Minimum power of diesel	15	kW
Maximum power of diesel	50	kW

-Scenario1: initial state of charge SOC (t_0) = 0.5

The optimal energy management by the two methods in studied microgrid is shown in Figure V.9.

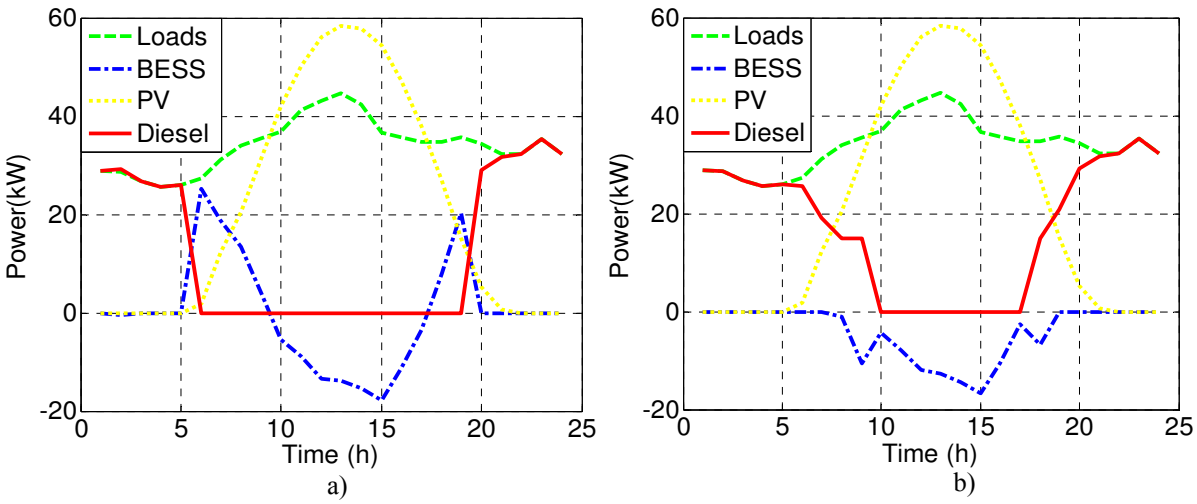

Figure V.9: Power schedule of a microgrid in isolated mode in scenario 1

The DP method **b) the rule-based method**

It can be seen that the load demand is satisfied by the sources. At the beginning of the day, when the load is low, the load demand is supplied by the diesel. After that, in the Figure V.9a, the BESS discharges to meet the load, the diesel does not work at 6am. On the other hand, the Diesel operate continually to supply for the load demand and charge for BESS in the Figure V.9b. The diesel stops operation for 13 hours (from 6am to 7pm) estimated by using the DP method and 7 hours (from 10am to 5pm) by the rule-based method. In this period, the consumption is supplied by the PV system production. When the PV power is sufficient to meet loads, the BESS is charged by the power excess. From the two Figures, one can see that the diesel cooperates with the BESS and PV in order to answer for the load in DP method. On the other side, there has not the cooperation between the diesel and the BESS in the rule-based method, the BESS is always charged as soon as possible. Figure V.10a shows that the state of charge at the end of day turns back the initial value (SOC=0.5) to prepare for the next day. Otherwise, the SOC at the end of the day is given as larger than this value at the beginning (in Figure V.10b).

The simulation results in the Figure V.9a and Figure V.10a show that the diesel generation is stopped for 13 hours per day, thus it leads to make good operating condition, increase the lifetime of diesel generators and reduce the cost fuel as well as the CO_2 emission. Furthermore, the final SOC equal with the initial one; thus the charge operation will be easily performed in the beginning of next day. In the ruled- based method, because there is no forecasting, the rule is to keep the BESS as full as possible, thus the final SOC is larger than the initial one (in Figure V.10). In this condition, the energy management of

the next day is restricted due to the fact that the BESS is almost fully charged. Therefore, the charge operation will not be possible at the beginning of next day. Therefore, the rule-based management is not the most suitable for day-ahead supervision.

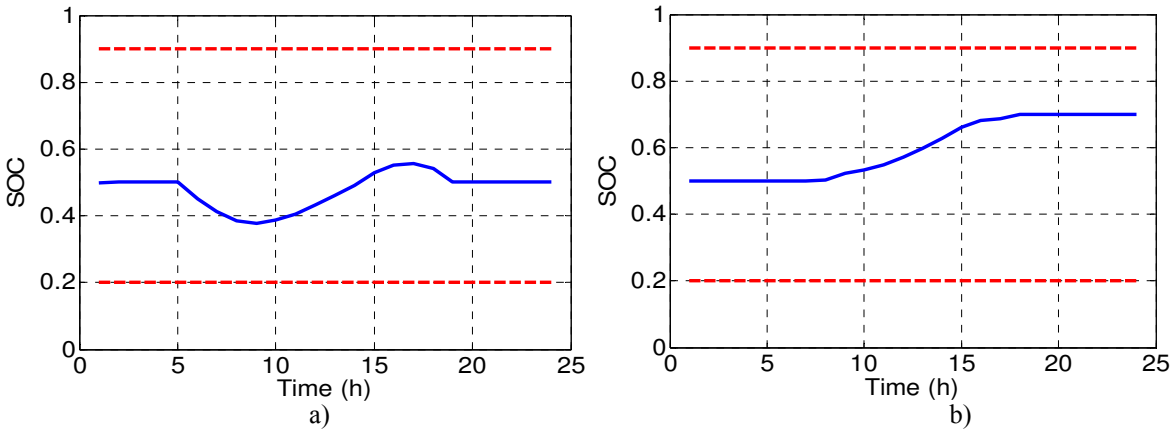

Figure V.10: The battery state of charge in a day optimal

a) The DP method **b) the rule-based method**

The final value of the objective function for the DP optimization and the rule-based management is presented in Table V.2. This value given by the DP algorithm is lower than that given by the rule-based method because it is optimization.

Table V.2: The final value of the objective function in case SOC= 0.5

	DP	Rule-based
Final value ($)	113.3	148.47

- Scenario2: The initial of the state of charge SOC(t_0) = 0.2

The optimal power schedule of sources is shown in Figure V.11a. In this case, the system begins to operate with the empty BESS, in fact that the initial state of charge SOC is 0.2. The load is low value at the beginning of the day; therefore the demand load is supplied by the diesel. After that, the BESS is charged to be ready to supply for load subsequently. At t=9am, the loads are supplied by the PV and BESS; therefore the diesel will be stopped. This situation is continued from 9am to 9pm. The BESS will be charged from the power excess. Then, the BESS discharges all of its energy to supply the loads. Finally, the diesel will operate to meet the load at 9pm. The estimated operation of system by rule-based method gives similar to the above case.

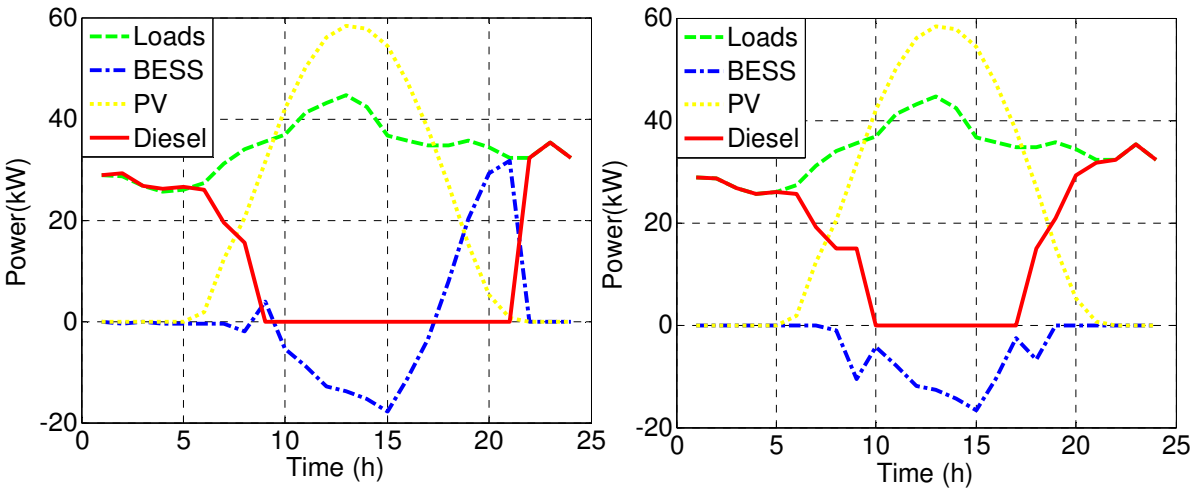

Figure V.11: power schedule of a microgrid in isolated mode in scenario 2

a) The DP method **b) the rule-based method**

The battery SOC value by two methods are shown in Figure V.12, they are always bounded by the limit values during a day.

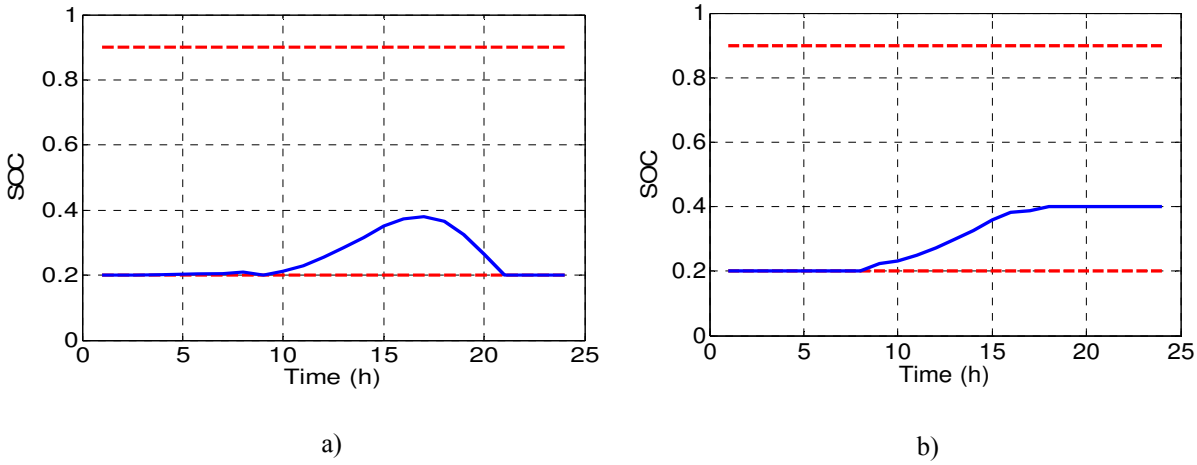

Figure V.12: BESS state of charge in a day optimal in scanerio2

a) The DP method **b) the rule-based method**

The final value of the objective function for the DP optimization and the rule-based management in this case is presented in Table V.3. The result given by the rule-based method is estimated the same the scenario 1. The value obtained using this method is greater than that given with the DP algorithm.

Table V.3: The final value of the objective function in case SOC= 0.2

	DP	Rule-based
Final value ($)	118	148.47

- Scenario3: initial state of charge SOC(t_0) = 0.9

Figure V.13a describes the optimal power schedule of sources. At the beginning of the day, the BESS is full. Generally, the operation of the system is the same with the operation of two previous scenarios. However, the diesel does not work at 5am. This is due to that the BESS has full energy at the beginning of the day. Furthermore, at 4pm, the BESS is almost fully charged to prepare for the next day. As can be seen from Figure V.13b, the BESS is not charged with the power excess from PV due to the fact that it has been fully charged. Thus, a large amount of PV power is lost daily duty cycle.

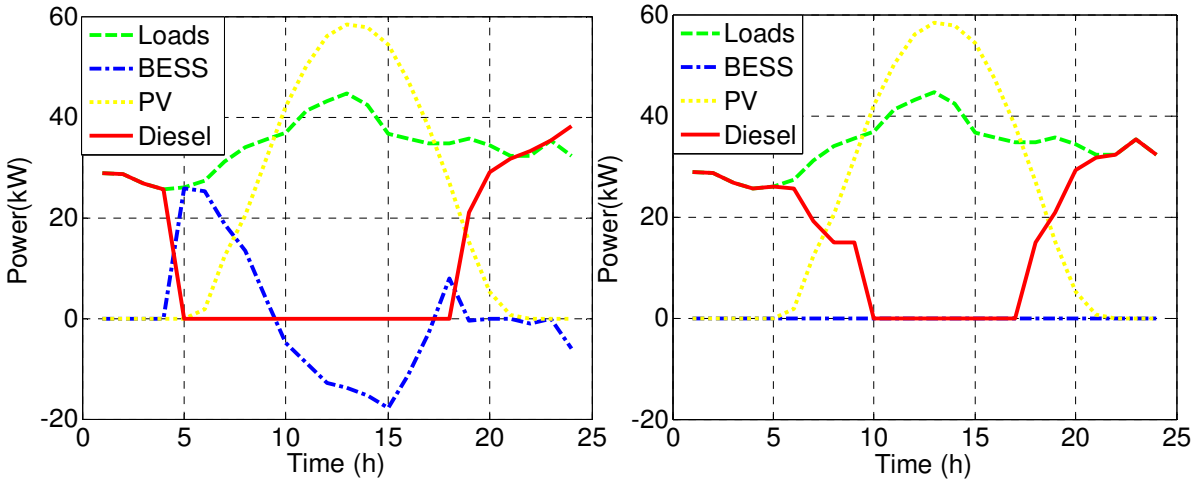

Figure V.13: power schedule of a microgrid in isolated mode in scenario 3

a) The DP method **b) the rule-based method**

The state of charge SOC in the scenario3 is shown in Figure V.14.

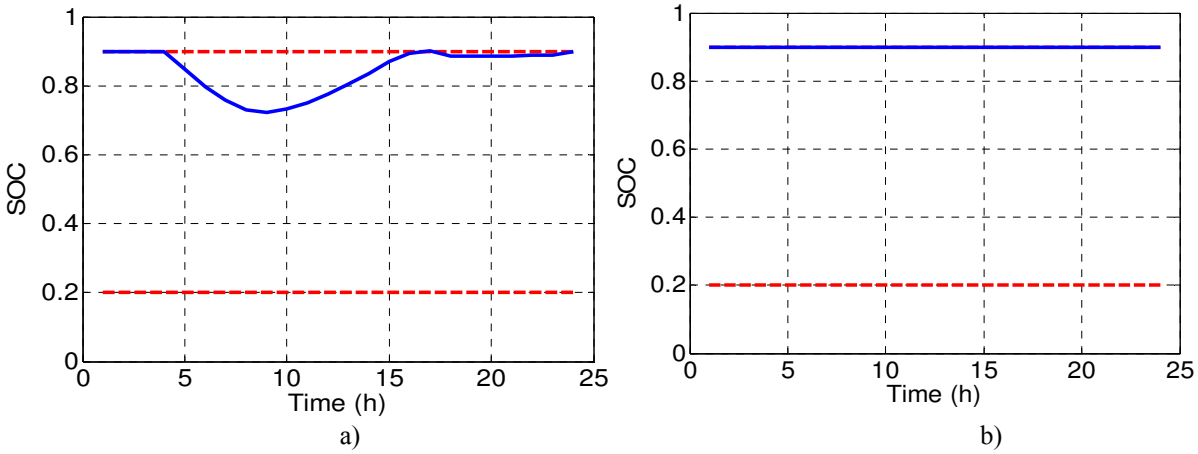

Figure V.14: BESS state of charge in a day optimal in scanerio3

a) The DP method **b) the rule-based method**

The final value of the objective function for the DP and the rule-based methods in this case is presented in Table V.4. This value in the rule-based method is smaller than that

value in two above case due to the fact that the BESS has no operation for a day.

Table V.4: The final value of the objective function in case SOC= 0.9

	DP	Rule-based
Final value ($)	116.13	136.7

The results obtained in Tables V.2-V.4 have proved that the energy management for an island microgrid determined by the DP method deduces the optimal result. Moreover, among three scenarios of the DP method, the scenario 1 (SOC = 0.5) gives the best result.

V.4. Optimization energy management for a microgrid in grid connected mode

The configuration of a microgrid in grid connected mode, which is estimated in Chapter IV, includes the main grid, PVs, and BESS. The main grid is connected by AC bus system, directly supply the power for the load demand. When the power from the PV system is not sufficient to meet the load demand, the remaining power will be covered by BESS and the main grid. On the other hand, the power excess from the PV will charge fully for the BESS and the remaining power will be sent to the main grid. It is necessary that the system has an energy management system in order to find the scheduling of sources which satisfies the objective function. In this section, the data of load is taken from the Chapter IV, while that of the PV radiation is given as equal to two out of three of the data in summer day in Chapter IV.

V.4.1. Objective function

The objective function, is expressed by (V.22) is to minimize the final value of the cash flow "CF" in [89] during the entire studied period. The cash flow includes the cash received "CR" and the cash pay "CP". The received cash is given as a negative value and the cash pay is expressed as a positive value.

Objective function:

$$\min(CF)=\min\left(\sum_{to}^{T} CR(t)+CP(t)\right) \quad (V.19)$$

The received cash "CR" is defined as the profit from the selling power excess to the main grid. It is determined by the following equation:

$$CR(t)=P_{grid}(t).FIT(t).t \quad (V.20)$$

where

P_{grid}: exchange power to the main grid (in this equation: $P_{grid}(t) \leq 0$);

FIT: Feed-in tariff

The cash pay "CP" includes the cost of electricity purchase from the grid and the battery's replacement cost. It is calculated by the following equation:

$$CP(t) = (P_{grid}(t).(t).EgP(t).t + BrC(t)) \quad (V.21)$$

where

P_{grid}: exchange power to the main grid (in this equation: $P_{grid}(t) \geq 0$);

EgP: electricity grid price

BrC: battery's replacement cost

Thus, the objective function of this problem is rewritten as follows

$$\min(CF)=\min \sum_{to}^{T} (P_{grid}(t).FIT(t).t)+(P_{grid}(t).EgP(t).t + BiC \frac{Z.(SOCx_i(t-\Delta t)-SOCx_j(t))}{1-SOH_{min}})$$

V.4.2. Constraints

** Power balance constraint:*

$$P_L(t)=P_{PV}(t) + P_B(t) + P_{grid}(t)$$

** BESS power output:*

$$P_{Bmin} \leq P_B(t) \leq P_{Bmax}$$

** BESS state of charge constraint:*

$$\Delta SOC_{min} \leq \Delta SOC(t) \leq \Delta SOC_{max}$$

$$SOC_{min} \leq SOC(t) \leq SOC_{max}$$

** BESS's ageing constraint:*

$$SOH(t) \geq SOH_{min}$$

** Grid power constraint:*

The exchange power is bounded as follows: $P_{grid}^{min} \leq P_{grid}(t) \leq P_{grid}^{max}$

In order to minimize the received power from the main grid, the P_{grid}^{max} value is limited as follow:

$$0 \leq P_{grid}^{max} \leq P_{peak\ load}$$

And

$$P_{grid}^{min} = - P_{grid}^{max}$$

In this section, the power of peak load is: $P_{peakload} = 50kW$.

V.4.3. A rule-based energy management strategy

In this part, a 'constraint' management strategy for grid connected microgrid is proposed with based on the predefined ruled. The principle of the ruled based energy management is based on the following main rules:

- PV system is primarily used to supply the loads
- The BESS only discharged when the PV and grid are not sufficient
- The BESS is charged as soon as possible with the first available source.

The proposed ruled based energy management has to assure the following constraints:

$$P_L(t)=P_{PV}(t) + P_B(t) + P_{grid}(t)$$

$$SOC_{min} \leq \Delta SOC\ (t) \leq SOC_{max}$$

$$P_{Bmin} \leq P_B(t) \leq P_{Bmax}$$

$$P_{grid}^{min} \leq P_{grid}(t) \leq P_{grid}^{max}$$

The approach is performed as follows:

- The grid power is predicted by the function of the PV and the load power.
- The corresponding BESS power is calculated by the equation V.12
- Verification the constraints compliance on the BESS and the grid
- The maximum import power from grid is the optimal value obtained by DP method

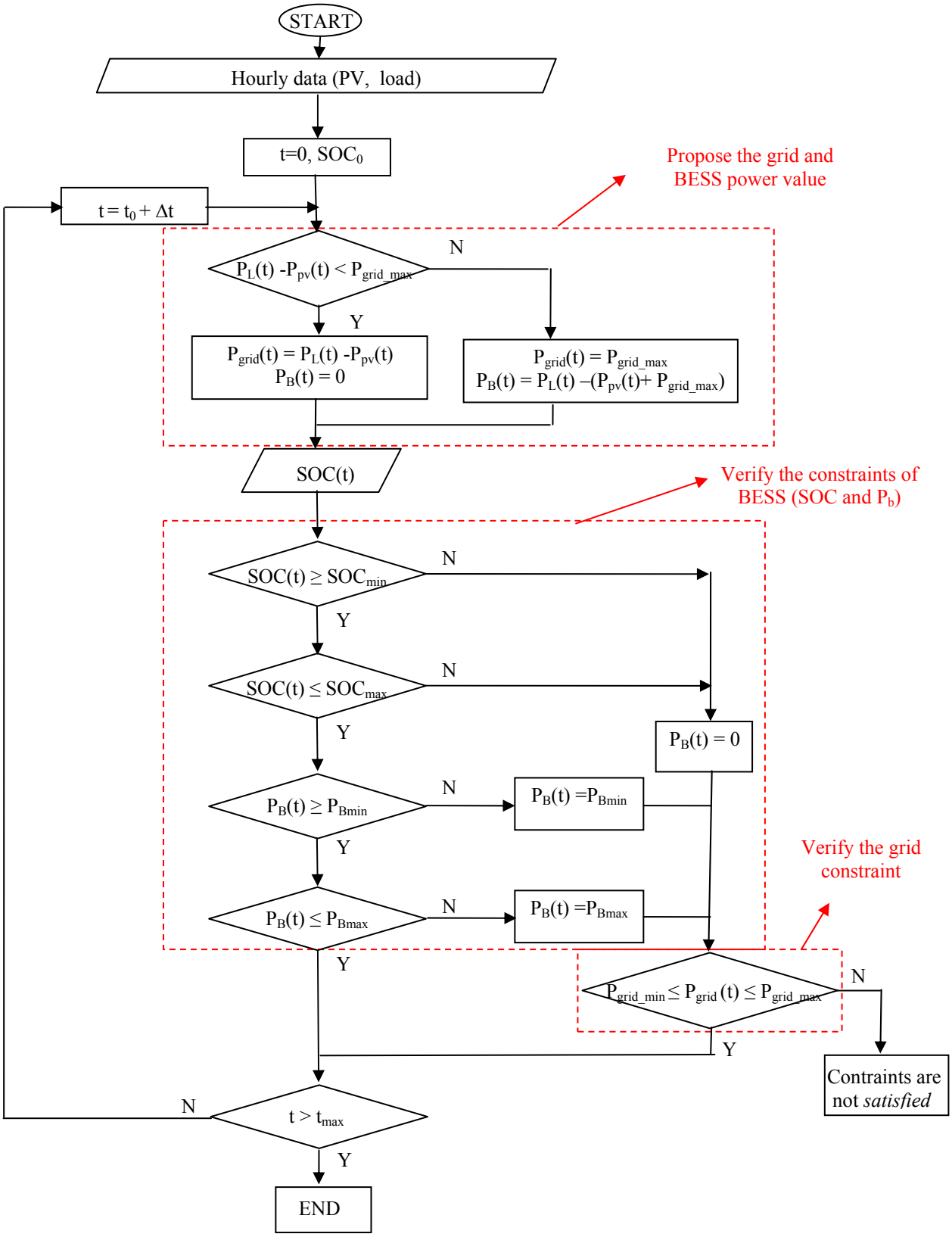

Figure V.15: The flowchart of rule-based management in island microgrid

V.4.4. Bellman algorithm Application in optimal energy management for a grid connected microgrid

The power of BESS (P_B) is estimated at each stage of charge variation ΔSOC. After that, the grid power is calculated following the P_B, P_L and P_{PV}. Then, the estimated P_{grid} has to satisfy the bound of grid power.

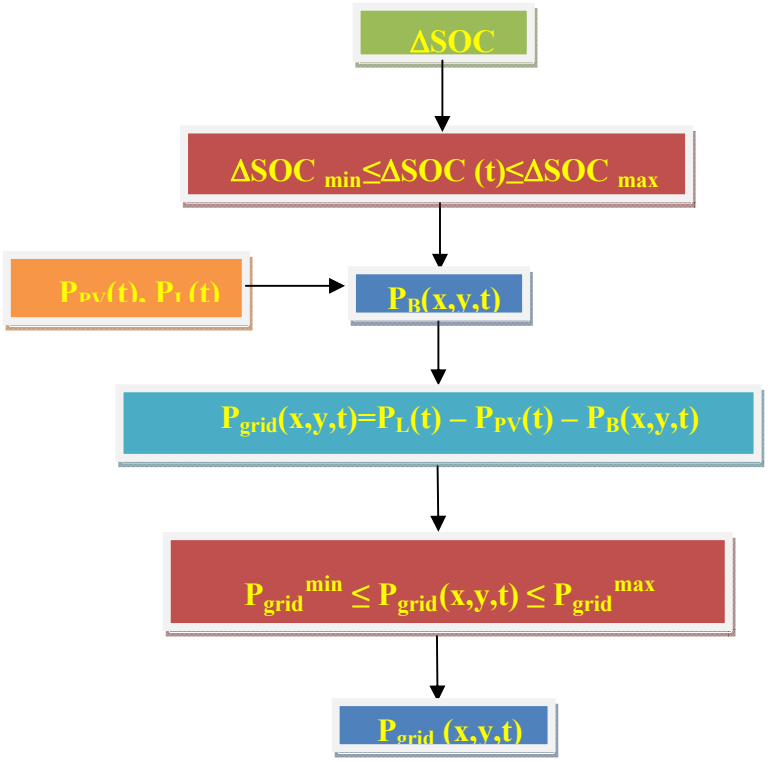

Figure V.16: Process of calculating the P_B and P_{grid}

Given an initial vector P_{grid}^{max}, defined as: $P_{grid}^{max} = \{P_{grid,i}^{max}\}$, i = 1,..k

For each element of P_{grid}^{max}, the Bellman algorithm is applied (similarly to island mode) to find the minimum of CF_i.

Assume that: $A_i = \text{argmin} CF_i$

After running all elements of P_{grid}^{max}, the optimal energy management for a grid-connected microgrid is obtained as the minimum value of vector A

$$\textbf{Min(A), A=\{A}_i\textbf{\}}$$

The flowchart of the algorithm with the computation of the weights of the edges is shown in the Figure V.17

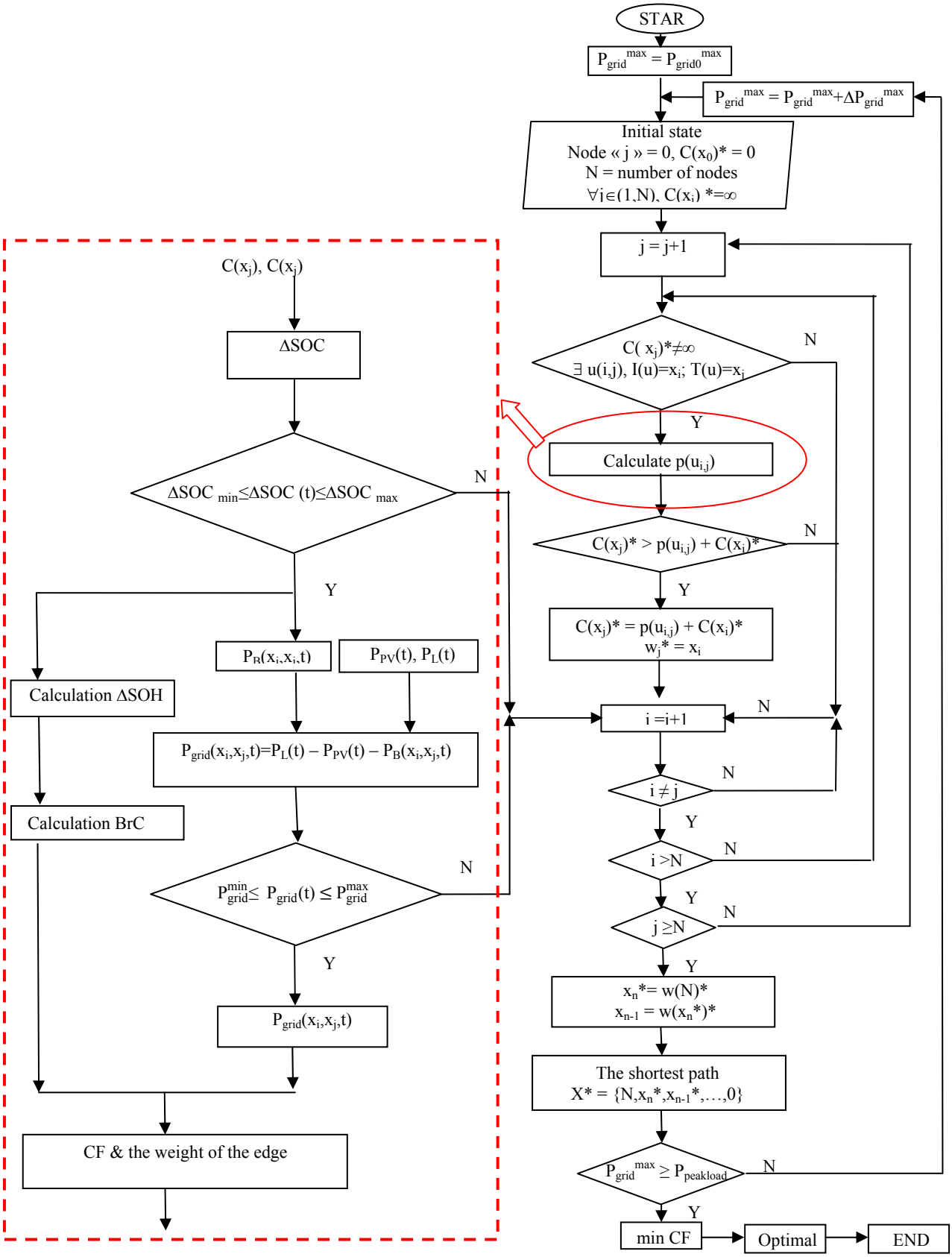

Figure V.17: The flowchart of the optimal management in grid connected mode

V.4.5. Simulation results and discussion

Optimal energy management of a microgrid in grid connected mode is to be presented in this part. The day-ahead forecast value of load and PV is shown in Figure V.18. The Table V.5 provides the simulations parameter values in this mode. The case studied with $SOC_{init} = SOC_{final\ (a\ day)} = 0.5$, has been chosen for simulation such that it gives the maximum flexible management in a day-ahead supervision. The economic data is taken in Table IV.1 of Chapter IV. In this part, the day-ahead simulation is performed to determine the minimum of the cash flow "CF" in 2 cases with the different tariffs: autonomy tariff and dynamic tariff. In each the maximum exchange power with the grid, the simulation is done when the state of charge SOC variable reaches its final state. The result simulation is achieved with the minimum of CF as well as its operation.

Objective

$$\min(CF)=\min\left(\sum_{to}^{T}(P_{grid}(t).FIT(t).t)+(P_{grid}(t).EgP(t).t + BrC(t))\right)$$

with

$$P_L(t)=P_{PV}(t) + P_B(t) + P_{grid}(t)$$

$$P_{Bmin} \leq P_B(t) \leq P_{Bmax}$$

$$\Delta SOC_{min} \leq \Delta SOC(t) \leq \Delta SOC_{max}$$

$$SOC_{min} \leq SOC(t) \leq SOC_{max}$$

$$SOH(t) \geq SOH_{min}$$

$$P_{grid}^{min} \leq P_{grid}(t) \leq P_{grid}^{max}$$

$$0 \leq P_{grid}^{max} \leq P_{peak\ load}$$

Table V.5: The simulation parameter values in the grid connected mode

Name	Value	Unit
T	24	h
Δt	1	h
δSOC	0.001	
SOC(t_o)	0.5	
SOC_{min}	0.2	
SOC_{max}	0.9	
ΔSOC_{min}	-0.7	
ΔSOC_{max}	0.7	
SOH_{min}	0.7	
$P_{peakload}$	50	kW

Figure V.18 shows the day-ahead forecast value of load and PV

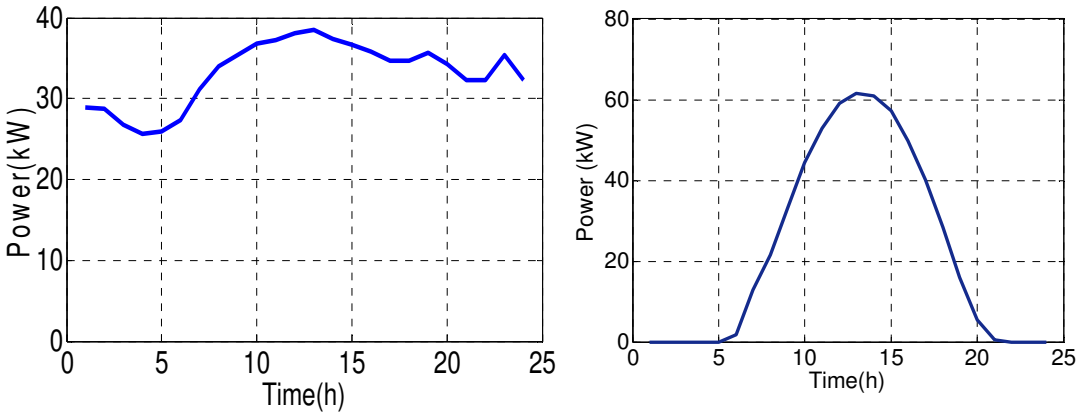

a) b)

Figure V.18: The day-ahead forecast value of load and PV in the grid connected mode

a. The day-ahead loads b. The output power of PV

- Scenario1: The power is sold/bought with the autonomy tariff

In this scenario, the power is bought/sold from/to the main grid with constant tariff for the whole day (EgP=constant, FiT=constant). The electricity grid price and the feed-in tariff is shown in Table V.6

Table V.6: The electricity grid price and the feed-in tariff in a day

Name	Value
Electricity grid price (EgP)	0.12€ (0.165$)
Feed-in tariff (FiT)	0.072€ (0.1$)

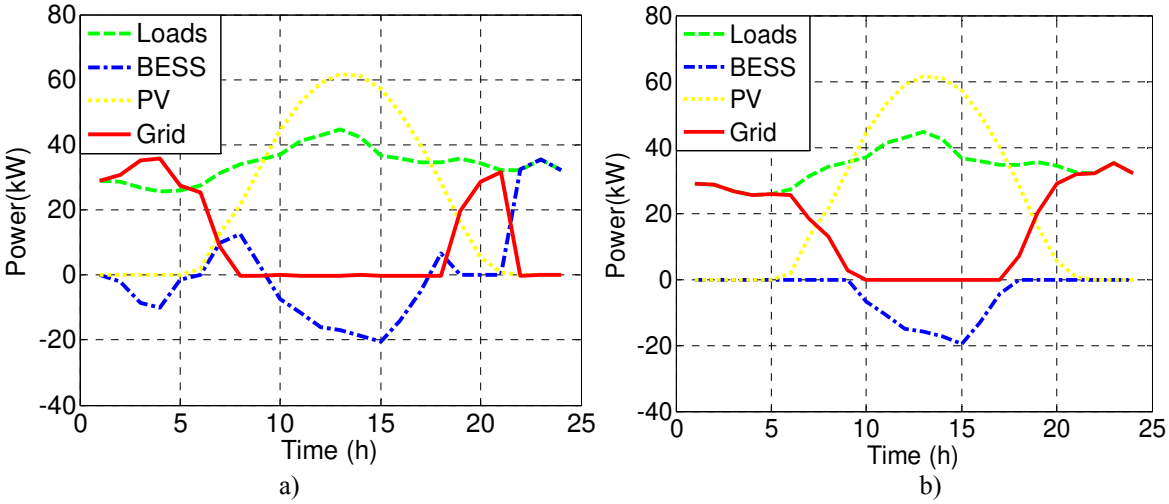

Figure V.19: power schedule of a microgrid in grid connected mode in scenario 1

a) The DP method **b) the rule-based method**

It can be seen from Figure V.19a, the power is bought from the grid at the beginning of the day to charge for the BESS. This leads to that the state of charge SOC increases, is shown in Figure V.20a. At 6am the batteries begin to discharge in order to provide a part of the load, the received power from grid decreases. At t=8am, the total power of BESS and PV meet the load demand; therefore, the exchange power is equal to zero. Then, when PV power exceeds the load demand, most of the power is charged for the BESS. The SOC value will increase to 0.85. After that, when the PV source is not available, the loads are mainly supplied by the main grid and the BESS until the end of the day. On the other hand, the grid plays a main role for supplying the demand loads in the rule-based strategy. The BESS is fully charged when the available PV power exceeds demand loads. The SOC increases from 0.5 (in the beginning day) to 0.85 (at the end of day), is shown in Figure V.20b.

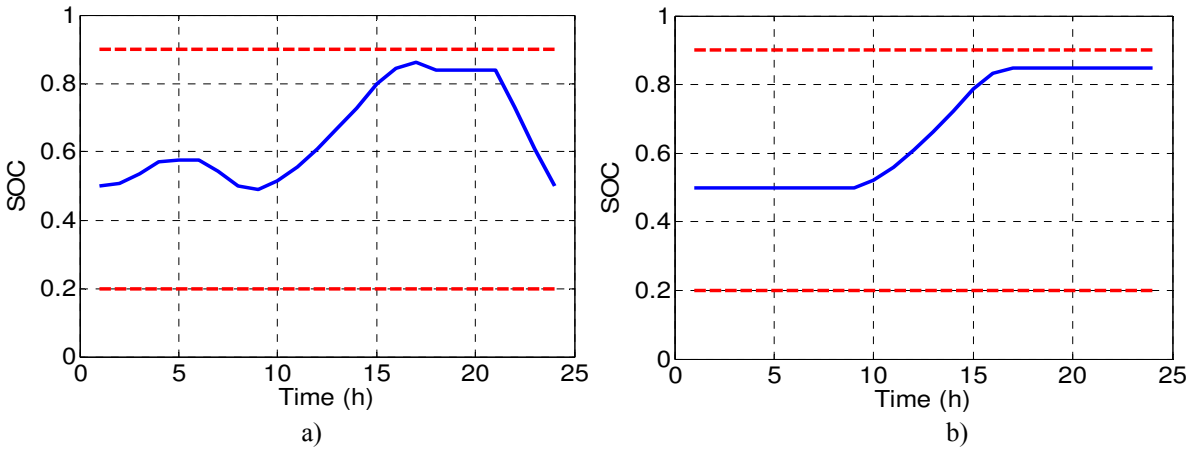

Figure V.20: BESS state of charge in a day optimal in scanerio1

(a. The DP method; b. The rule-based method)

The final value of the objective function for the DP optimization and the rule-based management is presented in Table V.8. The DP algorithm gives a lower value than this value given by the rule-based method.

Table V.7: The final value of the objective function

	DP	Rule-based
Final value ($)	44.6	63.2

On the other hand, based on the flow chart of DP method (Figure V.17) the proposed optimal energy management can find the optimization of the maximum imported power from grid. As can be seen from the Figure V.19, the optimal maximum value of the received power from grid is estimated as 36kW.

- Scenario2: The power is sold/bought with the dynamic tariff

In the scenario 2, the power is sold/bought to/from the main grid with dynamic tariff for a day. The electricity grid price (EgP) and the feed-in tariff (FiT) are shown in Figure V.21

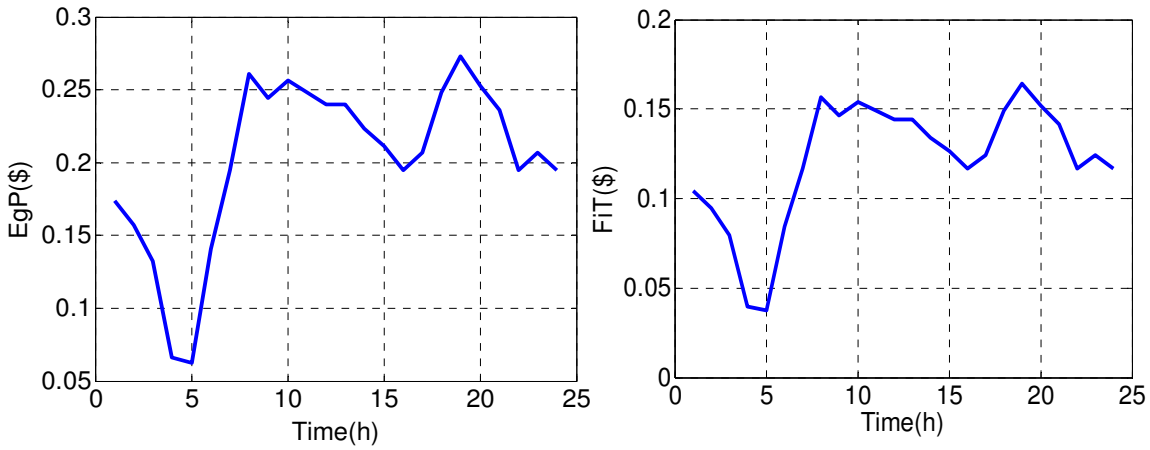

Figure V.21: The electricity grid price (EgP) and the feed-in tariff (FiT)

The optimal power schedule in scenario 2 is shown in Figure V.22a. The power from the main grid is supplied for the demand loads and charged for BESS in the beginning of the day. This is due to the fact that the tariff is given as low value in this period time. After that, the demand loads are supplied from the PV and the BESS from 7am to 5pm. Then, the BESS plays the main role to answer the demand loads. From the Figure V.22b, the demand loads is received the power from the main grid. The BESS is only used to charge the power excess from the PV production.

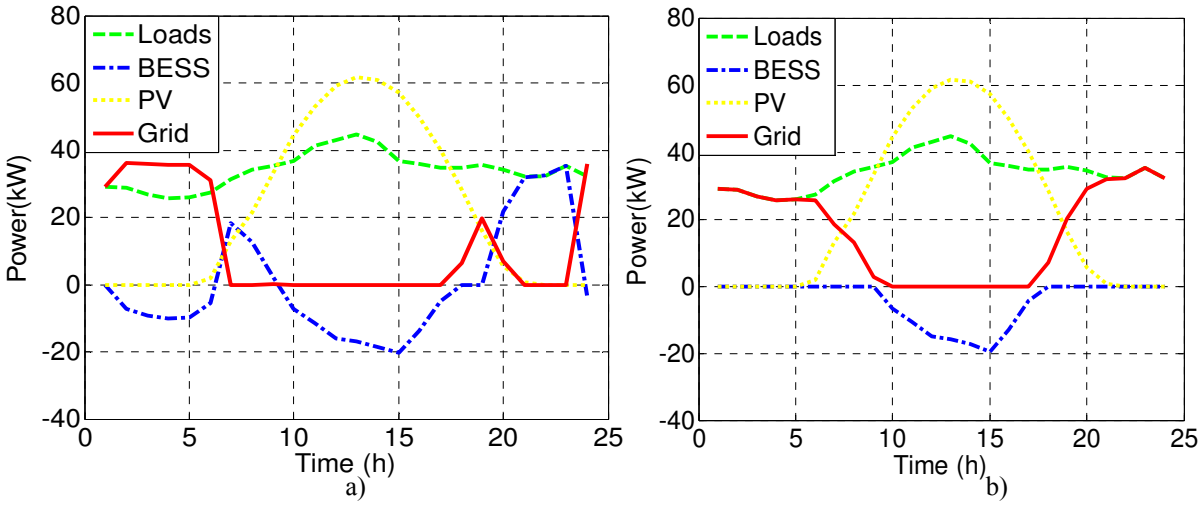

Figure V.22: Power schedule of a microgrid in grid connected mode in scenario 2

The BESS state of charge for a day optimal in this scenario is shown in Figure V.23. From this figure, one can see that the SOC value is always bounded by the limit values. During the day, the BESS performs charge /discharge cycle corresponding the tariff curve in DP method, thus the BESS is well controlled and got the high efficiency. On the other hand, the BESS is always charged as soon as possible in the rule-based method. This leads to the BESS is always fully state at the end of the day;

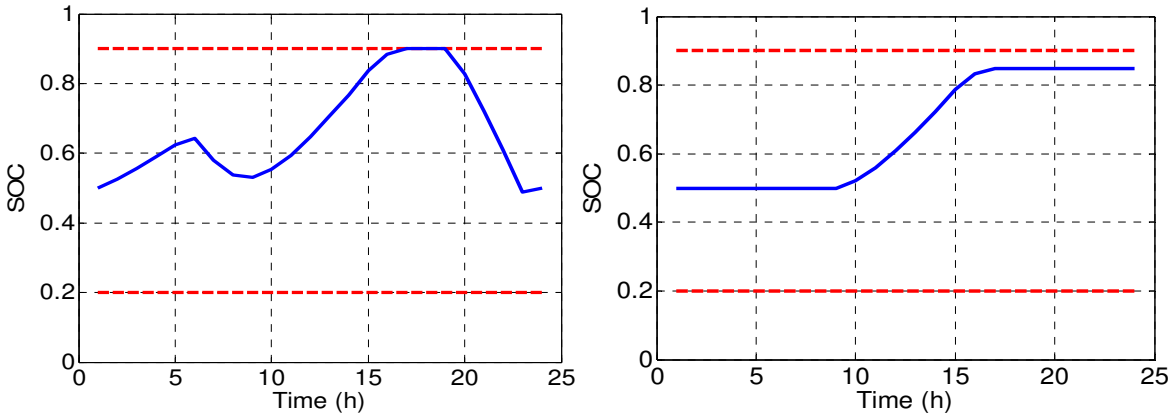

Figure V.23: BESS state of charge in a day optimal in scanerio2

The final value of the objective function for the DP optimization and the rule-based management is presented in the scenario 2, is shown in Table V.8. It is clear that the DP method gives better final value than the rule-based method

Table V.8: The final value of the objective function

	DP	Rule-based
Final value ($)	39.6	69

Similar to the above case, the optimal maximum value of imported power from grid is estimated in the DP method. This value in this scenario is 36kW a day.

V.5. **Conclusion**

In this chapter, the optimal energy management of PV-diesel-BESS hybrid and grid connected PV-BESS systems has been presented. Dynamic programming technique is used to find the optimal schedule of power sources as well as the export/ import with the main grid, and thus, minimizes the operation cost of the microgrid and CO2 emission. The final value obtained is compared with this value in the Rule-based method

In the optimal energy management of an island microgrid (PV-diesel-BESS hybrid), the minimum of CS, the CO2 emission as well as optimal the schedule of diesels and BESS in three scenarios with different the initial state of charge are achieved. The simulation results are carried out in the sense that the proposed method not only gives the global optimal of energy management but also finds the best of initial state of charge to get the best operation and management of an island microgrid.

In the optimal energy management of grid-connected microgrid, the minimum of cash flow CF in two types of tariff: autonomy tariff and dynamic tariff are achieved in order to optimize the schedule of sources, as well as the import/export power with the main grid. The simulation results are carried out that the method not only gives the global optimal of energy management in two scenarios but also to find the minimum value of maximum received power from the main grid. This leads to the optimization of the operation cost of a microgrid in grid connected mode.

CHAPTER VI :

Microgrid control

SUMMARY

VI.1. **Introduction**

Microgrid control includes two terms that are a coordinated (or energy management) and a local control [1]. This chapter concentrates on the local control. The efficient microgrid operation can be enhanced by using the intelligent local controllers for DER. In fact, these controllers participate in controlling the frequency and voltage in different operation modes of microgrid: islanded mode, grid connected mode; furthermore, they distribute efficiently for frequency and voltage regulation during transitions from interconnected to islanded operation.

The main tasks of DERs controller are expected to allow power sharing between different sources at different locations of them within the microgrid. In order to reach these tasks, the electronic converters which are the interfaces of DERs to the network, are adjusted. This allows that the frequency and the voltage of microgrid will be maintained in the predefined limits. Furthermore, in order to avoid the lost or lack of the communication as well as reducing the investment in communication line, a local controller strategy based on the frequency and voltage droop control is used. By this way, the local information of frequency and voltage at each DER are used to facilitate the power sharing between DERs in the microgrid. This is due to the fact that the active power and reactive power are related with the frequency and voltage, respectively.

In this chapter, the local control for DER is presented. Firstly, a control strategy based on the droop control is proposed to bring the voltage and frequency back to the normal values by using the primary and secondary controls. In the primary control, the implemented droop characteristic in the VSI is used to ensure that the frequency and voltage remain close to their set point values. After that, the secondary control is needed to restore the frequency and voltage to the nominal value. The simulation results of an island microgrid with the PV, battery and diesel are presented to assess the efficiency of the proposed method. Secondly, new microgrid architecture is used in which the diesel is not available. The fuzzy logic is added in the proposed control. In this method, the frequency is not only expressed as a function of power but also of the state of charge and initial operation condition. The simulation is performed in some cases such as: island mode and transition from the grid connected to islanded mode.

VI.2. **Control strategies for DERs**

When a microgrid is connected with the main power, the voltage and frequency is maintained by the main grid. Thus, all the inverters within microgird can be operated in PQ mode. However, when the disconnection with the main power occurs, the microgrid will be lost control. This is to the fact that there are not a generator (like the main grid) to keep the frequency, voltage as well as the balance between production and consumption. Thus, at least, a voltage source inverter (VSI) in V/f mode is needed to provide a reference for frequency in a microgrid. The VSI receive the useful information to provide a voltage and frequency primary regulation in the islanded microgrid. This leads the microgrid operation in islanded mode and transition to islanded operation can be performed without changing the control mode of any inverter [80].

In some literatures from the research developed within the MicroGrids project [80], [101], [102], there are two main control strategies for DERs:

- Master slave control
- Multi-master control

VI.2.1. Master slave control

A system with a voltage source, as a master and current sources as slaves (grid supporting units) is described in Figure VI.1 [1].

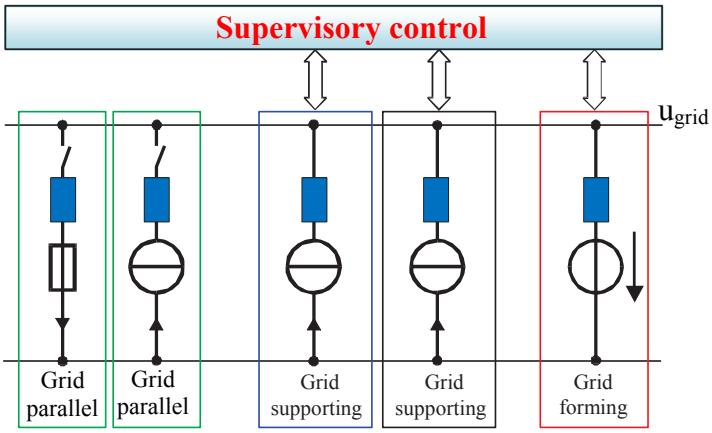

Figure VI.1: a system with one voltage source and current sources

This control method has been used for a system which has multiple parallel inverters. In this approach, an inverter plays a master unit to regulate the voltage and frequency whereas the other units keep the constant power. The master unit acts a V/f controller

inverter and the remaining units as the P/Q controlled. This method is a simple control, however it has some drawbacks such as: high communication requirement; the system is difficult to expand [103]; system reliability depends on the master unit. Thus, the multi-master control is used to overcome these disadvantages.

VI.2.2. Multi - Master control

In order to avoid using the communication line or extra cable, the multi-master method has been presented in [104]. In this method, the inverters themselves set immediately the active and reactive power. A 'droop' concept is applied for the DERs in microgrid, a similar way to this used by rotating machines in the large system. The active power- frequency droop and reactive power- voltage droop is shown in Figure VI.2 [87].

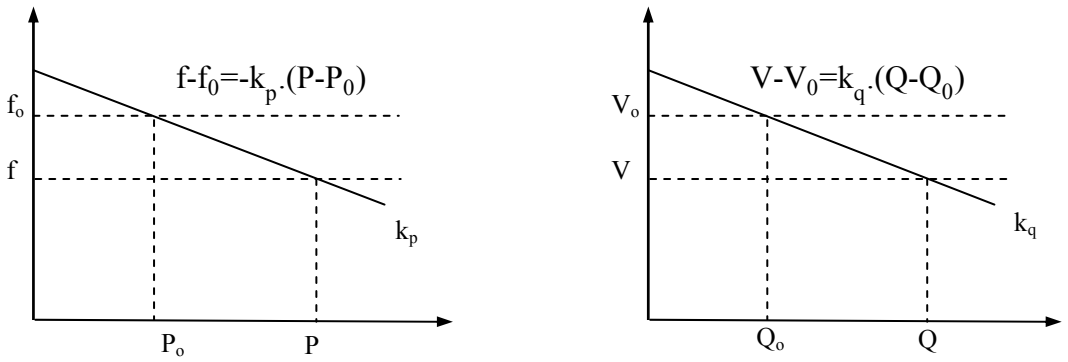

Figure VI.2: Frequency and voltage droop characteristics

VI.2.2.a. Primary droop control

Similar to the power flows between two power systems, the active power and the reactive power flow between two parallel inverters with negligible resistance is calculated in [1]:

$$P=\frac{U_1.U_2}{\omega.(L_1+L_2)}\sin(\delta) \quad \text{(VI.1)}$$

$$Q=\frac{U_1^2}{\omega.(L_1+L_2)}-\frac{U_1.U_2}{\omega.(L_1+L_2)}\cos(\delta) \quad \text{(VI.2)}$$

where

P: active power

Q: reactive power

U_1,U_2: voltage magnitudes (rms) of the voltage sources

δ: voltage phase shift between voltage sources

ω: angular frequency of the grid

L_1, L_2: coupling inductances

From equation VI.1 and VI.2, one can see that the active power can be controlled by controlling the voltage phase shift δ, while the reactive power can be controlled by controlling voltage magnitude. Furthermore, the angle difference is given by the integral of the frequency control. Thus, the active and reactive power sharing among the DGs are described as the function of frequency and voltage, respectively. The power sharing is presented in Figure VI.3

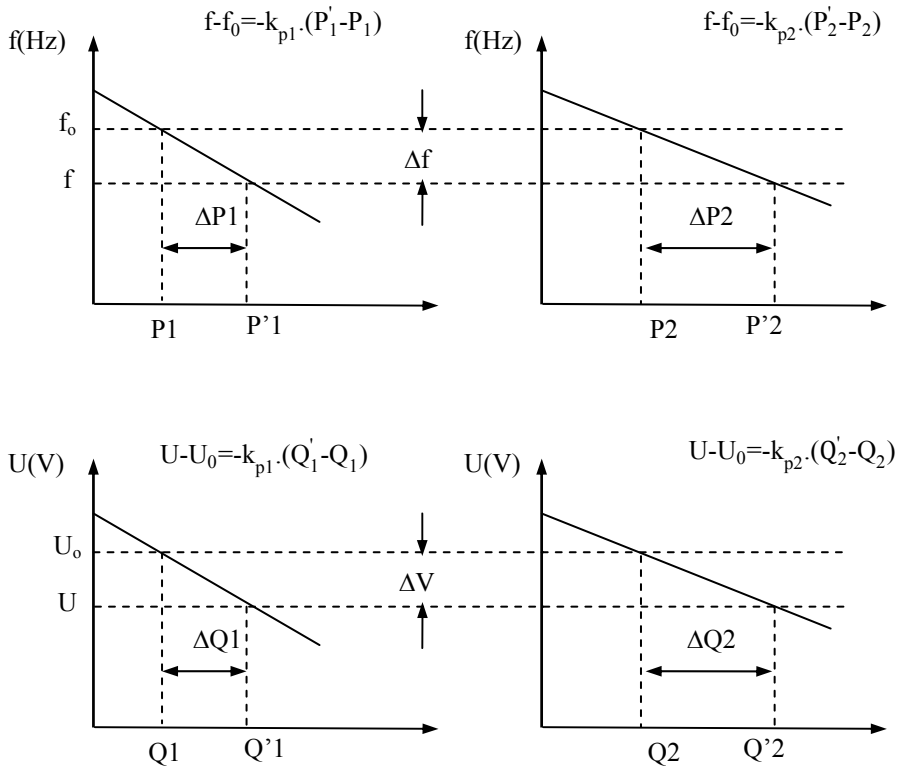

Figure VI.3: Power sharing of two parallel inverters

The frequency droop (f/P) and voltage droop (V/Q) is added in the voltage source inverters is shown in Figure VI.4. The frequency is measured from the phase-locked loop (PLL) with based on the three phase voltage. The frequency deviation is multiplied by a gain constant to obtain the set-point active power. Similarity, the measured voltage is compared with the reference voltage. The voltage dip is also multiplied with a gain to obtain the reactive power set point. The active power and reactive power variations are fixed as the input of power control of a DER unit.

The droop coefficients and the set-points are controlled by restoration process to adjust the operation of output of DER. The restoration process is performed by primary and secondary control

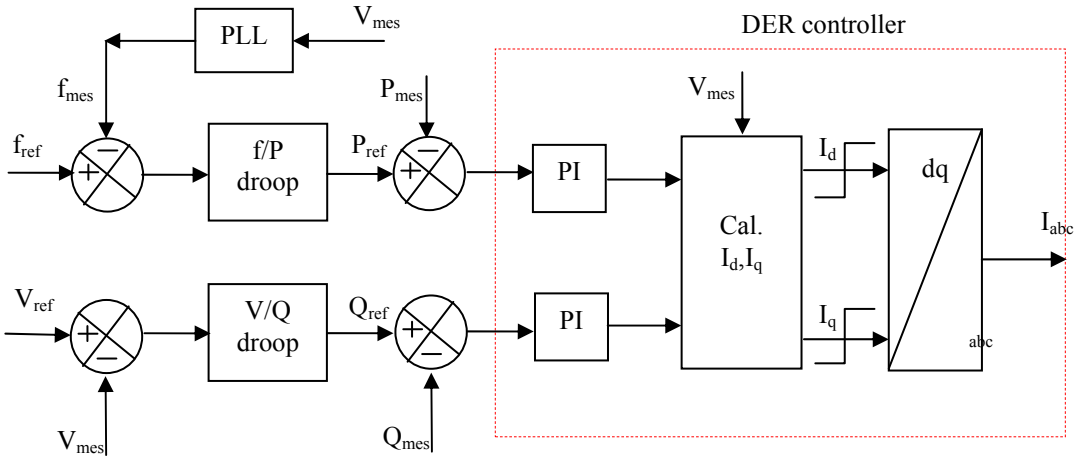

Figure VI.4: Primary droop control strategy

VI.2.2.b. Secondary droop control

First, the primary control responses rapidly in order to bring the frequency to a value close to the nominal value. Then, the secondary control is used to restore the frequency to the nominal value by controlling the power set point. The response of secondary control is slower than the primary control. The secondary control can be presented in Figure VI.5

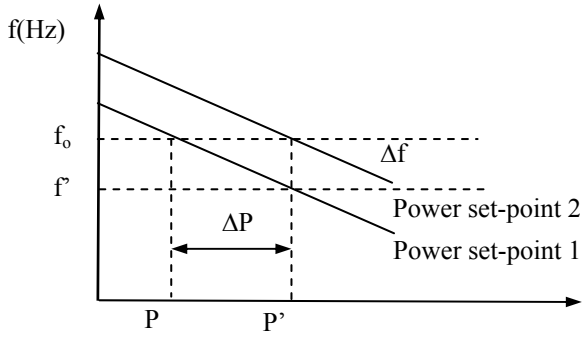

Figure VI.5: Secondary control with power set point changing

Assume that the disturbance occurs in the system. The frequency is maintained at new value (f') after the primary control. The new output power of the sources for secondary control can be estimated by following equation:

$$P'_i = P_i + \Delta P_{1i} + \Delta P_{2i} \quad \text{(VI.3)}$$

where

P_i: the initial active power value of DER i

ΔP_{1i}: the active power change according to the primary control of DER i.

ΔP_{2i}: the active power change according to the secondary control of DER i.

The total power change by the secondary control can be calculated such as:

$$\Delta P_{2\Sigma}=(f_{ref}- f'). (\sum \frac{1}{k_i}) \quad \text{(VI.4)}$$

where

k_i: the droop value of DER i

VI.2.2.c. Simulation case

A simulation case of an island microgrid is presented in Figure VI.6.

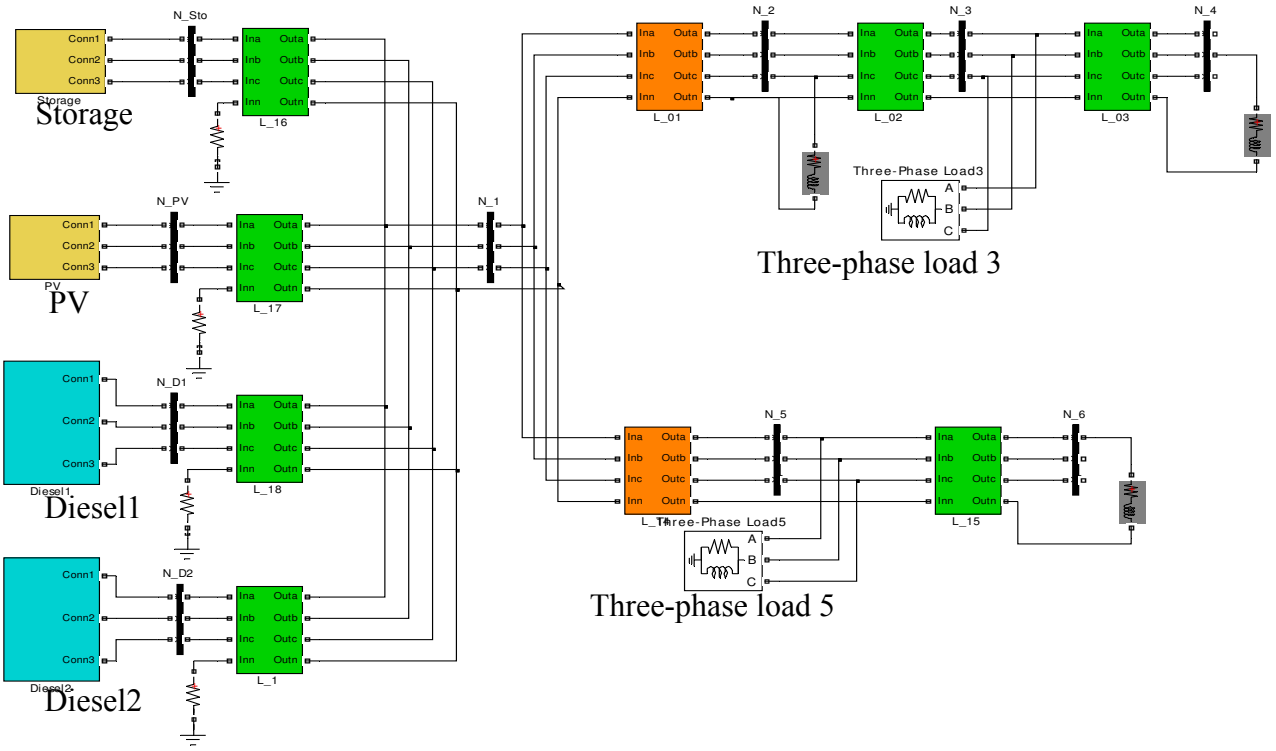

Figure VI.6: System modeling with MATLAB/Simulink

The system:

- Peak demand of the residential area of 70 kW
- PV system with a rated power of 60 kWp
- Two Diesel Generators of a rated power of 60 kVA
- Battery energy storage system (100 kWh).

The simulations are performed in the following cases:

* Normal operation

* Under disturbance operation

Scenario 1: Load variations

Scenario 2: Production variations (tripping diesel).

Scenario 3: PV power losing

Scenario 4: Tripping BESS.

**** Normal condition operation***

The active power variation of PV-Diesel-BESS for a day is shown in Figure VI.7. The first diesel (Diesel 1) is started at 6pm and stopped at 5am, whereas the second (Diesel 2) is connected between 4am and 9am; 5pm and 10pm, respectively. The daily load, is presented in Figure VI.6 (negative value) reaches a peak of 70kW at 7pm. The PV system production supply to load demand from 6am to 9pm.

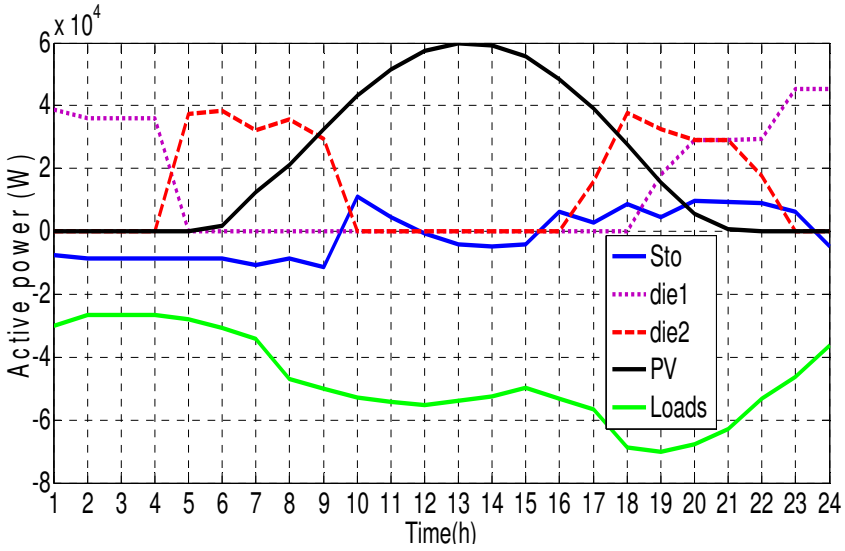

Figure VI.7: Active power variation of PV-Diesel-BESS and loads

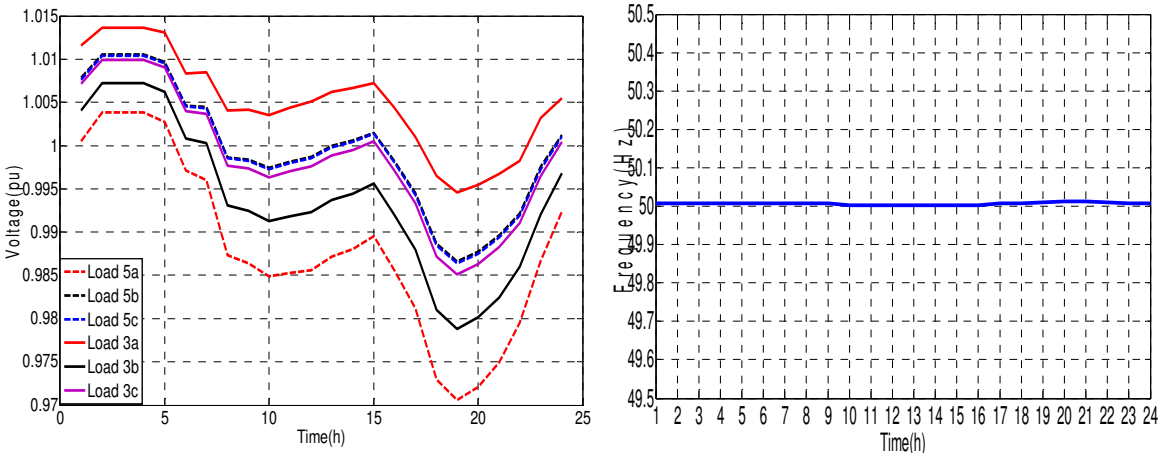

Figure VI.8: The voltage and frequency of PV-Diesel-Battery system

The voltage and frequency system are maintained within the permitted values as shown in Figure VI.8.

**** Under disturbance operaton***

- Scenario 1: Load Variation

In this case, the system includes: PV system with P_{PV} = 20kW, Diesel 1 and BESS. The total power of loads is given as 50kW. At t=3s, the loads are suddenly increased about 10%. As can be seen the Figure VI.9 and Figure VI.10, the diesel genset and the BESS power are adapted to answer the power load variation as well as regulate the voltage and the frequency (primary control). Then the secondary regulation is performed by changing the set-point to bring the frequency to the normal value

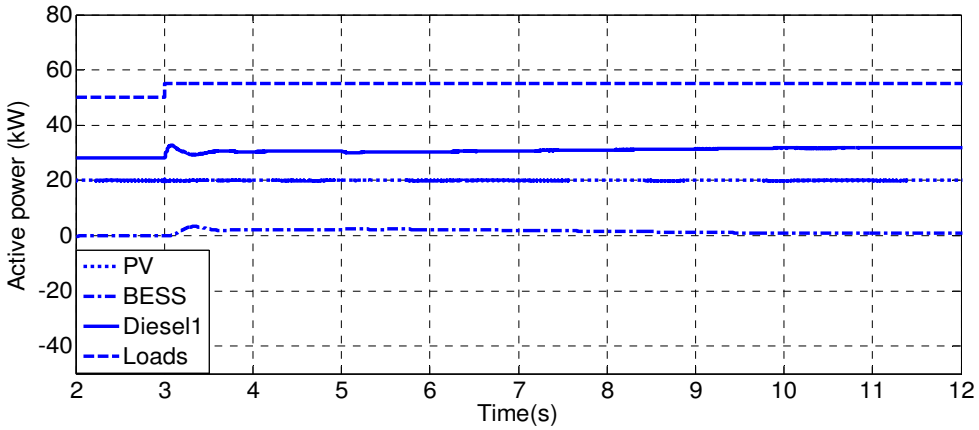

Figure VI.9: Active power variation of PV-Diesel-BESS in scenario 1

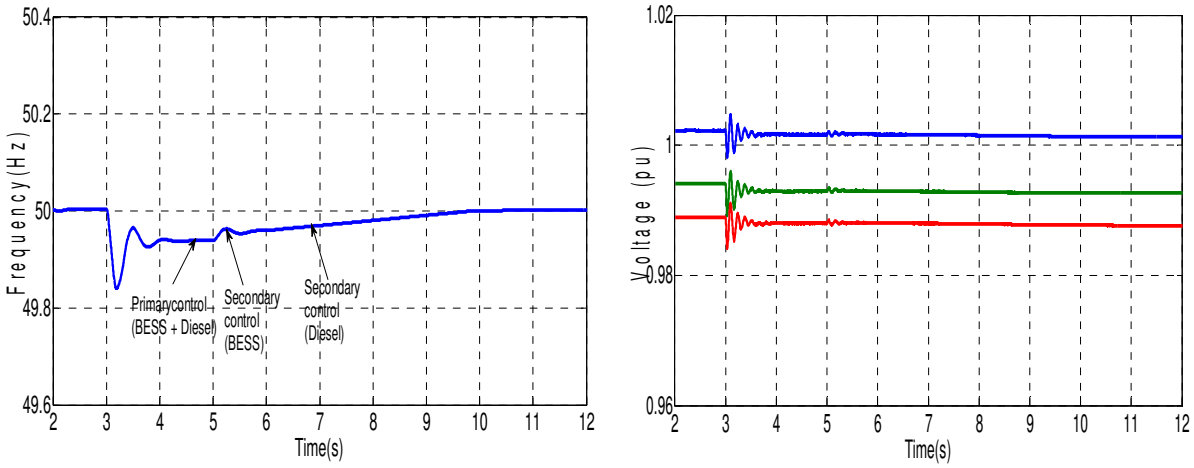

Figure VI.10: The voltage at load 3 and system frequency in scenario 1

- Scenario 2: A diesel generator tripping

In this scenario, the system includes two diesels, BESS and loads (50kW). The active power variation of Diesels and BESS is shown in Figure V11. The second diesel generator is tripped at t=5s. The power deficit is covered by the Diesel 1. Figure VI.12 describes the voltage at load 3 and system frequency. As can be seen from this Figure, one can see that the voltage is oscillated before it obtains the stable value within limit value.

The frequency drop to a stable value according to primary control and returns to the nominal value at t=12s.

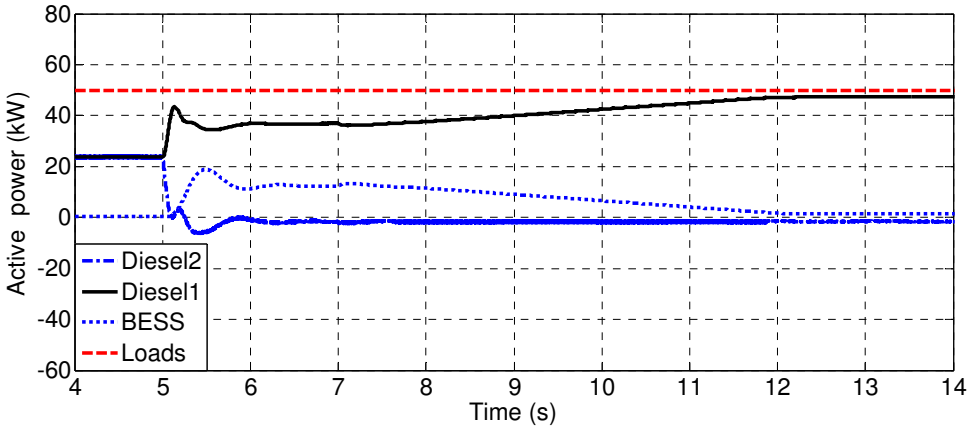

Figure VI.11: Active power variation of Diesels-BESS and loads in scenario 2

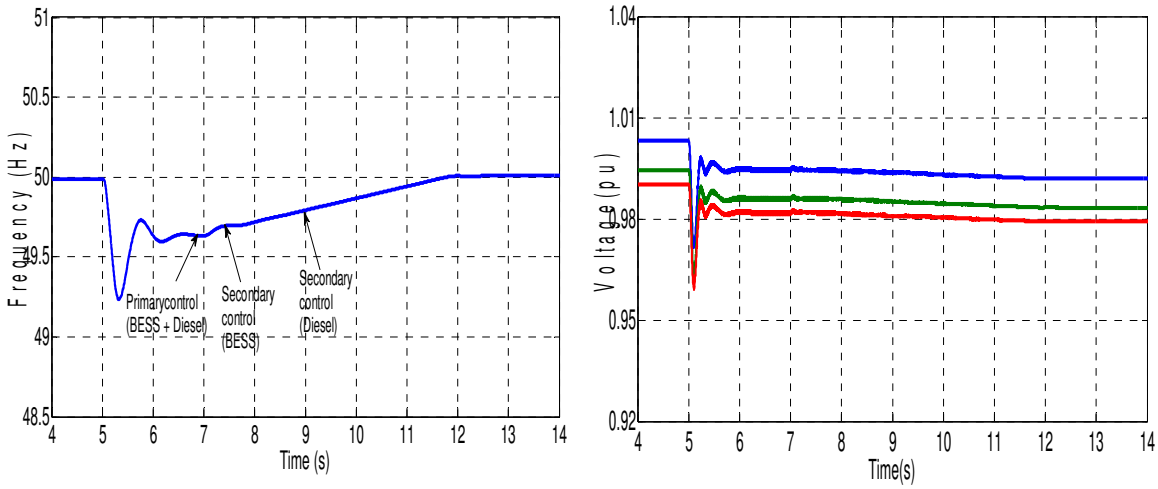

Figure VI.12: The voltage at load 3 and system frequency in scenario 2

- *Scenario 3: PV production suddenly decreasing*

In this case, the PV power suddenly reduces from 20kW to 5kW at t=3s. The simulation result is shown in Figure VI.13 and Figure VI.14. After the primary control, the active power is adapted to keep balance between productions and consumptions. The frequency turns back the nominal value after the BESS and the diesel adjust the set points according to the secondary control. On the other hand, the voltage at load 3 is maintained on the predefined threshold

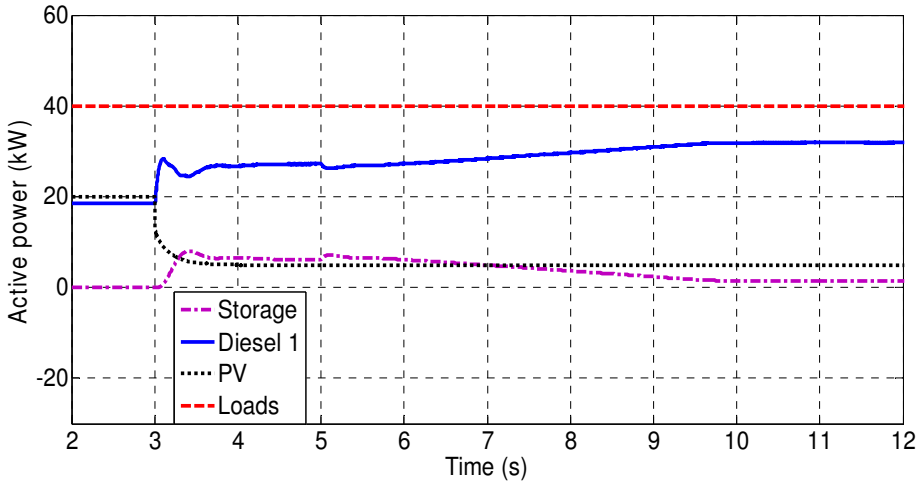

Figure VI.13: Active power variation of PV-Diesel-BESS and loads in scenario 3

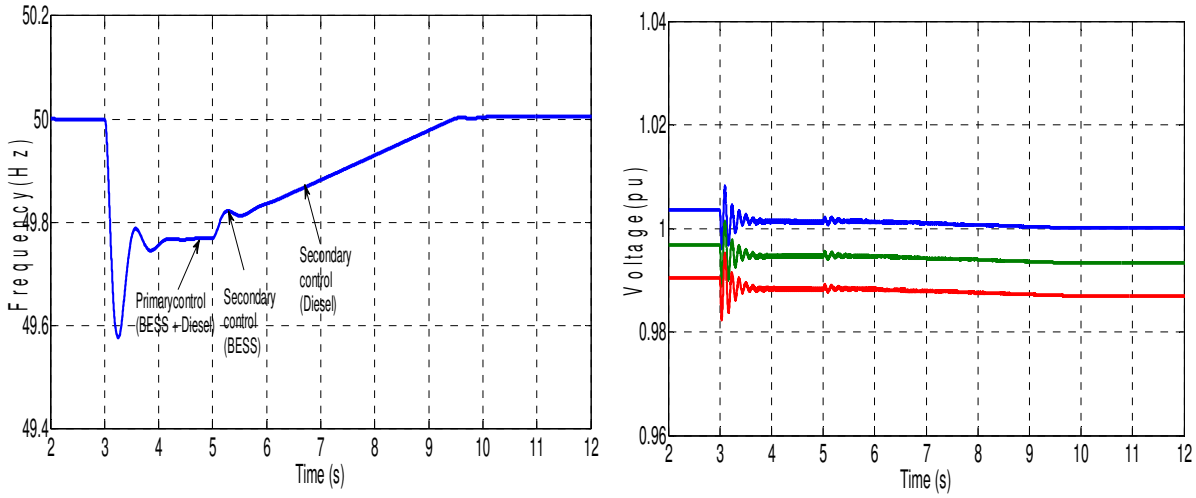

Figure VI.14: The voltage at load 3 and system frequency in scenario 3

- *Scenario 4: BESS tripping*

In this case, the system comprises of the battery banks (P_{sto} =1kW), PV system (P_{PV} = 20kW) and loads (60kW). At t=13s, the BESS is tripped from the system. As can be seen from the Figure VI.16, the voltage and system frequency is kept at stable state after some oscillation. After that, the secondary control process is performed to bring the voltage and frequency to nominal value.

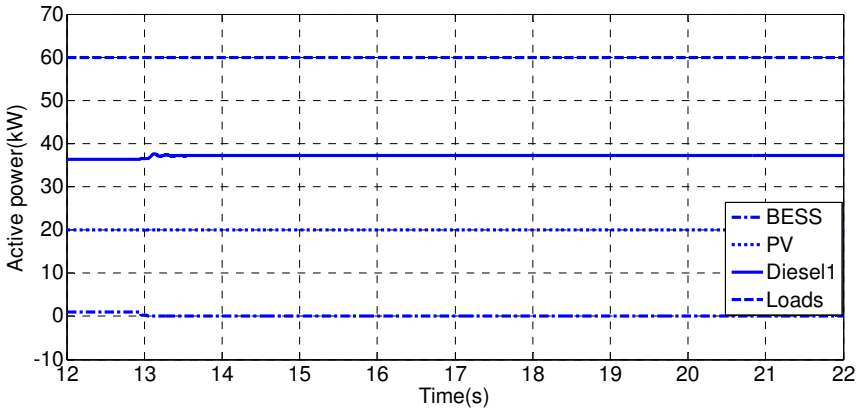

Figure VI.15: Active power variation of PV-Diesel-BESS and loads in scenario 4

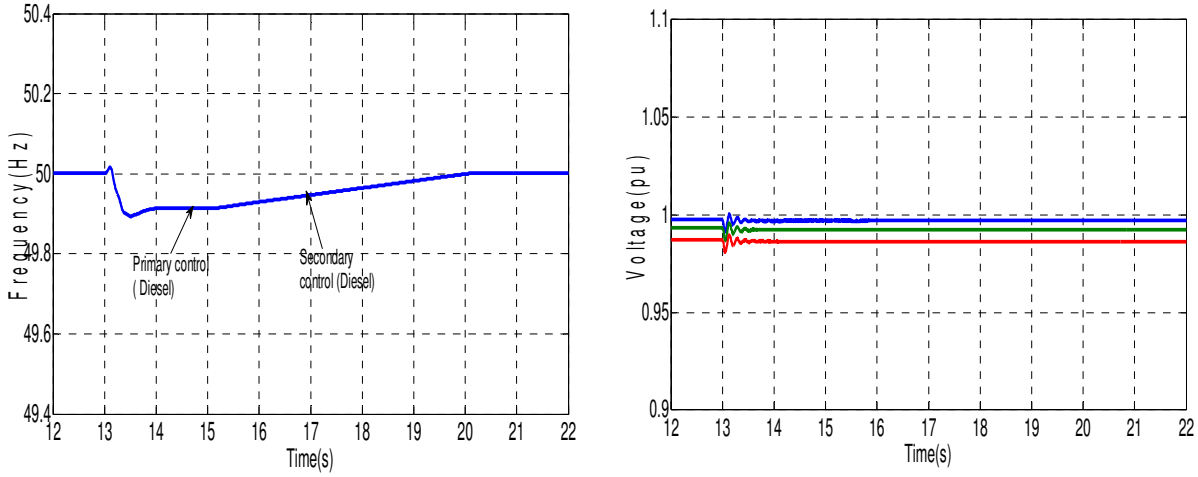

Figure VI.16: Active power, voltage and frequency of system in scenario 4

VI.2.3. An intelligent control strategy

In this subsection, an intelligent control strategy for microgrid is proposed. This can be used for microgrid operation modes such as: transition to the island mode and island mode. In this method, new microgrid architecture is defined. This architecture includes the microsources and the BESS without diesel gensets. In the connected mode, the voltage and frequency is regulated by the main grid. However, in the island mode, the BESS inverters with the V/f control play a role of the master unit. They substitute the diesel (in above case) to maintain the voltage and frequency in the permitted limit. Furthermore, the fuzzy logic is added to determine adaptively the control coefficient (k) of inverters. The fuzzy logic is used to calculate the control coefficient based on the local information of DERs such as: state of charge, measured power, measured frequency. The physical constraint of

the battery such as the state of charge SOC and the power is concerned in the proposed method. The input/output of used fuzzy logic is shown in Figure VI.17

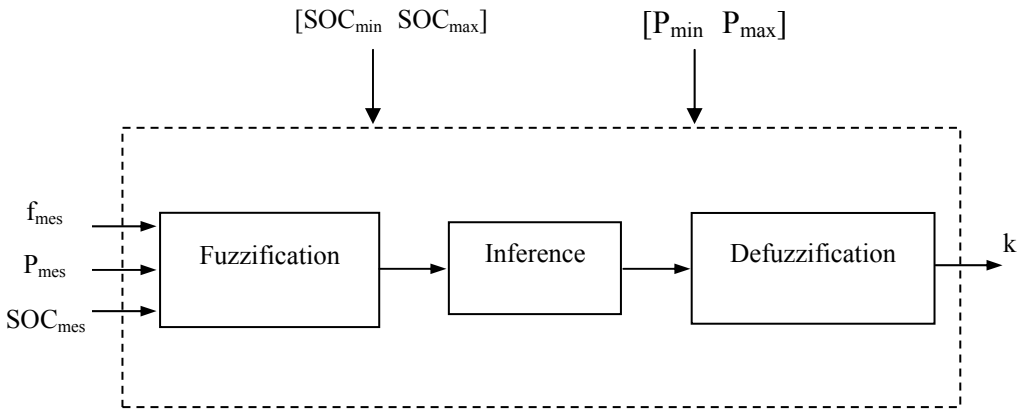

Figure VI.17: The method determines the control coefficient k

The detail of proposed control method is confidential

VI.2.4. Simulation results

In order to evaluate the efficiency of the proposed control method, the simulation test is performed for a rural network which is shown in Figure VI.18. This network is fed by a transformer of 250kVA, 20/0.4kV and it consists of single-phase and three-phase loads, PV production and BESS. The Matlab/simulink model of this microgrid is shown in Figure VI.15. Two scenarios are performed as follows:

- Scenario1: Transition from the connected mode to islanded mode with 4 cases depending on the initial operation conditions.

- Scenario2: The PV productions are suddenly varied in island mode.

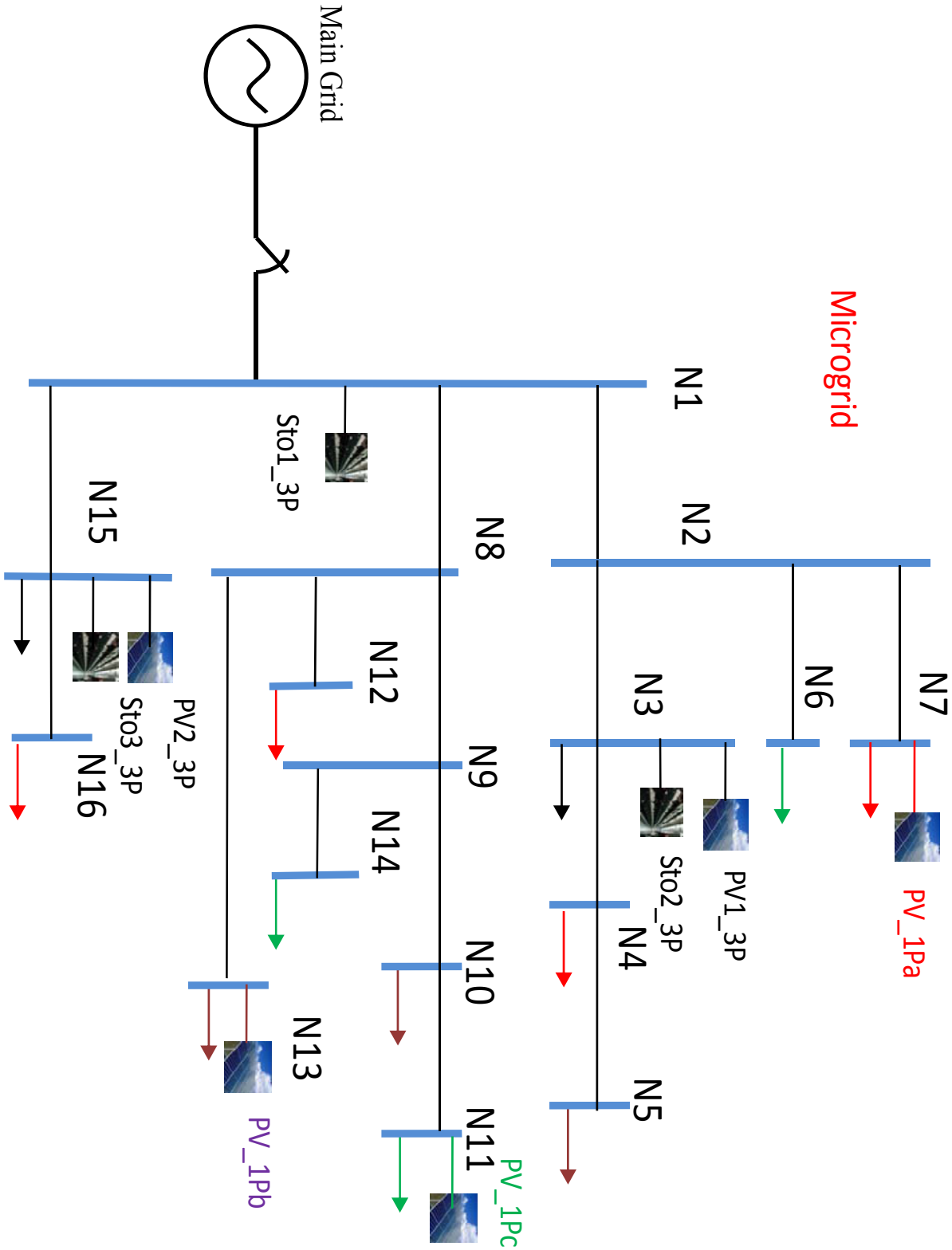

Figure VI.18: The study microgrid architecture

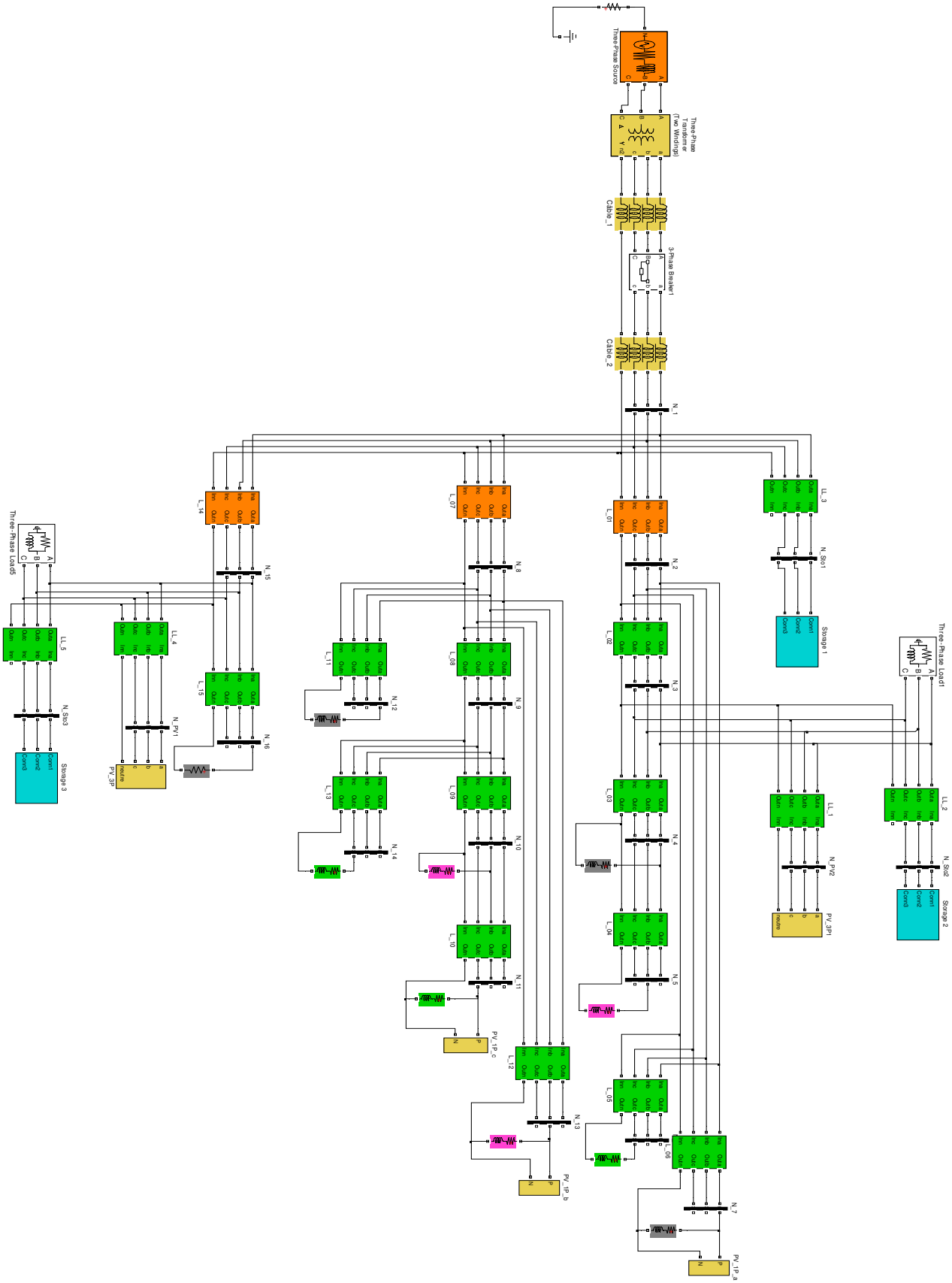

Figure VI.19: The modeling of study microgrid in Matlab simulink

A microgrid:

* 2 three-phase PV productions (nodes 3, 15):

  - P_PV_3P_1 (max) = 35kW

  - P_PV_3P_2 (max) = 25kW

* 3 single-phase PV productions (nodes 7, 11, 13):

  - P_PV1P_a (max) = P_PV1P_b (max) = P_PV1P_c (max) = 5kW

* 3 BESS (nodes 1, 3, 15):

  - Sto1: Pmax = 30kW

  - Sto2: Pmax = 30kW

  - Sto3: Pmax = 30kW

* Loads

  - Total load = 75kW

  - Single-phase loads 10 (nodes 4, 5, 6, 7, 10, 11, 12, 13, 14 and 16)

  - 2-three phase loads (nodes 3, 15).

Scenario1: transition from the connected mode to isolated mode

At time t = 2s, the network is switched to islanded mode.

Before islanding, the system includes:

- The total load: 75 kW
- PV productions P_PV_3P_1 = 15 kW
  P_PV_3P_2 = 20 kW;
  P_PV_1P = 3x5 kW
- The BESS power: 0kW (or charge or discharge).
- The power from the main grid: P_{sys} = 25kW

At t = 2s, the microgrid is switched to islanding. At this time, the PV power is fixed constant. The power deficit (25kW) is covered by the BESS to meet the load demand. The system frequency is controlled by the BESS with primary/secondary control to restore the frequency to 50 Hz. Therefore, the frequency and voltages are maintained at nominal values.

The simulation with different cases is performed to evaluate the efficiency of the proposed methods. The studied cases are shown in Table VI.1, are explained as follows:

Case1: - The initial power of BESS: $P_{ini} = 0$

- The initial of state of charge: SOC1=0.8; SOC2=0.8; SOC3=0.8;

Case2: - The initial power of BESS: $P_{ini} = 0$

- The initial of state of charge: SOC1=0.2; SOC2=0.5; SOC3=0.8;

Case3: - The initial power of BESS: $P_{ini1} = 0$; $P_{ini2} = 5kW$; $P_{ini2} = 10kW$;

- The initial of state of charge: SOC1=0.8; SOC2=0.8; SOC3=0.8;

Case4: - The initial power of BESS: $P_{ini1} = -5$; $P_{ini2} = 0kW$; $P_{ini2} = 5kW$;

- The initial of state of charge: SOC1=0.2; SOC2=0.5; SOC3=0.8;

Table VI.1: The initial operation conditions of BESS in 4 cases

		BESS 1	BESS 2	BESS 3
	P_n (kW)	**30**	**30**	**30**
Case 1	P_{ini}	0	0	0
	SOC	0.8	0.8	0.8
Case 2	P_{ini}	0	0	0
	SOC	0.2	0.5	0.8
Case 3	P_{ini}	0	5	10
	SOC	0.8	0.8	0.8
Case 4	P_{ini}	-5	0	5
	SOC	0.2	0.5	0.8

Case 1

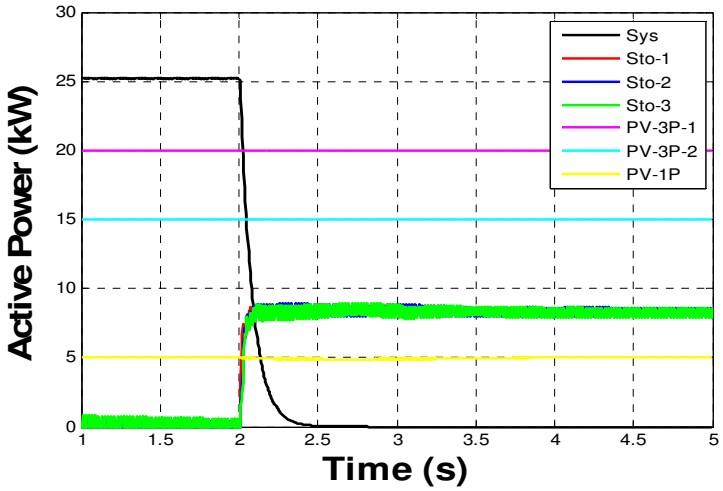

Figure VI.20: The simulation results of the microgrid active power in case 1

The simulation results of changing the active power, voltage and frequency of the microgrid are shown in Figure VI.20 and VI.21 respectively. It can be seen from the Figure VI.20, after the microgrid is disconnected from the main grid at t=2s, three BESS

discharge with the same of power value to meet the load demand. This is due to the fact that all BESS are given with the same initial conditions (SOC1=SOC2=SOC3=0.8; P_{ini} = 0). The voltage and frequency are maintained in the permitted limit. In the Figure VI.21, the frequency is maintained at 50 Hz rapidly after the actions of primary and secondary control of BESS.

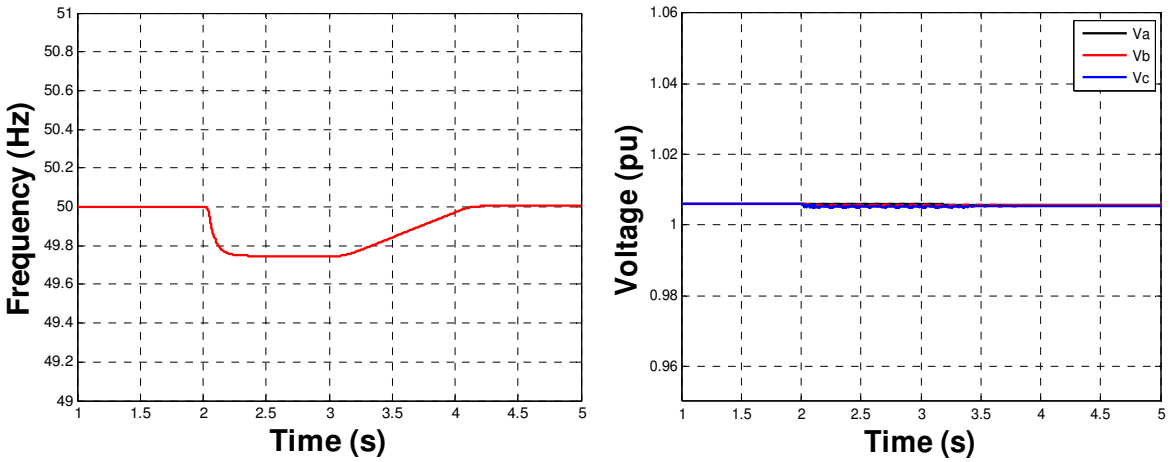

Figure VI.21: The simulation result of the microgrid frequency and voltage in case 1

Case2

The sharing of active power and the frequency of the microgrid are presented in Figure VI.22 and VI.23, respectively. As can be seen from the Figure VI.22, three BESS are adjusted different together. It is due to the fact that the STO3 is given with the largest initial capacitor (SOC3 = 0.8), thus the power deficit is almost supplied by this BESS. Otherwise, the STO1 (SOC1 = 0.2) supplies the least power to load demand.

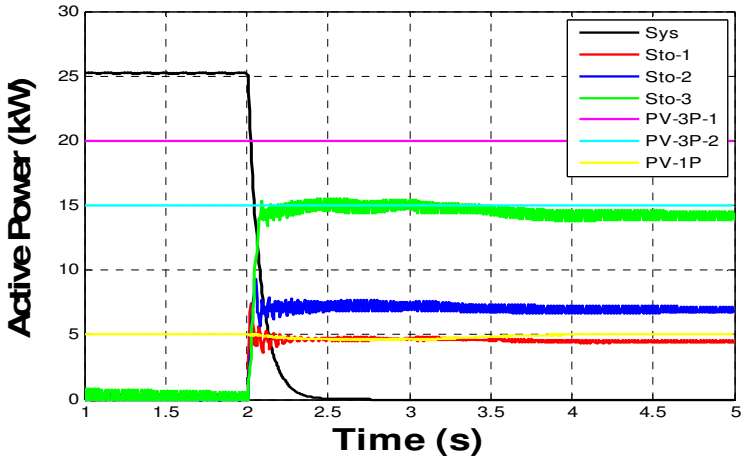

Figure VI.22: The simulation results of the microgrid active power in case 2

In this case, the frequency is maintained at 49.57 Hz by the primary control. Then it turns back the normal value 50Hz after the secondary control is performed

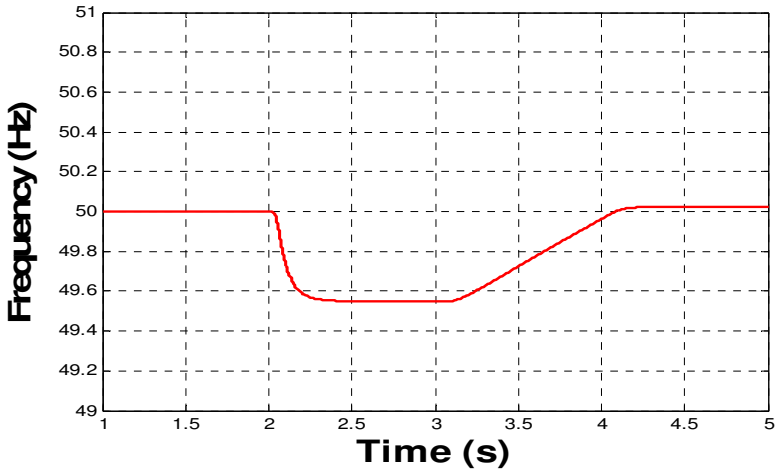

Figure VI.23: The simulation result of the microgrid frequency in case 2

Case 3

The active power and frequency are illustrated in Figure VI.24 and Figure VI.25, respectively. As can be seen from the Figure VI.25, we can see that the frequency reaches the nominal value after the secondary control. Although, three BESS are given with the states of charge SOC1= SOC2= SOC3, the discharge power of these is determined as different together. This is due to depend on the initial power of each BESS (the power at t=2s). In fact, in Figure VI.24, the initial power of BESS 3(STO-3) is given as the largest initial power (P_0 = 10kW), however the discharge power is estimated to the least value (2.7kW). In contrast, the largest power (4.5kW) is shared by the BESS 1(STO-1)

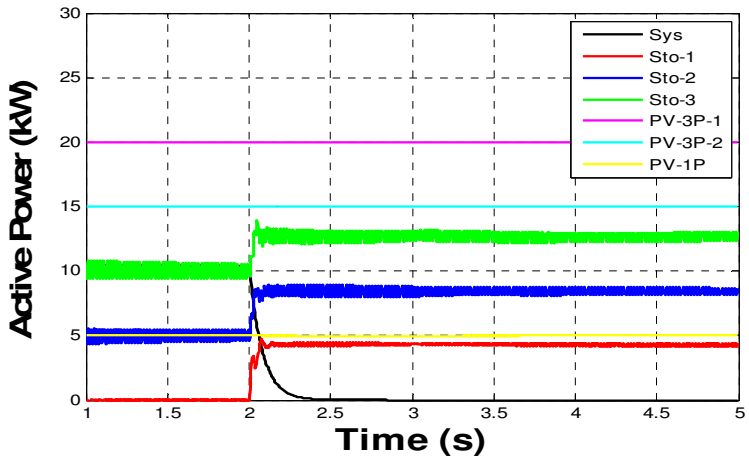

Figure VI.24: The simulation results of the microgrid active power in case 3

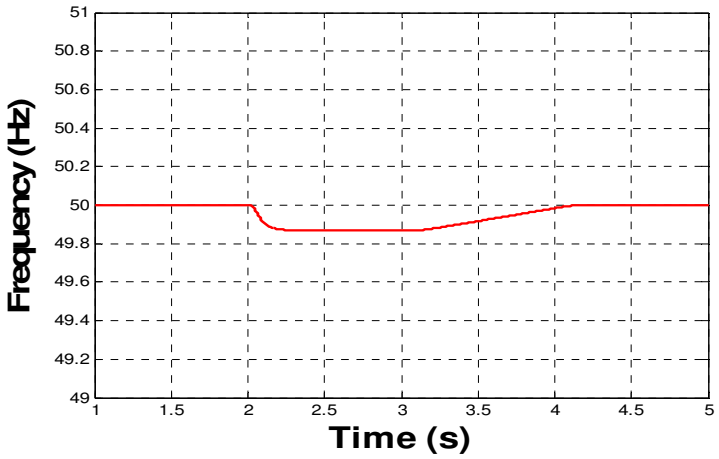

Figure VI.25: The simulation result of the microgrid frequency in case 3

Case 4

The simulation results are shown in Figure VI.26 and Figure VI.27. In this case, the frequency is maintained at 50 Hz after the actions of primary and secondary control. The discharge power of three BESS are taken into account the different together. The results are achieved as the combination of the results in the cases 2 and 3. In this case, the initial states of three BESSs were given as follows: BESS 1 (STO-1): discharge (P_{ini1} =5kW), BESS 2 (STO-2): rest state (P_{ini2} =0) and BESS 3 (STO-3): was charged (P_{ini1} =-5kW). After the transition, the BESS 3 stops the charging. Then, it moves to the rest state. On the other hand, the BESS 1 and BESS 2 discharge to supply for the demand loads in which the power is almost supplied by BESS 1.

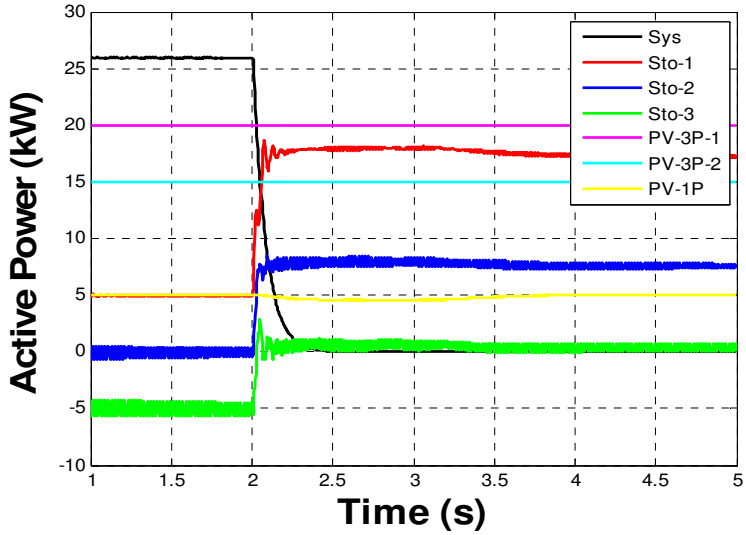

Figure VI.26: The simulation results of the microgrid active power in case 4

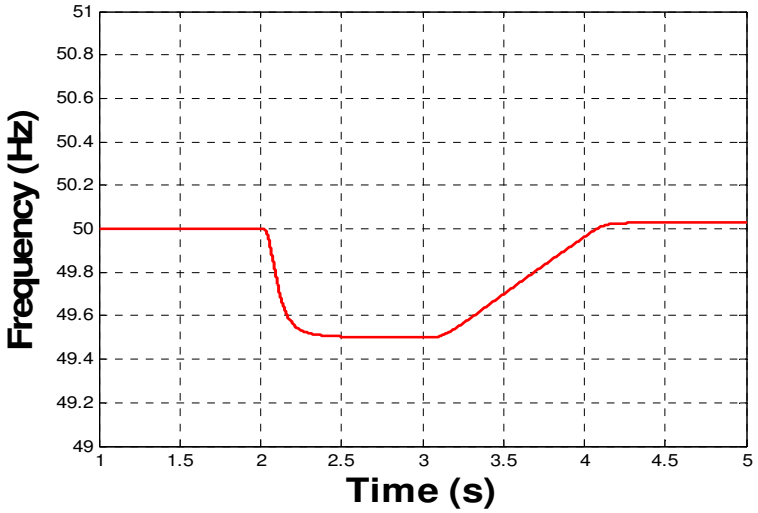

Figure VI.27: The simulation result of the microgrid frequency in case 4

Scenario2: Island microgird

In this scenario, the PV production is suddenly varied, for example: reducing from 100% to 40% after that increasing from 40% to 90%.

Before the events:

- The total load is 75 kW
- PV productions P_PV_3P_1 = 35 kW
  P_PV_3P_2 = 25 kW
  P_PV_1P = 3x5 kW
- 3 BESS Sto1: P_{max} = 30kW
  Sto2: P_{max} = 30kW
  Sto3: P_{max} = 30kW
- The BESS initial power equal to zero (or charge or discharge).
- The initial state of charge
  SOC1 = 0.7
  SOC2 = 0.5
  SOC3 = 0.3

Assumed that

- T = 3s: all PV production is reduced from 100% to 40%
- T = 7s: all PV production is increased to 90%.

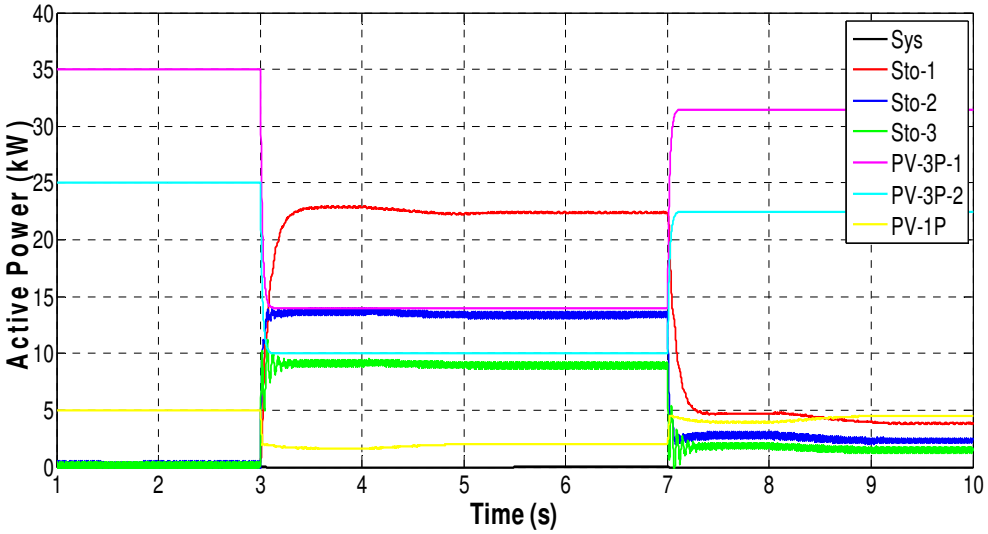

Figure VI.28: The simulation results of the microgrid active power in scenario 2

The active power and the frequency of microgrid are shown in Figure VI.28 and Figure VI.29, respectively. After the PV production reduces (from 100% to 40%), three BESS discharge to maintain the balance between production and consumption. In which, the largest power is provides by the BESS 1 due to the fact that this BESS has the largest initial capacitor (SOC1=0.7); in contrast, the BESS 3 discharge with the least power (SOC3=0.3). As can be seen from the Figure VI.29, the frequency is maintained at 50 Hz after the actions of primary and secondary frequency control. Then, at t = 7s, PV production increases to 90%, it leads to the frequency increasing. In order to prevent this increasing, the discharge power has to reduce. Finally, the frequency is maintained at the nominal value (50Hz) after the secondary control is performed.

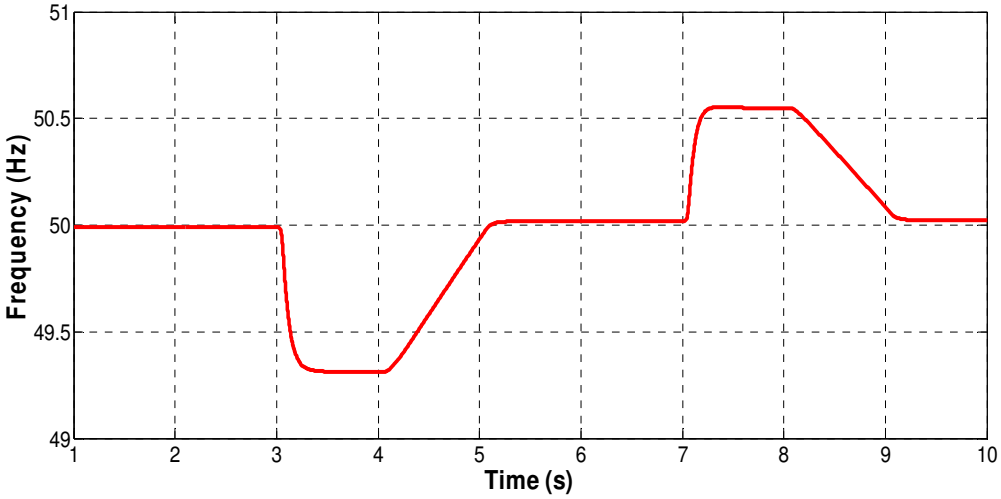

Figure VI.29: The simulation result of the microgrid frequency in scenario 2

VI.3. **Conclusion**

In this chapter, the microgrid controls in the island and transition from the grid connected to island modes have been presented. A conventional droop control method is performed for PV-BESS-diesel system. The simulation results are carried out to show that diesels and BESS participate to share the active, reactive power and control frequency and voltage system in both transient states and steady state. Thus, this system operates with high reliability. Moreover, an intelligent control method is also proposed in this chapter. In this method, fuzzy logic is used to deduce adaptively the control coefficient with considering the state of charge and the initial condition of BESS. The simulation results have shown the efficiency of the proposed method, especially in the transition from the grid connected mode to the island mode.

CHAPTER VII :

Conclusion and Future works

SUMMARY

VII.1. **Conclusion**

In this thesis, optimal sizing, control and energy management strategies for a microgrid have been studied and developed. The general conclusions of this thesis can be summarized as:

- The development of photovoltaic system and BESSs in all over the world and particularly Europe is illustrated to show that the microgrid with PV and BESSs are seen as the new trend for a 'smart grid'. The issues related with microgrid and their solutions are presented in literatures review. The objective, contribution and organization of this thesis are also presented.

- The general problem of a microgrid is viewed including definition, architecture and components as well as its operation.

- The models of microgrid components are developed for different purposes of this thesis. The efficiency of the developed models is illustrated by the simulation results.

- An iterative method is proposed to find an optimal sizing of a microgrid in two modes: island mode and grid connected mode. The optimal configurations not only satisfy technical conditions but also minimize the costs (economic issue) with respect to the low CO_2 value emissions (environmental aspect).

-The optimal energy management in operation for a microgrid is also developed under two operational modes: the island and the grid connected modes by using the dynamic programming (DP) method. In the island mode, the objective is to minimize the fuel cost and reduce emissions by scheduling of DERs, while the objective function in the grid-connected mode is to minimize the net power exchange with the main grid and the cash flow of the system considering the maximal usage of PV energy

- The strategies by using droop control for DER and BESS are developed to control the voltage and frequency of microgrid in two cases: island mode and transition from the grid-connected to island mode. On the other hand, the intelligent control strategies by using fuzzy logic are proposed in order to change adaptively the controllers. The proposed solutions permit to take into account BESS physical constraints such as SOC.

VII.2. **Future works**

Microgrid with BESS is an innovative solution in the future to facilitate the renewable energy sources integration such as PV. Furthermore, the microgrid is characterized as the “building blocks of smart grids” [1]. Thus, microgrid becomes an issue of great interest. Based on the results obtained in this thesis, the continuing work of this research area can be described as:

* Validate developed models by simulations and real time simulations

* In the future work, a sizing method by using stochastic approach can be used. It permits to take into account the incertitude of PV production and load demands.

* In this thesis, the control and the energy management are performed in a microgrid. Multi-microgrid control and management will be given as a potential problem for future work.

* The microgrid architecture can be expanded with more types of renewable energies, such as PV and wind generation association; as well as fuel cell and controllable load (electric vehicle…)

* The potential ancillary services furniture is an interesting issue to develop, the microgrid could be an efficient mean to participate not only on the voltage plan control but to the frequency plan as well. Other possibilities like power quality improvement could be explored too.

Appendix A

Résumé en Français

Sommaire

A.I : Introduction

A.I.1. Contexte

- Développement du PV

La puissance installée des ressources renouvelables en Europe, prévue pour 2050, est représentée dans la Figure A.I.1. De cette figure, l'énergie photovoltaïque et l'énergie éolienne sont données avec la plus forte croissance.

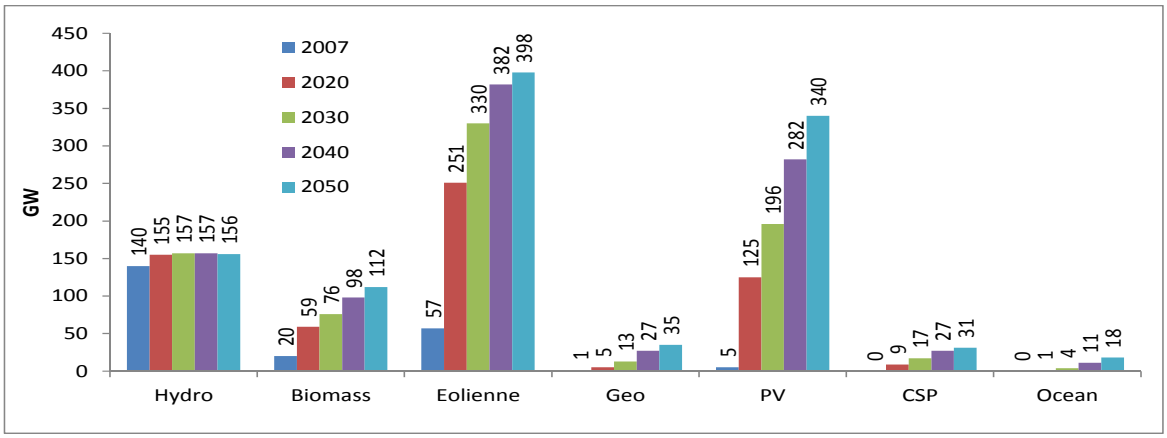

Figure A.I.1: The contribution of renewable sources in the total electricity generation

(Source: http://www.greenpeace.org; Energy (R)evolution-
Towards a fully renewable energy supply in the EU 27)

Figure A.I.2 illustre le prix de PV installée en Allemagne. Ce prix va diminuer constamment entre 2013 et2030

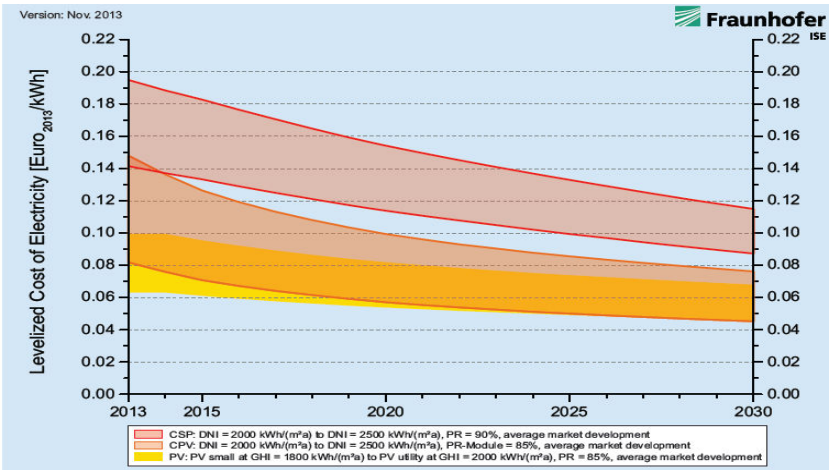

Figure A.I.2: The installed PV price in Germany

(Source : http://www.ise.fraunhofer.de/en/)

Développement du Stockage Électrochimique de l'Énergie

La capacité de stockage quotidien de l'électricité de quatre régions en 2011 et 2050 est décrite dans la Figure A.I.3. Dans cette figure, il y a une croissance significative de la capacité de stockage de l'électricité dans toutes les régions.

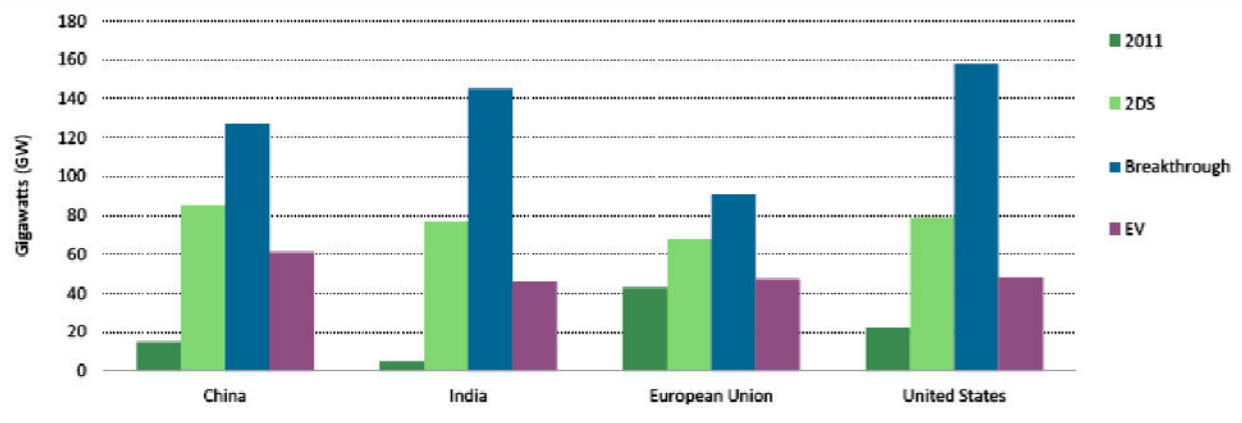

Figure A.I.3: Electricity storage capacity for daily electricity storage by region in 2011 and 2050

(Source: http://www.iea.org; Technology Roadmap: Energy Storage)

Figure A.I.4 montre l'évolution future du prix de la batterie; le prix devrait diminuer constamment à l'horizon 2030, et après il se stabilise à 2050.

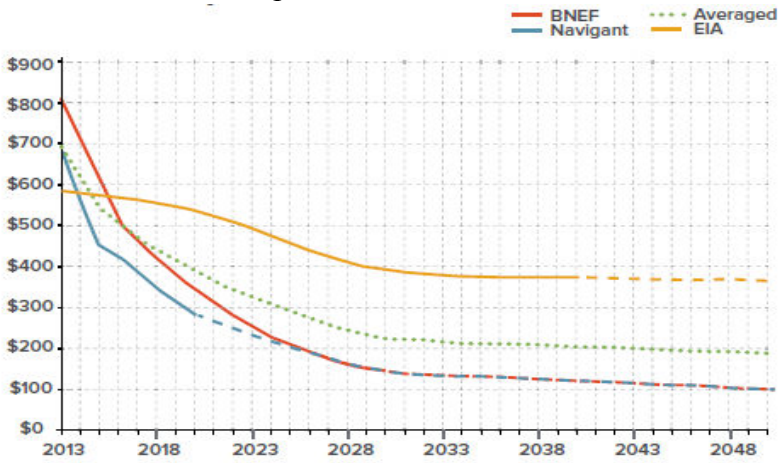

Figure A.I.4: The Battery price provision from 2013 to 2050

(Source: www.rmi.org; RMI - The Economics Of Grid Defection - When And Where Distributed Solar Generation Plus Storage Competes With Traditional Utility Service)

En ce qui concerne les questions ci-dessus, l'intégration de photovoltaïque au réseau est un sujet important à considérer. Le stockage est l'un des leviers qui peuvent augmenter le taux de pénétration de PV. Autres fonctions supplémentaires peuvent être prises à partir du stockage comme les services système et d'autres aspects de la qualité de l'alimentation. Ainsi, un concept de Microgrid, y compris PV et batteries, sera une nouvelle solution pour un 'smart grid'.

- Microgrid

Il y a des projets micro-réseaux qui ont été achevées avec succès, fournissant des solutions techniques de plusieurs d'innovation.

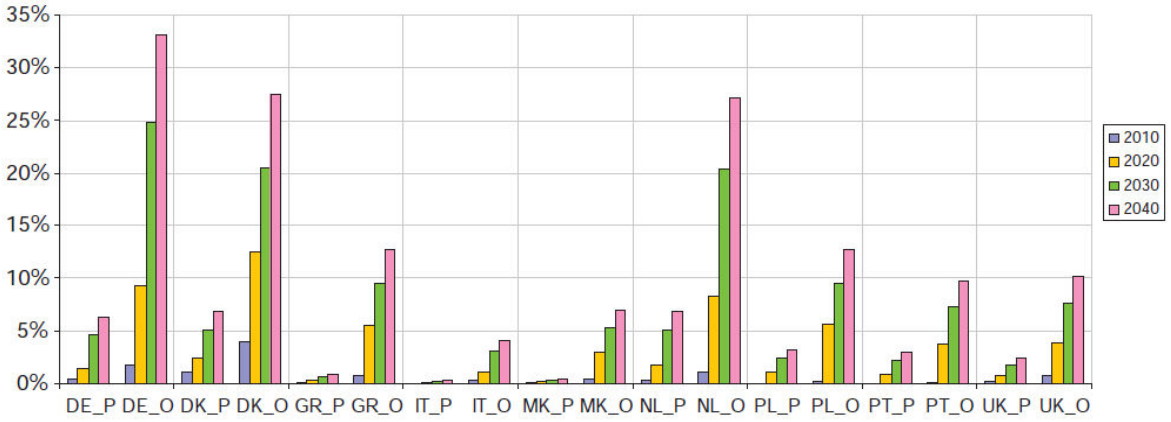

Figure A.I.5: Microgrid dissemination ratio in EU national grids scenarios

(O = optimistic assumptions, P = pessimistic assumptions). (DE=Germany, DK=Denmark, GR=Greece, IT=Italy, MK=FYROM, NL=The Netherlands, PL=Poland, PT=Portugal, UK=United Kingdom)

Pour illustrer le développement des Microgrids en Europe, quatre scénarios sont présentés pour 2010, 2020, 2030 et 2040. La part des Microgrids typiques dans les réseauxélectriques nationales (Microgrid ratio de diffusion) par pays et par région sont supposées comme sur la Figure A.I.5, pour 2010, 2020, 2030 et 2040, avec pessimistes (P) et optimistes (O) hypothèses [1]. De cette figure, le taux de croissance de Microgrid est donné et devrait augmenter continuellement.

Revue de la littérature Les stratégies de dimensionnement, de contrôle et de gestion optimale de l'énergie sont connues comme sujets de recherche importants. Premièrement, plusieurs méthodes de dimensionnement optimal ont été proposées dans la littérature. Certains des auteurs utilisent les méthodes d'intelligence artificielle (AI) telles que Genetic algorithm (GA), Particle Swarm optimization (PSO), tandis que d'autres utilisent la méthode itérative pour trouver la configuration optimale d'un Microgrid qui répond à la stratégie de fonctionnement optimal. Deuxièmement, l'optimisation pour la gestion de l'énergie de Microgrid est également présentée dans certaines recherches. La méthode basée sur des règles, méthodes globales optimales (Linear programming (LP), Mix-Integer-Linear-Programming (MILP) et la Dynamic programming (DP)) ainsi que les (AI) méthodes sont utilisés pour trouver la gestion optimale de l'énergie d'un Microgrid. Enfin, les contrôleurs locaux pour DER peuvent améliorer l'efficacité de fonctionnement de Microgrid en utilisant les méthodes classiques (single master (centralize control),

master/slave and droop control)). En outre, les variations de contrôle par statisme classique sont également abordées dans certaines publications.

A.I.2. Objectif de la thèse

L'objectif de cette thèse est de présenter les stratégies de configuration et de contrôle optimal pour assurer un fonctionnement sûr, fiable et efficace d'un Microgrid y compris de productions photovoltaïques (PV), Battery Energy Storage System (BESS) et / ou diesels. Dans cette thèse, le dimensionnement, le contrôle et la gestion d'énergie optimale de Microgrid sont proposées dans les deux modes: mode îloté et mode connecté au réseau. Les objectifs de cette thèse sont décrits comme suit:

- Un dimensionnement optimal d'un Microgrid est conçu pour trouver le coût minimum en tenant compte de l'optimisation des conditions de fonctionnement avec la plus grande fiabilité et des émissions plus bas

- Optimiser la répartition de puissance entre DER, le coût de consommation du carburant et les émissions pour un Microgrid en mode iloté

- Optimiser le coût de production, la puissance échangée entre le Microgrid avec le réseau principal et la répartition de puissance entre DER

- Controler la tension de Microgrid et la fréquence dans le mode iloté et la transition de mode connectée au mode iloté.

A.I.3. Contributions de la thèse

Les principales contributions de cette thèse sont comme suit:

- Une méthode pour optimiser le dimensionnement d'un Microgrid. La technique d'optimisation itérative a été utilisée pour suivre les Renewable Energy Fractions (FR), le excess energy ratio (EER) et le Annual Cost of System (ACS) en tenant compte de l'émission.

- La gestion optimale de l'énergie pour le fonctionnement d'un Microgrid est effectuée par la méthode de programmation dynamique (DP) et la méthode à base de règles. Ces méthodes sont utilisées pour déterminer le coût minimum de consommation de carburant en tenant compte des émissions dans un Microgrid en mode iloté ainsi que de minimiser le cash flows et la puissance échangée avec le réseau principal en mode

connecté au réseau.

- La thèse propose les stratégies de control de tension et de la fréquence pour un Microgrid en mode îloté en utilisant des méthodes de statisme

- La thèse propose en outre des stratégies de contrôle intelligent de tension et de fréquence en utilisant la logique floue pour ajuster de façon adaptative le statisme. De cette manière, la fréquence est exprimée non seulement que la fonction de la puissance active (dans la stratégie ci-dessus), mais aussi l'état de charge du BESS et les conditions de fonctionnement initiales.

A.I.4. Organisation de la thèse

Cette thèse comprend sept chapitres. Les contenus de chaque chapitre sont brièvement décrits comme suit:

- Chapitre I: présente le contexte, la revue de la littérature, l'objectif de cette thèse, la contribution de thèse et l'organisation de thèse.

- Chapitre II: présente le concept de Microgrid, la définition de Microgrid, l'opération de Microgrid, le contrôle de Microgrid et la protection de Microgrid.

- Chapitre III: fait ressortir la modélisation des composants micro-réseaux: productions photovoltaïques (PV), des systèmes de stockage d'énergie de la batterie, diesel et les charges.

- Chapitre IV: propose le dimensionnement optimal pour deux types de micro-réseaux: le Microgrid en îloté et de Microgrid en connectés au réseau.

- Chapitre V: présente la gestion optimale de l'énergie d'un microgrid en mode iloté et en mode connectée

- Chapitre VI: propose le contrôle de Microgrid. La stratégie de contrôle de tension et de la fréquence en utilisant le statisme classique pour un Microgrid îloté est présentée dans la première partie. Dans la deuxième partie, une stratégie de contrôle intelligent (par logique floue) est proposée pour le mode îloté et de la transition du mode connecté au mode îloté.

- Chapitre VII: contient les conclusion et perspectives.

A.II : Concept de Microgrid

A.II.1. Définition de Microgrid

- Microgrid est une intégration de microsources, des unités de stockage et des charges contrôlables situés dans un réseau de distribution local.

- Un Microgrid peut fonctionner dans les modes connecté ou déconnecté

- La gestion de l'énergie et le contrôle de la coordination entre microsources disponibles sont démontrées dans un Microgrid.

A.II.2. Structure et les composants du Microgrid

Un Microgrid comprend des ressources d'énergie distribuées (DER) (photovoltaïque, petites éoliennes, piles à combustible, les moteurs à combustion, microturbines, etc.), des dispositifs de stockage d'énergie distribués (de volants, inductances supraconductrices, batteries, etc.), et les charges. Les dispositifs de stockage d'énergie décentralisés peuvent être utilisés pour absorber l'excès de puissance et décharger pour couvrir le déficit de puissance. Ainsi, ils contribuent à améliorer la fiabilité de Microgrid ainsi que le rendant efficace et le fonctionnement économique. En outre, le stockage d'énergie est connu que des dispositifs à réponse rapide. Par conséquent, ils empêchent également l'instabilité transitoire et participent à contrôler la tension et la fréquence du Microgrid en fournissant la réserve.

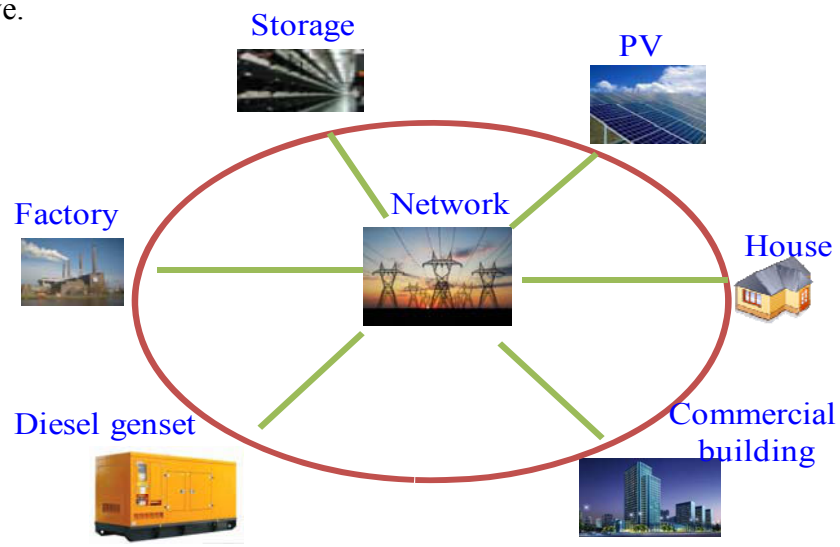

Figure A.II.1: A studied Microgrid structure

A.II.3. Opération de Microgrid

Deux modes de fonctionnement de Microgrid peuvent être définis comme suit:

• **Mode connecté**: le Microgrid (MG) est connecté au réseau. Le MG peut recevoir en totalité ou en partie par l'énergie du réseau principal (selon le partage de puissance). D'autre part, l'excédent d'énergie peut être envoyé au réseau principal (lorsque la production totale est supérieure à la consommation).

• **Mode iloté**: lorsque le réseau amont présente une défaillance, ou il y a des actions prévues (par exemple, pour effectuer des actions de maintenance), le MG peut facilement se déplacer à l'opération d'îlotage. Ainsi, la MG fonctionne de façon autonome, s'appellant le mode îloté, comme le réseau électrique d'une île.

Les stratégies d'exploitation de Microgrid sont présentées à la Figure A.II.2

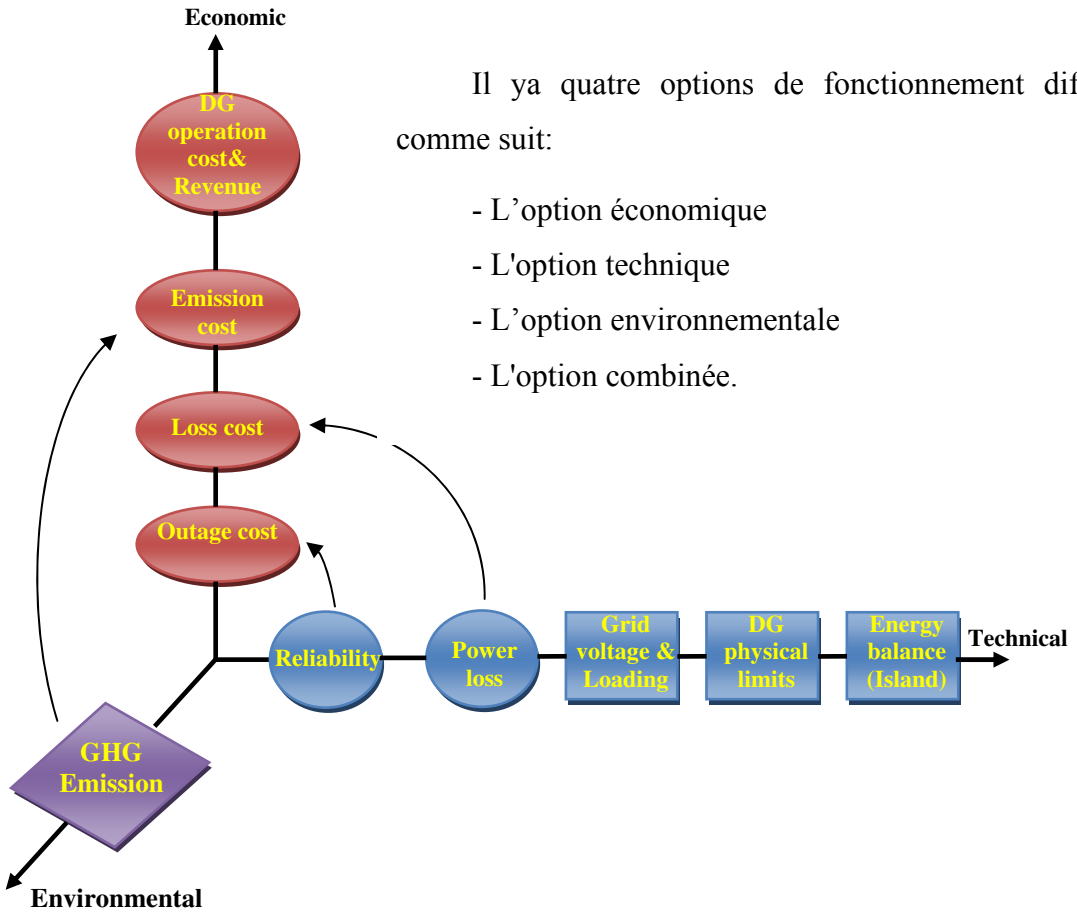

Il ya quatre options de fonctionnement différents comme suit:

- L'option économique
- L'option technique
- L'option environnementale
- L'option combinée.

Figure A.II.2: The Microgrid operation strategies

A.II.4. Contrôle de Microgrid

Le principe de base de la commande de Microgrid est présenté dans cette partie. La structure typique de contrôle de Microgrid est décrite à la Figure A.II.3.

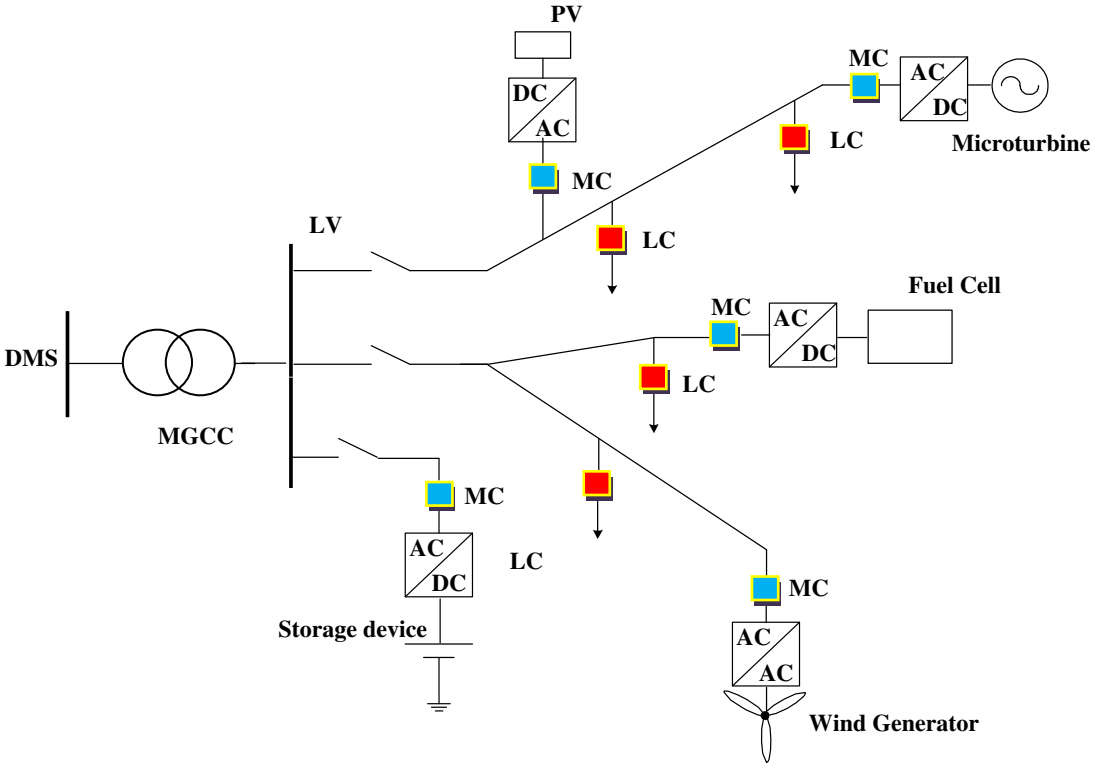

Figure A.II.3: The typical Microgrid control structure

*** Les fonctionnalités de contrôle dans un Microgrid sont présentées comme suit:**

- Système de gestion de distribution (DMS)

- Les fonctions de contrôleur central (MGCC):

- Contrôleur de Microsource (MC)

*** Le control d'un Microgrid comporte de 3 niveaux:**

- Contrôle primaire

- Contrôle secondaire

- Contrôle tertiaire

A.II.5. Protection de Microgrid

La protection de Microgrid doit réagir lorsque la perturbation se produit dans le

réseau de distribution ainsi que dans le Microgrid. Si la perturbation apparaît dans le réseau électrique, la protection doit être déclenché à débrancher le Microgrid avec le réseau principal aussi rapidement que possible par un commutateur appelé commutateur statique (SS). Si le défaut est dans le Microgrid, le système de protection isole la section en défaut pour éliminer le défaut [1].

La localisation de défauts rapidement et avec précision est très importante pour l'économie, la sécurité et la fiabilité de système d'alimentation. Dans [83] - [84], un algorithme de localisation de défaut sont présentées. Figure A.II.4 décrit les scénarios de défauts externes et internes dans un Microgrid simple. Par exemple, une panne se produit à la N1. Ce point se trouve dans le réseau de distribution; le commutateur statique au MCC s'ouvre pour isoler le Microgrid avec la grille principale. Après cela, le Microgrid fonctionne dans le mode d'îloté. Si la perturbation s'affiche en N2, le disjoncteur CB4-5 ouvrirait mais le CB 3-4 ne serait pas. La source à l'B5 doit arrêter alors que les sources restantes fonctionnent encore.

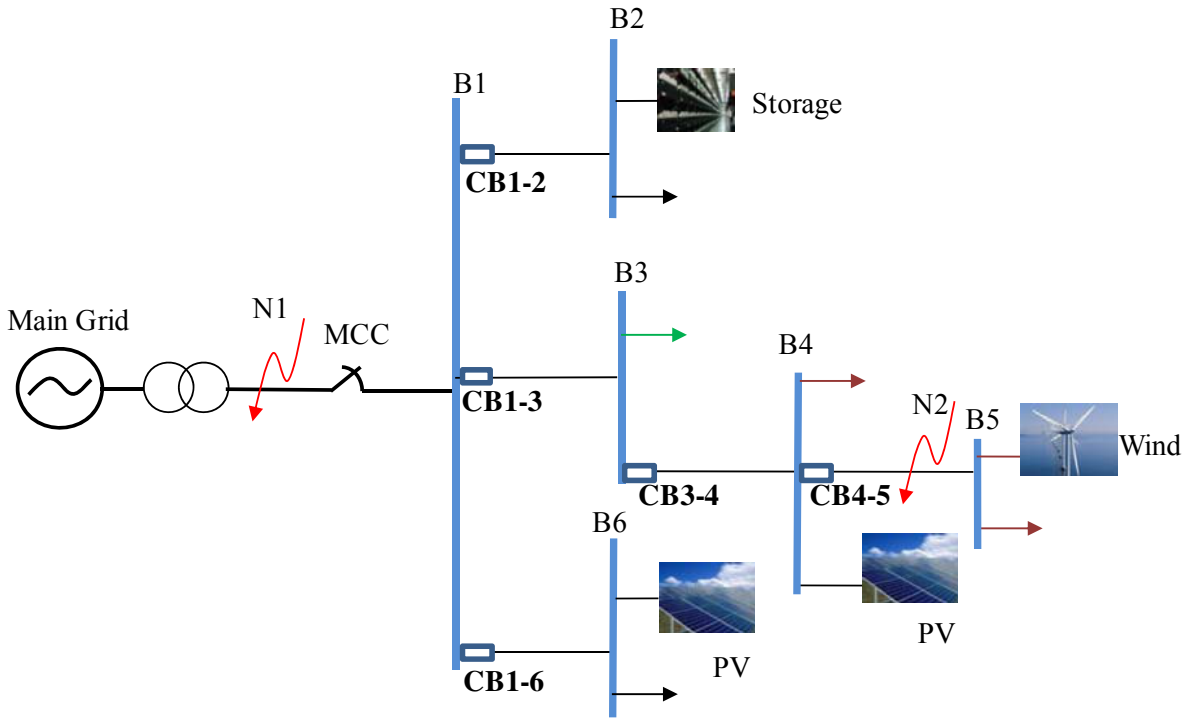

Figure A.II.4: External and internal fault scenarios in a Microgrid

A.III : Modélisation des composants de Microgrid

A.III.1. Introduction

Dans ce chapitre, le modèle de composants dans un Microgrid est illustré. Dans chaque appareil, on se concentrer sur des recherches sur le modèle de contrôle qui est décrit dans le chapitre VI. En outre, le modèle mathématique de ces composants est également conçu pour s'appliquer pour le dimensionnement optimal de Microgrid qui est décrit dans le chapitre IV. Dans cette thèse, le Microgrid présenté inclut le photovoltaïque système (PV), le diesel, le système de stockage et la charge. Ainsi, la modélisation de ces composants est représentée dans ce chapitre.

A.III.2. Modélisation du système photovoltaïque

- Dimensionnement d'un Système PV

Le dimensionnement de PV est présenté dans ce paragraphe pour déterminer le dimensionnement optimal de Microgrid. Les variables de dimensionnement PV sont données comme le numéro de panneau PV et la quantité de chaîne dans un tableau de PV.

Le nombre requis de panneaux photovoltaïques en série est estimé par le nombre de panneaux nécessaires pour accorder à la tension de fonctionnement du DC bus. Ainsi, le nombre de panneaux photovoltaïques en série est calculé comme suit:

$$n_{pv\ series} = \frac{U_{bus}}{U_{panel}} \tag{III.1}$$

Le nombre de panneaux PV peut varier de 0 à la plus grande quantité de panneaux photovoltaïques nécessaires quand un système PV autonome peut couvrir la demande de charge. Ainsi, $x_{PV,\ parellel}$ est délimité comme suit:

$$0 \leq x_{pv,parallel} \leq \frac{E_{L\_day}}{\eta . W . n_{pv\ series} . Hours_{sunshine/day}} \tag{III.2}$$

- Modélisation de système PV

Un système photovoltaïque est modélisé par une source de courant avec sa commande de puissance. Le modèle de système PV simplifié est donné comme une source de courant injecté avec régulation P / Q. Le but de ce contrôle est d'imposer à la sortie

d'une puissance active et réactive suivant la valeur de consigne P_{SP} et Q_{sp}, respectivement. Le fonctionnement de ce modèle est représenté sur la Figure A.III.1

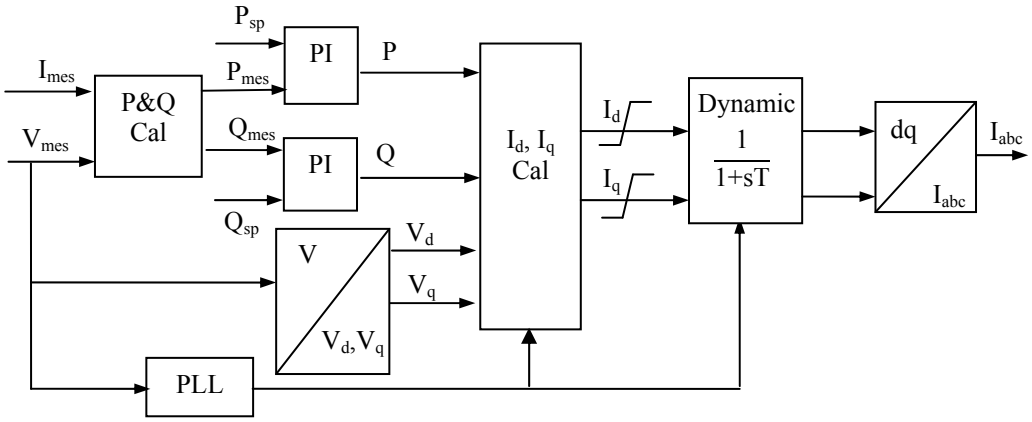

Figure A.III.1: Photovoltaic system with power electronic interface – P/Q control

A.III.3. Modélisation de stockage électrochimique

Dans cette thèse, le stockage électrochimique est utilisé. Dans cette partie de la modélisation de ces unités de stockage sera présentée. Le modèle de la batterie est présenté correspondant à la technologie de la batterie au plomb-acide.

-Paramètres de batterie

+ *Tension*

Dans [89], la tension des batteries est exprimée en fonction de la SOC; ainsi il a été considéré comme fonction linéaire. À partir des résultats expérimentaux effectués à l'institut INES, la tension des batteries de charge et de décharge sont calculés par (III. 3) et (III.4), où "N_{Bat}" est le nombre de batteries 12V connecté en série

- Si $I_{BAT} \geq 0$ (Charge ou de repos)

$$V_{BAT}(t) = (12.94 + 1.46.SOC(t)).\ N_{BAT} \quad \text{(III.3)}$$

- Si $I_{BAT} < 0$ (décharge)

$$V_{BAT}(t) = (12.13 - 1.54.(1-SOC(t))) .N_{BAT} \quad \text{(III.4)}$$

+ *État de charge (SOC)*

Le SOC est estimé comme suit

$$SOC = \frac{C(t)}{C_{ref}} \quad \text{(III.5)}$$

+ *État de la Santé (SOH)*

Le SOH de batteries est défini comme suit [39]

$$SOH = \frac{C_{ref}(t)}{C_{ref,nom}} \quad \text{(III.6)}$$

- Interface de Batterie

Le BESS sont connectés au réseau via l'interface électronique de puissance avec la puissance d » charge ou déchargedirectement à partir du réseau électrique. Dans ce mémoire, le convertisseur de batterie est commandé par un dispositif de commande V/f. Ces points de consigne peuvent être exprimés comme la référence de tension et de la fréquence de référence. Le contrôleur V/f de l'onduleur de la batterie est indiqué sur la Figure A.III.2.

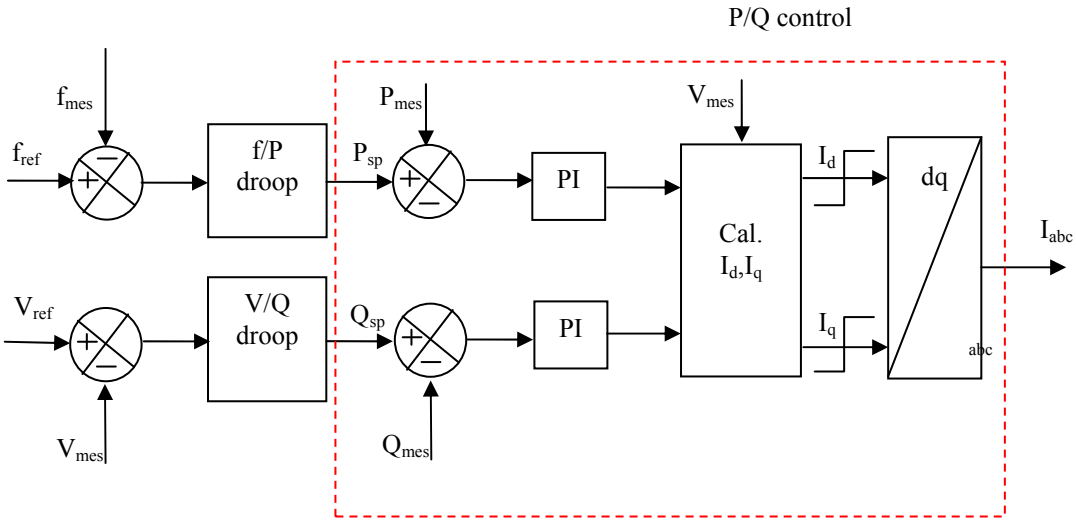

Figure A.III.2: Battery model with power electronic interface – V/f control

A.III.4. Modélisation de Diesel

- Dimensionnement d'un diesel

Le diesel doit être fonctioné à des niveaux de charge élevés pour maximiser l'efficacité de carburant et conçu de telle sorte qu'il respecte la fiabilité de charge [85]. Ainsi, la puissance nominale (P_R) du générateur diesel doit couvrir entre 0 et la demande maximale. Par conséquent, la limite du dimensionnement général diesel est donnée par:

$$0 \leq P_R \leq P_{L\_peak} \quad \text{(III.7)}$$

La puissance générée du générateur doit être délimitée dans la gamme comme suit

$$P_{Die\_min} \leq P_D(t) \leq P_{Die\_max} \quad \text{(III.8)}$$

- La modélisation de commande

Un générateur de diesel comprend d'une combustion interne (IC) couplé à un moteur générateur synchrone. Le moteur à combustion interne est intégré avec un régulateur pour commander la vitesse de sortie de l'arbre du moteur par réglage de la quantité de carburant fournie. La commande d'un tel system se comporte en général de deux blocs comme décrit dans les figure ci dessous. Un régulateur PID est utilisé pour commander le régulateur de vitesse (Figure A.III.3). Le générateur synchrone est incorporé avec un excitateur et un régulateur de tension (Figure A.III.4). La commande de régulateur de tension maintient la tension aux bornes requis

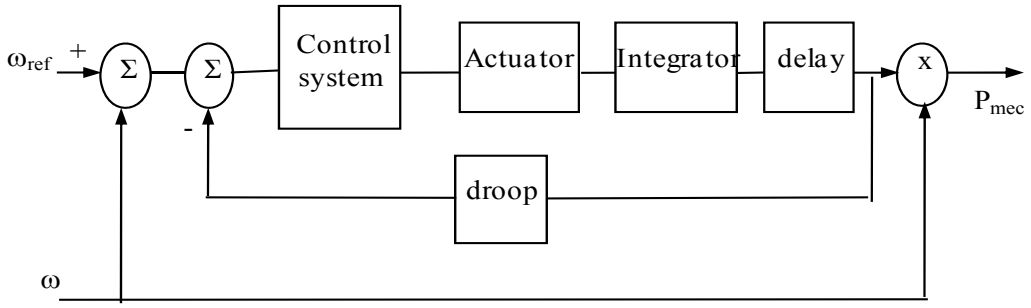

Figure A.III.3: Schéma du système de régulation de vitesse

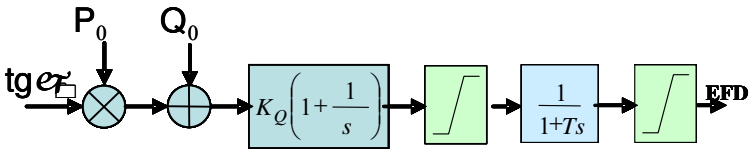

Figure A.III.4: Régulation de tension automatique

A.III.5. Modélisation de charge

La modélisation de charge est compliquée en raison du grand ensemble de périphériques connectés tels que réfrigérateur, chauffage, ... Ainsi, il est difficile d'estimer la modélisation de charge exacte. En outre, les changements de charge en fonction de nombreux facteurs tels que le temps, des conditions météorologiques, et économie [94]. Dans [94], le modèle de charge peut être divisé en deux types: modèle statique et le modèle dynamique. Dans ce mémoire, le modèle de charge est supposé que les constantes de puissance active et réactive. La courbe de charge journalière en deux jours qui sont jours d'été et les jours d'hiver, est illustré à la Figure A.III.5.

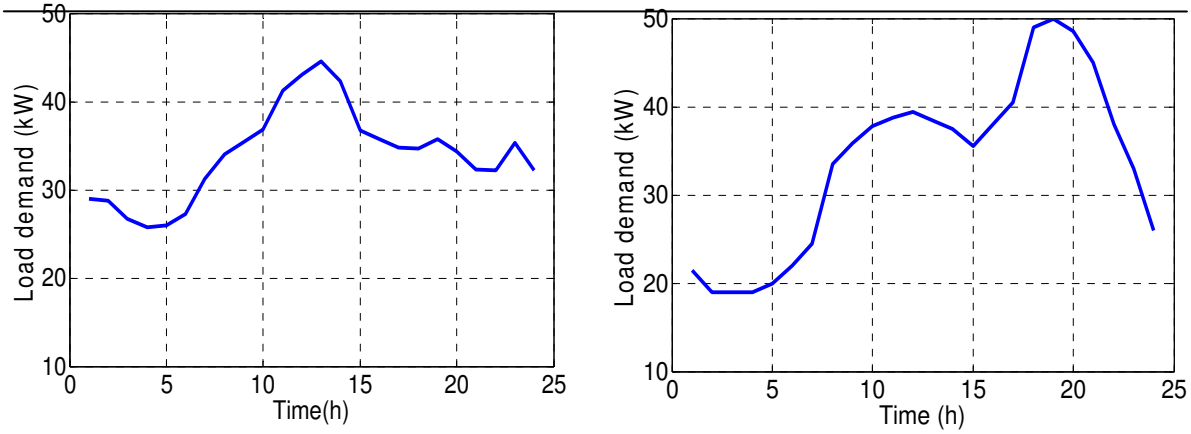

Figure A.III.5: Daily loads in a summer day and winter day

A.III.6. Conclusion

Afin d'optimiser le dimensionnement et la commande, les composants de microgrid sont modélisés pour les différents buts. En outre, chaque modèle a été testé et évalué par des résultats de simulation. Ces modèles développés seront utilisés dans les chapitres suivants.

A.IV : Un dimensionnement optimal du Microgrid

A.IV.1. Introduction

Un Microgrid est un système d'alimentation à petite échelle des DERs comme renouvelables et non renouvelables ressources avec stockage. Récemment, l'augmentation des prix du carburant et le développement de technologies d'énergies renouvelables donnent plus de possibilités d'utilisation des sources renouvelables dans Microgrid. Cependant, l'énergie photovoltaïque et l'énergie éolienne sont des sources intermittentes en raison du fait qu'ils dépendent de la météo. Par conséquent, il est difficile de maintenir l'équilibre entre la production et la demande. Cela rend le processus complexe de dimensionnement dans de nombreux aspects techniques/économiques combinés avec des préoccupations sociales. Ainsi, un dimensionnement optimal d'un Microgrid nécessite de l'optimisation de l'ensemble des composants et des flux d'énergie.

Le dimensionnement optimal d'un Microgrid prend en compte non seulement la valeur ajoutée des bénéfices directes, mais aussi d'autres questions comme la disponibilité de puissance, la fiabilité, la condition environnementale, la qualité de l'alimentation, le taux de l'intégration des sources renouvelables et donc pour les deux modes connecté au réseau ou déconnecté.

Dans ce chapitre, le dimensionnement optimal d'un Microgrid en mode îloté et en mode relié au réseau est présenté. La technique d'optimisation itérative est utilisée pour suivre les 'Renewable Energy Fractions (FR)', le 'Excess Energy Ratio (EER)' et le coût annuel du système (ACS) en tenant compte de l'émission de CO_2. Tout d'abord, sur la base d'une simulation itérative, les configurations possibles du système sont calculées pour remplir les conditions de système de charge souhaitée. Afin de trouver la configuration optimale, ces configurations sont évaluées en fonction FR, EER et le coût annuel du système avec la faible émission de CO_2 (off-grid Microgrid).

A.IV.2. Un dimensionnement optimal d'un Microgrid en mode îloté

- La configuration du système

Dans cette section, un Microgrid en mode îloté comprend de PV système, Diesel, BESS et de charge. Les générateurs diesel sont connectés avec le réseau, qui alimentent directement à la charge. Alors que le PV et BESS sont couplés au réseau avec l'onduleur. Les groupes électrogènes peuvent être utilisés comme source principale ou comme back up (associée ou non à BESS) dans le cas, par exemple, de l'insuffisance de la production photovoltaïque. En outre, la production de PV doit être utilisée avec la plus grande efficacité. Par conséquent, il est nécessaire d'une stratégie d'opération pour trouver la solution optimale économique. D'autre part, la capacité de BESS doit être assez grande pour pouvoir être chargé à partir de l'excédent de puissance et de absorber le déficit d'énergie.

- Méthodologie

Fonction objectif

La fonction objectif est de minimiser le coût annuel du système (ACS) en tenant compte de l'émission de CO2. Il comprend le coût d'investissement initial et des coût de fonctionnements pendant toute la durée de vie de l'installation. Pour ce chapitre, la durée de vie des composants est considéré comme le même.

Le (ACS) comprend le coût annuel du capital (ACC), l'entretien annuel d'exploitation (AOM), le coût annuel de remplacement (ARC), le coût annuel en carburant (AFC) et le coût annuel d'émissions (AEC) comme dans [96].

$$ACS=ACC + AOM + ARC + AFC + AEC \quad (IV.1)$$

Contraintes

** Les contraintes de configuration*

$$0 \leq N_{pv} \leq \frac{E_{L\_day}}{\eta.W.Hours_{sunshine/day}} \quad (IV.2)$$

$$0 \leq C_b \leq \frac{5.E_{L\_day}}{DOD.\eta_b} \quad (IV.3)$$

$$0 \leq P_R \leq P_{L\_peak} \quad (IV.4)$$

** Les contraintes d'exploitation*

$$P_L(t)=P_{PV}(t) + P_B(t) + P_D(t) \quad (IV.5)$$

$$SOC_{min} \leq SOC(t) \leq SOC_{max} \quad (IV.6)$$

$$P_{Bmin} \leq P_B(t) \leq P_{Bmax} \quad (IV.7)$$

Les autres contraintes

$$FR_{design} \leq FR \leq 1 \quad \text{(IV.8)}$$

$$0 \leq EER \leq EER_{design} \quad \text{(IV.9)}$$

- Les résultats de simulation et discussion

Un dimensionnement optimal en mod d'îloté de Microgrid est révélé dans cette partie. La simulation annuelle est effectuée pour déterminer le ACS et l'émission de CO_2. La simulation sera terminée lorsque les variables atteignent leurs valeurs maximales.

Table A.IV.1: Optimal sizing PV-diesel-BESS hybrid results

	Hybrid system	Diesel only system
Maximum PV power (kW)	103.4 (440x235)	-
BESS capacity (kWh)	495	-
Diesel generator capacity (kW)	50	50
Diesel generator minimum power (%)	30	30
SOC_{min} (%)	20	-
SOC_{max} (%)	90	-
FR (%)	50	-
EER (%)	1	-
Annual load energy (kWh)	286853.5	286853.5
Annual CO_2 emission (Ton/year)	34.8	100.6
Annual cost of system ACS (US$)	53.296	71.060
Price (US$/kW)	0.19	0.24

Dans le Tableau A.IV.1, les résultats de dimensionnement optimal du système sont présentés et comparés avec un système de diesel seul. De ce résultat, nous pouvons conclure que le système hybride est plus économique ainsi que moins d'émissions que le système avec diesel seul.

A.IV.3. Gestion de l'énergie optimale dans d'un Microgrid en mode connecté

- La configuration du système

Dans ce cas, il n'y a pas de générateur diesel; Ainsi, le réseau principal alimentera à la demande de charge quand elle dépasse la puissance de PV and BESS. D'autre part, lorsque la puissance PV est supérieure à la demande de charge, l'excédent de puissance peut être revendu au réseau principal ou à la charge BESS. Dans ce système, les solutions de traitement de charge/décharge du BESS et de l'achat/vente de l'énergie à partir du réseau principal sont obtenues après la résolution de l'économie optimale basée sur le fonctionnement du système.

- Méthodologie

Fonction objectif

Dans ce paragraphe, la fonction objectif est de minimiser le coût annuel du système (ACS). Il comprend le coût de l'investissement initial, le coût de fonctionnement pendant toute la durée de vie de l'installation et les recettes provenant de la vente d'électricité au réseau électrique principal. Le coût annuel du système dans cette partie peut être proposé avec des éléments comme suit:

Dans cette partie, le coût annuel du système (ACS) comprend le coût annuel du capital (ACC), l'entretien annuel d'exploitation (AOM), le coût annuel de remplacement (ARC), le coût d'achat annuel (ABC) et le revenu de la vente de l'électricité au réseau principal (vente annuelle des coûts de l'ASC). L'ACS est estimé comme suit:

$$ACS=ACC + AOM + ARC +ABC-ASC \quad (IV.10)$$

Contraintes

** Les contraintes de configuration*

Les contraintes (IV.21), (IV23).

** Les contraintes d'exploitation*

Les contraintes (IV.21), (IV23) et

$$P_{grid}^{min} \leq P_{grid} \leq P_{grid}^{max} \quad (IV.11)$$

**Les autres contraintes*

$$FR_{design} \leq FR \leq 1 \quad (IV.12)$$

$$0 \leq EER \leq EER_{design} \quad (IV.13)$$

- Les résultats de simulation et discussion

Un dimensionnement optimal de Microgrid connecté au réseau est présenté dans ce

paragraphe. La simulation annuelle est effectuée pour déterminer l'ACS. La simulation s'arrête lorsque les variables (N_{pv} et E_b) atteignent leurs valeurs maximales.

Table A.IV.2: Optimal sizing grid connected PV-BESS system results

	Grid connected PV-BESS system	PV- diesel-BESS system
Maximum PV power (kW)	108.1 (460x235)	103.4 (440x235)
BESS capacity (kWh)	295	495
Diesel generator capacity (kW)	-	50
Diesel generator minimum power (%)	-	30
SOC_{min} (%)	20	20
SOC_{max} (%)	90	90
FR (%)	50	50
EER (%)	1	1
Annual load energy (kWh)	286853.5	286853.5
Annual cost of system ACS (US$)	45.861	53.296
Annual average price (US$/kW)	0.16	0.19

Dans le Tableau A.IV.2, les résultats de dimensionnement optimal d'un Microgrid en mode connecté au réseau sont présentés et comparés. De ce tableau, on peut en conclure que le le Microgrid en mode connecté au réseau est plus économique que le Microgrid en mode îloté.

A.IV.4. Conclusion

Dans ce chapitre, le dimensionnement optimal de Microgrid en mode îloté et de Microgrid raccordé au réseau a été présenté. Une technique itérative est utilisée pour trouver la configuration optimale avec le nombre de panneaux photovoltaïques, la capacité BESS et la capacité de diesel (dans le système hybride). Ensuite, les comparaisons de la configuration de système optimale avec le système îloté (avec diesel) et en mode connecté au réseau ont été réalisées afin d'évaluer la méthode proposée.

A.V : Gestion de l'énergie optimale dans d'un Microgrid

A.V.1. Introduction

Quand un Microgrid a plus que deux DER, il est nécessaire d'avoir un système de gestion d'énergie (EMS) qui devrait optimiser le partage de puissance entre DER, le coût de la production d'énergie et d'émission. Les fonctions de EMS sont présentés dans la Figure A.V.1. Le système de gestion de l'énergie reçoit les valeurs de prévision de demande de charge, les ressources énergétiques distribuées et le prix de l'électricité sur le marché dans chaque heure le lendemain afin de déterminer la puissance de sortie de DER, l'importation / exportation de puissance avec le réseau principal, le coût et la émission. La configuration de Microgrid présentée dans le chapitre IV, sera utilisée dans ce chapitre.

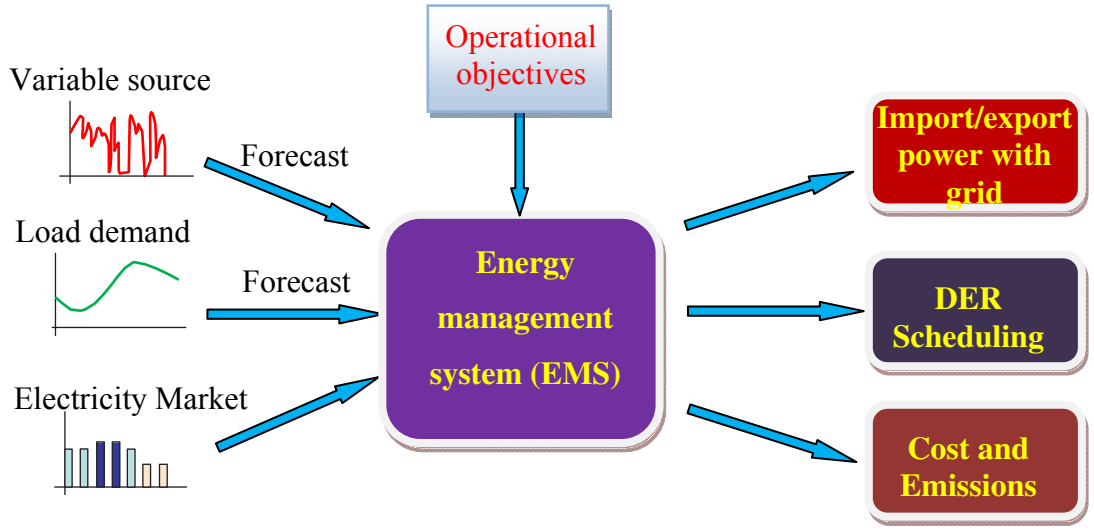

Figure A.V.1: The EMS in a Microgrid

La gestion optimale de l'énergie pour un Microgrid est effectuée sous deux modes de fonctionnement : connecté au réseau et îloté en utilisant la méthode de programmation dynamique DP. Dans le Microgrid îloté, la fonction objectif est de minimiser le coût de consommation de carburant et de réduire les émissions. Alors que pour le mode connecté au réseau, l'objectif est de minimiser les 'cash flow' du système ainsi que pour satisfaire l'importation de la puissance nette du réseau principal, qui est considéré comme une contrainte du problème d'optimisation. La gestion de l'énergie obtenue par la méthode DP est comparée à une méthode basée sur des règles. Les résultats de simulation sont effectués pour évaluer l'efficacité de la méthode proposée (DP).

A.V.2. Méthodes d'optimisation

- Programmation dynamique et Algorithme de Bellman

La programmation dynamique est connue comme une technique d'optimisation qui transforme un problème complexe en problème plus simple en découpant un problème en une série de sous-problèmes. Un algorithme de programmation dynamique appelé l'algorithme Bellman est utilisé pour trouver le chemin le plus court de tous les nœuds d'un graphe. Dans ce chapitre, l'algorithme Bellman est appliqué à trouver la séquence minimale de l'état de charge (SOC).

L'algorithme Bellman pour le SOC est décrit comme la Figure A.V.2. L'état du système à chaque fois est estimé par un ensemble de variables d'état. Il est discrétisé avec un pas de "δSOC". L'état initial de charge (SOC_0) est donné comme le nœud initial sans le nœud précédent. De même, on met de l'état de charge final (SOC_T). Toutes les arêtes sont orientées dans une direction de temps t à t + Δt temps. Ainsi, le processus de SOC de changement est considéré comme un graphe orienté avec nœud initial (SOC_0) et le noeud final (SOC_T)

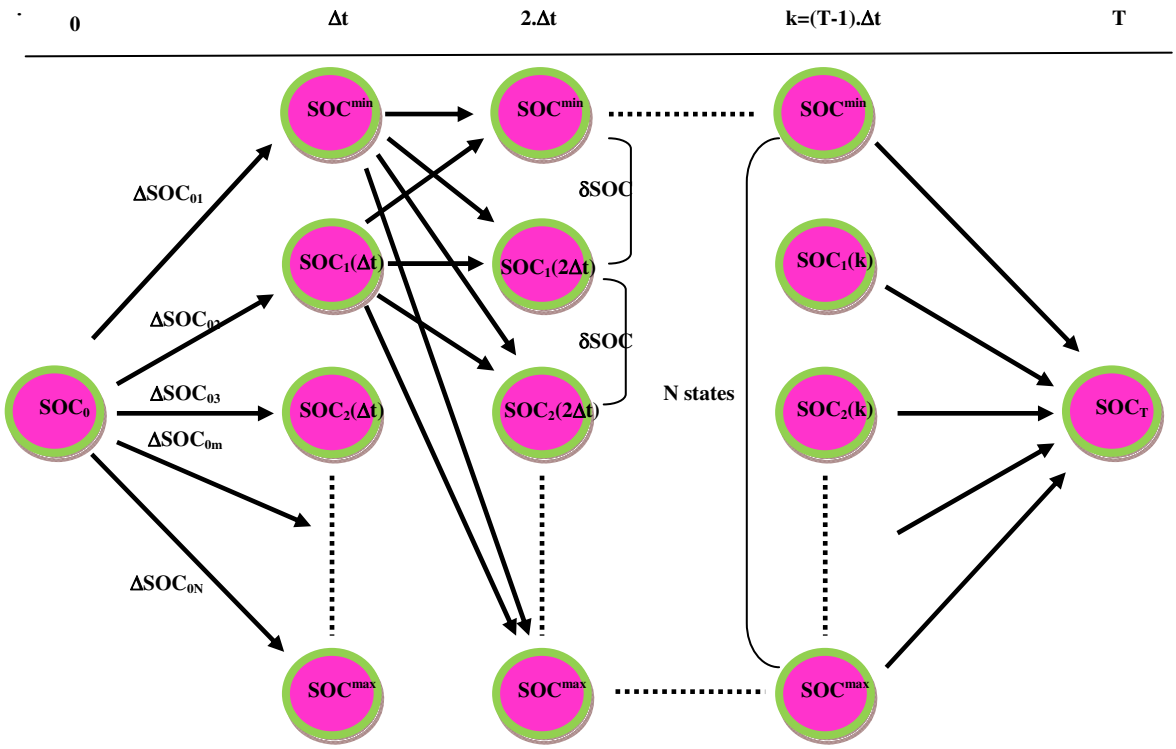

Figure V.2: Bellman algorithm application for battery's SOC space

A.V.3. Gestion de l'énergie optimale dans d'un Microgrid en mode îloté

La configuration d'un Microgrid îloté comprend un système PV, Diesels, BESS et les charges. Les systèmes de diesel fournissent directement à la demande de charge. Lorsque la puissance PV n'est pas suffisante pour répondre à la demande de charge, la puissance restante sera couverte par le diesel et BESS. De l'autre côté, l'excédent de puissance de la production photovoltaïque sera à la charge du BESS. Ainsi, la gestion de l'énergie est effectuée pour estimer la répartition optimale de la puissance entre les sources. Dans cette section, les données de charge sont extraites du chapitre IV, tandis que celle du rayonnement de PV est donnée en jour d'été dans le chapitre IV.

- Fonction objectif

L'objectif est de minimiser le coût de système (CS) en tenant compte de l'émission de CO2. Le CS comprend le coût du carburant (FC), le coût d'émission (EC) et le coût des batteries de remplacement (BrC). Dans ce chapitre, le coût du système peut être déterminé comme suit:

$$CS= \sum_{t=1}^{24} FC(t)+EC(t)+BrC\,(t) \tag{V.1}$$

- Contraintes

** Contrainte de l'équilibre de puissance:*

$$P_L(t)=P_{PV}(t) + P_B(t) + P_D(t) \tag{V.2}$$

** Contrainte de puissance BESS:*

$$P_{Bmin} \leq P_B(t) \leq P_{Bmax} \tag{V.3}$$

$$\Delta SOC_{min} \leq \Delta SOC\,(t) \leq \Delta SOC_{max} \tag{V.4}$$

** Contrainte d'État de charge de la batterie:*

$$SOC_{min} \leq SOC(t) \leq SOC_{max} \tag{V.5}$$

** Contrainte de vieillissement de batterie:*

$$SOH(t) \geq SOH_{min} \tag{V.6}$$

** Contrainte des générateurs diesel:*

$$P_{die\_min} \leq P_D(t) \leq P_{die\_max} \tag{V.7}$$

- Une stratégie de gestion de l'énergie à base de règles

Dans ce paragraphe, une stratégie de gestion de «contrainte» est proposée sur la base des règles prédéfinies. Le fonctionnement du système est prélevé en fonction de la puissance et de la consommation de PV. Ce mode de gestion est limité en raison du fait que l'état de la batterie n'est pas pris en compte dans les règles prédéfinies.

Le principe de la gestion de l'énergie est basé sur les règles principales suivantes:

- L'énergie photovoltaïque est principalement utilisée pour fournir des charges
- Le BESS décharge lorsque la production de système PV et Diesels ne sont pas suffisantes
- Le BESS est chargé dès que possible avec l'excès de puissance (lorsque la production est plus que les charges)

- L'application de l'algorithme Bellman dans la gestion optimale de l'énergie pour un Microgrid îloté

L'algorithme de Bellman est appliqué pour ce système hybride afin de trouver le coût minimum de système par le moyen de trouver la séquence optimale de transition de SOC à partir du moment initial et de temps final. C'est un problème d'optimisation discrétisée en temps Δt. Ainsi, le coût du système (CS) peut être décrit comme suit:

$$CS= \sum_{t=1}^{24} C_f.FC(t)+\frac{E_f.E_{cf}P_{DG}(\Delta t)}{1000}+BrC(t) \qquad (V.8)$$

L'algorithme Bellman est appliqué à construire un graphe d'état de charge à partir du moment initiale à la dernière fois que la Figure V.2. En outre, la variation de SOC (ΔSOC) est liée à la puissance de la batterie. Ainsi, pour chaque ΔSOC le P_B et P_D sont estimés en fonction de la valeur prévue de la PV disponible. Par conséquent, le CS correspondant est obtenu

- Les résultats de simulation et discussion

La gestion optimale de l'énergie de Microgrid îloté est présentée dans le présent paragraphe. La simulation est effectuée pour déterminer le minimum de CS, les émissions de CO2 ainsi que le planning optimal de fonctionnement des diesels et BESS. La simulation est terminée lorsque l'état de la variable charge SOC atteint son état final. Dans cette partie, trois scénarios sont effectués avec différents SOC initiaux

Table A.V.1: The final value of the objective function in case SOC= 0.5

	DP	Rule-based
Final value ($)	113.3	148.47

Table A.V.2: The final value of the objective function in case SOC= 0.2

	DP	Rule-based
Final value ($)	118	148.47

Table A.V.3: The final value of the objective function in case SOC= 0.9

	DP	Rule-based
Final value ($)	116.13	136.7

Les résultats obtenus dans les Tableaux A.V.1-A.V.3 ont prouvés que la gestion de l'énergie pour un Microgrid îloté déterminée par la méthode DP donne le résultat optimal. En outre, parmi les trois scénarios du procédé DP, le scénario avec SOC = 0,5 donne le meilleur résultat.

A.V.4. Gestion de l'énergie optimale dans d'un Microgrid en mode connecté

La configuration d'un Microgrid en mode connectée comprend le réseau principal, système PV, et BESS. Le réseau principal fournit directement à la demande de charge. Lorsque la puissance du système de PV n'est pas suffisante pour répondre à la demande de charge, la puissance restante sera couverte par BESS et le réseau principal. D'autre part, l'excès d'alimentation de la PV sera chargé complètement pour le BESS et la puissance restante sera envoyée au réseau principal.

- Fonction objectif

La fonction objectif est de minimiser la valeur finale de cash flow "CF" pendant toute la période étudiée. Le cash flow comprend la cash reçue "CR" et l'argent payé "CP". L'argent reçu est donné comme une valeur négative et l'argent de revenue est exprimé comme une valeur positive.

Fonction objectif:

$$\min(CF)=\min\left(\sum_{to}^{T} CR(t)+CP(t)\right) \quad (V.9)$$

- Constraints

** Contrainte de l'équilibre de puissance:*

$$P_L(t)=P_{PV}(t) + P_B(t) + P_{grid}(t)$$

** Contrainte de puissancede BESS:*

$$P_{Bmin} \leq P_B(t) \leq P_{Bmax}$$

** Contrainte d'État de charge de la batterie:*

$$\Delta SOC_{min} \leq \Delta SOC(t) \leq \Delta SOC_{max}$$

$$SOC_{min} \leq SOC(t) \leq SOC_{max}$$

** Contrainte de vieillissement de batterie:*

$$SOH(t) \geq SOH_{min}$$

** Contrainte de puissance de réseau:*

La puissance de l'échange est limitée comme suit: $P_{grid}^{min} \leq P_{grid}(t) \leq P_{grid}^{max}$

Afin de minimiser la puissance reçue à partir du réseau principal, la valeur Pgridmax est limitée comme suit:

$$0 \leq P_{grid}^{max} \leq P_{peak\ load}$$

- Une stratégie de gestion de l'énergie à base de règles

Le principe de la gestion de l'énergie à base statué est basé sur les règles principales suivantes:

- Le système PV est principalement utilisé pour alimenter les charges
- Le BESS est déchargé lorsque la production PV et le réseau ne sont pas suffisants
- Le BESS est chargé dès que possible avec la première source disponible.

- L'application de l'algorithme Bellman dans la gestion optimale de l'énergie pour Microgrid connecté au réseau

L'algorithme Bellman est appliqué à déterminer la valeur de FC minimum en trouvant la séquence optimale de transition SOC dans l'ensemble de la période étudiée. La puissance de BESS (P_B) est estimée à chaque étape de variation de charge ΔSOC. Après

cela, la puissance de réseau est calculée suivant le P_B, P_L et P_{PV}. Ensuite, le P_{grid} estimée doit satisfaire la limite de la puissance du réseau. Enfin, les FC correspondant sont atteints et c'est l'arête du graphe SOC.

- Les résultats de simulation et discussion

La gestion optimale de l'énergie d'un Microgrid en mode connecté au réseau est présentée dans cette partie. La simulation est effectuée pour déterminer le minimum de cash flow "CF" dans 2 cas avec les différents tarifs: tarif de l'autonomie (fixe) et de la tarification dynamique. Dans chaque la puissance maximale d'échange avec le réseau, la simulation se fait lorsque l'état de la variable charge SOC atteint son état final. Les résultats de simulation de sont obtenus avec un minimum de FC ainsi que son fonctionnement.

Table A.V.4: The final value of the objective function in the autonomy tariff case

	DP	Rule-based
Final value ($)	44.6	63.2

Table A.V.5: The final value of the objective function in the dynamic tariff case

	DP	Rule-based
Final value ($)	39.6	69

Les résultats obtenus dans les Tableaux A.V.4-A.V.5 ont approuvé que la gestion de l'énergie pour un Microgrid connectée au réseau, déterminée par la méthode DP donne le résultat optimal. La valeur maximale optimale de la puissance reçue à partir du réseau est estimée à 36kW.

A.V.5. Conclusion

Dans ce chapitre, la gestion optimale de l'énergie de Microgrid en mode îloté et en mode connectée au réseau a été présentée. La technique de programmation dynamique est utilisée pour trouver le plan de fonctionnement optimal des sources d'énergie ainsi que l'import/export avec le réseau principal, et donc, de minimiser les coûts de fonctionnement du Microgrid et émissions de CO_2. La valeur finale obtenue est comparée à cette valeur dans le procédé à base de règles

A.VI : Contrôle de Microgrid

A.VI.1. Introduction

Le contrôle de Microgrid comprend deux termes qui sont coordonné ou locale [1]. Ce chapitre se concentre sur le contrôle local. Le fonctionnement efficace de Microgrid peut être amélioré en utilisant les contrôleurs locaux de DER intelligents. Ces contrôleurs participent au contrôle de la fréquence et de la tension dans les différents modes de fonctionnement de Microgrid : le mode îloté, mode connecté au réseau; en outre, ils distribuent efficacement pour la régulation de la fréquence et de la tension pendant les transitions de mode connecté à l'opération d'îlotage.

Tout d'abord, une stratégie de contrôle basée sur le contrôle de statisme est proposée pour ramener la tension et la fréquence aux valeurs normales en utilisant les contrôles primaires et secondaires. Dans le réglage primaire, la caractéristique de statisme mis en œuvre dans le VSI est utilisée pour veiller à ce que la fréquence et la tension restent proches de leurs valeurs de consigne. Après cela, la commande secondaire est nécessaire pour rétablir la fréquence et la tension à la valeur nominale. Deuxièmement, la nouvelle architecture de Microgrid est utilisée dans lequel le diesel n'est pas disponible. La logique floue est ajoutée à la commande proposée. Dans ce procédé, la fréquence n'est pas seulement exprimée comme une fonction de puissance mais aussi de l'état de charge et l'état de fonctionnement initial.

A.VI.2. Les stratégies de contrôle pour DERs

- Multi - Master control (droop control)

Afin d'éviter d'utiliser la communication, la méthode 'Multi-Master' est utilisée. Dans cette méthode, les onduleurs se fixent immédiatement la puissance active et réactive. Un concept de 'statisme ou droop' est appliqué pour les DERs en Microgrid.

*** Réglage primaire**

Comme pour les flux d'énergie entre deux systèmes d'alimentation, le partage de la puissance active et réactive entre les DERs sont décrites comme la fonction de la fréquence et de la tension, respectivement. La répartition de puissance active est présentée à la Figure

A.VI.1

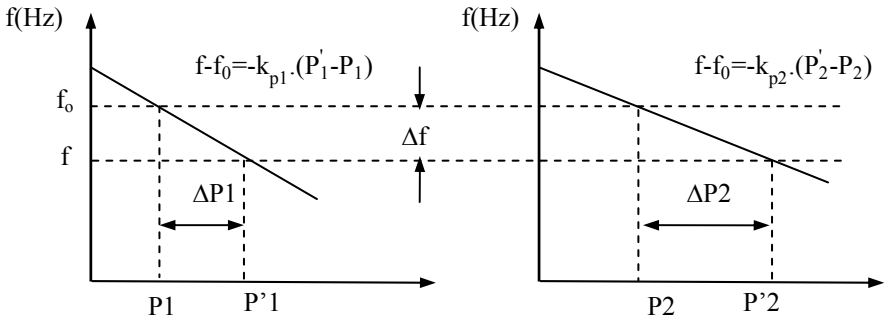

Figure A.VI.1: Power sharing of two parallel inverters

*** Réglage secondaire**

Tout d'abord, les réponses de contrôle primaires rapidement afin de ramener la fréquence à une valeur proche de la valeur nominale. Ensuite, la commande secondaire est utilisée pour restaurer la fréquence à la valeur nominale par ajuster la consigne de puissance. Le réglage secondaire est présenté à la Figure A.VI.2

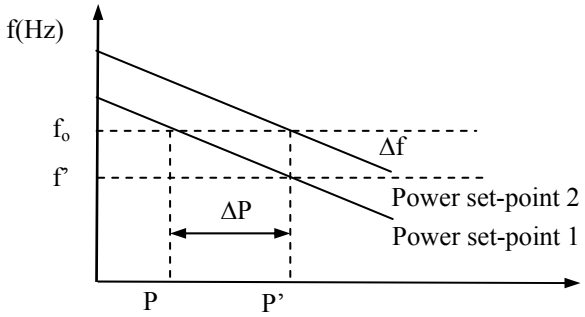

Figure A.VI.2: Secondary control with power set point changing

*** Cas de simulation**

- Fonctionnement normal
- Fonctionnement perturbation

**** Fonctionnement normal***

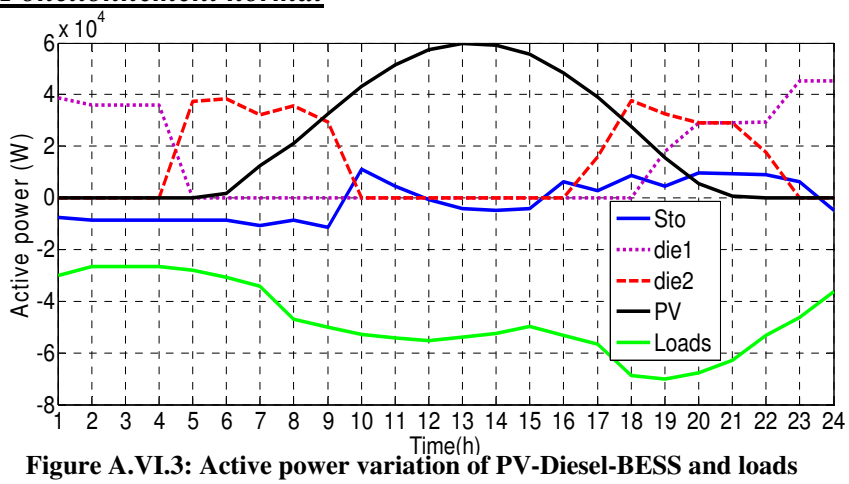

Figure A.VI.3: Active power variation of PV-Diesel-BESS and loads

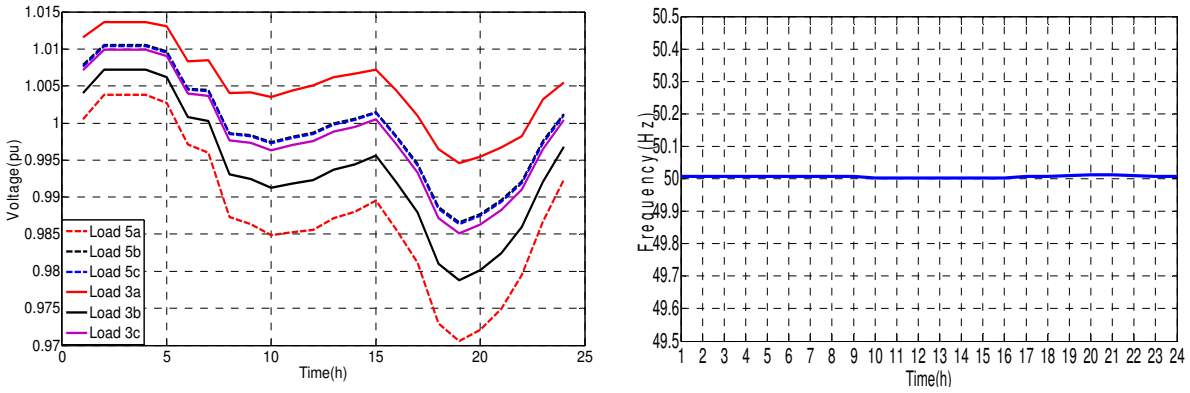

Figure A.VI.4: The voltage and frequency of PV-Diesel-Battery system

La tension et la fréquence sont maintenus au sein de la valeur autorisée.

**** Fonctionnement perturbation***

- Scénario 1: Les variations de charge
- Scénario 2: Variations de production (déclenchement diesel).
- Scénario 3: Perte de production PV
- Scénario 4: Déclenchement de BESS.

Les résultats de la simulation sont présentés dans le chapitre VI.

- Une stratégie de contrôle intelligent

Dans ce paragraphe, une stratégie de contrôle intelligent pour Microgrid est proposée. Ceci peut être utilisé pour les modes de fonctionnement microgrid: transition du mode connecté au mode îloté. Dans cette méthode, nouvelle architecture de Microgrid est défini. Cette architecture comprend les microsources et l'BESS sans groupes électrogènes diesel. En mode connecté, la tension et la fréquence sont imposées par le réseau principal. Cependant, dans le mode îloté, les onduleurs BESS avec le contrôle V/f jouent un rôle de l'unité maître. Ils remplacent le diesel (dans le cas ci-dessus) pour maintenir la tension et la fréquence dans la limite autorisée. En outre, la logique floue est ajoutée pour déterminer de manière adaptative le coefficient de commande (k). La logique floue est utilisée pour calculer le coefficient de contrôle basé sur les informations locales de DER tels que: l'état de charge, puissance mesurée, la fréquence mesurée. La contrainte physique de la batterie tels que l'état de charge SOC et puissance disponible. L'entrée / sortie de la logique floue utilisée est représentée sur la Figure A.VI.5.

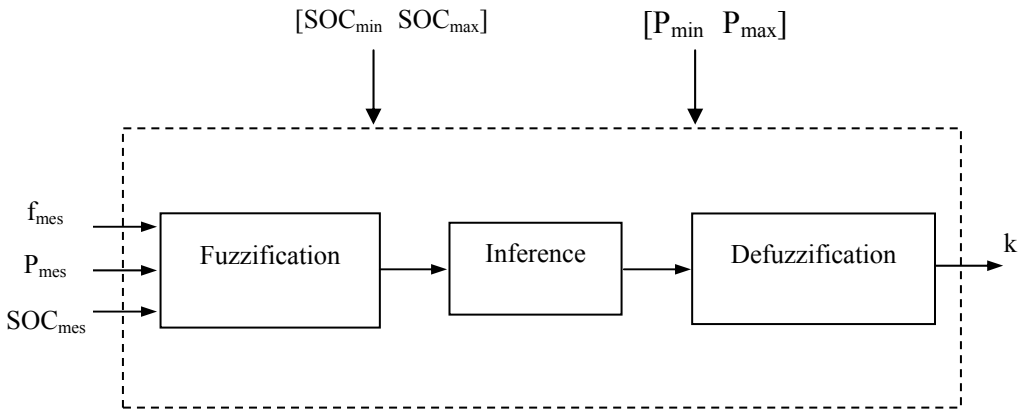

Figure A.VI.5: The method determines the control coefficient k

Le détail de la méthode de contrôle proposée est confidentiel (brevet en cous de déposer)

*** Les résultats de simulation**

Afin d'évaluer l'efficacité de commande proposé, le critère de simulation est effectué pour un réseau rural. Deux scénarios sont effectués comme suit:

- Scénario 1: Transition de la mode connecté au mode îlotage avec 4 cas en fonction des conditions de fonctionnement initiales.

- Scénario 2: Les productions photovoltaïques sont soudainement variées en mode îloté.

Scénario 1: passage du mode connecté au mode d'îloté

La simulation effectuée avec les différents cas sont présentés dans le Tableau A.VI.1:

Table A.VI.1: The initial operation conditions of BESS in 4 cases

		BESS 1	BESS 2	BESS 3
	P_n (kW)	**30**	**30**	**30**
Case 1	P_{ini}	0	0	0
	SOC	0.8	0.8	0.8
Case 2	P_{ini}	0	0	0
	SOC	0.2	0.5	0.8
Case 3	P_{ini}	0	5	10
	SOC	0.8	0.8	0.8
Case 4	P_{ini}	-5	0	5
	SOC	0.2	0.5	0.8

Les résultats de la simulation est présentés dans le chapitre VI.

Scénario 2: Microgrid îloté

Dans ce scénario, la production photovoltaïque est brusquement variée, par exemple:

la réduction de 100% à 40% et puis l'augmentation de 40% à 90%.

La puissance active et de la fréquence de Microgrid sont représentés sur la Figure A.VI.6. Après la réduction de production de PV (de 100% à 40%), trois BESS décharge pour maintenir l'équilibre entre production et consommation. De plus, la fréquence est maintenue à 50 Hz après l'action de réglage de fréquence primaire et secondaire. Puis, à t = 7s, production PV s'élève à 90%, elle conduit à la croissance de fréquence. Afin d'éviter cette augmentation, la puissance de BESS doit diminuer. Enfin, la fréquence est maintenue à la valeur nominale (50 Hz) après le réglage secondaire.

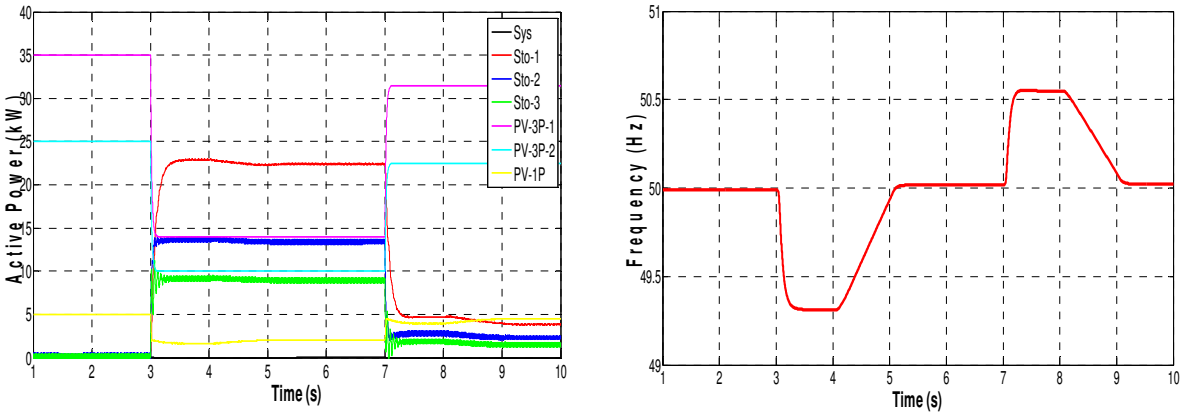

Figure A.VI.6: Active power and system frequency in scenario 2

A.VI.3. Conclusion

Dans ce chapitre, les commandes de microgrid en mode îloté et de la transition du mode connecté au réseau à mode isolé ont été présentées. Une méthode de contrôle de statisme classique est effectuée pour le système PV-BESS-diesel. Les résultats des simulations obtenus montrent que les diesels et BESS participent à répartir la puissance active et réactive pour régler la fréquence et les tensions. Ainsi, ce système fonctionne avec une grande fiabilité. En outre, une méthode de contrôle intelligent est également proposée dans ce chapitre. Dans cette méthode, la logique floue est utilisée pour déterminer de façon adaptative le coefficient de contrôle en tenant compte de l'état de charge et de l'état initial du BESS. Les résultats de simulation ont montré l'efficacité de la méthode proposée notamment dans la transition du mode connectée au mode îloté.

A.VII : Conclusion et perspectives

A.VII.1. Conclusion

Dans cette thèse, les stratégies de dimensionnement, de contrôle et de gestion de l'énergie optimale pour un Microgrid ont été étudiés et développés.

- Les questions liées à Microgrid et leurs solutions sont présentées par une étude bibliographique. L'objectif, la contribution et l'organisation de cette thèse sont également présentés.

- Le problème général d'un Microgrid est considéré y compris la définition, l'architecture et les composants ainsi que son fonctionnement.

- Les modèles de composants de micro-réseaux sont développés pour les différentes applications de cette thèse. L'efficacité des modèles développés est illustrée par les résultats de la simulation.

- Une méthode itérative est proposée pour déterminer un dimensionnement optimal d'un Microgrid en deux modes: le mode îloté et le mode connecté.

-La gestion optimale de l'énergie de fonctionnement pour un Microgrid est également développé sous deux modes de fonctionnement: le mode îloté et le mode connecté en utilisant la méthode DP et la méthode à base de règles.

- Les stratégies en utilisant le contrôle de statisme pour DER et BESS sont développées pour contrôler la tension et la fréquence de Microgrid. D'autre part, les stratégies de contrôle intelligent en utilisant la logique floue sont proposées pour modifier de manière adaptative les coefficients de réglage du système.

A.VII.2. Perspectives

* Valider des modèles développés par des simulations et des simulations en temps réel

* Effectuer les simulations en utilisant l'approche stochastique. Il permet de prendre en compte l'incertitude de production PV et de charge.

* Le contrôle et la gestion multi-Microgrids seront effectués comme un potentiel du problème

* L'architecture de Microgrid peut être étendue avec plusieurs types d'énergies renouvelables, et de charges pilotables

* Le potentiel de service système est une question intéressante à développer.

References

[1] Hatziargyriou, N. “Microgrids:Architectures and Control” Wiley-IEEE Press, 2014

[2] http://www.iec.ch/whitepaper/pdf/iecWP-energystorage-LR-en.pdf

[3] Johnson, Jay; Schenkman, Benjamin; Ellis, Abraham; Quiroz, Jimmy; Lenox, Carl, "Initial operating experience of the 1.2-MW La Ola photovoltaic system," *Photovoltaic Specialists Conference (PVSC), Volume 2, 2012 IEEE 38th* , vol., no., pp.1,6, 3-8 June 2012

[4] Vechiu, I., Camblong, H., Tapia, G., Dakyo, B., & Nichita, C. (2004). Dynamic simulation model of a hybrid power system: performance analysis. Wind Energy Conference, London, England

[5] Mahamadou, A. T., Mamadou, B. C., Brayima, D., & Cristian, N. (2011). Ultracapacitors and batteries integration for power fluctuations mitigation in wind-PV-diesel hybrid system. International Journal of Renewable Energy Research (IJRER), 1(2), 86-95

[6] Xiangjun Li; Dong Hui; Xiaokang Lai, "Battery Energy Storage Station (BESS)-Based Smoothing Control of Photovoltaic (PV) and Wind Power Generation Fluctuations," *Sustainable Energy, IEEE Transactions on* , vol.4, no.2, pp.464,473, April 2013

[7] Bernal-Agustın, Jose L., and Rodolfo Dufo-Lopez. "Simulation and optimization of stand-alone hybrid renewable energy systems." *Renewable and Sustainable Energy Reviews* 13 (2009): 2111-2118.

[8] Phrakonkham, S., Le Chenadec, J. Y., Diallo, D., Remy, G., & Marchand, C. (2010). Reviews on Micro-Grid Configuration and Dedicated Hybrid System Optimization Software Tools: Application to Laos. Engineering Journal, 14(3), 15-34. SIZING

[9] Kébé, A., Phrakonkham, S., Remy, G., Diallo, D., & Marchand, C. (2012, March). Optimal Design of a renewable energy power plant for an isolated site in Senegal. In Renewable Energies and Vehicular Technology (REVET), 2012 First International Conference on (pp. 336-343). IEEE. SIZING

[10] S. Phrakonkham, J.Y. Lechenadec, D. Diallo, C. Marchand, Optimisation Software Tool Review and the Need of Alternative Means for Handling the Problems of Excess Energy and Mini-Grid Configuration: A Case Study from Laos, ASEAN Symposium

on Power and Energy Systems, Hua Hin, TH, 28 September 2009, pp. 53-58, Proceedings of ASEAN Symposium on Power and Energy Systems

[11] HOMER (The Hybrid Optimization Model for Electric Renewables). [Online]. Available: http://www.homerenergy.com

[12] HOGA (Hybrid Optimization by Genetic Algorithms). [Online]. Available http://www.unizar.es/rdufo.hoga - eng.htm

[13] T. Khatib, A. Mohamed, K. Sopian "A review of photovoltaic system size optimization techniques," Renewable and Sustainable Energy Reviews, 22 (2013), pp. 454–46

[14] H. Suryoatmojo, A. Elbaset, Syafaruddin and T. Hiyama "Genetic algorithm based optimal sizing of PV–wind–diesel–hydrogen–battery systems," Innovative Computing, Information and Control, vol 6 (2010), pp.

[15] J.L. Bernal-Agustín, R. Dufo-López, D.M. Rivas-Ascaso, "Design of isolated hybrid systems minimizing costs and pollutant emissions," Renew Energy, 31 (14) (2006), pp. 2227–2244

[16] R. Dufo-López, J.L. Bernal-Agustín, "Multi-objective design of PV–wind–diesel–hydrogen–battery systems," Renew Energy, 33 (12) (2008), pp. 2559–2572

[17] R. Dufo-López et al, "Multi-objective optimization minimizing cost and life cycle emissions of stand-alone PV–wind–diesel systems with batteries storage," Applied Energy,88 (2011), pp. 4033–4041

[18] S. Diaf, M. Belhamelb, M. Haddadic, A. Louchea, "Technical and economic assessment of hybrid photovoltaic/wind system with battery storage in Corsica Island," Energy Policy, 36 (2) (2008), pp. 743–754

[19] H.X. Yang, J. Burnett, L. Lu, "Weather data and probability analysis of hybrid photovoltaic/wind power generation systems in Hong Kong," Renewable Energy, 28 (2003), pp. 1813–1824

[20] H.X. Yang, L. Lu, W. Zhou, "A novel optimization sizing model for hybrid solar–wind power generation system," Solar Energy, 81 (1) (2007), pp. 76–84

[21] A. Kaabeche, M. Belhamel, R. Ibtiouen, "Sizing optimization of grid-independent hybrid photovoltaic/ wind power generation system," Energy, 36 (2011), pp. 1214–1222

[22] Yu Ru; Kleissl, J.; Martinez, S., "Storage Size Determination for Grid-Connected Photovoltaic Systems," Sustainable Energy, IEEE Transactions on , vol.4, no.1, pp.68-81, Jan. 2013

[23] Kornelakis, A., and E. Koutroulis. "Methodology for the design optimisation and the economic analysis of grid-connected photovoltaic systems." IET Renewable Power Generation, vol. 3, no 4, p. 476-492, 2009.

[24] Kaldellis, J. K., D. Zafirakis, and E. Kondili. "Optimum sizing of photovoltaic-energy storage systems for autonomous small islands." International journal of electrical power & energy systems vol. 32, no 1, p. 24-36, 2010.

[25] Hernández, J. C., A. Medina, and F. Jurado. "Optimal allocation and sizing for profitability and voltage enhancement of PV systems on feeders." Renewable Energy 32.10 (2007): 1768-1789

[26] Kornelakis, Aris, and Yannis Marinakis. "Contribution for optimal sizing of grid-connected PV-systems using PSO", vol. 35, no 6, p. 1333-1341, 2010.

[27] C.Wang and M. H. Nehrir, "Power management of a stand-alone wind/photovoltaic/fuel cell energy system," IEEE Trans. Energy Convers.,vol. 23, no. 3, pp. 957–967, Sep. 2008.

[28] S. Jain and V. Agarwal, "An integrated hybrid power supply for distributed generation application fed by nonconventional energy sources," IEEE Trans. Energy Convers., vol. 23, no. 2, pp. 622–634, Jun. 2008.

[29] M. Urbina and Z. Li, "A fuzzy optimization approach to PV/battery scheduling with uncertainty in PV generation," in Proc. 38th North American IEEE Power Symp. (NAPS 2006), Carbondale, IL, 2006, pp.561–566.

[30] A. W. Yang, "Design of energy management strategy in hybrid vehicles by evolutionary fuzzy system part I: Fuzzy logic controller development," in Proc. 6th World Congress on Intelligent Control and Automation, Dalian, China, Jun. 21–23, 2006.

[31] A. Borghetti, C. D'Ambrosio, A. Lodi, and S. Martello, "An MILP approach for short-term hydro scheduling and unit commitment with head-dependent reservoir," IEEE Trans. Power Syst., vol. 23, no. 3, pp. 1115–1124, Aug. 2008.

[32] T. T. Ha Pham, F. Wurtz, and S. Bacha, "Optimal operation of a PV based multi-source system and energy management for household application," in Proc. IEEE Int. Conf. Industrial Technology (ICIT), Gippsland, Victoria, Australia, 2009, pp. 1–5.

[33] B. Lu andM. Shahidehpour, “Short term scheduling of battery in a grid connected PV/battery system,” IEEE Trans. Power Syst., vol. 20, no. 2, pp. 1053–1061, May 2005.

[34] M. Koot, J. T. B. A. Kessels, B. de Jager, W. P. M. H. Heemels, P. P. J. Van Den Bosch, and M. Steinbuch, “Energy management strategies for vehicular electric power systems,” IEEE Trans. Veh. Technol., vol. 54, no. 3, pp. 771–782, May 2005.

[35] Faisal A. Mohamed. “Microgrid modeling and online management”. Helsinki University of Technology Control Engineering, Finland. PhD Thesis, June 2008

[36] C. Chen, S. Duan, T. Cai, B. Liu and G. Hu, "Smart energy management system for optimal microgrid economic operation," IET Renew. Power Gener., vol. 5, Iss. 3, pp.258-267, 2011.

[37] E. Sortomme and M. A. EI-Sharkawi, "Optimal power flow for system of microgrids with controllable loads and battery storage," IEEE PES Power System Conf. and Exposition, pp. 1-5, 2009.

[38] Bhuvaneswari Ramachandran, Sanjeev K. Srivastava, Chris S. Edrington, and David A. Cartes, "An intelligent auction scheme for smart grid market using a hybrid immune algorithm," IEEE Trans. Industrial Electronics, vol. 58, No. 10, October 2011.

[39] Yann Riffonneau. “Gestion des flux energetiques dans un systeme photovoltaique avec stockage connecte au reseau”. Universite Joseph Fourier, France. PhD Thesis, October 2009

[40] Zheng Zhao “Optimal Energy Management for Microgrids”. Clemson University, United State. PhD Thesis, October 2009

[41] Microgrids. [Online] www.microgrids.eu

[42] More Microgrids. [Online] www.microgrids.eu

[43] J. M. Guerrero, J. C. Vásquez, J. Matas, M. Castilla, L. G. D. Vicuña, and M. Castilla, “Hierarchical control of droop-controlled AC and DC microgrids—A general approach toward standardization,” IEEE Trans.Ind. Electron., vol. 58, pp. 158–172, Jan. 2011.

[44] A. Mehrizi-Sani and R. Iravani, “Potential-function based control of a microgrid in islanded and grid-connected models,” IEEE Trans. Power Syst., vol. 25, pp. 1883–1891, Nov. 2010.

[45] C. Yuen, A. Oudalov, and A. Timbus, “The provision of frequency control reserves from multiple microgrids,” IEEE Trans. Ind. Electron., vol. 58, pp. 173–183, Jan. 2011.

[46] K. D. Brabandere, K. Vanthournout, J. Driesen, G. Deconinck, and R. Belmans, “Control of microgrids,” in Proc. IEEE Power & Energy Society General Meeting, 2007, pp. 1–7.

[47] Y. A. R. I. Mohamed and A. A. Radwan, “Hierarchical control system for robust microgrid operation and seamless mode transfer in active distribution systems,” IEEE Trans. Smart Grid, vol. 2, pp. 352–362, Jun. 2011.

[48] J. A. P. Lopes, C. L. Moreira, and A. G. Madureira, “Defining control strategies for microgrids islanded operation,” IEEE Trans. Power Syst., vol. 21, pp. 916–924, May 2006.

[49] P. Piagi and R. H. Lasseter, “Autonomous control of microgrids,” in Proc. IEEE Power Eng. Soc. General Meeting, 2006.

[50] F. Katiraei, M. R. Iravani, and P. W. Lehn, “Microgrid autonomous operation during and subsequent to islanding process,” IEEE Trans. Power Del., vol. 20, pp. 248–257, Jan. 2005.

[51] Y. Li, D. M. Vilathgamuwa, and P. C. Loh, “Design, analysis, and real-time testing of a controller for multibus microgrid system,” IEEE Trans. Power Electron., vol. 19, pp. 1195–1204, Sep. 2004.

[52] H. Nikkhajoei and R. H. Lasseter, “Distributed generation interface to the CERTS microgrid,” IEEE Trans. Power Del., vol. 24, pp. 1598–1608, Jul. 2009.

[53] Jiefeng HU. “Advanced Control in Smart Microgrids”. University of Technology, Sydney, Australia. PhD Thesis, June 2013

[54] A. P. Martins, A. S. Carvalho, and A. S. Araujo, “Design and implementation of a current controller for the parallel operation of standard UPSs,” in Proc. IEEE IECON, 1995, pp. 584-589.

[55] Chandorkar M, Divan D. Decentralized operation of distributed ups systems. In: International conference on power electronics, drives and energy systems for industrial growth, vol.1;1995.p.565–71.

[56] Guerrero J, Berbel N, deVicun˜a L, MatasJ, MiretJ, Castilla M “Droop control method for the parallel operation of online uninterruptible power systems using resistive

output impedance". In: IEEE applied power electronics conference and exposition (APEC); 2005.p.1716–22.

[57] Guerrero J, Garcia de Vicu na L, Matas J, Castilla M, Miret J. "Output impedance design of parallel-connected ups inverters with wireless load-sharing control". IEEE Transactions of Industrial Electronics 2005; 52(4): 1126–35.

[58] Bidram, A.; Davoudi, A., "Hierarchical Structure of Microgrids Control System," Smart Grid, IEEE Transactions on , vol.3, no.4, pp.1963,1976, Dec. 2012

[59] F. Katiraei, R. Iravani, N. Hatziargyriou, and A. Dimeas, "Microgrids management," IEEE Power Energy Mag., vol. 6, pp. 54–65, May/Jun. 2008

[60] G. Diaz, C. Gonzalez-Moran, J. Gomez-Aleixandre, and A. Diez, "Scheduling of droop coefficients for frequency and voltage regulation in isolated microgrids," IEEE Trans. Power Syst., vol. 25, pp. 489–496, Feb. 2010

[61] C. K. Sao and W. Lehn, "Autonomous load sharing of voltage source converters," IEEE Trans. Power Del., vol. 20, pp. 1009–1016, Apr.2005.

[62] C. K. Sao and W. Lehn, "Control and power management of converter fed microgrids," IEEE Trans. Power Syst., vol. 23, pp. 1088–1098, Aug. 2008.

[63] M. N. Marwali, J. W. Jung, and A. Keyhani, "Control of distributed generation systems–Part II: Load sharing control," IEEE Trans. Power. Electron., vol. 19, pp. 1551–1561, Nov. 2004.

[64] T. L. Lee and P. T. Cheng, "Design of a new cooperative harmonic filtering strategy for distributed generation interface converters in an islanding network," IEEE Trans. Power. Electron, vol. 22, pp. 1919–1927, Sep. 2007.

[65] J. C. Vasquez, J. M. Guerrero, A. Luna, P. Rodriguez, and R. Teodorescu, "Adaptive droop control applied to voltage-source inverters operating in grid-connected and islanded modes," IEEE Trans. Ind. Electron., vol. 56, pp. 4088–4096, Oct. 2009.

[66] K. D. Brabandere, B. Bolsens, J. V. D. Keybus, A. Woyte, J. Driesen, and R. Belmans, "A voltage and frequency droop control method for parallel inverters," IEEE Trans. Power Electron., vol. 22, pp. 1107–1115, Jul. 2007.

[67] Y. Li and Y. W. Li, "Power management of inverter interfaced autonomous microgrid based on virtual frequency-voltage frame," IEEE Trans. Smart Grid, vol. 2, pp. 30–40, Mar. 2011.

[68] W. Yao,M. Chen, J. Matas, J. M. Guerrero, and Z. Qian, "Design and analysis of the droop control method for parallel inverters considering the impact of the complex

impedance on the power sharing," IEEE Trans. Ind. Electron., vol. 58, pp. 576–588, Feb. 2011.

[69] Savaghebi, M.; Jalilian, A.; Vasquez, J.C.; Guerrero, J.M., "Autonomous Voltage Unbalance Compensation in an Islanded Droop-Controlled Microgrid," Industrial Electronics, IEEE Transactions on , vol.60, no.4, pp.1390,1402, April 2013

[70] D. Yazdani, A. Bakhshai, G. Joos, and M. Mojiri, "A nonlinear adaptive synchronization technique for grid-connected distributed energy sources," IEEE Trans. Power Electron., vol. 23, pp. 2181–2186, Jul.2008.

[71] B. P. McGrath, D. G. Holmes, and J. J. H. Galloway, "Power converter line synchronization using a discrete fourier transform (DFT) based on avariable sample rate," IEEE Trans. Power Electron., vol. 20, pp.877–884, Jul. 2005.

[72] S. J. Lee, H. Kim, S. K. Sul, and F. Blaabjerg, "A novel control algorithm for static series compensators by use of PQR instantaneous power theory," IEEE Trans. Power Electron., vol. 19, pp. 814–827, May 2004.

[73] A. Yazdani and R. Iravani, "A unified dynamic model and control for the voltage source converter under unbalanced grid conditions," IEEE Trans. Power Del., vol. 21, pp. 1620–1629, Jul. 2006.

[74] Savaghebi, M.; Jalilian, A.; Vasquez, J.C.; Guerrero, J.M., "Secondary Control Scheme for Voltage Unbalance Compensation in an Islanded Droop-Controlled Microgrid," Smart Grid, IEEE Transactions on , vol.3, no.2, pp.797,807, June 2012

[75] K. Vanthournout, K. D. Brabandere, E. Haesen, J. Driesen, G. Deconinck, and R. Belmans, "Agora: Distributed tertiary cotrol of distributed resources," in Proc. 15th Power Systems Computation Conf., 2005, pp.1–7.

[76] Myles, Paul, Joe Miller, Steven Knudsen, and Tom Grabowski. "430.01.03 Electric Power System Asset Optimization". Morgantown, WV: National Energy Technology Laboratory, 2011.

[77] Campbell, Richard J. Weather "Related Power Outages and Electric System Resiliency". Report for Congress, Washington, D.C. Congressional Research Service, 2012

[78] Microgrids: "Large Scale Integration of Micro-Generation to Low Voltage Grids", ENK5-CT-2002-00610. 2003–2005.

[79] More microgrids: "Advanced Architectures and Control Concepts for More microgrids", FP6 STREP, Proposal/Contract no.: PL019864. 2006–2009.

[80] Lopes, J.A.P., Moreira, C.L., Madureira, A.G "Defining control strategies for microgrids islanded operation". IEEE Trans. Power Syst. 21, 916–924 (2006)

[81] R. H. Lasseter and P. Piagi, "Control and design of microgrid components," PSERC Publication 06-03, University of Wisconsin-Madison, January 2006.

[82] Nikkhajoei, H.; Lasseter, R.H., "Microgrid Protection," *Power Engineering Society General Meeting, 2007. IEEE* , vol., no., pp.1,6, 24-28 June 2007

[83] A studying of single ended fault locator on siemens relay. Authors: Le Kim Hung,Vu Phan Huan, Nguyen Hoang Viet. Journal of Electrical and Control Engineering, 2013 Vol.3, No.2

[84] A fault location system for transmission lines using data measurements from two ends. Authors: Le Kim Hung, Nguyen Hoang Viet, Vu Phan Huan. 2012 International Conference on Green technology and Subtainable development- Ho Chi Minh City, 29-30 september 2012

[85] Gabriele Seeling-Hochmuth "Optimisation of hybrid energy systems sizing and operation control". University of Kassel, Germany. PhD Thesis, October 1998

[86] T. Tran-Quoc, N.A. Luu, and al., "Dynamic analysis of a stand-alone hybrid PV-diesel system with battery storage", International Conference 6th European Conference on PV-Hybrids and Mini-Grids. pp: 274-281. April 2012

[87] Luu Ngoc An; Tran Quoc-Tuan; Seddik, B., "Control strategies of a hybrid PV-diesel-battery system in different operation modes," PowerTech (POWERTECH), 2013 IEEE Grenoble , vol., no., pp.1,6, 16-20 June 2013

[88] Electrical energy storage-White paper. [Online] www.iec.ch

[89] Riffonneau, Y.; Bacha, S.; Barruel, F.; Ploix, S., "Optimal Power Flow Management for Grid Connected PV Systems With Batteries," Sustainable Energy, IEEE Transactions on , vol.2, no.3, pp.309,320, July 2011

[90] A. Delaille, F. Huet, E. Lemaire, F. Mattera, M. Perrin, and M. Vervaart, "Development of a battery fuel gauge based on ampere-hour counting," in Proc. 21st Eur. Photovoltaic Solar Energy Conf.,Dresden, Germany, Sep. 4–8, 2006.

[91] Y. Riffonneau, A. Delaille, F. Barruel, and S. Bacha, "System modeling and energy management for grid connected PV systems with storage," in Proc. 24th EU Photovoltaic Solar Energy Conf., Valencia, Spain, 2008.

[92] Microgrid Operation and Control. [Online] www.igrid.net.au

[93] Heri Suryoatmojo. “Artificial intelligent based optimal configuration of hybrid power generation sytem”. Kumamoto University, Japan. PhD Thesis, 2010

[94] P. Kundur “Power System Stability and Control”. Book, McGrall-Hill, 1994

[95] T. Senjyu, D. Hayashi, A. Yona, N. Urasaki and T. Funabashi “Optimal configuration of power generating systems in isolated island with renewable energy,” Renewable Energy, vol. 32 , pp. 1917–1933, 2007

[96] H. Suryoatmojo, A. Elbaset, Syafaruddin and T. Hiyama “Genetic algorithm based optimal sizing of PV–wind–diesel–hydrogen–battery systems,” Innovative Computing, Information and Control, vol 6 (2010)

[97] Z. Wei, "Simulation and Optimum design of hybrid Solar-wind and Solar-wind-diesel power generation systems," Ph.D. dissertation, Dep. Building service engineering, Univ. Hong Kong polytechnic, Hong Kong, 2007.

[98] Maria-Florina Balcan “Design and Analysis of Algorithms” Online http://www.cc.gatech.edu/~ninamf/Algos11/lectures/lect0318.pdf

[99] R.Bellman, “The theory of dynamic programming”, RAND Corporation, Proceedings of the National Academy of Sciences, pp.503-715, 1952

[100] R.Bellman, “On a routing problem”, Quarterly of Applied Mathematics, Vol.16, pp.87-90, 1958

[101] J. A. Peças Lopes, C. L. Moreira, A. G. Madureira, F. O. Resende, X. Wu, N. Jayawarna, Y. Zhang, N. Jenkins, F. Kanellos, N. Hatziargyriou, "Control strategies for microgrids emergency operation," in International Journal of Distributed Energy Resources, vol. 2, 2006, pp. 211-232.

[102] J. A. Peças Lopes, C. L. Moreira, A. G. Madureira, F. O. Resende, P. G. Abia, X. Wu, N. Jayawarna, Y. Zhang, N. Jenkins, F. Kanellos, N. Hatziargyriou, C. Duvauchelle, "Emergency strategies and algorithms," MicroGrids Project, Deliverable DD1,
http://microgrids.power.ece.ntua.gr/micro/micro2000/index.php?page=deliverables

[103] Chen, J.F. and Chu, C.-L. (1995) Combination voltage-controlled and current-controlled PWM inverters for UPS parallel operation. IEEE Trans. Power Electronics, 10 (5), 547–558

[104] Lasseter, B. (2001) “Microgrids Distributed Power Generation”, IEEE Power Engineering Society Winter Meeting Conference Proceedings, Columbus, Ohio, vol. 1, pp. 146–149.

Publications

[1] **A. Luu-Ngoc**, T. Tran-Quoc, S. Bacha "Control strategies of a hybrid PV-diesel-battery system in different operation modes"; IEEE/PES (Powertech-2013), Grenoble, France, June 2013

[2] **A. Luu-Ngoc**, T. Tran-Quoc, S. Bacha "Sizing Optimization of an Isolated Photovoltaic-Diesel-Battery Hybrid System", IEEE/PES General Meeting, Washington DC, USA, July 2014

[3] **A. Luu-Ngoc**, T. Tran-Quoc, S. Bacha, Van Linh NGUYEN "Optimal sizing of a Grid connected ", IEEE/ICIT, Spain, March 2015.

[4] **A. Luu-Ngoc**, T. Tran-Quoc, S. Bacha "Optimal energy management for a island microgrid by using Dynamic Programming (DP) Algorithm", submit to IEEE PowerTech conference, Eindhoven, The Netherlands from 29 June - 2 July 2015

[5] T. Tran-Quoc, **A. Luu-Ngoc**, X. Le Pivert, J. Merten, B. Lazpita, K. Mamadou, M. Vervaart "Dynamic analysis of a stand-alone hybrid PV-diesel system with battery storage ", 6th European conference on PV-Hybrids and Mini-Grids, Chambery, France April 2012.

[6] T. Tran-Quoc, **A. Luu-Ngoc**, X. Le-Pivert, J. Merten, F. Barruel, "Probabilistic Analysis of Photovoltaic Generation Impacts on Distribution Networks", 27th European PV Solar Energy conference and Exhibition, Frankfurt, Germany, Sep. 2012

[7] Van Linh NGUYEN, Tuan Tran Quoc, Seddik Bacha, **Ngoc An Luu**, "Charging Strategies to Minimize the Energy Cost for an Electric Vehicle Fleet", ISGT, Istanbul, Turkey,2014

Brevet:

Quoc Tuan TRAN, **Ngoc An LUU**, " Procédé de réglage de la fréquence d'un réseau électrique ", Déposé le 19/11/2013